ANALYTICA CHIMICA ACTA

International monthly devoted to all branches of analytical chemistry
Revue mensuelle internationale consacrée à tous les domaines de la chimie analytique
Internationale Monatsschrift für alle Gebiete der analytischen Chemie

Editors

Philip W. West *(Baton Rouge, La., U.S.A.)*
A. M. G. Macdonald *(Birmingham, Great Britain)*

ELSEVIER PUBLISHING COMPANY
AMSTERDAM

Anal. Chim. Acta, Vol. 58, No. 1, 1–252, January 1972
Published monthly

Publication Schedule for 1972

Vol. **58**, No. **1**	January 1972	
Vol. **58**, No. **2**	February 1972	**(completing Vol. 58)**
Vol. **59**, No. **1**	March 1972	
Vol. **59**, No. **2**	April 1972	
Vol. **59**, No. **3**	May 1972	**(completing Vol. 59)**
Vol. **60**, No. **1**	June 1972	
Vol. **60**, No. **2**	July 1972	**(completing Vol. 60)**
Vol. **61**, No. **1**	August 1972	
Vol. **61**, No. **2**	September 1972	
Vol. **61**, No. **3**	October 1972	**(completing Vol. 61)**
Vol. **62**, No. **1**	November 1972	
Vol. **62**, No. **2**	December 1972	**(completing Vol. 62)**

Subscription price: $20.80 or Dfl. 72.80 per volume plus postage. Total subscription price for 1972: $104.00 or Dfl. 364.00 plus postage. Additional cost for copies by airmail available on request. For subscribers in the U.S.A. and Canada, 2nd class postage paid at Long Island City, N.Y. and at additional mailing offices. For advertising rates apply to the publishers.

Subscriptions should be sent to:

ELSEVIER PUBLISHING COMPANY P.O. Box 211, Amsterdam, The Netherlands

---

GENERAL INFORMATION

Languages

Papers will be published in English, French or German.

Submission of papers

Papers should be sent to:

PROF. PHILIP W. WEST,
Coates Chemical Laboratories,
College of Chemistry and Physics,
Louisiana State University,
Baton Rouge 3,
La. 70803 (U.S.A.)

or to:

DR. A. M. G. MACDONALD,
Department of Chemistry,
The University,
P.O. Box 363
Birmingham B15 2TT (Great Britain)

Reprints

Fifty reprints will be supplied free of charge. Additional reprints (minimum 100) can be ordered at quoted prices. They must be ordered on order forms which are sent together with the proofs.

An Important Encyclopaedic Work of Reference

COMPREHENSIVE CHEMICAL KINETICS

edited by C. H. BAMFORD
and C. F. H. TIPPER

The aim of this series is to cover in a critical way the practice and theory of kinetics and the kinetics of inorganic and organic reactions in the gas and condensed phases or at interfaces.
Each chapter is written by an expert in the field so that the series as a whole will serve as a direct source of reference and information over the whole range of kinetics.
The vast amount of material scattered through the literature has never before been gathered together and presented in this accessible form.

Elsevier
Book Division, P.O. BOX 3489,
AMSTERDAM - THE NETHERLANDS

Volume 1. The Practice of Kinetics

1. Experimental methods for the study of slow reactions (L. Batt)
2. Experimental methods for the study of fast reactions (D.N. Hague)
3. Experimental methods for the study of heterogeneous reactions (D. Shooter)
4. The detection and estimation of intermediates (R.P. Wayne)
5. The treatment of experimental data (D. Margerison)

**6½ × 10″, xiii + 450 pages, 32 tables, 161 illus., 1160 lit. refs., 1969, Dfl. 95.00 (ca. $ 26.25)
ISBN 0-444-40673-5**

Volume 2. The Theory of Kinetics

1. Kinetic characterization of complex reaction systems (Z.G. Szabó)
2. Chain reactions (V.N. Kondratiev)
3. Theory of the kinetics of elementary gas phase reactions (R.P. Wayne)
4. Theory of elementary reactions in solution (I.D. Clark and R.P. Wayne)
5. Theory of solid phase kinetics (L.G. Harrison)

**6½ × 10″, xiii + 486 pages, 13 tables, 77 illus., 794 lit. refs., 1969, Dfl. 100.00 (ca. $ 27.75)
ISBN 0-444-40674-3**

Volume 3. The Formation and Decay of Excited Species

1. Effect of low energy radiation (C.S. Burton and W.A. Noyes, Jr.)
2. Effect of high energy radiation (G. Hughes)
3. The chemical production of excited states (T. Carrington and D. Garvin)
4. The transfer of energy between chemical species (A.B. Callear and J.D. Lambert)

**6½ × 10″, xii + 300 pages, 30 tables, 53 illus., 783 lit. refs., 1969, Dfl. 70.00 (ca. $ 19.50)
ISBN 0-444-40802-9**

The series as a whole will comprise about 25 volumes divided into a number of sections:

Section 1. The practice and theory of kinetics (3 volumes)
Section 2. Decomposition and isomerization reactions (2 volumes)
Section 3. Inorganic reactions (2 volumes)
Section 4. Organic reactions (6 volumes)
Section 5. Polymerization reactions (2 volumes)
Section 6. Oxidation and combustion reactions (2 volumes)
Section 7. Selected elementary reactions (2 volumes)

Other sections are planned on heterogeneous reactions, solid state reactions, and kinetics and technological processes.

VERLAG
CHEMIE

Soeben erscheint Band 1 der neuen Reihe
»WERKSTOFFE — Aufbau, Eigenschaften, Untersuchung, Anwendung«!

Erhard Hornbogen

Durchstrahlungs-Elektronenmikroskopie fester Stoffe

Die Verwirklichung jeder technischen Idee erfordert geeignete Werkstoffe. Deren Verfügbarkeit entscheidet zunehmend häufiger über den Erfolg eines Konzepts und beeinflußt so das Ausmaß des technischen Fortschritts. Oft sind Werkstoffprobleme die eigentliche Schwierigkeit bei Projekten, deren grundlegende physikalische und konstruktive Zusammenhänge gelöst sind. So rückt die Optimierung vorhandener und die Entwicklung neuer Werkstoffe immer mehr in den Blickpunkt der technischen Entwicklung. Fragen nach Werkstoffen mit geeigneten Eigenschaften, nach ihrem Aufbau, ihrer Untersuchung und ihrer Anwendung stellen sich in allen Bereichen der Technik in zunehmendem Maße; sowohl Ingenieure als auch Wissenschaftler werden mit Ihnen konfrontiert. Zur Beantwortung dieser Fragen soll die Buchreihe »Werkstoffe« beitragen, deren erster Band nun vorliegt.

Für Werkstoffentwicklungen ist es immer weniger sinnvoll, den früher allein üblichen empirischen Weg zu gehen. Es ist vielmehr zweckmäßig, die Eigenschaften eines Werkstoffes aus dem atomaren Aufbau abzuleiten. Voraussetzung dazu ist in jedem Fall, daß der mikroskopische Aufbau eines Stoffes lückenlos bekannt ist.

Das vorliegende Buch vermittelt eine Einführung, die praktisches Arbeiten im Labor ermöglichen soll. Es ist für alle gedacht, die die direkte Durchstrahlung mit Elektronen zur Untersuchung des Gefüges von Werkstoffen anwenden wollen. Bekanntlich sind solche Untersuchungen nicht ohne Kenntnisse über das Entstehen der Abbildungen möglich. Ziel des Buches ist es, ausgehend von einfachen Kontrastbedingungen — z. B. der Versetzung, des Stapelfehlers, der Antiphasengrenze — zu einem Verständnis der in der Praxis vorkommenden Gefüge zu gelangen.

Dieses Buch beschränkt sich auf die direkte Durchstrahlung der Werkstoffe. Diese Methode wird im ersten Kapitel in den Rahmen der anderen optischen Untersuchungsverfahren eingeordnet. Im Mittelpunkt steht die Abbildung mit Streuabsorption, d. h. Streuung der Elektronen in der Probe und Absorption dieser Elektronen in einer Objektiv-Aperturblende. Der hier am ausführlichsten behandelte Sonderfall ist der Beugungskontrast, d. h. Beugung in der kristallinen Probe und Absorption der gebeugten Strahlen in der Blende.

Den Abschluß des Bandes bildet je ein Abschnitt über Zusatzeinrichtungen zur Probenbehandlung im Mikroskop und über Mikroskopie bei sehr hoher Spannung.

»Werkstoffe — Aufbau, Eigenschaften, Untersuchung, Anwendung« Band 1. Herausgegeben von G. Petzow und H. Warlimont. 1971. XI, 151 Seiten mit 109 Abb. und 17 Tab. Broschiert DM 31,50. ISBN: 3-527-25386-6. LC Catalog Card No.: 71-150730.

Wir übersenden Ihnen gern unseren Sonderprospekt.

VERLAG CHEMIE · GMBH · WEINHEIM/BERGSTR.

410Ga

ANALYTICA CHIMICA ACTA

Vol. 58 (1972)

ANALYTICA CHIMICA ACTA

International monthly devoted to all branches of analytical chemistry
Revue mensuelle internationale consacrée à tous les domaines de la chimie analytique
Internationale Monatsschrift für alle Gebiete der analytischen Chemie

ELSEVIER PUBLISHING COMPANY
AMSTERDAM

Anal. Chim. Acta, Vol. 58 (1972)

PRINTED IN THE NETHERLANDS

Analytica Chimica Acta
Elsevier Publishing Company, Amsterdam
Printed in The Netherlands

AN INTEGRATOR FOR LOW ABSORBANCE SAMPLES IN ATOMIC ABSORPTION SPECTROSCOPY

H. NISHITA, R. FARMER* AND S. PETERSON

Laboratory of Nuclear Medicine and Radiation Biology, University of California, Los Angeles, Calif. 90024 (U.S.A.)

(Received 8th July 1971)

Since its establishment as a viable method by Walsh[1] in 1955, atomic absorption spectroscopy has become a very important technique for chemical analyses. More than 60 elements are determined routinely by this technique[2]. The sensitivity and the detection limits of these elements under specified analytical conditions have been reported in many books and reviews. The limiting sensitivity that is usually reported represents the concentration of a metal that will produce 1% absorption. The detection limit is defined generally as the concentration in water solution that gives a signal twice the size of background variability[2]. The background variability is the intrinsic instrumental fluctuation. Thus, by definition, an elemental detection limit is a form of signal-to-noise ratio. From an analytical point of view, the important quantity is the minimum concentration of metal that can be measured with useful precision. It is common knowledge that the precision and accuracy of sample absorption measurements become increasingly unsatisfactory as the detection limit is approached. This condition prevails for measurements made at less than 5% sample absorption unless stable scale-expansion methods can be employed[3].

A large percentage of the analytical work done in this laboratory entails analyses of low absorbance samples. Consequently, in order to improve the precision and accuracy of measurements, an integration readout system was incorporated into the spectrophotometer system. By integrating the output signal from the spectrophotometer for a given period of time, the net charge consisting of information signal and noise can be accumulated. In this process, if the noise is random and the information signal is unidirectional, the information signal-to-noise ratio is improved because the noise component, at least to some extent, cancels itself out and thus accumulates at a relatively slower rate. There are expensive, sophisticated systems that can do this efficiently, but for our purposes, the relatively inexpensive analog integration system was used. The system was that of Harrison and Berry[3] with several modifications. The analog integrator as presented by Harrison and Berry[3] was unstable with our spectrophotometer system when the input signal was small. This instability was traced to the time-delay relay that was specified by Harrison and Berry[3]. The relay caused baseline drift as its temperature increased after being energized. This is to be expected since the manufacturers' specification was 5% tolerance of the time delay. This paper presents the modified version that showed

---

* Present address: Los Angeles Trade-Technical College, Los Angeles, Calif. 90015, U.S.A.

greater stability in the range of low input signal. The use and performance of the modified version of the integrator is presented.

EXPERIMENTAL

Spectrophotometer

A Perkin-Elmer Model 303 atomic absorption spectrophotometer equipped with Model 403 burner mount (Part No. 303–0410) was used to produce the signal for integration. The spectrophotometer was equipped also with an automatic recorder readout accessory (Model 303–0103), which produced an output signal proportional to the absorption of the sample and prepared it for presentation to a 10-mV potentiometric recorder (Perkin-Elmer Model 165). The recorder readout accessory had provision for selecting absorption scale expansions of 1, 3, 10, 30 and 100 ×. Any portion of the scale could be expanded. Since scale expansions increase the noise, the recorder readout accessory was provided also with filter circuits, which provided any of 5 damping times between 0.5 sec and 2 min. The filter circuits sharply reduced the increased noise levels present at high scale expansions, but did not eliminate them. Thus, there was a practical limit of scale expansion, which varied with the element to be determined.

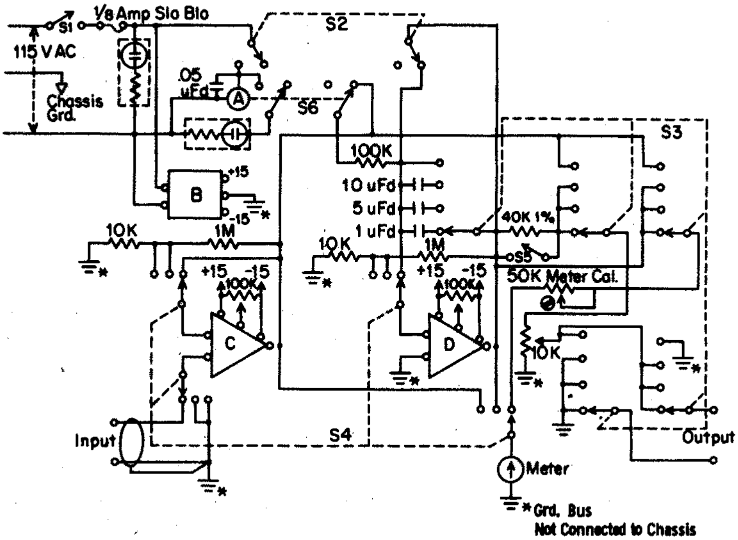

Fig. 1. Circuit diagram of the integrator. Major parts: A, timer motor; B, power supply-analog devices 904; C, amplifier-analog devices 183 K; D, amplifier-analog devices 230 J. Switches: S 1, power; S 2, integrate-standby; S 3, time constant-amplifier; S 4, balance-operate; S 5, integrator gain; S 6 time delay.

Integrator

The integrator that was constructed was inserted in-line in the above spectrophotometer system between the recorder readout accessory and the recorder. The circuit diagram is shown in Fig. 1.

A two-conductor shielded cable feeds the signal voltage from the recorder readout accessory to the input (buffer) amplifier (Analog Devices, Inc. Model 183 K). The feedback current to the selected integrating capacitor (1 μF, 5 μF or 10 μF) on the second amplifier (Analog Devices, Inc., Model 230J) produces an output voltage which is impressed across a voltage divider, the variable portion of which is a 10-turn miniature potentiometer (Helipot, 7240 Series). This controls the percentage of the output voltage applied to the recorder. Depending on the input signal magnitude, the output voltage range can be increased by a factor of 5 by shorting out the 40 K resistor with switch S5. Switch S3 provides a selection of 3 integrating capacitors listed above or the amplifier circuit which bypasses the integrating circuit. The integrating periods are initiated by throwing switch S2 to the integrating mode. This removes the shorting bypass from the integrating capacitor and applies a 115-V activating voltage to the time-delay synchronous motor, which controls switch S6. This unit is equivalent to a model-78 Eagle reset timer. This timer has a repeatability of ±1.5%, an adjustable time cycle of 0–60 sec and a reset time of 1 sec. The switch in this timer unit, which was originally a SPDT switch, was replaced with DPDT micro switch (Micro Switch No. DT-2R-A7). At the end of the timing cycle, a neon light goes on to indicate the end of the integration period and the readout trace on the recorder holds at the peak. Then, when switch S2 is thrown to the standby mode the integration capacitor is shorted and the readout trace on the recorder returns to zero (baseline). Also, the neon light goes out and the timer resets to the starting position.

Switch S4 has 3 positions. One position is used when the buffer amplifier is amplified. The second is used when the integration amplifier is balanced. These amplifiers are balanced with the use of the null meter while switch S3 is in the amplifier position. When necessary because of the input signal strength, the sensitivity of the null meter may be changed with the 50K potentiometer (Ohmite, 2 W), which is not a front panel control. The third position of switch S4 is the operating position, which is used after the amplifiers have been balanced. The amplifiers are powered by a ±15 V 4 mA power supply (Analog Devices, Inc., Model 904). Balance controls are 10-turn miniature potentiometers (Helipots). Hermetically sealed, low-leakage capacitors (Southern Electronics) were used for all integration time constants. The resistors used were low noise.

The preceding paragraph gives the components and the general operation of the integrator itself. In actual practice, the balancing of the integrator amplifiers was done by the use of both the integrator null meter and the recorder. The integrator null meter was used for coarse adjustment only. For fine adjustment, switch S2 was thrown to the integrating mode and the amplifier balance control was adjusted until the trace on the recorder chart showed no drift.

After the integrator amplifiers had been balanced, the chart baseline for sample analysis was set by adjusting the absorption range control of the recorder readout accessory until the trace on the recorder chart showed no drift. This was done with water (or other solvents) aspirating in the flaming burner and the integrator set for operation, *i.e*, switches S2 and S4 in the integrating and the operating modes, and switch S3 at the selected integrating capacitor. In order to obtain easier control, the original 1 K potentiometer on the recorder readout accessory was changed to a two-section, single-turn, 800-ohm potentiometer (Helipot, 5610 series) in the conjunction with a 200-ohm, 10-turn miniature potentiometer (Helipot, 7240 series). The former was used for coarse adjustment and the latter for the fine.

Procedure

Cesium was selected for testing the performance of the spectrophotometer with and without the use of the integrator. Cesium was selected firstly because it occurred in very low concentrations in the plant, soil and other materials that were of interest. Secondly, cesium required the use of vapor-discharge lamps, because a hollow-cathode lamp is not commercially available. The use of vapor-discharge lamps exposed the integrator to a more rigorous test than when a hollow-cathode lamp was used; in our experience with the lamps of other alkali metals (K, Na, Rb), discharge lamps always were noisier than the hollow-cathode lamps. Additionally, cesium has its sensitive resonance lines in the near-infrared spectral region where the monochromator efficiency and the detector sensitivity are at the lowest. This, of course, would give poorer signal-to-noise ratio. Aqueous solutions of cesium (as nitrate) at the 0.5 μg ml^{-1} level were used throughout. The spectral line used for the analyses was 852.1 nm. The spectrophotometer operational parameters were always kept the same in comparing the results with and without the use of the integrator. The three-slot Boling burner head with air–acetylene flame was used. The solution aspiration rate was 5.2 ml min^{-1}.

RESULTS AND DISCUSSION

Figure 2 shows the recorder traces of the absorption from a 0.5 μg Cs ml^{-1} solution with and without the use of the integrator. In Chart 1, 0.5 μg Cs ml^{-1} is seen to absorb about 1% when a scale expansion (S.E.) of 1 × and a noise suppression (N.S.) setting of 2 were used. The letter "A" represents the beginning of the sample aspiration period and "B" indicates the end. In Chart 2, the scale expansion was set at 3 × at the same noise suppression setting (N.S. 2). It is evident that the trace looks considerably noisier. By changing the noise suppression to a setting of 3, the noise was greatly reduced (Chart 3). This procedure of alternate change of the scale expansion and the noise suppression is continued through a scale expansion of 30 × and a noise suppression setting of 5. Scale expansion of 100 × was beyond the capacity of the chart paper. The traces obviously became noisier as the scale expansion was increased. Thus, it was necessary to increase the noise suppression also. By the use of sufficiently high noise-suppression setting, most of the noise was eliminated. The peak and the baseline on the traces became easier to establish, but a certain amount of uncertainty involved in establishing these was not eliminated. Furthermore, high noise suppression, particularly setting 5, was very rarely used in our work, because of limited samples. The minimum recommended sample aspiration times when noise-suppression settings of 4 and 5 are used, are 40 and 120 sec, respectively. These disadvantages are made minimal by the use of the integrator.

Chart 8 shows the trace for a scale expansion of 3 × and noise-suppression setting of 3 on the recorder readout accessory and the 1-μF capacitor with a gain setting (G.) of 0.5 × 1 on the integrator. The minimum recommended sample aspiration time for a noise-suppression setting of 3 is 15 sec. The letters "C" and "D" indicate the beginning and the end of the integration period, which was set at 45 sec for all this work. The operating parameters shown gave the most stable baseline with the 1-μF capacitor; therefore, the trace shown was the best that could be obtained with this capacitor. Charts 10 and 13 give the traces with 5-μF and 10-μF capacitors, respecti-

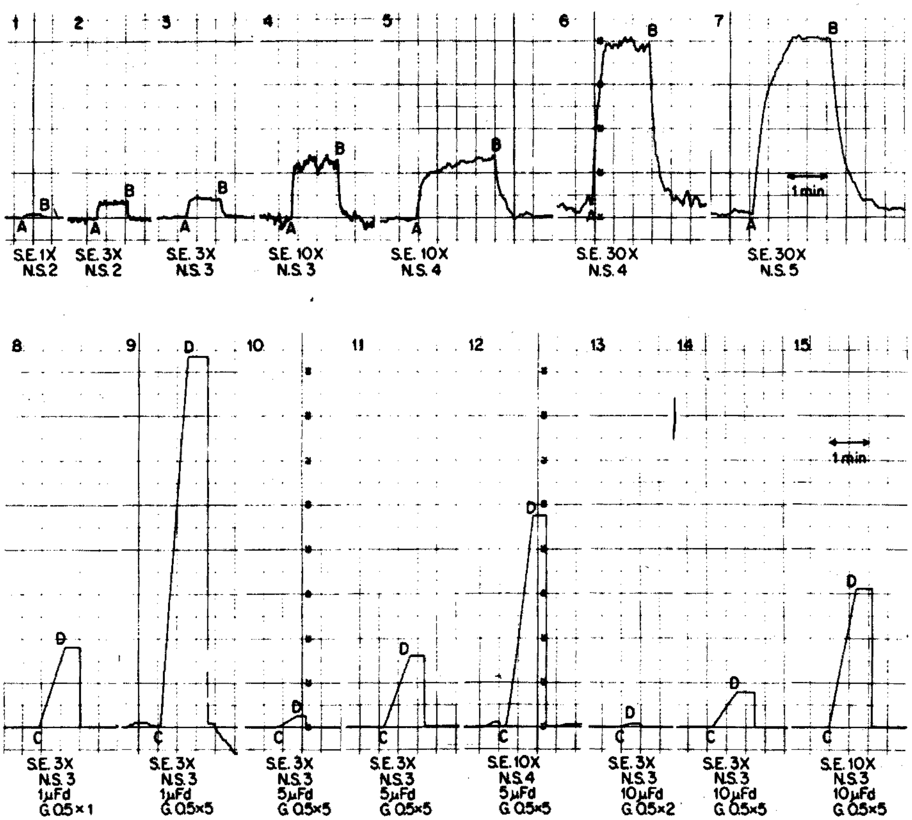

Fig. 2. Recorder traces of the absorption of cesium (0.5 μg ml^{-1}). (A) Without integrator; (B) with integrator.

vely, when all other parameters were kept the same. It is evident that the peak height decreased as the size of the capacitor was increased, making the absorption measurement less sensitive. These capacitors, however, could be used when the gain was increased. Charts 11 and 14 show the increase of peak heights caused by increasing the gain setting to 0.5 × 5. This gain could not be used with the 1-μF capacitor, since it caused severe baseline drift (Chart 9).

Another way to increase the sensitivity is by changing the scale expansion on the recorder readout accessory. Changing the scale expansion to 10× , while keeping the other parameters constant (compare Charts 14 and 15) gave good workable trace with the 10-μF capacitor. In fact, this combination of operational parameters (Chart 15) showed higher peak than the best that could be obtained with the 1-μF capacitor (Chart 8). The scale expansion of 10 × with the gain of 0.5 × 5 could not be used with the 5-μF capacitor because of the baseline drift (Chart 12). It was necessary to reduce the gain to obtain a good baseline with the 5-μF capacitor. From these results, it is evident that several workable operational parameter combinations can be used. With the 1-μF capacitor, the minimum input voltage to the integrator to obtain stable baselines was 0.5 mV. In general, because of its high sensitivity, the 1-μF capacitor was found to be difficult to use. Most of our sample analyses have been done with the use of the 5-μF capacitor. In any case, the use of the integrator has improved the instrument sensitivity and the operator readability of the recorder traces of low absorbance samples.

These studies were supported by Contract AT (04-1) GEN-12 between the Atomic Energy Commission and the University of California. The authors are indebted to T. Hartsock and R. M. Haug for technical assistance.

SUMMARY

An analog integrator for samples giving low absorbance in atomic absorption spectroscopy is described. Its performance is demonstrated by the use of aqueous solutions of cesium (0.5 μg ml^{-1}).

RÉSUMÉ

On décrit un intégrateur pour spectroscopie par absorption atomique spécialement conçu pour des échantillons donnant une faible absorption. On a choisi comme exemple de démonstration des solutions aqueuses de césium (0.5 μg ml^{-1}).

ZUSAMMENFASSUNG

Es wird ein Analogintegrator für Proben beschrieben, die bei der Atomabsorptionsspektroskopie niedrige Extinktionen ergeben. Seine Leistung wird am Beispiel wässriger Cäsiumlösungen (0.5 μg ml^{-1}) gezeigt.

REFERENCES

1 A. Walsh, *Spectrochim. Acta*, 7 (1955) 108.
2 H. L. Kahn, *J. Chem. Educ.*, 43 (1966) A7.
3 W. W. Harrison and F. E. Berry, *Anal. Chim. Acta*, 47 (1969) 415.

Analytica Chimica Acta
Elsevier Publishing Company, Amsterdam
Printed in The Netherlands

EVALUATION OF ATOMIC ABSORPTION WITH A HEATED GRAPHITE ATOMIZER FOR THE DIRECT DETERMINATION OF TRACE TRANSITION METALS IN SEA WATER*

D. A. SEGAR AND J. G. GONZALEZ
University of Miami, Rosenstiel School of Marine and Atmospheric Science, Miami, Fla. 33149 (U.S.A.)

(Received 2nd August 1971)

Atomic absorption spectrophotometry has been extensively employed in the analysis of trace transition elements in sea water. With the normal technique, when the sample is nebulized into a flame to produce the atomic vapor, the sensitivities attainable are such that direct analysis without preconcentration is precluded, particularly when the strong light scattering effects in the flame and the clogging of nebulizers by the high salt content of sea water is considered. Fabricand *et al.*[1] have reported the direct analysis of sea water for Cu, Fe, Mn, Ni and Zn by this technique but their results do not appear to have been reproduced by other workers.

The development of atomizers such as the graphite tube furnace[2-4] and the carbon rod atomizer[5] has led to an increase in the sensitivity of the atomic absorption technique by about 2 to 3 orders of magnitude. In addition, it has been suggested that the use of atomization techniques such as these can allow the determination of trace elements without interference in the presence of considerable concentrations of elements with volatilities differing from the element being determined[2]. The trace transitional elements in sea water are in just such a matrix. Accordingly, the heated graphite atomizer has been evaluated for its applicability in the direct determination of several elements in sea water.

The only previous application of a selective volatilization technique to the analysis of trace transition elements in sea water appears to be the use of a sampling boat system for zinc determination[6].

EXPERIMENTAL

A Perkin-Elmer Model 403 atomic absorption spectrophotometer equipped with a Sargent-Welch Model SRG recorder, a deuterium arc background corrector and a Perkin-Elmer HGA-70 heated graphite atomizer was employed.

A simple modification was made to the spectrophotometer to allow the use of the deuterium arc signal in the emission mode. A phasing switch was installed in the circuit controlling the light chopper which modulates the deuterium arc and hollow-cathode lamp beams before passage through the flame. In this way, the broad band spectrum of the deuterium arc was used to study light scattering absorption or molecular absorption within the graphite atomizer. This phasing switch is currently

---

* Contribution Number 1428 from the Rosenstiel School of Marine and Atmospheric Science.

installed on all new Perkin Elmer Model 403 instruments.

The heated graphite atomizer electronics were also modified to enable selective volatilization analysis to be carried out[7].

All temperature settings used in the tube furnace are reported in terms of the applied voltage measured directly across the atomizer terminals, and the corresponding temperature determined from the instrument manual is indicated in parentheses. This procedure is adopted because the relationship between the applied voltage and the actual temperature achieved in the graphite tube may be variable from tube to tube, and during the lifetime of any particular tube. No attempt has been made to measure such variations but it may be assumed that they are relatively small except when the graphite tube ages badly. Thus, with the same voltage settings, reproducible selective volatilization of various salts was achieved even after changing graphite tubes. The graphite tubes were used for a maximum of 100 injections and were not found to age significantly during such use, with a flow rate of the argon purge gas of 1.5 l min^{-1}.

All sample injections were made with Eppendorf microlitre pipettes with disposable plastic tips.

RESULTS AND DISCUSSION

Preliminary investigation of sea water injections

The elements Fe, Mn, Cd, Zn, Pb, Co, Ni, Cu, Ag, Cr and V are present in sea water at concentrations which suggest that direct analysis by atomic absorption with a heated graphite atomizer may be possible (Table I). Thus, the potential of direct injection analysis of sea water for these metals was evaluated.

TABLE I

FEASIBILITY OF GRAPHITE TUBE FURNACE FOR ANALYSIS OF SEA WATER

Element	*Concentration in sea water* ($\mu g\ l^{-1}$)[a]	*Sensitivity of graphite tube furnace techniques* (*pg*)[b]
Fe	10–100	25
Mn	0.5–3.0	11
Cd	0.03–0.17	1.3
Zn	0.3–10.0	1.8
Pb	0.03–9	38
Co	0.04–20.0	73
Ni	0.07–7.0	140
Cu	1–2.0	60
Cr	0.04–2.5	26
Ag	0.15–2.9	10
V	0.2–7.0	320

[a] Values taken from Riley[8].

[b] Values from Fernandez and Manning[9] except V from Manning and Fernandez[3] and Ag determined in the present study.

Preliminary injections of 20 μl of sea water indicated that atomization at voltages higher than 3.5 V (*ca.* 1100°) led to the production of a visible "smoke" within the graphite tube. The attenuation of the light beams of the deuterium arc and hollow-cathode lamp passing through the tube was almost total and thus the range of compensation of the deuterium arc background corrector was far exceeded.

Injections of the component salts of sea water at their sea water concentrations ($35^{\circ}/_{\circ\circ}$ salinity) were made to investigate the production of this smoke. The production of smoke was monitored by measuring the drop in intensity of the beam from the deuterium arc after passage through the atomizer. The atomic absorption instrument was operated in the emission mode at a variety of wavelengths within the range used for atomic absorption. Attenuation of the light beam passing through the atomizer was detectable for each of the following solutions containing salts at their sea water concentrations: (*i*) $NaCl$; (*ii*) Na_2SO_4; (*iii*) $MgCl_2$, $CaCl_2$ plus $SrCl_2$; (*iv*) KCl, $NaHCO_3$ plus KBr; (*v*) H_3BO_3 plus NaF. However, for all except the sodium chloride and sodium sulphate solutions, the attenuation was small and well within the compensation capabilities of the deuterium arc background corrector used in the atomic absorption mode.

Analysis of sea water samples by direct atomization was not possible because of the production of this smoke during the volatilization of the major component salts, particularly sodium chloride and sulfate. Therefore, it was necessary to devise a selective volatilization method to allow the elements under study to be volatilized separately from the bulk of the salts. In selective volatilization analysis for volatile elements the voltage applied to the atomizer during the atomization step can be set below that required to atomize the interfering substances. For involatile elements, the interfering substances must be removed initially and then the element itself atomized with a higher applied voltage.

The voltage range over which atomization of a 20-μl sea water sample produced a scattering absorption sufficient to override the deuterium background corrector was determined. Significant smoke was not formed at atomization voltages less than 3.5 V (*ca.* 1100°) and it was necessary to heat the atomizer for a minimum of 25 sec at 3.8 V (*ca.* 1250°) to ensure that most of the salt was removed. Residual amounts of the major sea water salts, particularly the calcium and magnesium salts, remained in the atomizer after this treatment. However, the quantities of these residual salts were small enough to give a scattering signal well within the compensation range of the deuterium arc background corrector during subsequent atomization at higher voltages.

If injections of 50 μl or more of sea water were made, it was necessary to heat the atomizer at 5.2 V (*ca.* 1650°) for more than 45 sec to remove a sufficient quantity of the bulk salts to allow atomization at a higher temperature without scattering interference. Thus, the practical limit of sample volume for water of salinity $35^{\circ}/_{\circ\circ}$ is about 20 μl, when selective volatilization for all but the most involatile elements is attempted.

Volatile elements

Cadmium was the most volatile of the metals investigated. Accordingly, the possibility of volatilizing the cadmium from the furnace at a temperature low enough to avoid interference from the major salts of sea water was evaluated. The optimal voltage for atomization of cadmium salts from distilled water solution injections was found to be 3.0 V (*ca.* 875°). This is below the voltage required to atomize the major salts. However, under identical conditions, cadmium was not detected in a sea water sample spiked with an identical concentration of cadmium(II). Apparently, the very great excess (more than $3 \cdot 10^7$ times) of total dissolved salts retarded the atomization of cadmium. Increasing the voltage of atomization of the spiked sea water sample did not atomize the cadmium until the sodium salts were atomized and thus the absorption signal from the cadmium in sea water was masked by the scattering signal caused by these sodium salts.

Zinc, lead and silver behaved similarly to cadmium. From sea water, they were atomized only when the major salts were volatilized. Thus, the absorption signals for each of these metals were lost in the background attenuation caused by the sodium salts. The behavior of zinc is particularly interesting. Burrell and Wood[6] have reported that selective volatilization of zinc can be achieved with the tantalum boat technique. Zinc could not be volatilized before the major salts from the heated graphite atomizer in the present study even though the continuously variable applied voltage allowed the possibility of such separation to be investigated under optimal conditions. It seems likely that the differences in behavior of the tantalum boat and the heated graphite atomizer are related to their different configurations and perhaps surface properties.

Involatile elements

The elements Co, V, Cu, Fe, Mn, Ni and Cr have volatilities less than those of the bulk of sea water salts. Preliminary removal of the salts at as low a temperature as possible followed by atomization of the element in question was attempted. For all of these elements, it was possible to remove the bulk of the salts without completely removing the element itself and then to obtain an absorption signal for the element by atomization at a higher temperature. However, with the exception of iron, and possibly manganese and copper, it does not seem likely that this technique can be successfully applied to the analysis of sea waters unless they are heavily polluted with the metal concerned.

It was not possible to analyse for chromium in sea water, owing to the low intensity of the deuterium arc source at the analytical wavelengths available. Thus, to balance the deuterium arc beam and the chromium lamp beam, it was necessary to decrease the hollow-cathode lamp current, and consequently emission, to a point at which the noise level in the signal received by the photomultiplier was unacceptable. It was not possible to analyse for chromium without the background corrector, because of a residual amount of salt which was atomized with the chromium producing an absorption signal by scattering.

Copper is not volatilized from the graphite atomizer at an applied voltage below 4.0 V (*ca.* 1300°) when the injection is made in distilled water. Injections of natural sea water (Florida Current) spiked with 100 μg Cu l^{-1} were made. The water was evaporated off by heating for 40 sec at 1.0 V (*ca.* 230°) and the salt bulk was selectively removed by heating for 24 sec at 3.8 V (*ca.* 1250°). The copper was then atomized by heating for 40 sec at 6.5 V (*ca.* 1900°). It was found that the response for 100 μg Cu l^{-1} in sea water was less than 10% of the response obtained for the same concentration in distilled water under identical atomization conditions. To investigate the effect of total salt content on selective volatilization of copper, diluted sea water samples were each spiked with 100 μg Cu l^{-1} and atomized by the procedure used above. The total salt content critically affects the recovery of copper in selective volatilization analysis (Fig. 1). With total salt contents of as little as 0.1 g l^{-1} (salinity 0.1°/₀₀), the response is only 87% of that obtained in distilled water. The response in

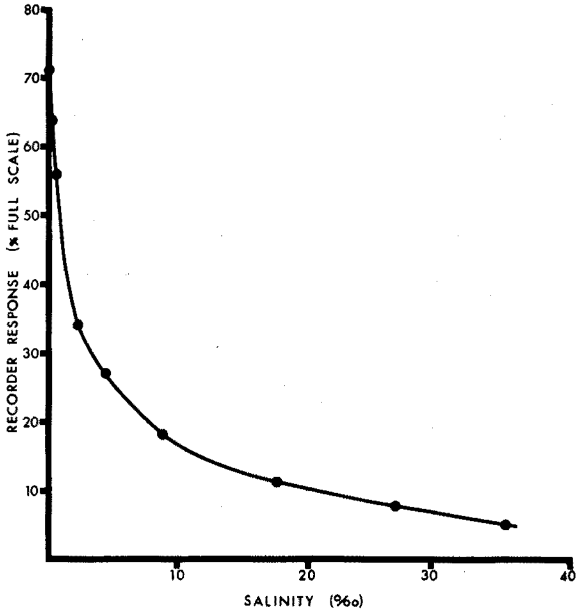

Fig. 1. Effect of salinity on copper response with selective volatilization.

this case is measured by determining the peak height. Some broadening of the copper absorption peak is noticeable with increasing salt content but peak area measurement showed this to be insufficient to account for more than a small fraction of the loss in sensitivity. Thus, it appears probable that some covolatilization of copper occurs with the sodium salts. Analysis of copper in varying concentrations of single salt solutions show that this covolatilization is not simply related to total salt concentration. Thus, magnesium salts attenuate the copper response more than sodium salts at the same concentrations whilst sulphates apparently attenuate the copper response less than chlorides. These effects have not yet been thoroughly investigated and further results will be reported at a later date.

Despite the loss of sensitivity caused by covolatilization of copper with the sodium salts, a linear calibration curve passing through the origin was obtained with the above technique for a series of natural sea water samples spiked with varying amounts of copper (30–500 μg l^{-1}). The practical detection limit is about 30 μg l^{-1}, somewhat above the reported range of concentrations in natural unpolluted sea waters (Table I) but sufficiently low to permit detection in heavily polluted coastal waters. Because the response is dependent upon the salt content, the method of standard additions must be employed in the direct analysis of natural waters for copper by this technique. No naturally occurring samples with copper concentrations sufficiently high for direct analysis were available during the present study.

Analysis for manganese, cobalt and nickel by the same selective volatilization technique used for copper was attempted. The final atomization voltage was in each instance adjusted to the optimum determined for these metals in distilled water *i.e.*, Mn 8.0 V (*ca.* 2250°), Ni 7.4 V (*ca.* 2150°) and Co 6.5 V (*ca.* 1900°). A reduction in sensitivity owing to the presence of bulk salts in the sea water was observed for each of these elements. The reduction in sensitivity was analogous to that observed for copper but of smaller magnitude. For manganese, the sensitivity was reduced to about 35‰, for nickel to about 25‰, and for cobalt the reduction was to about 15‰ of the corresponding distilled water values. The detection limits for direct injection analysis of sea water for cobalt and nickel were found to be about 50 μg l^{-1} whilst that for manganese was about 5 μg l^{-1}. Thus, determination of manganese, cobalt and nickel concentrations in natural saline waters appears to be precluded except in some coastal areas and possibly in areas where pollution occurs (Table I).

Selective volatilization analysis of sea water for vanadium and iron concentrations was attempted under the same conditions employed for the copper determinations except that the atomization voltages were adjusted to 7.3 V and 6.5 V, respectively. The presence of salts in solution did not affect the sensitivity for either element and the responses obtained in sea water and distilled water were identical for solutions having equal concentrations of vanadium or iron. Thus, no covolatilization of either vanadium or iron occurs during the selective removal of the sodium salts.

The sensitivity for vanadium was such that a practical detection limit of about 50 μg l^{-1} was obtained with 20-μl injections. This figure is somewhat worse than that claimed by Manning and Fernandez[3]. Thus, it is not possible to determine vanadium directly in sea water, as the maximum reported concentrations in sea water are of the order of 7 μg l^{-1}.

The detection limit obtained for iron was 3 μg l^{-1}, which is sufficiently low to permit determination in natural sea waters. The reproducibility of results in natural sea water was poor but was improved by acidification (pH 1) and thorough mixing. This is perhaps an indication of the colloidal dispersed nature of the major proportion of the iron in the "dissolved" state in sea water. The calibration curve

TABLE II

SEA WATER ANALYSIS FOR IRON BY DIRECT INJECTION AND BY EXTRACTION

Sample	*Direct injection* ($\mu g\ l^{-1}$)[a]	*Extraction* ($\mu g\ l^{-1}$) ($\pm$0.3–0.5)[b]
1	3±3	2.2
2	3±3	5.9
3	10±3	10.7
4	11±4	1.5
5	16±4	6.2
6	11±4	4.5
7	5±3	1.6
8	7±3	6.1
9	3±3	6.8
10	10±3	9.1
11	17±4	17.4
12	17±4	9.4
13	6±3	5.4
14	3±3	5.8
15	9±3	10.3
16	13±3	13.5

[a] Average of five injections.

[b] Method of Brewer *et al.*[10], single determination only.

obtained for natural sea water spiked with various concentrations of iron was found to be linear up to at least 100 μg l^{-1}, the recorder response for this concentration being *ca.* 60% of full scale. The reproducibility of the analysis was assessed by making a series of injections of Florida Current sea water (*ca.* 3 μg Fe l^{-1}) spiked with 50 μg Fe l^{-1}. The standard deviation of ten injections was ±6.3% of the average. This is somewhat worse than the reproducibility attained by Fernandez and Manning[9] for direct atomization analysis of iron in fresh water.

The accuracy of the method was assessed by analysis of a series of filtered (0.45-μm membrane) samples of water from a series of stations in South Biscayne Bay, Florida (salinity range 38.9–39.2 $^0/_{00}$). These same samples were also analysed by the method of Brewer *et al.*[10]. The results are presented in Table II. It can be seen that the agreement between the two methods is good for most of the samples. However, for samples 4, 5 and 6, the results by direct injection are considerably higher than those obtained by the extraction technique. These three samples were from adjacent stations and the results may reflect the presence in this area of a large fraction of the dissolved iron in a physical state that renders it non-extractable by the method of Brewer *et al.*[10].

DISCUSSION

It has been shown that direct analysis of sea water for iron in sea water and for Ni, Co, V and Mn in polluted saline water samples can be achieved by means of a selective volatilization technique. The precision is relatively poor and thus direct injection analysis is not ideal for most oceanographic purposes. However, as the analysis is many times faster than any other known method for saline waters, it represents an ideal technique for monitoring large numbers of samples for polluting elements.

A more satisfactory analytical technique for general oceanographic use involves the separation of the trace transition elements from the major sea water salts before analysis with the graphite tube furnace[11].

This research was carried out with the support of AEC contract AT401-3801 Sub 2 and the National Science Foundation Grant GU103302 Sub 32.

SUMMARY

The heated graphite atomizer has been evaluated for its potential utilization in the direct injection analysis of sea water for trace transition metals. Direct atomization was found to be impossible owing to the scattering interference of the major salts. Selective volatilization techniques were unsuccessful in separating Zn, Cd, Pb and Ag from the major salts. Selective volatilization was successful in analyses for Cu, Fe, Mn, Co, Ni and V, the major salts being removed at a lower temperature than required for subsequent atomization of the element concerned. Covolatilization losses of copper, manganese, cobalt and nickel with the major salts reduce the sensitivity attainable, so that only iron may be determined in unpolluted sea water by this method.

RÉSUMÉ

On examine les possibilités d'utilisation de l'atomiseur de graphite chauffé pour l'analyse par injection directe de l'eau de mer, en vue de doser les métaux de transition à l'état de traces. Une atomisation directe est impossible, en raison des interférences causées par la plupart des sels. Des techniques par volatilisation sélective donnent des résultats satisfaisants avec Cu, Fe, Mn, Co, Ni et V et non avec Zn, Cd, Pb et Ag. Des pertes par covolatilisation de cuivre, de manganèse, de cobalt et de nickel diminuent la sensibilité. Seul le fer peut être dosé par cette méthode dans l'eau de mer non polluée.

ZUSAMMENFASSUNG

Die Methode der Atomdampferzeugung mit erhitztem Graphit wurde für die direkte Bestimmung von Übergangsmetallspuren in Meerwasser geprüft. Die direkte Atomisierung stellte sich wegen der Streustörungen durch die Salzmatrix als undurchführbar heraus. Methoden der selektiven Verdampfung waren ohne Erfolg bei der Abtrennung von Zn, Cd, Pb und Ag von den Salz-Hauptbestandteilen. Die selektive Verdampfung war erfolgreich bei der Bestimmung von Cu, Fe, Mn, Co, Ni und V; die Salz-Hauptbestandteile wurden bei einer niedrigeren Temperatur entfernt, als für die nachfolgende Atomisierung des betreffenden Elementes erforderlich war. Die Verluste von Kupfer, Mangan, Cobalt und Nickel bei der gemeinsamen Verdampfung mit den Hauptsalzen vermindern die erreichbare Empfindlichkeit, so dass nur Eisen in nicht verunreinigtem Meerwasser nach dieser Methode bestimmt werden kann.

REFERENCES

1 B. P. Fabricand, R. R. Sawyer, S. G. Ungar and S. Adler, *Geochim. Cosmochim. Acta*, 26 (1962) 1023.
2 B. V. L'Vov, *Spectrochim. Acta*, 24B (1969) 53.
3 D. C. Manning and F. Fernandez, *Atomic Absorption Newsletter*, 9 (1970) 65.
4 H. Massman, *Spectrochim. Acta*, 23B (1968) 215.
5 J. P. Matousek, *American Laboratory*, June (1971) 45.
6 D. C. Burrell and G. G. Wood, *Anal. Chim. Acta*, 48 (1969) 45.
7 D. A. Segar and J. G. Gonzalez, *Atomic Absorption Newsletter*, 10 (1971) 94.
8 J. P. Riley, in J. P. Riley and G. Skirrow, *Chemical Oceanography, Vol. 2*, Academic Press, London, 1965, pp. 343–360.
9 F. Fernandez and D. C. Manning, *Atomic Absorption Newsletter*, 10 (1971) 65.
10 P. G. Brewer, D. W. Spencer and C. L. Smith, *Atomic Absorption Spectroscopy*, ASTM STP 443, American Society for Testing and Materials, 1969, p. 70.
11 D. A. Segar, *Proc. 3rd Int. Atomic Absorption and Fluorescence Spectrometry Congr., Paris, Oct., 1971*, in press.

Analytica Chimica Acta
Elsevier Publishing Company, Amsterdam
Printed in The Netherlands

ANALYSIS OF METALS FOR TRACE IMPURITIES BY SEALED CELL ATOMIC ABSORPTION

J. P. PEMSLER AND E. J. RAPPERPORT

Ledgemont Laboratory, Kennecott Copper Corporation, Lexington, Mass. 02173 (U.S.A.)

(Received 18th June 1971)

In several recent papers, the application of atomic absorption spectroscopy to the measurement of thermodynamic quantities in metal solutions has been examined[1-4]. During these investigations, it became apparent that the technique developed could be applied to the detection of extremely dilute impurities in well characterized metals and alloys. This paper discusses the technique in general and describes its application to the determination of trace quantities of zinc in copper.

THEORY

The concentration of an element i in an alloy may be determined through a measurement of its thermodynamic activity a_i in the alloy. The activity is related to the atom fraction x_i in the alloy by the equation

$$a_i = x_i \gamma_i \tag{1}$$

where γ_i is the activity coefficient of the element in the alloy. In the general case, γ_i depends on both composition and temperature. In sufficiently dilute solutions, however, γ_i is a constant independent of composition (Henry's law). The temperature dependence of γ_i, either at constant composition or in the Henry's law region, is expressed by the Clapeyron equation

$$\ln \gamma_2/\gamma_1 = \frac{\overline{\Delta H}_i}{R}\left(\frac{T_2 - T_1}{T_2 T_1}\right) \tag{2}$$

where γ_2 and γ_1 are the activity coefficients at temperatures T_2 and T_1, respectively, R is the gas constant, and $\overline{\Delta H}_i$ is the partial heat of solution of the solute in the solvent.

The activity may be determined experimentally by measuring the partial pressure of the element in equilibrium with the alloy at a given temperature. The quantities are related by the equation

$$a_i = p_i^{\text{alloy}}/p_i^0 \tag{3}$$

or

$$\ln a_i = \ln p_i^{\text{alloy}} - \ln p_i^0 \tag{4}$$

where p_i^0 is the equilibrium vapor pressure of pure element i, and p_i^{alloy} is the vapor pressure of element i in equilibrium with its alloy at a given temperature.

The Beer–Lambert law may be applied to measuring the partial pressure of gaseous atoms in equilibrium with a pure metal or an alloy contained in a sealed cell.

The equation may be written as

$$I = I_0 \exp(-K_\lambda l n_i) \tag{5}$$

or

$$\ln(I_0/I) = K_\lambda l n_i \tag{6}$$

where I_0 is the incident intensity, I the attenuated intensity, K_λ the absorption coefficient of atomic species i at its resonant wavelength, λ, l the cell length, and n_i is the number of atoms of absorbing element i.

At the moderately low pressures here considered, the number of absorbing atoms n_i in a static, isothermal cell is related to the vapor pressure p_i of the absorbing element and the absolute temperature T by

$$n_i = A(p_i V/RT) = K_1 p_i l/T \tag{7}$$

where A is Avogadro's number, V the cell volume, R the gas constant, K_1 is a constant, and l is the cell length.

Combining eqns. (6) and (7) and rearranging, one obtains a relationship linking the measured intensities and absolute cell temperature to the desired vapor pressure:

$$p_i = \frac{\ln(I_0/I)T}{K_1 K_\lambda l} \tag{8}$$

or

$$p_i = \frac{\ln(I_0/I)T}{Kl} \tag{9}$$

where K is a constant, calculable in terms of K_λ and other determinable constants.

In order to obtain absolute values of the vapor pressure, it is necessary to evaluate the absorption coefficient independently. While such constants can be estimated in some instances[5], it is not generally feasible to calculate accurate values of K_λ. However, absorption measurements on pure elements, together with the knowledge of their absolute vapor pressures from other sources, enable calculations of values of the constant K in eqn. (9). Determination of K then allows computation of p_i from relative intensity measurements and absolute temperature measurements.

EXPERIMENTAL

Materials and specimen preparation

The alloys used in this study may be divided into two groups. The more concentrated group comprising the 2.749, 2.002 and 1.004 at.-% zinc alloys, were made in this laboratory by electron beam-melting high-purity ASARCO copper and 99.999% COMINCO zinc in a vacuum better than 10^{-8} torr. The alloys so made were cold worked by swagging to 75% reduction in area and then given homogenization anneals of 114 h at 1000° in evacuated silica tubes. The second group of alloys had zinc concentrations of 2280, 360, 171, and 42 p.p.m., respectively, and were obtained (Johnson-Matthey Company, England) as high-purity homogeneous rods. These rods also were homogenized for 114 h at 1000°.

After the homogenization anneals, all the bars were sectioned and examined in detail by electron beam micro-analysis for macro and micro segregation. No segregation was found within the counting statistics of the samplings.

Each rod was milled under alcohol to provide about 5 g of coarse chips for the absorption cells. The chips were loaded into 25-mm diameter silica absorption cells 10–20 cm long which had been thoroughly cleaned. Initial evacuation of the cells was followed with a backfill of one-half atmosphere of a 2% hydrogen–98% argon gas mixture and an anneal of 1 h at 325°. This evacuation backfill anneal procedure was repeated twice more and then the cell was evacuated to 10^{-6} torr and sealed.

A series of chemical analyses on the bars and on the chips was made by means of conventional atomic absorption analysis as well as differential polarography. The results of these analyses are shown in Table I.

TABLE I

CHEMICAL ANALYSIS OF COPPER–ZINC BAR STOCK AND PORTIONS OF MILLED MATERIAL IN ABSORPTION CELLS
(Concentrations are given in at.-% zinc)

Analyses of bars adjacent to sample millings		*Analyses of sample millings*		*Analyses used in computations in this work*
Atomic absorption	*Differential polarography*	*Atomic absorption*	*Differential polarography*	
2.749				2.75
2.002				2.00
1.004				1.00
0.2340	0.2216		0.2216	0.2280
0.0479	0.0435	0.0441	0.0437	0.0450
0.0181	0.0169	0.0153	0.0164	0.0170
0.0042	0.0051	0.0043	0.0049	0.0042

Instrumentation

The atomic absorption apparatus is described in detail elsewhere[6], and only a summary is presented here. A schematic diagram is shown in Fig. 1, and a block diagram of the electronic components is shown in Fig. 2. The hollow-cathode source operated from a constant current power supply is separated from the two monochromators by a distance of about 4 feet. Radiation from the hollow cathode is chopped by a mechanical chopper and collimated by a system of diaphragms and collimating lenses to form a narrow beam of light about 3/8 in. in diameter which is further focused onto the entrance slit of the monochromator by a single lens 3.5 in. from the monochromator. A neutral density filter is used as a beam splitter to deflect a portion of the light to a second monochromator set at a nearly nonabsorbing wavelength. This serves to monitor intensity changes in the source and any loss in transmissivity of the cell windows due to condensation of metal vapor. A furnace, contained in the space between the hollow-cathode lamp and the monochromator, is fitted with four 1.25-in. diameter silica tubes which run axially along the entire length of the furnace and extend out about 6 in. on each end. The tubes are arranged on a circle of 1.5-in. radius within the 4-in. muffle of the furnace, and are held in place by an Inconel jig within the furnace and by end plates attached to the end of the muffle. The ends of each tube are sealed with stainless steel fittings containing O-ring seals to the tube and to a high u.v. transmission quartz window. One end of each tube contains

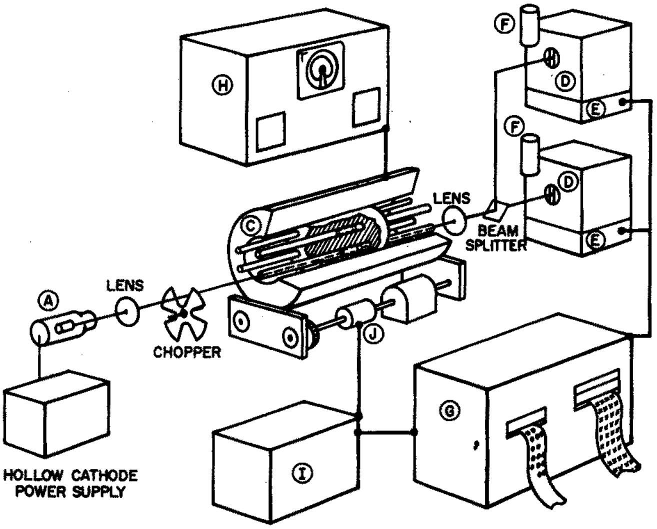

Fig. 1. Schematic diagram of atomic absorption apparatus. (A) Hollow-cathode source; (B) evacuated absorption cells; (C) furnace; (D) spectrometers; (E) lock-in amplifiers; (F) photomultipliers; (G) data processing system, (H) oven and temperature control; (I) timing and command system; (J) oven rotating system.

an evacuation port connected to a manifold so that the tubes may be evacuated. Each tube contains a 0.75-in. diameter 8-in. long sealed silica sample cell.

The furnace is wound in three separate zones with Kanthal A heating element. The center zone temperature is sensed by a thermocouple near the furnace windings and controlled by a current proportioning controller connected to a magnetic amplifier. The temperature-control point is determined by a programmed curve follower so that the temperature of the furnace may be set to rise and fall along a fixed schedule for a 24-h period. The two outer zone temperatures are sensed by thermo-

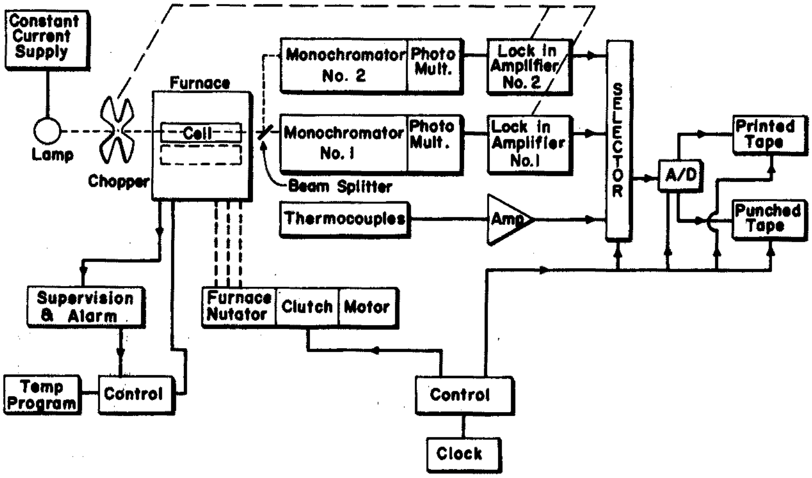

Fig. 2. Block diagram illustrating the subsystem relationships.

couples connected to detect temperature differences between the end zones and center zone, and connected to d.c. null detectors. The output of the null detectors is used in conjunction with current proportioning controllers and magnetic amplifiers to control current to the windings.

A motor and magnetic clutch rotate the position of the furnace on command so that, in sequence, each of the four separate optical channels intercepts the hollow-cathode beam. The photomultiplier output is fed to a lock-in amplifier, whose output is converted to a four-digit number which is printed on a paper tape as well as on punch tape suitable for computer input. After each set of 8 intensity readings (one for each of the four channels at each of the two wavelengths), the three thermocouple outputs representing the temperatures at the center and extrema of the cells are recorded.

Method

An experiment consists of loading three sample-containing cells and a blank into the four channels of the furnace and then evacuating the tubes. The proper hollow-cathode lamp is selected as the source, and the monochromators are set at appropriate resonant and reference wavelengths. The temperature range and the rate of rise of the furnace are set and the furnace power turned on. The remainder of the experiment is fully automated and the intensities in each of the four channels are recorded as functions of temperature. The punched data tape is then read and processed by computer.

RESULTS AND DISCUSSION

Absorption cells containing pure zinc have been repeatedly run in previous work[3,4] in order to obtain reliable values for the constant K of eqn. (9). The values obtained for the two zinc lines used in this work are

$$\ln K_{307.6\,\mathrm{nm}} = 16.05 \pm 0.02 \text{ deg atm}^{-1}\,\mathrm{cm}^{-1} \tag{10}$$

and

$$\ln K_{213.9\,\mathrm{nm}} = 25.01 \pm 0.02 \text{ deg atm}^{-1}\,\mathrm{cm}^{-1} \tag{11}$$

The experimental data collected consisted of the incident and attenuated intensities, along with the corresponding thermocouple voltages. These were computer-processed to yield tabular values of $[\ln \ln(I_0/I) + \ln T]$, the equivalent to $\ln (Kp_i l)$ from eqn. (9). Knowledge of the internal cell lengths and the absorption coefficient thus allowed computation of the absolute zinc partial pressures over any of the alloys. The data for the six alloys listed in Table I were used to determine the zinc activity in dilute copper alloys. An analysis of the data[4] indicated that Henry's law is obeyed over the concentration range studied, 42 p.p.m. to 2.75 at.-% zinc. The activity coefficient of zinc is therefore constant with composition at concentrations at or below 2.75 at.-%. The relation between activity coefficient and temperature may be expressed as

$$\ln \gamma_{\mathrm{Zn}} = -0.7360 - \frac{2977}{T} \pm 0.04 \tag{12}$$

A knowledge of the activity coefficient of zinc in dilute alloys allows the

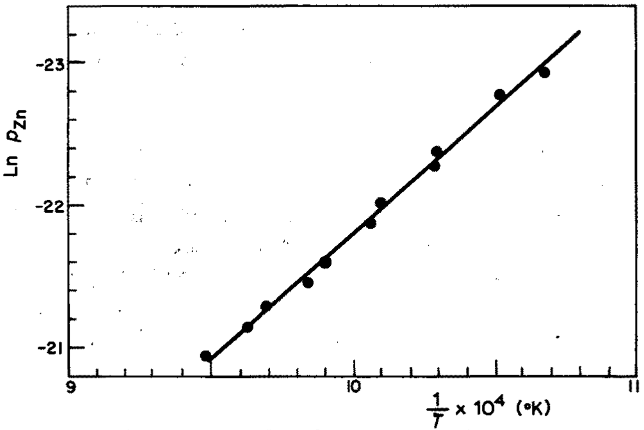

Fig. 3. Plot of ln p_{Zn} *vs.* $1/T$ for ASARCO 99.9999% Cu.

determination of extremely low concentrations of zinc in copper. ASARCO copper with a stated purity level of 99.9999% was examined by this technique. The data taken at 213.0 nm are shown in Fig. 3, which is a plot of ln p_{Zn} *vs.* $1/T$. The line shown was obtained from a least-squares regression analysis of 78 points and only a representative number of points are shown. The equation for the line is given by

$$\ln p_{Zn} = -4.115 - 17{,}688/T \pm 0.039 \qquad (13)$$

When the values for p_{Zn}, γ_{Zn}, and p^0_{Zn} at 1000°K are used, a value of the atomic concentration of zinc in this sample of ASARCO copper of 80 p.p.b. is obtained. This value is not a lower limit of detectability, for by raising the temperature further, lower values could be determined if purer material were available.

The limitations of the technique depend on the system in question. The basic factor necessary for an analysis is the ability to obtain sufficient vapor pressure of the trace impurity to attenuate the beam. This will depend on the vapor pressure of the pure element, the absorption coefficient of the most sensitive atomic absorption line and the activity coefficient of the element in the particular metal matrix.

Another crucial factor in analyses of this kind is the need for a measurable portion of the elemental vapor to be in the atomic state. Many elements, such as P, As, S, Sb, Se and Te, exist as polymeric vapor species and hence are insensitive to atomic absorption.

As the temperature of the sample is raised, the interaction of the sample and the cell becomes important. At temperatures of the order of 1200°, silica devitrifies and softens, limiting its useful temperature. When cells having alumina bodies and sapphire windows with a seal made within an evacuated tube by a spring fit holding together lapped surfaces of the cell body and window are used, the temperature range is increased and the reactivity with many materials is decreased.

The atomic absorption technique measures the thermodynamic activity of volatile species in solution. In dilute solutions a substantial fraction of the solute may be associated with other elements in compound formation and as such not exhibits its normal vapor pressure. In such a situation, the vapor pressure sensed would be characteristic of the remainder of the solute in solid solution. Weaker interactions in very dilute solutions where nearest neighbor distances between impurities are quite large, are not expected to affect the activities of the separate components, and measurable effects are expected only with compound formers such as oxygen, sulfur and phosphorus. The fact that Henry's law was obeyed in the copper–zinc system down to 42 p.p.m. is indicative of the fact that any impurities present did not strongly interact with the zinc in solution.

We wish to express our appreciation to John K. Litchfield for aid in the construction and operation of the equipment, and to Richard D. Leite for aid in material and cell preparation.

SUMMARY

The concentration of extremely dilute impurities in well characterized metals and alloys may be determined by atomic absorption spectroscopy in a sealed cell. The vapor pressure of the trace element is determined at a suitable temperature by measuring the attenuation of a resonant atomic line. A knowledge of the activity coefficient of the trace element in dilute alloys, either from literature or determined experimentally, allows the measured vapor pressure to be related directly to concentration. The method is illustrated by the determination of zinc in 99.9999% ASARCO copper, which was found to contain 80 p.p.b. Advantages and limitations of the method are discussed.

RÉSUMÉ

On propose une méthode spectroscopique par absorption atomique, en cellule scellée, pour le dosage d'impuretés à l'état de traces, dans des métaux et des alliages. Elle consiste à déterminer la tension de vapeur de l'élément à doser, à une température donnée, en mesurant l'atténuation d'une ligne atomique de résonance.

Le dosage du zinc (80 p.p.b.) dans un cuivre ASARCO à 99.9999% est donné comme exemple. On examine les avantages et les inconvénients de cette méthode.

ZUSAMMENFASSUNG

Die Konzentration von extrem verdünnten Verunreinigungen in gut charakterisierten Metallen und Legierungen kann durch Atomabsorptionsspektroskopie unter Anwendung einer verschlossenen Küvette bestimmt werden. Der Dampfdruck des Spurenelements wird bei einer geeigneten Temperatur ermittelt, indem die Verminderung einer Resonanz-Atomlinie gemessen wird. Die Kenntnis der Aktivitätskoeffizienten des Spurenelements in verdünnten Legierungen, der entweder aus der Literatur entnommen oder experimentell bestimmt worden ist, ermöglicht, den gemessenen Dampfdruck unmittelbar mit der Konzentration in Beziehung zu setzen. Die Methode wird an Hand der Bestimmung von Zink in 99.9999%igem ASARCO-Kupfer erläutert; der Gehalt wurde zu 80 p.p.b. bestimmt. Vorteile und Grenzen der Methode werden diskutiert.

REFERENCES

1 E. J. Rapperport and J. P. Pemsler, *Trans. TMS-AIME*, 242 (1968) 151.
2 J. P. Pemsler and E. J. Rapperport, *Trans. TMS-AIME*, 245 (1969) 1395.
3 J. P. Pemsler and E. J. Rapperport, *Met. Trans.*, 2 (1971) 79.
4 E. J. Rapperport and J. P. Pemsler, presented *AIME Centennial Meeting, New York, March 1, 1971*; to be published in *Met. Trans.*
5 P. T. Cunningham and J. K. Link, *J. Opt. Soc. Amer.*, 57 (1967) 1000.
6 E. J. Rapperport, J. P. Pemsler and E. Adler, *Rev. Sci. Instr.*, 41 (1970) 1168.

Analytica Chimica Acta
Elsevier Publishing Company, Amsterdam
Printed in The Netherlands

THE DETERMINATION OF NOBLE AND BASE METALS IN OSMIRIDIUM, NATIVE PLATINUM AND SPERRYLITE BY ATOMIC ABSORPTION SPECTROPHOTOMETRY

J. G. SEN GUPTA
Geological Survey of Canada, Ottawa, Ontario KlA OE8 (Canada)

(Received 23rd July 1971)

Studies on the geochemistry of the precious metals in Canada have required the determination of each of these metals in a variety of naturally occurring platiniferous materials. The complete analysis of certain materials is complicated by their resistance to chemical attack and the need to separate the noble and base metals from one another. As classical separation methods are time-consuming, and subject to manipulative errors, it seemed reasonable to look for alternative rapid methods where separations could be avoided without sacrifice of accuracy. Atomic absorption techniques offered promising possibilities in this direction.

Studies of the atomic absorption behaviour of the noble metals have been reported[1-6], but there have been few applications in the complete analysis of precious metals minerals. This paper describes analytical methods evolved for determining the noble and base metals in such samples. It is hoped that subsequent papers will describe further work on native silver, native gold, iron meteorites and sulfide minerals.

EXPERIMENTAL

Apparatus

A Techtron AA-3 atomic absorption spectrophotometer, equipped with a Hamamatsu R-213 photomultiplier tube, a type IM-5 amplifier-readout unit, a flat-topped 10-cm slot laminar-flow burner head for air–acetylene (Type AB 41) and a grooved titanium 6-cm slot burner head for nitrous oxide–acetylene flame, was used. A Beckman gas control unit (Model 9220) replacing the Techtron unit, and a variable-flow nebulizer (uptake rate of 4 ml min^{-1} used as standard) were employed. Individual ASL shielded-cathode hollow-cathode lamps were used for the determination of the six platinum group metals and iron. Perkin-Elmer individual Intensitron hollow-cathode lamps were used for silver and gold, and two- or multi-element Intensitron hollow-cathode lamps for copper and nickel.

Operating parameters

Instrumental parameters and apparent sensitivities are recorded in Table I. Where necessary, the burner head was rotated to reduce sensitivity, and for maximum accuracy the absorbance readings were taken between 0.1 and 0.4.

TABLE I

OPERATING PARAMETERS AND APPARENT SENSITIVITIES OF THE NOBLE METALS

Element	*Wavelength (nm)*	*Slit-width (μm)*	*Lamp current (mA)*	*Flame*	*Apparent sensitivity*[b]
Ru	349.8	25	8	Air–C_2H_2[a]	0.06
Rh	343.4	100	5	Air–C_2H_2[a]	0.01
Pd	244.7	50	6	Air–C_2H_2[a]	0.02
Ag	328.0	50	4	Air–C_2H_2	0.003
Os	290.9	50	15	N_2O–C_2H_2[a]	0.25
Ir	263.9	50	24	Air–C_2H_2[a]	0.16
Pt	265.9	150	8	Air–C_2H_2[a]	0.13
Au	242.8	300	4	Air–C_2H_2	0.01

[a] A mask with a 5-mm diameter opening was placed on the lens between burner and slit to increase sensitivity by restricting the area of flame observed.

[b] That concentration (p.p.m.) giving an expanded absorbance signal of 0.004 (in 0.5% Cu–0.5% Cd spectroscopic buffer). Approximate scale expansion between 7.5 and 10 times, where a stable and reproducible reading was obtained, was used.

Reagents

Standard solutions of the noble metals. Standard solutions of the platinum metals were prepared by procedures described previously[7]. Standard solutions of gold and silver were prepared from the "Specpure" metal (Johnson Matthey Chemicals, Ltd.). Gold was dissolved in aqua regia and converted to chloride by three evaporations with hydrochloric acid on the steam bath. Silver was dissolved in dilute nitric acid and the solution evaporated to dryness on the steam bath. The residue was dissolved in 0.1 *M* nitric acid.

Standard solutions of base metals. A standard solution of iron was prepared by dissolving a weighed quantity of pure iron (G. F. Smith Chemical Co., electrolytic) in hydrochloric acid, that of copper by dissolving a weighed quantity of pure copper (99.9%) in (1+1) nitric acid and then converting to chloride with hydrochloric acid. A solution of nickel was obtained by dissolving nickel chloride hexahydrate ("Baker Analyzed" reagent) in dilute hydrochloric acid; an aliquot was standardized by the dimethylglyoxime method.

Standard solutions at the $\mu g\ ml^{-1}$ level were prepared by freshly diluting the stock solutions with 0.12 *M* acid solution (same acid as present in the original stock solution).

Mixed copper–cadmium buffer solution[2]. This was prepared by dissolving 49.1 g of copper sulfate pentahydrate and 28.5 g of cadmium sulfate ($3CdSO_4 \cdot 8H_2O$) in 500 ml of warm 6 *M* hydrochloric acid.

Lanthanum chloride buffer solution[8]. This was prepared by dissolving 11.7 g of lanthanum oxide (SPEX Industries, Inc.) in 200 ml of 6 *M* hydrochloric acid on a hot plate.

Strontium chloride buffer solution. Reagent-grade strontium carbonate (16.85 g) was dissolved in dilute hydrochloric acid, the solution was evaporated to dryness on the steam bath, and the residue was dissolved in 200 ml of 6 *M* hydrochloric acid.

TABLE II

INTERFERENCE STUDY IN THE ATOMIC ABSORPTION DETERMINATION OF THE NOBLE METALS IN VARIOUS SYNTHETIC MIXTURES

Synthetic soln.	*Element (p.p.m.)*											*Comment on inter-element interferences*
	Ru	*Rh*	*Pd*	*Ag*	*Os*	*Ir*	*Pt*	*Au*	*As*	*Cu*	*Fe*	
Mixture 1	—	4	6	0.8	—	4.5	6	0.8	—	—	—	Inter-element interferences observed in HCl soln. without any buffer. No interference in 0.5% Cu–0.5% Cd, or 1% La, or 1% Sr buffer medium.
Mixture 2	—	6	15	2	—	14.8	20	2	—	—	—	
Osmiridium 1	118.2	7	2.5	0.8	294.2	277.2	19	0.8	—	—	—	No interference for Pd, Ag and Au. Serious interference for Rh and Pt.
Osmiridium 2	14.8	0.88	0.31	0.1	36.8	34.7	2.4	0.1	—	—	—	No interference
Sperrylite 1	2.6	126	0.6	0.2	—	2	3600	0.2	2800	—	—	No interference for Pd, Ag and Ru. Serious interference for Rh.
Sperrylite 2	0.1	5.04	0.02	0.01	—	0.08	144	0.01	112	—	—	No interference
Native Pt 1	6.4	8	52	0.6	—	40	1800	0.6	—	64	224	No interference for Pd, Ag and Ru. Serious interference for Rh.
Native Pt 2	0.26	0.32	2.08	0.02	—	1.6	72	0.02	—	2.56	8.96	No interference

Interference study

Inter-elements effects of the precious metals were studied in solutions containing osmium, iridium, ruthenium, platinum, arsenic and iron as major components, in the ranges expected in the samples (osmiridium, native platinum and sperrylite).

Various synthetic mixtures were prepared (see Table II) and the solutions were evaporated to dryness on the steam bath in the presence of sodium chloride to eliminate the excess of acid and to prevent the thermal decomposition of the salts. After the salts had been dissolved in dilute hydrochloric acid or in a spectroscopic buffer solution, the volume was made up with water. The final concentration of the acid was adjusted to 1.2 *M*. In Table II the composition of "synthetic osmiridium 1" corresponds to 8 mg of original sample per 10 ml and that of "synthetic osmiridium 2" to 1 mg per 10 ml. "Synthetic sperrylite 2" and "native platinum 2" were obtained by diluting "synthetic sperrylite 1" and "native platinum 1" to 25 times the original volumes. All these solutions (Table II) had a final concentration of 1.2 *M* hydrochloric acid and 0.5% Cu–0.5% Cd spectroscopic buffer. The solutions were aspirated into the atomic absorption spectrophotometer and the absorption of each noble metal

TABLE IIIA

COMPOSITION OF SYNTHETIC MIXTURES OF OSMIRIDIUM, SPERRYLITE AND NATIVE PLATINUM AND PREPARATION OF VARIO SOLUTIONS FROM ALIQUOTS FOR STUDY OF THE RECOVERIES OF NOBLE AND BASE METALS BY ATOMIC ABSORPTION SPECTROPHOTOMETRY

Elements (mg in 25 ml) present in the synthetic mixture (main soln.)	*Element(s) to be determined*	*Aliquot taken (ml)*	*Buffer added*	*Final volume of the buffered soln.*	*Soln. identification for results given in Table IIIB*
Osmiridium					
Ir =3.855; Pt=0.265;	Ir	2.5	1 ml Cu–Cd	5	a
Rh=0.1125; Pd=0.010;	Rh, Pd, Pt, Ag and Au	6	1 ml Cu–Cd	5	b
Ag=0.001; Au=0.015;					
Fe=0.2975; Cu=0.152;	Fe, Cu and Ni	10	1 ml Sr	5	c
Ni=0.070; NaCl=170 mg					
Sperrylite					
Pt =53.18; As=38;	Pt	1	2 ml Cu–Cd	10	d
Ag=0.25; Fe=0.35;	Ag	5	1 ml Cu–Cd	5	e
Cu=0.05; Ni=0.08;	Fe, Cu and Ni	5	1 ml Sr	5	f
NaCl=400 mg					
Native platinum 1					
Pt =88.0; Ir=6.5;	Pt	1	2 ml Cu–Cd	10	g
Rh=0.90; Pd=0.325;	Pd, Ag and Au	5	2 ml Cu–Cd	10	h
Ag=0.0035; Au=0.024;	Rh	0.5	5 ml Cu–Cd	25	i
Fe =11.9; Cu=1.094;	Ir	2.5	2 ml Cu–Cd	10	j
Ni =0.15; NaCl=300 mg	Fe	1	5 ml La	25	k
	Cu and Ni	5	2 ml La	10	l
Native platinum 2					
Pt =88.65; Ir=1.77;	Pt	1	2 ml Cu–Cd	10	m
Rh=1.25; Pd=0.55;	Pd, Ag, Ir, Au	2.5	1 ml Cu–Cd	5	n
Ag=0.17; Au=0.025;	Rh	0.5	5 ml Cu–Cd	25	o
Fe =7.00; Cu=0.85;	Fe	1	5 ml La	25	p
Ni =0.08; NaCl=300 mg	Cu and Ni	5	1 ml La	10	q

in the synthetic mixture was compared with that of a solution containing the same quantity of that metal, of sodium chloride and of acid. The observations of this study are incorporated in Table II. During this study it was also observed that in 0.5% Cu–0.5% Cd spectroscopic buffer medium, the sensitivity of ruthenium is the same in air–acetylene and nitrous oxide–acetylene flames, that of osmium four times higher in nitrous oxide–acetylene than air–acetylene, and that of iridium 1.5 times higher in air–acetylene than nitrous oxide–acetylene. The sensitivities of these three elements are higher in 0.5% Cu–0.5% Cd buffer medium than in 1% La or 1% Sr buffer.

Rhodium absorption is more sensitive with the lanthanum buffer than with the other two. Platinum is equally sensitive with both lanthanum and strontium. In general, the strontium buffer (1%) is not suitable for gold, osmium and iridium determinations because of erratic absorbance readings. From the standpoint of general applicability to the determination of all noble metals, 0.5% Cu–0.5% Cd spectroscopic buffer is by far the best choice, since reproducible absorbance readings and straight line calibration curves are always obtained.

Lanthanum (1%) and strontium (1%) buffers were found equally effective in determining the base metals.

Study of the recovery of the precious and common metals from synthetic mixtures of osmiridium, sperrylite and native platinum

Each synthetic mixture shown in Table IIIA was prepared by pipetting individual solutions of the noble and the base metals into a beaker; an appropriate amount of sodium chloride* was added and the solution evaporated to dryness on the steam bath. After the residue had been dissolved in 1 *M* hydrochloric acid, the solution was diluted to 25 ml with the same acid. To determine different elements, aliquots were taken in 20-ml beakers and evaporated to dryness on the steam bath. An appropriate amount of a spectroscopic buffer was added to each, and after brief warming on the steam bath, the solution was diluted with water to a known volume. The final concentration of the buffer metal(s) in each solution was 1%. The atomic absorption measurements of the elements in the mixtures were carried out in an air–acetylene flame and the absorbances were compared with those of the "pure" standards prepared identically and measured immediately before and after the synthetic mixtures. The results given in Table IIIB indicate quantitative recovery.

Recommended procedures for analyses of osmiridium, native platinum and sperrylite

For complete analysis, the osmiridium and native platinum samples were brought into solution by dry chlorination at 700°. For this, the procedure of Westland and Beamish[9] was modified to suit decomposition of about 10 mg of osmiridium and 100 mg of native platinum. Sperrylite was decomposed by a combination of treatment with Br_2–KBr and dry chlorination at 700°.

For atomic absorption determination, standard solutions were prepared, containing known amounts of each element together with the same amount of sodium chloride, acid and buffer as present in the sample solutions. Calibration curves were

---

* Sodium chloride was added to prevent decomposition of salts to free metals during evaporation, and the amount was the same which would be used in decomposing the naturally occurring sample by dry chlorination at elevated temperature.

TABLE IIIB

ATOMIC ABSORPTION STUDY OF THE RECOVERIES OF NOBLE AND BASE METALS FROM ALIQUO

(All results are given as μg ml^{-1})

Solution (see Table IIIA for details)	*Iridium*		*Rhodium*		*Palladium*		*Platinum*	
	Sought	*Found*	*Sought*	*Found*	*Sought*	*Found*	*Sought*	*Found*
a	77.1	77.1						
b			5.4	5.4	0.48	0.48	12.72	12.72
c								
d							212.7	212.7
e								
f								
g							352.0	351.0
h					6.5	6.5		
i			0.72	0.72				
j	65.0	65.0						
k								
l								
m							354.6	354.6
n	35.4	35.4			11.0	11.0		
o			1.0	1.0				
p								
q								

prepared from these standards immediately before and after the sample readings.

The method of analysis is schematically represented in Fig. 1 and additional details are described below in the procedures.

Analysis of osmiridium and native platinum (*Procedure* 1, *see Fig.* 1)

Dry chlorination. Accurately weigh the sample (10 mg of osmiridium, or 100 mg of native platinum) and transfer it to a quartz boat. Cover with finely powdered sodium chloride (A.C.S. grade, 100 mg for osmiridium, 300 mg for native platinum) and introduce at the center of a 18-cm long clear quartz tube, each end of which has been coated with 10 mg of sodium chloride by fusion. The quartz tube bears a 14/35 ground joint on either end. Introduce the tube into the apparatus assembly for dry chlorination[9], and place the bulb at the exit end of the tube outside the hot zone of the 12.5-cm long furnace (Lindberg Hevi-duty, tube type).

Place 10 ml of water in the first receiver (500-ml round bottom distillation flask) and 30 ml, 10 ml and 10 ml of 6 *M* hydrochloric acid in the subsequent three receivers. Saturate the solutions in the receivers with sulfur dioxide gas and introduce chlorine (pre-dried by bubbling through concentrated sulfuric acid) through the system. Always maintain an excess of sulfur dioxide in the receivers. Heat the furnace to 700° and chlorinate the sample for 7 h. After cooling, displace the chlorine from the tube by nitrogen and remove the tube from the assembly.

Wash the chlorinated product in the tube into a 20-ml beaker with about 10 ml of 1 *M* hydrochloric acid. If necessary, warm the tube with little hydrochloric acid (1 *M*) and dislodge any solid from the heated zone with a glass rod. Filter, if

F SYNTHETIC SOLUTIONS OF OSMIRIDIUM, SPERRYLITE AND NATIVE PLATINUM

Silver		*Gold*		*Iron*		*Copper*		*Nickel*	
Sought	*Found*	*Sought*	*Found*	*Sought*	*Found*	*Sought*	*Found*	*Sought*	*Found*
0.05	0.05	0.72	0.72						
				23.8	23.8	12.1	12.2	5.6	5.6
10.0	10.0								
				14.0	14.0	2.0	2.0	3.2	3.2
0.07	0.07	0.48	0.48						
				19.1	19.2				
						21.8	21.5	3.0	3.0
3.4	3.4	0.5	0.5						
				11.2	11.2				
						17.0	16.8	1.6	1.5

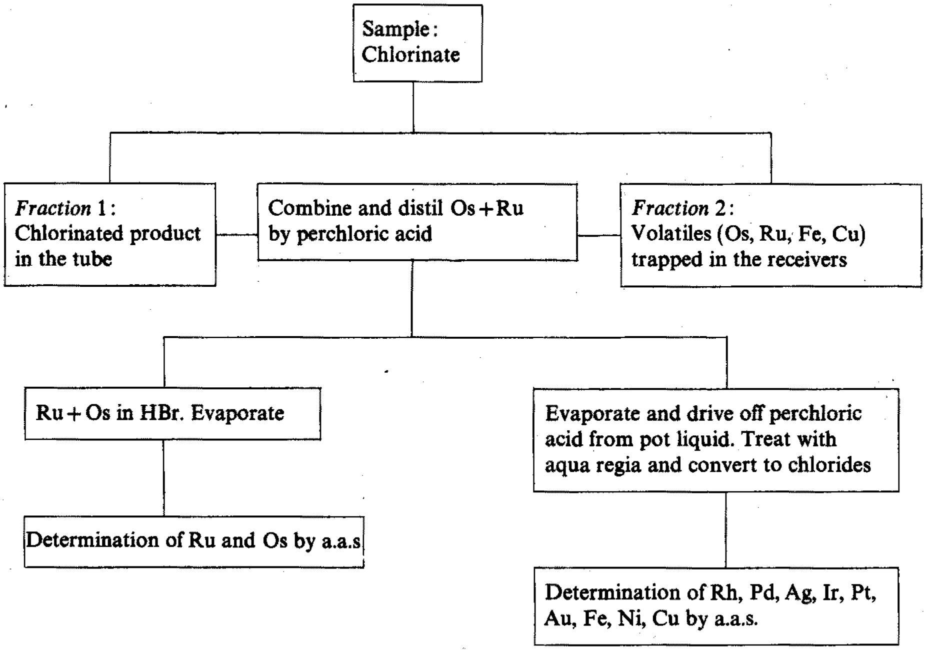

Fig. 1. Flow-sheet outlining analytical scheme (*Procedure* 1 for osmiridium and native platinum).

TABLE IV

ANALYSIS OF OSMIRIDIUM (NEW GUINEAN) BY ATOMIC ABSORPTION SPECTROPHOTOMETRY AND COMPARISON WITH SOME FIRE ASSAY VALUES

Element	*Atomic absorption (%, this work)*		*Fire assay (%)*[a,b]
	Procedure 1 (sample = 10.15 mg)	*Procedure 2 (sample = 10.64 mg)*	
Ru	13.7	14.2	14.1–15.2[b]
Rh	1.06	0.87	0.9[a]
Pd	0.06	0.09	< 0.3[a]
Ag	0.01	0.01	—[c]
Os	38.5	38.2	35.8–38.0[b]
Ir	36.6	36.7	33.3–34.8[a]
Pt	2.82	2.40	2.33[a]
Au	0.05	0.05	—[c]
Fe	2.80	—[c]	—[c]
Cu	1.43	—[c]	—[c]
Ni	0.66	—[c]	—[c]

[a] Faye *et al.*[13].
[b] Faye[14].
[c] Not determined.

necessary, any solid material by suction through a porous bottom porcelain filter crucible (Coors, 767-5/0) collecting the filtrate in a 50-ml flask, and transfer the solid quantitatively to the crucible with a minimum quantity of 1 *M* hydrochloric acid. Dry the crucible in air, add 50–100 mg of sodium chloride and chlorinate in upright position in a bigger tube (clear quartz, 2.5 cm inner diameter) at 700° for 5–7 h. During this chlorination, the exit end of the chlorination tube should remain attached via a polyvinyl tube and a 14/35 inner joint to the afore-said four receivers in which the volatiles liberated during the first chlorination have been trapped. After cooling and displacement of chlorine by nitrogen, detach the tube and wash the chlorinated product with 1 *M* hydrochloric acid into the beaker containing the main solution. Disconnect the three receivers (6 *M* hydrochloric acid saturated with sulfur dioxide), combine their contents into a 150-ml beaker and evaporate to about 5 ml. Transfer to the 500-ml flask by rinsing with water and also add the main solution to this flask.

Distillation of osmium and ruthenium by perchloric acid. Insert the flask containing the main solution as above into the distillation train, which contains a 300-ml trap for perchloric acid vapour, a water condenser and three receivers connected in series[7]. Distil osmium and ruthenium by boiling to fuming with 70% perchloric acid and collect osmium and ruthenium in 48% hydrobromic acid (ice-cold).

Determination of osmium and ruthenium by atomic absorption. Combine the hydrobromic acid receiving solutions as above into a 400-ml beaker and rinse the tubes and connections with 10% hydrobromic acid. Add 20 mg of sodium chloride and evaporate to a small volume on a hot plate and finally to dryness on a steam bath. If the sample is osmiridium, dissolve the residue in 0.1 *M* hydrobromic acid (briefly warm, if necessary) and dilute to 25 ml. Take a 5-ml aliquot, add 2 ml of the Cu–Cd buffer, dilute to 10 ml and determine osmium and ruthenium by atomic absorption.

If the sample is native platinum, dissolve the residue in 1 ml or 2 ml of Cu–Cd buffer (depending on the osmium content) and dilute to 5 ml or 10 ml with water giving a total buffer metals concentration of 1%. Determine osmium and ruthenium by atomic absorption.

Removal of perchloric acid from the pot liquid and atomic absorption determination of Rh, Pd, Ag, Ir, Pt, Au, Fe, Ni and Cu. Transfer the perchloric acid pot liquid to a 600-ml beaker, add 10 ml of concentrated nitric acid and evaporate to dryness on a medium hot plate (perchloric acid fume hood). Rinse the sides with concentrated hydrochloric acid and evaporate to dryness. Repeat this operation once more. Cool, add 15 ml of aqua regia, cover and digest on the steam bath. Evaporate and convert to chlorides by three evaporations with concentrated hydrochloric acid (steam bath). Dissolve the residue in 3 *M* hydrochloric acid and transfer to a 25-ml volumetric flask and make up the volume with the same acid.

Atomic absorption determination of Rh, Pd, Ag, Ir, Pt, Au, Fe, Ni and Cu. Osmiridium. Evaporate a 10-ml aliquot to dryness on the steam bath. Dissolve in 1 ml of Cu–Cd buffer and dilute to 5 ml in a volumetric flask. Determine Ag, Au, Pd and Pt by atomic absorption.

Evaporate a 5-ml aliquot to dryness on the steam bath. Dissolve in 1 ml of Cu–Cd buffer and dilute to 5 ml in a volumetric flask. Determine Rh and Ir by atomic absorption.

Evaporate a 5-ml aliquot to dryness on the steam bath. Dissolve in 1 ml of La or Sr buffer. If a white precipitate appears, filter through a glass fiber filter paper, wash and dilute to 5 ml in a volumetric flask. Determine Fe, Cu, Ni by atomic absorption.

Native platinum. Evaporate a 10-ml aliquot to dryness on a steam bath. Dissolve in 1 ml of Cu–Cd buffer and dilute to 5 ml in a volumetric flask. Determine Ag, Au and Pd by atomic absorption.

Evaporate a 5-ml aliquot to dryness (steam bath). For native platinum 2 (see Table V), add 1 ml of Cu–Cd buffer and dilute to exactly 5 ml. For native platinum 1 or 3 (*cf.* Table V), add 2 ml of Cu–Cd buffer and dilute to exactly 10 ml. Determine iridium by atomic absorption.

Transfer 0.5 ml (native platinum 2) or 1.0 ml (native platinum 1 or 3) aliquot of the solution used for iridium to a 25-ml volumetric flask, add Cu–Cd buffer (4.9 ml to native platinum 2; 4.8 ml to native platinum 1 or 3) and dilute to volume with water. Determine rhodium by atomic absorption.

Evaporate a 1-ml aliquot to dryness (steam bath). Dissolve in 2 ml of Cu–Cd buffer and dilute to exactly 10 ml. Determine platinum by atomic absorption.

Evaporate a 5-ml aliquot to dryness (steam bath). Add 2 ml of lanthanum buffer and dilute to exactly 10 ml. Determine nickel and copper by atomic absorption.

Transfer a 2-ml aliquot of the solution used for copper and nickel to a 25-ml volumetric flask, add 4.8 ml of lanthanum buffer and dilute to volume with water. Determine iron by atomic absorption.

Alternative methods (*Procedure* 2)

Osmiridium. Dilute Fraction 1 (see Fig. 1) to exactly 25 ml with 1 *M* hydrochloric acid and determine Ir, Ru, Os, Pt, Pd, Rh, Ni, Fe and Cu from different aliquots by atomic absorption (see *Procedure* 1).

Distil osmium and ruthenium from Fraction 2 (see Fig. 1) with perchloric acid,

TABLE V

ANALYSIS OF NATIVE PLATINUM BY ATOMIC ABSORPTION SPECTROPHOTOMETRY[a]

Element	*Specimen no.*[b]		
	1	2	3
Ru	0.06	0.07	1.00
Rh	0.84	1.11	1.14
Pd	0.31	0.53	0.84
Ag	0.004	0.001	0.13
Os	0.36	0.27	5.06
Ir	6.01	1.52	6.66
Pt	80.92	89.35	77.81
Au	0.03	0.024	0.36
Fe	10.51	6.37	6.07
Cu	0.99	0.74	0.85
Ni	0.14	0.07	0.15
Total	100.174	100.055	100.07

[a] Average of two analyses (except osmium) expressed in %.

[b] 1 = Native platinum, Similkameen River, British Columbia, Canada; 2 = Native platinum, Horsefly River, British Columbia, Canada; 3 = Native platinum, North Saskatchewan River, Near Edmonton, Alberta, Canada.

collect in hydrobromic acid and determine osmium and ruthenium by atomic absorption (see *Procedure* 1 for details). Combine the osmium and ruthenium values to obtain the total.

For the determination of iron and copper in Fraction 2 (Fig. 1), remove perchloric acid from the pot liquid by evaporation. Evaporate with hydrochloric acid twice and dilute to exactly 25 ml with 0.1 *M* hydrochloric acid. Determine the iron and copper content by atomic absorption and combine with the amounts obtained in Fraction 1 to obtain the total.

Native platinum. Attack the sample (100 mg) with aqua regia. Filter off any insoluble material (*e.g.* osmiridium), reduce in hydrogen and chlorinate at 700° in the presence of sodium chloride. Mix the chlorinated product with the main portion and determine the noble metals (osmium excepted) and the base metals from different aliquots by atomic absorption (see *Procedure* 1 for details).

Analysis of sperrylite ($PtAs_2$)

Treat the sample (*ca.* 100 mg) in a 100-ml beaker with 2 ml of bromine solution (0.3 g of potassium bromide + 0.2 ml of liquid bromine + 1.8 ml of water), cover the beaker and allow to stand for 15 min with occasional swirling. Add three 2-ml portions of concentrated nitric acid and heat on a hot plate until the reaction ceases. Raise the glass cover by three glass hooks and evaporate to dryness on a steam bath. Convert the soluble salts to chlorides by repeated evaporation with hydrochloric acid (steam bath). Warm the residue with 25 ml of 1 *M* hydrochloric acid. Although the major portion of sperrylite dissolves in the above treatment, some material may remain unattacked. Filter the solution through a Whatman #40 (5.5-cm) filter paper, quantitatively transfer the unattacked material to the filter paper, and wash with hot dilute hydrochloric acid (0.12 *M*). Reserve the filtrate (main solution), and burn the paper with the residue in a porcelain crucible (Coors 4/0) at 350–400° in a muffle furnace. Carefully transfer the residue to a small quartz boat (2.7 cm × 0.6 cm), and mix and cover with a total of 50 mg of finely powdered sodium chloride. Place the boat at the center of a clear quartz tube (1 cm i.d., 18 cm long) and chlorinate at 700° in an electric furnace for 7 h. Cool the tube, displace chlorine by nitrogen and dissolve the chlorinated product in 0.12 *M* hydrochloric acid. Filter the solution through a Whatman #40 (5.5 cm) filter paper, and transfer the white siliceous residue quantitatively to the paper. Wash with hot 0.12 *M* hydrochloric acid, dry and ignite to constant weight in a porcelain crucible. X-Ray powder pattern diffraction of the residue identified it as cristobalite (SiO_2).

Combine the filtrate (chlorinated product) with the main solution and evaporate to dryness on the steam bath. Dissolve the residue in 10 ml of 0.12 *M* hydrochloric acid by warming on a steam bath and cool overnight to allow the separation of potassium hexachloroplatinate crystals. Filter the supernate through a borosilicate medium-porosity sintered crucible (8-ml capacity) previously washed with dilute hydrochloric acid, distilled water and heated to constant weight at 110°. Wash three times by decantation with 80% ethanol and finally transfer to the sintered crucible with the same wash liquid. After two more washings with small amounts of 80% ethanol, heat the crucible to constant weight at 110°. The gravimetric factor is 0.4014.

Small amounts of platinum (about 3% of the total) which escape the potassium hexachloroplatinate precipitation and traces of some other noble and base metals can be determined in the filtrate by atomic absorption spectrophotometry by the following procedures.

Transfer the filtrate to a 100-ml beaker by washing the flask with 0.12 *M* hydrochloric acid and evaporate to 5 ml. Transfer to a 20-ml beaker, and evaporate to dryness on a steam bath. Treat the residue with 10 ml of aqua regia and evaporate to dryness on a steam bath. Convert the salts to chlorides by evaporating to dryness (3 times on steam bath) with concentrated hydrochloric acid. Add 5 ml of 1 *M* hydrochloric acid and dissolve the salts by heating on a steam bath. Cool to room temperature, transfer the solution to a 10-ml volumetric flask and dilute to volume with 1 *M* hydrochloric acid. Transfer an aliquot (2 ml) to a 5-ml volumetric flask, add 1 ml of strontium buffer and dilute to volume with water (solution A). To the remaining 8 ml, add 2 ml of Cu–Cd buffer and mix well (solution B). Transfer 1 ml of solution B to a 2-ml volumetric flask, add 0.8 ml of Cu–Cd buffer and dilute to volume with water (solution C).

Determine platinum, iridium, ruthenium, palladium and gold by atomic absorption spectrophotometry in solution B, rhodium in solution C, and iron, copper and nickel in solution A. These determinations should be done on the day on which the solutions are prepared in order to minimize the effect of post-precipitation of potassium hexachloroplatinate. The platinum value thus obtained is added to the gravimetric value to calculate the percentage in sperrylite.

For osmium and silver, decompose 80 mg of sperrylite by dry chlorination at 700° in the presence of sodium chloride (see *Procedure* 1 for native platinum). Determine osmium by spectrophotometry[7] and silver by atomic absorption spectrophotometry in the presence of 0.5% Cu–0.5% Cd buffer.

Determination of arsenic in sperrylite. Place an accurately weighed amount of sperrylite (*ca.* 40 mg) in a zirconium crucible, mix and cover with a total of 1 g of sodium peroxide. After covering, slowly heat the crucible to dull red heat for 10–15 min with occasional swirling of the molten mass. After cooling, place the crucible in a 250-ml Teflon beaker and pour 20 ml of hot water into the crucible. After the solid mass disintegrates, stir with a Teflon rod, filter through a 1.3-ml Coors filter crucible (5/0) by suction, and wash by decantation with hot water.

Collect the filtrate in a polyethylene flask, neutralize to a colorless end-point (phenolphthalein) with (1+1) sulfuric acid, again make slightly alkaline with very dilute sodium hydroxide solution, and then just discharge the pink color with 0.2 *M* acetic acid. Transfer the solution to a 150-ml beaker, cover with a borosilicate glass cover and boil on a hot plate to expel carbon dioxide. Allow the small dark precipitate which appears to settle overnight, filter through a filter crucible by suction, and wash with water. Reject the residue. Treat the filtrate with 13 ml of (1+1) sulfuric acid, dilute to 75 ml with water and add 1 g of potassium iodide. Reduce the solution by boiling down to 50 ml, cool and treat with 0.03 *M* sodium thiosulfate solution (yellow color just discharged). Dilute to 75 ml, neutralize the free acid with concentrated ammonia (methyl orange), and then render slightly acidic with dilute sulfuric acid. Add 2 g of sodium bicarbonate, mix and titrate the arsenite with 0.03 *M* iodine solution using starch-iodide as the indicator[10]. Standardize the iodine solution against a sodium thiosulfate solution which was pre-standardized against a potassium iodate solution.

Determination of total sulfur in sperrylite. Determine the sulfur content of sperrylite by combustion of 10-mg sample in a high-frequency induction furnace[11], absorbing the liberated sulfur dioxide in sodium tetrachloromercurate solution and making a spectrophotometric finish with *p*-rosaniline hydrochloride and formaldehyde[12].

RESULTS AND DISCUSSION

In Table IV the results for osmiridium obtained by atomic absorption spectrophotometry are given, and a comparison is made with some of the precious metals values obtained by Faye *et al.*[13,14] who used the tin-collection scheme of fire-assaying. However, there is one significant difference in the sample treatment before analysis. The present author obtained from the donor the white lustrous grains of osmiridium (non-magnetic) which was separated from the black magnetic material by hand-picking under a microscope. Faye *et al.* (private communication) analyzed the mixture of white lustrous grains and the black magnetic material without such separation, and this is possibly the reason for their somewhat lower results for osmium, iridium and platinum (Table IV). Recent examination by electron microprobe[15] showed that individual grains of the New Guinean osmiridium specimen are highly variable in composition and the osmium–iridium phase contains inclusions of other phases such as iridium arsenic sulfide, quartz, platinum alloy and iridium–osmium phase. Therefore, the results as obtained in this work as well as those of Faye *et al.* (Table IV) are the average of 10–30 small grains per 10 mg of sample.

Table V gives the average of two results on each of three native platinum samples, the determinations being completed by atomic absorption spectrophotometry following two different dissolution processes: (*a*) dry chlorination alone at

TABLE VI

REPRODUCIBILITY OF RESULTS (%) OF THE ANALYSES OF NATIVE PLATINUM BY ATOMIC ABSORPTION SPECTROPHOTOMETRY

Sample[a]	*Wt. taken (mg)*	*Procedure followed*	*Ru*	*Rh*	*Pd*	*Ag*	*Ir*	*Pt*	*Au*	*Fe*	*Cu*	*Ni*
1	109.566	2	0.05	0.83	0.31	0.003	5.93	81.00	0.02	10.50	0.99	0.14
	106.690	1	0.06	0.84	0.31	0.005	6.09	80.84	0.04	10.51	0.99	0.14
2	102.266	2	0.08	1.12	0.54	0.001	1.63	89.22	0.024	6.36	0.84	0.07
	101.977	1	0.06	1.10	0.52	0.001	1.40	89.48	0.024	6.37	0.63	0.07

[a] See footnote (*b*) of Table V.

700°, and (*b*) aqua regia plus dry chlorination. In Table VI the agreement between results obtained by the two dissolution processes is demonstrated.

In Table VII the analytical data for a sperrylite sample are presented and a comparison is made with earlier data in the literature. The present sample resembles closely the Russian samples in the composition of major elements. Spectrographic analysis of the present sperrylite sample showed that in addition to the elements listed in Table VII, traces of bismuth, aluminium, titanium and tin, and faint traces of magnesium and calcium, are also present.

TABLE VII

SPERRYLITE ($PtAs_2$): ANALYTICAL DATA (%) OF THIS WORK COMPARED WITH EARLIER DATA

Element	1[a] (*this work*)	2	3	4
Pt	56.30	52.57	56.2	56.40
Pd	0.024	Trace	—	—
Rh	0.013	0.72	—	—
Ru	0.021	—	—	—
Os	< 0.01	—	—	—
Ir	0.04	—	—	—
Ag	0.23	—	—	—
Au	0.07	—	—	—
As	40.21	40.98	40.6	40.90
Sb	0.30[b]	0.50	—	—
S	0.12	—	—	—
Fe	0.34	0.07	0.4	0.56
Cu	0.05	—	0.7	—
Ni	0.07	—	—	—
Rem.	0.61	4.62	1.3	1.62
Total	98.40	99.46	99.2	99.48

[a] 1=Frood mine, Sudbury, Ontario, Canada, J.G. Sen Gupta analyst. Residue is cristobalite (SiO_2). 2=Vermillion mine, Sudbury, Canada, Residue is cassiterite[16]. 3=Nikolaev mine, Timptonskiy area, Yakutsk, U.S.S.R. Residue is SiO_2[17]. 4=Alexandro-Nevskiy mine, River M. Zalta, Tributary of river Ilikan, Amur Province, U.S.S.R.[18].

[b] Spectrographic value (W. H. Champ and G. Bender analysts).

I thank R. W. Boyle for providing background information on sperrylite and native platinum samples, H. R. Steacy for osmiridium samples, and S. Abbey and G. H. Faye for critical reading of the manuscript.

SUMMARY

Atomic absorption spectrophotometric methods for determining the noble and base metals in osmiridium, native platinum and sperrylite have been developed and applied to the analysis of some naturally occurring samples. The sample is decomposed by dry chlorination at 700° in the presence of sodium chloride, or by treatment with aqua regia (native platinum) or Br_2–KBr (sperrylite) followed by dry chlorination of the insoluble residue. Osmium and ruthenium are separated by distillation with perchloric acid and collected in hydrobromic acid. From different aliquots the noble metals are determined in the presence of 0.5% Cu–0.5% Cd buffer and the base metals in the presence of 1% lanthanum or strontium buffer.

RÉSUMÉ

Des méthodes spectrophotométriques d'absorption atomique sont proposées pour le dosage de métaux nobles et de métaux de base dans l'osmiridium, le platine natif et la sperrylite. L'échantillon à analyzer est décomposé soit par chloruration sèche à 700°, en présence de chlorure de sodium, soit par traitement à l'eau régale, ou au Br_2–KBr et chloruration sèche du résidu insoluble. L'osmium et le ruthénium sont séparés par distillation avec acide perchlorique et recueillis dans l'acide bromhydrique. Les métaux nobles sont finalement dosés en présence d'un tampon 0,5% Cu–0,5 % Cd; les métaux de base en présence d'un tampon à 1 % de lanthene ou de strontium.

ZUSAMMENFASSUNG

Für die Bestimmung der Edelmetalle und unedlen Metalle in Osmiridium, gediegenem Platin und Sperrylith wurden Methoden der Atomabsorptionsspektrophotometrie entwickelt und auf die Analyse von einigen in der Natur vorkommenden Proben angewendet. Die Probe wird durch trockene Chlorierung bei 700° in Gegenwart von Natriumchlorid aufgeschlossen. Der Aufschluss kann auch durch Behandlung mit Königswasser (gediegenes Platin) oder Br_2–KBr (Sperrylith) mit anschliessender trockener Chlorierung des unlöslichen Rückstandes erfolgen. Osmium und Ruthenium werden durch Destillation mit Perchlorsäure abgetrennt und in Bromwasserstoffsäure aufgefangen. In verschiedenen aliquoten Anteilen werden die Edelmetalle in Gegenwart eines 0.5% Cu–0.5% Cd-Puffers und die unedlen Metalle in Gegenwart eines 1%igen Lanthan- oder Strontiumpuffers bestimmt.

REFERENCES

1 F. E. Beamish, C. L. Lewis and J. C. van Loon, *Talanta*, 16 (1969) 1.
2 M. M. Schnepfe and F. S. Grimaldi, *Talanta*, 16 (1969) 591; 17 (1970) 617.
3 S. Kallman and E. W. Hobart, *Talanta*, 17 (1970) 845.

4 A. E. Pitts, J. C. van Loon and F. E. Beamish, *Anal. Chim. Acta*, 50 (1970) 181.
5 A. Simonsen, *Anal. Chim. Acta*, 49 (1970) 368.
6 J. C. van Loon, *At. Abs. Newsletter*, 8 (1969) 6.
7 J. G. Sen Gupta, *Anal. Chim. Acta*, 42 (1968) 481.
8 J. C. van Loon, *Z. Anal. Chem.*, 246 (1969) 122.
9 A. D. Westland and F. E. Beamish, *Anal. Chem.*, 30 (1958) 414.
10 N. H. Furman (Editor), *Standards Methods of Chemical Analysis*, Vol. I, 6th Edn., D. Van Nostrand, New York, 1962, p. 109.
11 J. G. Sen Gupta, *Anal. Chim. Acta*, 49 (1970) 519.
12 J. G. Sen Gupta, *Anal. Chem.*, 35 (1963) 1971.
13 G. H. Faye, W. R. Inman and P. E. Moloughney, *Anal. Chem.*, 36 (1964) 366.
14 G. H. Faye, *Anal. Chem.*, 37 (1965) 696.
15 D. C. Harris, Mines Branch, Dept. of Energy, Mines and Resources (Canada), private communication.
16 H. L. Wells, *Amer. J. Sci.*, 37 (1889) 67; J. D. Dana and E. S. Dana, *The System of Mineralogy*, Vol. I, John Wiley, New York, 1946, p. 292.
17 P. P. Pilipenko, *Izv. Akad. Nauk Peterb.*, 9 (1915) 1229; *Mineraly, Spravochnik*, Tom I, Izdatel'stvo Akademii Nauk SSSR, Moskva, 1960, p. 133.
18 S. D. Popov and A. M. Popova, *Tr. Lomon. in-ta AN SSSR, Ser. Min.*, 7 (1936) 269; *Mineraly, Spravochnik*, Tom I, Izdatel'stvo Akademii Nauk SSSR, Moskva, 1960, p. 133.

Analytica Chimica Acta
Elsevier Publishing Company, Amsterdam
Printed in The Netherlands

ATOMIC ABSORPTION AND FLUORESCENCE SPECTROSCOPY WITH A CARBON FILAMENT ATOM RESERVOIR

PART VIII. THE DETERMINATION OF MANGANESE BY ATOMIC ABSORPTION SPECTROSCOPY

L. EBDON, G. F. KIRKBRIGHT AND T. S. WEST
Department of Chemistry, Imperial College, London, S.W. 7 (England)

(Received 20th June 1971)

Earlier papers in this series have described various aspects of the use of the carbon filament as an atom reservoir in trace element analysis by atomic absorption spectroscopy (a.a.s.) and atomic fluorescence spectroscopy (a.f.s.). In particular, the use of an unenclosed cell[1], limited field viewing to minimise vapour phase interferences[2,3] and of a fast-response recording system[3] have been reported. In this paper the determination of manganese by a.a.s. is reported with limited field viewing in an unenclosed cell. A storage oscilloscope was used to display the signals obtained.

Manganese is an interesting element for such a study owing to its importance as a trace element in many matrices, and also because manganese, whose melting and boiling points are 1247 and 2030° respectively, is typical of a number of analytically important elements of only moderate volatility. This element may, therefore, act as a model for its type with respect to its vaporization from the carbon filament. While in an earlier paper[4] a detection limit of $5 \cdot 10^{-12}$ g was noted for manganese in a.f.s., no systematic examination of the determination of this element by a.a.s. with the carbon filament atom reservoir has been described.

EXPERIMENTAL

Apparatus

A Unicam SP 900A thermal emission/atomic absorption flame spectrophotometer fitted with an EMI 9601B photomultiplier was employed. The recorder output from the spectrophotometer was led directly to the Y-axis amplifier of a storage oscilloscope (Telequipment, type DM 53A fitted with K-type amplifier). A manganese hollow-cathode lamp (Atomic Spectral Lamps Pty. Ltd.) was used as the spectral source. The modified filament atomic reservoir and its use with the Unicam SP 900A has been described previously[1]. In the present experiments the filament was rotated 90° in the horizontal plane relative to the spectrometer slit, *i.e.* the filament was at 90° to the optical axis of the monochromator, and it was possible to view radiation between 0 and 2 mm above the rod without obstruction from the electrode heads. In the cell used, titanium electrodes were employed. A small copper tube (4 mm internal diameter, 40 mm in length) was positioned between the filament and the slit of the spectrometer to act as a collimator. Immediately before passing into the collimator the light beam traversed a horizontal slit with a fixed width of 0.7 mm. By varying the height of this slit the dependence of analytical signal upon height of observation above the filament was investigated. A nickel foil screen was placed between the filament and the slit to prevent any radiation from the glowing filament from directly entering the slit.

The SP 900A was used in the thermal emission mode, *i.e.* the light entering the monochromator is modulated at 100 Hz by a rotating sector and the signal is reconverted to a d.c. level by the a.c. amplifier of the SP 900A spectrophotometer.

Sample volumes of 5 μl or 1 μl were used throughout the studies; the use of 5-μl samples permits higher reproducibility to be attained compared to 1-μl samples.

Radiation from the hollow-cathode source was focussed as sharply as possible onto the filament so that the surface onto which the sample was placed lay immediately beneath the level of the horizontal diameter of the image of the hollow cathode.

The power supply, preparation of the filament, sheathing gas supply and sample pipettes have been described previously[1,2,4].

Reagents

All reagents were of analytical-reagent grade and the water used was glass-distilled and then deionized. The water used to prepare the solution, and the reagents used in the interference studies, were periodically checked for contamination by manganese.

The sample pipettes and all glassware were treated with "Repelcote" as described previously[2,4].

Procedure

The following procedure was used in routine determinations. The wavelength, electronic gain, slit-width, shielding gas flow-rate, water-cooling and hollow-cathode lamp current were adjusted to previously determined optimal values. The filament was then heated to the working temperature. After 30 sec a 5-μl sample was placed on the prepared surface, and the water was then driven off slowly by heating the rod to *ca.* 120°. The filament was then switched off and the Variac set to the value required for atomization. Whilst waiting 30 sec, the 0 and 100% transmission signals were stored on the screen of the oscilloscope. The filament was switched on for 2 sec, the signal from the SP 900A being recorded on the oscilloscope and stored using the "single-shot" facility. The percentage absorption was then calculated from the traces stored by

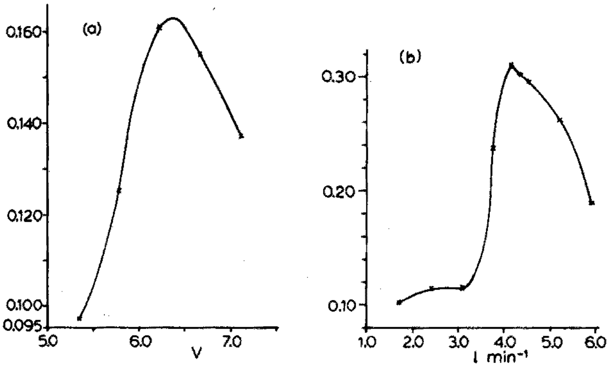

Fig. 1. Effect of (a) filament voltage, (b) nitrogen flow-rate, on manganese absorbance at 279.5 nm.

the oscilloscope. It should be noted that reproducibility is improved when this regular timing sequence is observed.

RESULTS AND DISCUSSION

Effect of filament voltage on absorbance due to manganese

The manganese analytical signal varies with the applied filament voltage. This relationship is illustrated in Fig. 1a, from which it is evident that the optimal applied voltage is *ca.* 6.4 V. This corresponds to a terminal filament temperature of *ca.* 2300°, as measured by an optical pyrometer. The analytical manganese absorption signal, however, is observed well before this temperature is reached. Manganese is completely removed from the filament at the voltage and heating time employed. This is demonstrated by the absence of a second manganese absorption signal (memory effect) when the filament voltage was applied for a second time.

Effect of shielding gas flow-rate and height of observation on absorbance

Figure 1b shows the variation of manganese absorbance with the nitrogen shielding gas flow-rate for a filament voltage of 6.4 V and a height of observation 0–2 mm above the filament. The optimal flow-rate was observed to be 4.1 l min^{-1} of nitrogen. This is high compared to previously reported flow-rates for the cell[1-3]; it was found that this high flow-rate produced the sharpest absorption peaks. No significant enhancement of absorbance was observed when argon was employed as shielding gas in place of nitrogen. With the optimal filament voltage and shielding gas flow-rate the sensitivity obtained for manganese was observed to be relatively independent of the height of observation above the filament between 0 and 2 mm. However, it was noted that the effect of foreign ions on the absorbance observed for manganese was critically related to height of observation and that least interference was obtained in the region 0–1 mm above the filament.

Effect of hollow-cathode lamp current and monochromator slit-width on absorbance

The optimal monochromator slit-width for the measurement of the manganese absorption at 279.5 nm was 0.02 mm (which corresponds to a spectral bandwidth of 0.2 nm at this wavelength). The optimal hollow-cathode lamp current was observed to be 10 mA. Neither of these parameters critically affected the sensitivity attained, however, and therefore with limited field viewing, *i.e.* viewing less than 1 mm above the rod, the monochromator slit was opened to 0.03 mm and the lamp current increased to the manufacturers' suggested maximum of 30 mA. This resulted in increased light flux entering the monochromator and permitted operation at lower amplifier gain settings to minimize the recorded noise level.

Detection limits and calibration curves

With the established optimal conditions the detection limits (signal-to-noise ratio 2:1) and sensitivities (for 1% absorption) were determined at 280 nm and 403 nm. The detection limits are listed in Table I. Comparison of the results obtained with previous a.a.s. work with premixed flames shows that it is possible to determine solutions of comparable concentrations to those used with flame cells. The system described here, however, is suitable for the detection of much lower absolute amounts of man-

TABLE I

DETECTION LIMITS FOR THE DETERMINATION OF MANGANESE BY ATOMIC ABSORPTION SPECTROSCOPY

Atom reservoir	*Detection limits at*	
	280 *nm*	403 *nm*
Carbon filament: 5-μl sample	0.01 p.p.m.[a] ($5 \cdot 10^{-11}$ g)	0.05 p.p.m.[b] ($2.5 \cdot 10^{-10}$ g)
1-μl sample	0.03 p.p.m. ($3 \cdot 10^{-11}$ g)	
20 × 5-μl sample	0.0005 p.p.m. ($5 \cdot 10^{-11}$ g)	
Air–acetylene flame[6]	0.005 p.p.m.[c]	
Carbon filament surrounded[7] by hydrogen diffusion flame		
1-μl sample	0.0005 p.p.m. ($5 \cdot 10^{-13}$ g)	

Sensitivities (for 1% absorption): [a] 0.01 p.p.m. manganese; [b] 0.10 p.p.m. manganese; [c] 0.05 p.p.m. manganese.

ganese. The limit of detection with this system for 1-μl samples is 0.03 p.p.m., but when the same detection system was used for the a.a.s. of manganese in an air–acetylene flame[5] it was necessary to use a sample volume of 2 ml to obtain a useful signal at the detection limit of 0.1 p.p.m. Thus the advantage in terms of absolute amounts of sample is several orders of magnitude. This advantage can be exploited by placing several 5-μl samples of a very dilute solution on the rod and carefully driving off the water between applications. Table I includes the detection limit obtained when twenty 5-μl samples were placed on the rod in this manner; 20 applications of 5-μl samples of blank solutions gave no signal.

The sensitivity corresponding to 1% absorption at the 5-μl sample level was 0.01 p.p.m., indicating the relatively high noise levels of the fast-response system.

The calibration curve at 280 nm is shown in Fig. 2. Several factors may account for the non-linear nature of the working curve; these are at present under investigation. The analytically useful working range is from 0.05–10 ng.

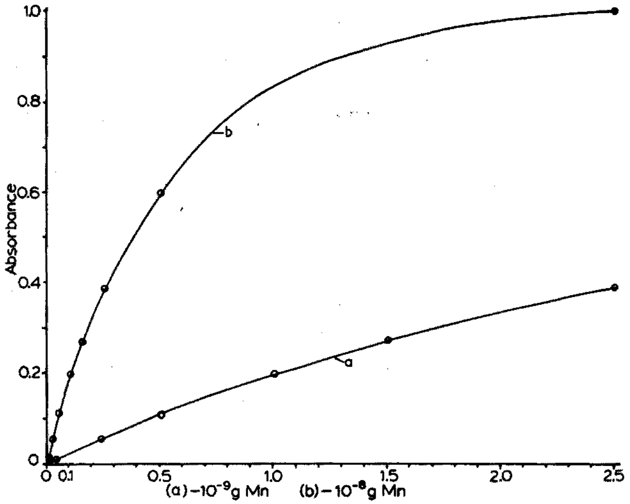

Fig. 2. Analytical calibration curves at 279.5 nm. (a) 0–2.5 ng Mn; (b) 0–25 ng Mn.

The possibility that the absorption signals might arise from scatter of the incident source radiation was excluded by using the lead line at 283 nm. No absorption signal was obtained from 5 μl of a 10-p.p.m. manganese solution with a high-intensity lead hollow-cathode lamp.

At the 1-ng level, a relative standard deviation of 6% was obtained for twelve 5-μl samples.

Interference studies

An extensive examination of the effect of foreign ions on the absorbance of manganese was made. Solutions of manganese (0.4 p.p.m.) containing 1000, 100 or 10-fold weights of 24 different foreign ions were employed. The results obtained for the 1000- and 100-fold levels are shown in Table II; no interferences were found from any of these ions at the 10-fold level. The effects of the interferences are listed as percentage suppressions or enhancements of the percentage absorption signal. Only results which showed a change of signal of 5% or more are regarded as significant interferences.

TABLE II

INTERFERENCES IN THE A.A.S. DETERMINATION OF MANGANESE ($2 \cdot 10^{-9}$ g) AT 280 nm WITH A CARBON FILAMENT ATOM RESERVOIR

Ion added	*Salt*	*% Change of signal from 1000- and 100-fold amounts of ions*[a]	
		1000	100
Na	NaCl	− 40	−20
K	KNO_3	− 60	−40
Ca	$Ca(NO_3)_2$	+ 30	0
Hg	$HgNO_3$	0	0
Mg	$MgCl_2$	−100	−80
Ga	Ga/HCl	− 50	0
Zn	$ZnSO_4$	0	0
Tl	$TlNO_3$	− 7	0
Th	$Th(NO_3)_4$	− 20	0
Fe	Fe/HCl	− 45	−15
Ni	$Ni(NO_3)_2$	− 60	0
Cr	$CrCl_3$	− 70	−67
Mo	NH_4MoO_4	0	0
Pb	$Pb(NO_3)_2$	0	0
Si	Si/HF	+ 16	0
Al	$Al(SO_4)_3$	− 8	0
W	$W/HNO_3/HF$	0	0
V	V/HNO_3	− 20	−17
Ta	Ta/HF	− 20	0
PO_4^{3-}	$(NH_4)_2HPO_4$	0	0
SO_4^{2-}	H_2SO_4	0	0
NO_3^-	HNO_3	0	0
NH_4^+	NH_4OH	0	0
Cl^-	HCl	0	0

[a] Each value represents the average of 6 values in good agreement.

While no interference was observed from any of the ions studied at the 20-ng level, interference was observed from 200-ng amounts of the relatively volatile elements. At the 1000-fold level (2 μg) most of the cations investigated produced serious de-

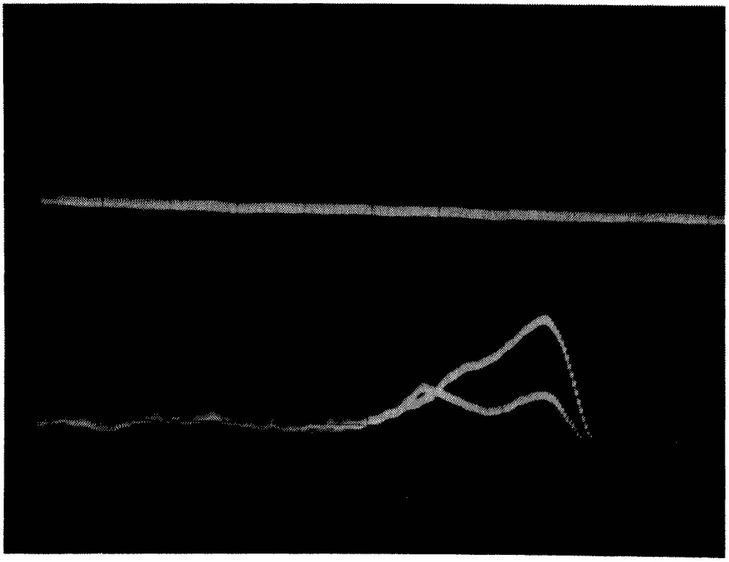

Fig. 3. Suppression of the absorption signal for 2 ng of manganese by 2 μg of sodium. The upper trace corresponds to 100% absorption, the middle trace shows the manganese absorption signals and the lower trace the signal from manganese in the presence of sodium.

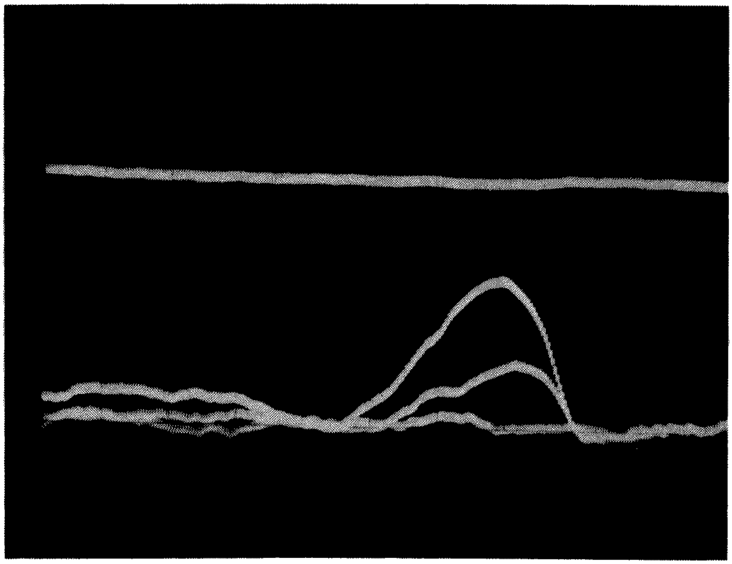

Fig. 4. Enhancement of the absorption signal for 2 ng of manganese by 2 μg of calcium. The uppermost trace corresponds to 100% absorption and the lowest to the signal when no sample is added. Of the traces in the centre of the photograph the lower shows the manganese absorption signal and the upper the signal from manganese in the presence of calcium.

pressions; no interference was noted from the anions studied. It can be seen that volatile elements tend to interfere more than involatile elements. This is in contrast to the behaviour in the atomic spectroscopy of manganese in the air–acetylene flames, but confirms previous conclusions that interferences in the carbon filament technique arise largely from vapour-phase interaction[1-3]. All the interferences observed were depressions of signal, except in the case of calcium and silicon where 400-p.p.m. solutions of these cations produced an absorption signal which appeared to be caused by scatter of the source radiation by particulate material produced above the filament.

Photographs of oscilloscope traces showing interference are reproduced in Figs. 3 and 4. Figure 3 shows the suppression of the absorption signal for 2 ng of manganese by a 1000-fold amount of sodium. Figure 4 shows the enhancement of the absorption signal by a similar amount of calcium. The interferences illustrated are slightly larger than those in Table II as in this case limited field viewing restrictions were relaxed to enable more light to reach the detector.

It may be observed from Table II that where serious interference was observed in many cases the cations studied were added as their chlorides. It was therefore thought that the more volatile chlorides might lead to more serious interference than if a less volatile compound was present. The interference on a 0.4-p.p.m. manganese solution by a 1000-fold amount of iron present as its sulphate was only -12%, whereas the interference from the same weight of iron present as its chloride was -45% (see Table II). However, it was shown that the atomic absorption signals obtained for iron by the carbon filament technique are identical for given concentrations of iron whether it is applied to the filament as the chloride or sulphate. This indicates that the interferences observed cannot be explained simply by volatility of the matrix compound.

In a study of interferences on the determination of manganese in the air–acetylene flame[5], it was found that magnesium depressed both the atomic fluorescence and absorption produced for manganese and this was ascribed to a chemical effect. In this study magnesium was again the most serious interference, depressing the manganese absorption when present in both 1000- and 100-fold amounts. The extent of interference was found to depend on the height of observation above the filament, as reported elsewhere[2,3], and the interferences reported in Table II were obtained by making observations as close to the filament as possible, *i.e.* in the zone 0–0.7 mm above the filament. Amos[7] has recently reported the use of a modified filament in which the source radiation passes through a hole in the filament into which the sample is placed, the filament being surrounded by a hydrogen diffusion flame. Although Amos reports no interference studies, it might be expected that the atomic population of analyte would cool less rapidly on this type of filament and thus vapour-phase interferences would be reduced.

The present experiments confirm that the degree of interference depends more on the absolute amount of concomitant element than on its ratio to the analyte[2,3], *i.e.* less severe interference was observed for 1000-fold amounts of foreign ions when the manganese concentration employed was lower.

DISCUSSION

The carbon filament method offers a sensitive method for the determination of manganese by a.a.s., particularly in very small samples. The use of a fast-response recording system and limited field viewing are to be recommended. The detection system employed might be modified by elimination of the SP 900A amplifier and the need to convert the signal to an a.c. level. This may be achieved by modifying the photomultiplier circuit to supply a negative EHT to the photomultiplier tube from an independent power supply and direct input of the d.c. signal to the amplifier of the oscilloscope. Preliminary work indicates that this rapid response system permits use of higher filament voltages (up to 12 V) and an improvement of an order of magnitude in sensitivity is obtained to produce a detection limit of $5 \cdot 10^{-12}$ g Mn.

We are grateful to the Ministry of Aviation Supply for support of this work.

SUMMARY

The atomic absorption characteristics of manganese with a carbon filament atom cell and hollow-cathode lamp source are described. With limited field viewing conditions and direct oscilloscopic presentation of the absorption signals, a detection limit of $5 \cdot 10^{-11}$ g Mn (5 μl of 0.01 p.p.m. Mn solution) is obtained at 279.5 nm. The effect of the presence of 24 foreign ions has been examined; 14 ions interfere at the 1000-fold level, but only 6 ions interfere at the 100-fold level.

RÉSUMÉ

On décrit les caractéristiques d'absorption atomique du manganèse, avec cellule atomique à filament de carbone et lampe à cathode creuse. Dans les conditions indiquées, on arrive à une limite de détection de $5 \cdot 10^{-11}$ g Mn (5 μl de solution de manganèse à 0.01 p.p.m.), à 279.5 nm. On examine l'influence de 24 ions étrangers. Quatorze ions interfèrent en concentration 1000 fois supérieure, mais six seulement gênent en concentration 100 fois supérieure.

ZUSAMMENFASSUNG

Die Atomabsorptionseigenschaften von Mangan bei Verwendung einer Graphitheizfadenküvette und einer Hohlkathodenlampe werden beschrieben. Unter den Bedingungen eines begrenzten Sichtfeldes und bei direkter oszilloskopischer Darstellung der Absorptionssignale wird eine Nachweisgrenze von $5 \cdot 10^{-11}$ g Mn (5 μl einer 0.01 p.p.m. Mn-Lösung) bei 279.5 nm erhalten. Der Einfluss von 24 Fremdionen wurde untersucht; 14 Ionen stören bei 1000-fachem Überschuss, jedoch nur 6 Ionen bei 100-fachem Überschuss.

REFERENCES

1 J. F. Alder and T. S. West, *Anal. Chim. Acta*, 51 (1970) 365.
2 J. Aggett and T. S. West, *Anal. Chim. Acta*, 55 (1971) 349.
3 D. Alger, R. G. Anderson, I. S. Maines and T. S. West, *Anal. Chim. Acta*, 57 (1971) 271.
4 R. G. Anderson, I. S. Maines and T. S. West, *Anal. Chim. Acta*, 51 (1970) 355.
5 L. Ebdon, G. F. Kirkbright and T. S. West, *Talanta*, 17 (1970) 965.
6 W. Slavin, *Appl. Spectrosc.*, 20 (1966) 281.
7 M. D. Amos, *American Laboratory*, Aug. (1970) 33.

Analytica Chimica Acta
Elsevier Publishing Company, Amsterdam
Printed in The Netherlands

THE DETERMINATION OF LEAD IN BLOOD BY ATOMIC ABSORPTION WITH THE HIGH-TEMPERATURE GRAPHITE TUBE

ELSA NORVAL AND L. R. P. BUTLER
National Physical Research Laboratory, C.S.I.R., Pretoria (South Africa)

(Received 14th August 1971)

Lead is one of the most ubiquitous of the natural substances which man concentrates in his immediate environment. It is present in food, drinking water and air and is one of the most insidiously toxic of the heavy metals to which man is exposed, particularly in its ability to accumulate in the body and to damage the central nervous system, including the brain. There is evidence that lead wastes have been accumulating, particularly in congested urban areas. The chipping paint in older buildings is the primary source of lead poisoning in young children. The most urgent need is to control the hazard of lead poisoning in certain subgroups within the general population that run the risk of clinical plumbism. These groups are young children in whom the habit of chewing objects as a means of environmental examination still persists and workers in certain industries such as lead mines and battery manufacturing plants. A high concentration of airborne lead is particularly noxious because about 50% of this lead may be absorbed on inhalation, in contrast to the 5–10% absorbed from lead-contaminated food and water[1].

The determination of lead in blood is one of the most useful diagnostic tests for lead poisoning[2]. It is known that lead is bound in the red blood corpuscles[3] and consequently whole blood must be analyzed for diagnostic purposes. In the past, most of the methods used for this determination included a time-consuming ashing procedure[4–6], and usually required more than 4 cm^3 of blood for one determination[4,5]. Furthermore, the sensitivity of conventional atomic absorption for lead determination is marginal for the direct analysis of normal blood, apart from the fact that for blood some pre-treatment is necessary, because even diluted whole blood cannot be routinely aspirated into the burner. Because of these considerations, it was decided to study the use of the high-temperature tube system for the determination of lead in blood.

THE HIGH-TEMPERATURE TUBE TECHNIQUE

The basic principles of the high-temperature graphite tube system are illustrated in Fig. 1. With this method the sample is not aspirated into a flame but is placed in a tube which is heated by means of electrical resistance, a welding transformer serving as a stable current source. The chief difference between the tube and flame techniques is that the tube is a static system, whereas the flame is a dynamic system. With the tube a definite quantity of the sample is used and the total absorption recorded, while with the flame the sample is continuously aspirated and the absorption registered when a constant value is reached. With the tube, the energy necessary to volatilize

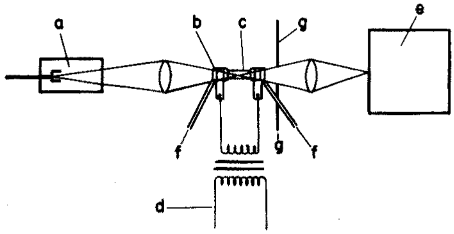

Fig. 1. Atomic absorption system with graphite cuvette. (a) Hollow-cathode lamp, (b) graphite cuvette, (c) point of sample introduction, (d) welding transformer, (e) spectrophotometer, (f) water-cooling, (g) diaphragm.

and dissociate the sample is obtained from an external source, while with the flame, use is made of the exothermal reactions of oxidizing and reducing gases to supply the necessary energy. In the tube, the dilution factor of the solvent and flame gases and their combustion products are absent.

The cuvette holder and cuvette

As it was felt that the apparatus described by L'vov[7] and Massmann[8] was too complicated for routine use, a simpler system was developed. This has no enclosure around the cuvette holder and since the cuvettes are not protected by an inert atmosphere, they have to be discarded after one measurement—a not prohibitively expensive step. This meant that samples could be interchanged very rapidly during the analysis and that they could be prepared in batches beforehand. The tubes are shorter than the L'vov tubes[7], the dimensions being approximately the same as those used by Massmann[8], with a slightly larger inner diameter and walls only 2/3 the thickness. The design of the cuvette holder is shown in Fig. 2. The holder was made of titanium, after several other materials had been tried and abandoned because of contamination and other failures, on account of the high temperatures to which they were subjected. The

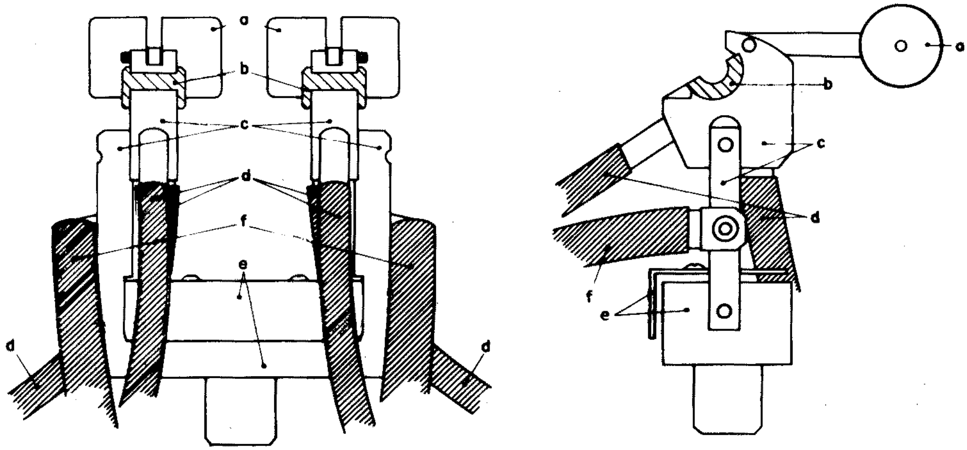

Fig. 2. Cuvette holder. (a) Weights of stainless steel for clamping cuvette into position, (b) graphite insert at points of contact with cuvette, (c) titanium, (d) water-cooling, (e) asbestos base shielded by aluminium plate, (f) cables to welding transformer.

holder has graphite inserts at the points of contact with the cuvette. This eliminates the possibility of arcing caused by corrosion of the titanium. As graphite arcs much less easily than titanium, a margin of variation in cuvette diameter can be tolerated, and when worn, the inserts are easily replaced by others. The holder is water-cooled and heavy cables connect the end blocks to terminals from the welding transformer. The weighted levers swing over to hold the cuvette firmly enough in place for good electrical contact. The power supply is a simple variable reactance welding transformer capable of supplying 400 A.

A diaphragm was tried out in the path of the radiation just after the cuvette. The idea was to separate a central bundle of radiation and so eliminate possible adverse effects arising from small irregularities in the cuvette shapes or from shielding of radiation by particles from the cuvette walls. Such effects were, however, not observed with the lead lamp which has a 4-mm cathode diameter, and a diaphragm was found to be unnecessary. It may be useful with other cathode and cuvette dimensions.

The dimensions of the cuvette (Fig. 3) were determined by the relevant optical system and by the requirements for high sensitivity. The latter are a long tube length which increases the retention time of the atoms and a small diameter which makes for a high atom density. The cuvettes differ from those of L'vov and Massmann in that the walls are machined down along the middle portion which results in a higher resistance and higher temperature in that part of the cuvette where the sample is initially concentrated. Sample solutions are introduced through the small hole (2.4 mm diameter). The cuvettes are not lined with any other material, and so a high-density graphite is required. Both the density and the electrical resistance of the graphite are important, which implies that the same type must be used throughout a particular analysis. The graphite used in this study had a distinctly negative thermal resistance characteristic.

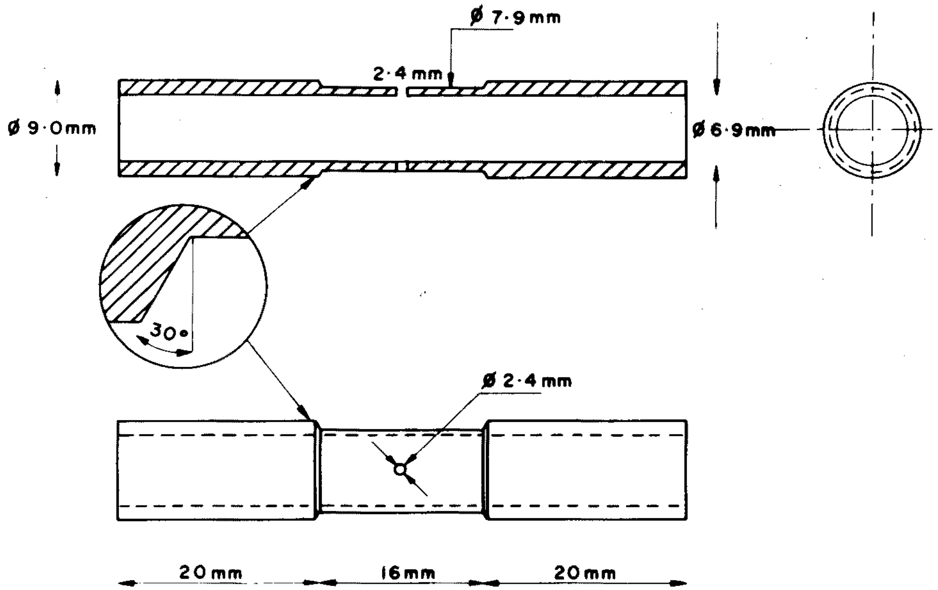

Fig. 3. Cuvette dimensions.

In spite of selecting the highest purity grade of graphite for making the cuvettes, a severe lead absorption signal was obtained when these were heated. This was doubtless due partly to contamination and partly to residual impurities in the graphite, shown up by the high sensitivity of the method. A special purifying device was consequently designed. In this, the cuvette is held in a vertical position with water-cooled stainless steel contacts at the top and bottom, and is encased in a quartz cylinder through which a stream of spectrographically pure argon is passed. When the cuvettes were heated for 2 min in this device, with a current of 330 A, zero blank values were obtained. The purifying device is shown in Fig. 4. As they had been enclosed in an argon atmosphere, there was no oxidation of the cuvettes and purified cuvettes were found to heat up and behave very similarly. After being purified, the cuvettes were kept in lidded grooved stainless steel containers throughout the procedure, except for the actual time of the absorption measurement. The cuvettes can be handled in these containers, also when standards and samples are introduced, and can be kept covered whenever possible.

Test of apparatus and method

In order to determine the most suitable working conditions, temperature–time graphs were drawn for various currents. These are shown in Fig. 5, and it can be seen that equilibrium is generally reached within 20–25 sec.

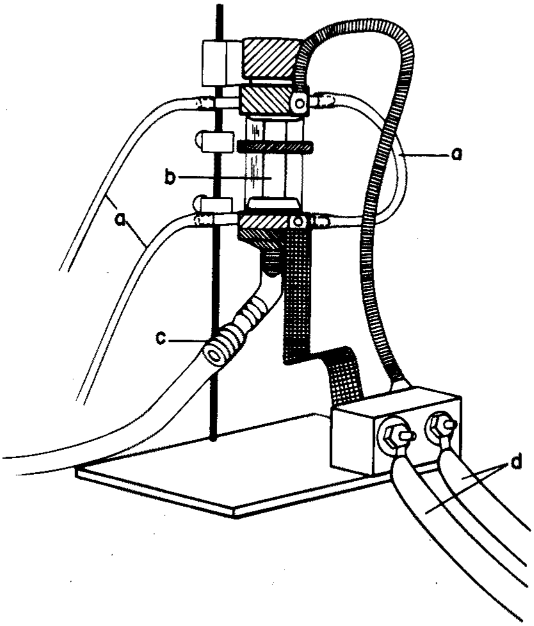

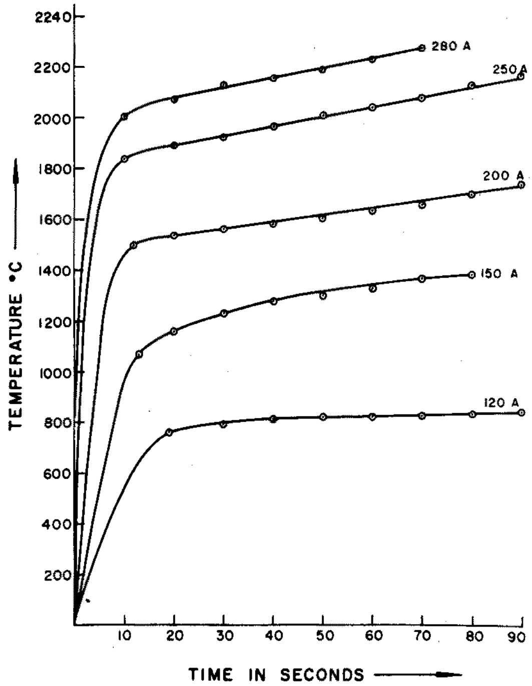

Fig. 4. Device for purifying cuvettes. (a) Water-cooling, (b) cuvette, (c) argon flow, (d) cables to welding transformer.

Fig. 5. Temperatures obtained with different currents.

The spectrophotometer used was equipped with both a pen recorder and a simple electronic integrator designed in this laboratory. There was some doubt as to whether it would be better to use the peak absorbance or the total integrated absorbance. It was found that when blood samples were analyzed for lead, the integrated absorbance gave a much better calibration curve as well as better accuracy, because of variations in the shape of the curves. Figure 6 illustrates the type of curve obtained; A was recorded with an aqueous standard which contained 8 ng of lead and B was obtained with a 0.02-cm^3 blood sample. A has a 77% peak absorbance and an integrated area of 45.09 cm^2 whereas B has a peak absorbance of 87% and an area of 43.22 cm^2.

In order to determine the optimal working temperature and the effect of anions, curves were obtained for lead as the chloride, nitrate and sulphate at 5 different currents. For the first three currents, 20 ng and for the last two currents, 12.5 ng of lead were used. In order to be able to measure the long flat curves recorded with a current of 150 A, the planimeter was set to measure in arbitrary units. These units were also

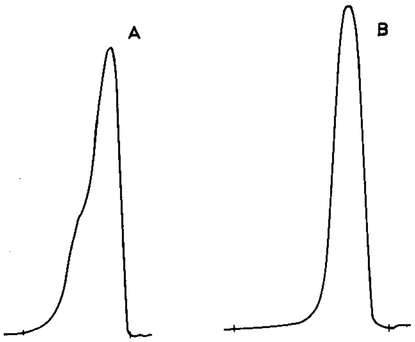

Fig. 6. Absorption curves obtained with (A) an aqueous standard containing 8 ng lead, and (B) a 0.02-cm^3 blood sample.

TABLE I

INTEGRATED AREAS OF ABSORPTION CURVES OBTAINED WITH DIFFERENT CURRENTS

Lead compound	*Area in arbitrary units*			*Area (cm^2)*	
	150 *A* (1000° *after* 10 sec)	200 *A* (1480° *after* 10 sec)	220 *A* (1560° *after* 10 sec)	250 *A* (1840° *after* 10 sec)	280 *A* (2005° *after* 10 sec)
$PbCl_2$	2.59	6.81	10.13	74.82	54.63[a]
	1.87	6.68	9.46	69.66	
Average	2.23	6.75	9.80	72.24	—
$Pb(NO_3)_2$	2.37	5.55	9.05	68.31	59.66
	2.50	7.24	8.88	68.43	56.31
Average	2.44	6.40	8.97	68.37	57.99
$PbSO_4$	1.53	5.60	8.14	68.37	47.02
	1.51	5.68	8.18	69.66	47.09
Average	1.52	5.64	8.16	69.02	47.06

[a] Approximate value of first part of double-peaked curve.

used for the curves obtained with 200 and 220 A. Those recorded with currents of 250 and 280 A were measured in cm^2. The curve areas are given in Table I. With the exception of the curves recorded with a current of 150 A (1000° after 10 sec), where it was difficult to decide on the starting and end points, sensitivities increase in the order $SO_4^{2-} < NO_3^- < Cl^-$. In interpreting the results in terms of the heats of formation of the different molecules, other effects should also be borne in mind. These are: cooling with consequent condensation at the cuvette ends and possible secondary reactions after the initial dissociation of the molecules. From the results listed in Table I it seems, however, that there may be a relationship. The heats of formation in kJ mole^{-1} are the following: $PbSO_4-917.95$; $Pb(NO_3)_2-448.94$; $PbCl_2-359.02$. It is known that with conventional atomic absorption, the sensitivity of an element in the presence of sulphate ions is often poorer than that of the same element in the presence of other anions, and that sulphates are more subject to chemical interferences. This study shows that with both the tube and the flame, the poorer sensitivity when an element is present in the sulphate form, is very probably connected with the heat of formation of the molecule. The integrated absorbances for lead sulphate and lead nitrate with a current of 280 A (2005° after 10 sec) are lower than with a current of 250 A (1840° after 10 sec). This may be due to the fact that at the higher temperature, the ratio between the rate of diffusion of the atoms through the open ends of the tube and the atomization rate differs from that at the lower temperature. The absorbance curves of lead chloride at a current of 280 A showed double peaks. In one case of the four recorded, the signal returned nearly to zero before forming a second peak. There was great variation in the shape and size of the area under the second peak. The formation of a second peak was probably due to condensation and redissociation of the compound after the initial atomization. As a result of the values listed in Table I, it was decided to undertake the analysis at a current of 250 A.

When dried biological material is analyzed by means of the high-temperature tube, two signals are obtained. The first, with a current of 70 A, is due to the combustion products of the sample and the second, obtained with a higher current, arises from the absorption of the lead atoms. It was found that direct ashing on the spectrophotometer with a current of 70 A usually resulted in the remaining inorganic material being left in the cuvette in the form of a small plug or web. This shielded off some of the radiation from the hollow-cathode lamp. Some form of pre-ashing was therefore required. Attempts were made to convert the lead to the sulphate or the chromate and, after drying, to ash the samples at 700° in a muffle furnace. This was unsatisfactory, as there were some apparent lead losses from standards treated in the same way as well as large differences between triplicate determinations on samples, all the lead probably not being converted to the desired compound. Pre-ashing was then done according to Delves' method^9 and after a final ashing on the instrument, the inorganic residue was deposited in such a way that no radiation was shielded off.

Because of the remarkably high sensitivity of the method, every possible measure had to be taken against contamination. As it was not possible to work in a completely lead-free atmosphere, the 283.3-nm line was used, the 217.0-nm line being too sensitive.

Of several anticoagulants tested, heparin gave a zero blank reading. If blood is not analyzed immediately after being drawn, it must be stored in a freezer. On storing blood for some time, the erythrocytes may "clump" or group together in masses; this process of agglutination is different from that of coagulation^{10}. If blood samples have been stored, alternately defrosting and freezing them a couple of times will cause the blood to haemolize and ensure that a homogeneous liquid is obtained.

LEVELS OF LEAD IN BLOOD

There is considerable difference of opinion concerning biologically allowable and toxic levels of lead in blood. As maximum biologically allowable concentrations, figures of 36[2] (for children), 40[11] and 60 μg/100 cm^3 [12] are mentioned, and as toxic 80[2] (for children), 70[13,14] and 100 μg/100 cm^3 [12]. An international group of medical specialists in lead problems suggested four categories of blood levels in adults and implied that lead poisoning does not occur at blood levels below 80 μg/100 cm^3 [15] (Table II).

TABLE II

FOUR CATEGORIES OF BLOOD LEAD CONCENTRATION IN ADULTS[15]

Category	*Blood lead level (μg/100 cm^3)*	*Description*
A Normal	< 40	"Normal" population with no occupational or abnormal exposure.
B Acceptable	40–80	Increased absorption resulting from occupational or abnormal exposure which is occupationally acceptable.
C Excessive	80–120	Increased absorption from excessive occupational or other exposure which may be associated with mild symptoms or signs, or, rarely, with severe symptoms or signs. These levels are unacceptable.
B Dangerous	> 120	Dangerous absorption from occupational or other exposure in which mild and severe symptoms and also long-term sequelae are increasingly probable.

EXPERIMENTAL

Equipment

Glassware was cleaned with a solution containing hydrogen fluoride and nitric acid of analytical-reagent quality, a detergent and double-distilled water. Tweezers used for handling cuvettes were cleaned with methanol (analytical-reagent standard) and the stainless steel containers used for the cuvettes were rinsed with double-distilled water and dried in a specially cleaned drying oven after each series of analyses.

Standard lead solution

Superpure nitric acid was diluted and used to make up a stock solution of 2000 p.p.m. of lead from "Specpure" lead oxide. This was diluted with double-distilled water to obtain standards containing 0.1, 0.2, 0.3 and 0.4 p.p.m. of lead.

Treatment of standards

As it was decided not to use any kind of lining in the cuvettes, they were dried immediately after the aqueous standards were introduced, in order to limit the degree of penetration into the graphite. The standards were treated in the same way as the samples and blanks were consistently run on the water used.

Treatment of blood samples

When blood samples had to be diluted, the dilution was done on a weight basis. The samples were placed in the purified cuvettes, 0.04 cm^3 being introduced by means of a micro-pipette. The blood was then rapidly dried on a hot-plate before the addition of 0.08 cm^3 of hydrogen peroxide (30%) to each sample. The initial drying of the blood was necessary as addition of hydrogen peroxide to the wet samples caused violent frothing which could lead to mechanical losses. After the addition of peroxide, the samples were again dried at 140° on a hot-plate, according to Delves' method[9]. During this drying which takes only about 2 min, a white froth extended above the rim of the opening in the cuvette for sample introduction. This froth collapsed back into the cuvette at 140°. Above 150° the solution boiled too vigorously and above 160° spontaneous ignition could occur. At temperatures below 130° the drying step was time-consuming. The samples were then sufficiently oxidized for the rapid final ashing on the spectrophotometer at 70 A for *ca.* 30 sec to leave the inorganic residue deposited in such a way that there was no interference with the radiation signal from the hollow-cathode lamp. By testing standards treated in the same way, it had been established that no lead losses occurred during the final ashing. The current was then switched to 250 A and the lead absorption recorded at the 283.3-nm line. Blank determinations done on the hydrogen peroxide showed no lead absorption.

RESULTS AND DISCUSSION

The technique was tested by using the addition method. The graph obtained is shown in Fig. 7. The particular sample had been diluted (1 + 3) with water and 0.02 cm^3 of sample plus 0.02 cm^3 of the different lead standards had been used. As 0.02 cm^3 of the diluted sample contained 1 ng of lead, the lead concentration present in the undiluted sample was 0.2 p.p.m. or 20 $\mu g/100\ cm^3$. As this compared well with a direct analysis, it was considered unnecessary that each blood sample should be analyzed by means of lead additions. Other considerations were that the total solids in blood are 19–23%[10] and the total percentage of inorganic materials less than that, so that the quantity of solid sample finally analyzed is far below the limit of 1 mg set by Massmann[8] where interferences may be serious. Furthermore, it had been demonstrated that even blood samples with low lead levels could be diluted before analysis.

The coefficient of variation calculated on 11 analyses of the same sample was 10.5%, which falls within the range of 4–12% mentioned by Massmann[8], and is quite adequate for the purpose of the particular analysis. With the use of some kind of background correction, the reproducibility of the method could be improved.

When the 283.3-nm resonance line is used, the detection limit for lead may be conservatively set at 0.5 ng.

Table III gives the lead concentrations in the blood of five workers in a lead mine. The samples were also analyzed in the mine laboratories by means of a colorimetric method involving dithionate. Considering the very low concentrations determined, the agreement between the two sets of results may be regarded as fair.

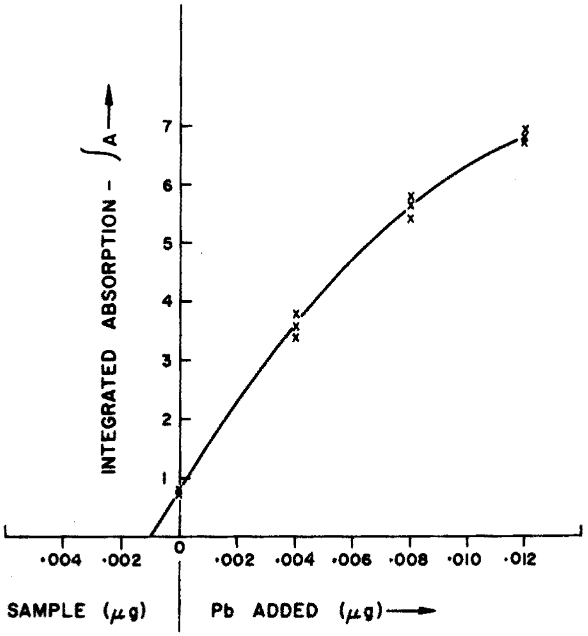

Fig. 7. Analysis of diluted blood sample by means of the method of additions.

TABLE III

LEAD CONCENTRATIONS (μg/100 g) IN THE BLOOD OF WORKERS IN A LEAD MINE

Sample no.	*Cuvette method*	*Colorimetric method*
1	126	130
2	109	110
3	44	25
4	59	55
5	67	55

In conclusion it may be said that the cuvette technique for the determination of lead in whole blood is much more rapid than present techniques. Done in batches of 20 samples (each analyzed in duplicate), the whole series can be completed in about 5 h. On a routine basis, considerably more samples could be analyzed in the same time. The use of very small quantities of sample has obvious advantages for purposes of routine screening. Very little sample preparation is needed and as the ashing is done in the cuvettes, the possibilities of contamination are kept to a minimum.

SUMMARY

The use of the high-temperature graphite tube with atomic absorption constitutes an exceptionally sensitive analytical method. Since only very small quantities of sample are needed, this method is highly suitable for the determination of lead in whole blood, especially when blood must be drawn from children. A technique which requires little preparation of the sample has been developed for such determinations. The graphite tube system developed can be used on any of a number of atomic absorption spectrophotometers and is better suited to routine analyses than the methods of L'vov and Massmann who pioneered the use of graphite tubes.

RÉSUMÉ

L'absorption atomique avec tube de graphite, à haute température, constitue une méthode d'analyse exceptionnellement sensible. Cette méthode convient très bien pour le dosage du plomb dans le sang, spécialement lorsqu'il s'agit d'enfants, car elle ne nécessite que de très petites quantités d'échantillons. Le système proposé convient mieux aux analyses de routine que les méthodes avec tube de graphite proposées précédemment par L'vov et Massmann.

ZUSAMMENFASSUNG

Die Anwendung einer Graphitrohr-Küvette für hohe Temperaturen bei der Atomabsorption ergibt eine aussergewöhnlich empfindliche analytische Methode. Da nur sehr geringe Probenmengen benötigt werden, eignet sich diese Methode besonders für die Bestimming von Blei in Blut, vor allem wenn das Blut von Kindern entnommen werden muss. Es wurde für solche Bestimmungen ein Verfahren entwickelt, das nur eine geringe Vorbereitung der Probe erfordert. Das entwickelte Graphitrohrsystem kann an zahlreichen Atomabsorptions-Spektrophotometern verwendet werden, und es eignet sich besser für Routineanalysen als die Methoden von L'vov und Massmann, die die Anwendung von Graphitrohr-Küvetten einführten.

REFERENCES

1 D. BRYCE-SMITH, *Chem. Br.*, 7 (1971) 54.
2 A. A. MONCRIEFF, O. P. KOUMIDES, B. E. CLAYTON, A. D. PATRICK, A. G. C. RENWICK AND G. E. ROBERTS, *Arch. Dis. Child.*, 39 (1964) 1.
3 J. B. HURSH, A. SCHRAUB, E. L. SATTLER AND H. P. HOFMANN, *Health Phys.*, 16 (1969) 257.
4 A. A. CERNIK, *Br. J. Ind. Med.*, 24 (1967) 289.
5 P. P. DONOVAN AND D. T. FEELEY, *Analyst*, 94 (1969) 879.
6 H. T. DELVES AND P. E. VINTER, *J. Clin. Pathol.*, 19 (1966) 504.
7 B. V. L'VOV, *Spectrochim. Acta*, 24B (1961) 53.
8 H. MASSMANN, *Rev. GAMS*, 4 (1968) 193.
9 H. T. DELVES, *Analyst*, 95 (1970) 431.
10 P. B. HAWK, B. L. OSER AND W. H. SUMMERSON, *Practical Physiological Chemistry*, 13th Edn., McGraw-Hill, New York, 1954, p. 468.
11 L. J. GOLDWATER AND A. W. HOOVER, *Arch. Environ. Health*, 15 (1967) 60.
12 H. L. KAHN AND J. S. SEBESTYEN, *At. Absorpt. Newsl.*, 9 (1970) 33.
13 L. COGHI AND E. BELLELI, *Ann. Ig. Microbiol. (Rome)*, 18 (1967) 1.
14 N. I. SAX, *Dangerous Properties of Industrial Materials*, 2nd Edn., Reinhold, New York, 1966, p. 931.
15 A. L. MILLS, *Chem. Br.*, 7 (1971) 160.

Analytica Chimica Acta
Elsevier Publishing Company, Amsterdam
Printed in The Netherlands

THE USE OF A GLOW-DISCHARGE LAMP AS A LIGHT SOURCE IN THE SPECTROMETRIC ANALYSIS OF GOLD

H. JÄGER
National Physical Research Laboratory, CSIR, Pretoria (South Africa)

(Received 5th July 1971)

There are various surveys on glow-discharge and cathode sputtering[1-3]. This kind of discharge is used for analytical purposes in the hollow-cathode lamp[4]. The present work deals with the practical application of the glow-discharge lamp developed by Grimm[5]. As the lamp is relatively well known, a description is not necessary, but it should be mentioned that the sample material is removed by cathodic sputtering in an argon atmosphere (2–20 Torr) and excited to light emission in the negative glow.

Gold with silver and copper contents in the per cent range and with lead and other impurities in the trace range, have been investigated. This report deals only with the gold–silver–copper system.

EXPERIMENTAL

Apparatus and samples

Data were obtained from a direct-reading 2-m grating spectrograph (RSV). Table I shows the spectral lines used.

TABLE I

ANALYTICAL LINES

Element	*Line and wavelength (Å)*	*Excitation energy (eV)*
Silver	Ag I 3382.89	3.66
Copper	Cu I 3247.54	3.82
Gold	Au I 3122.78	5.10

The glow-discharge lamp (RSV) was operated at constant argon pressure (3 Torr), constant voltage, and variable current (pulsed with 50 c.p.s.). The integration time was 30 sec, but a 10-sec integration time normally suffices for routine operation. Special gold standards were available containing constant amounts of silver and copper.

Calibration curves

The calibration curves for silver and gold obtained at constant integration time are shown in Figs. 1 and 2. The calibration curves for copper are similar to those

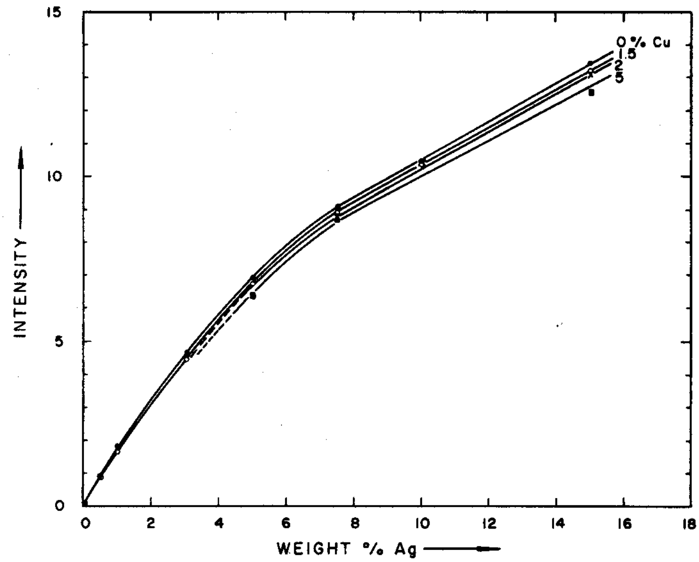

Fig. 1. Calibration curves for silver in Au–Ag–Cu alloys at constant integration time (3 Torr).

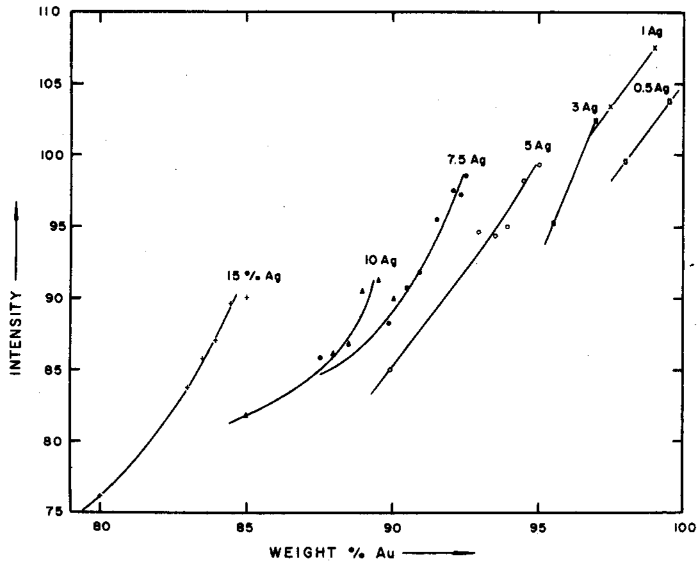

Fig. 2. Calibration curves for gold in Au–Ag–Cu alloys at constant integration time (3 Torr).

for silver. From these results it is obvious that the curves are non-linear, and that they split as a function of a third partner.

The curves cannot be used for routine analyses because of unsatisfactory reproducibility in spite of the small standard deviation of a single measurement.

Therefore, a mathematical treatment of the measured data has been introduced, and this will be described and discussed.

TREATMENT OF DATA

For the analysis of high alloys, where the composition of the alloying elements varies considerably, the use of one of these elements as an internal standard is not practicable. The sputtering rate in the glow-discharge has been taken as reference for the present problem. This is possible because the sample removal by sputtering is steady and controllable.

The emitting plasma of the glow-discharge source consists of argon and metal vapour. The emitting line intensity I is proportional to the number of particles n in the plasma. If the metal component consists of elements A, B and C, then

$$I_A \sim n_A, \quad I_B \sim n_B, \quad I_C \sim n_C$$

On multiplication of I_A, I_B, and I_C by factors a, b and c, respectively, so that the condition

$$a\,I_A : b\,I_B : c\,I_C = C_A : C_B : C_C$$

is fulfilled, where C_A, C_B and C_C are the respective concentrations of A, B and C in the sample, the sputtering rate S is defined as

$$a\,I_A + b\,I_B + c\,I_C = S$$

The conversion factors a, b and c are obtained by measuring a standard sample with known concentrations:

$$a = (C_A/I_A)_{\text{standard}} \quad b = \ \ldots.$$

All intensities of unknown samples are then referred to constant sputtering rates which have been determined for each sample:

$$J_A = \frac{aI_A}{S} \quad J_B = \frac{bI_B}{S} \quad J_C = \frac{cI_C}{S}$$

This method does, of course, require the complete analysis of the investigated material.

RESULTS

Improved analysis

The transformation of the data (from Figs. 1 and 2) leads to the calibration curves shown in Figs. 3 and 4. The calibration curves for silver (Fig. 3) are still non-linear and split, but the splitting direction has changed. The calibration curves for copper are again similar. The calibration curves for gold (Fig. 4) are now a well arranged system of single curves for constant concentrations of silver and copper.

This system contains all the information necessary for the determination of gold, silver and copper. A computer program* has therefore been written to solve the problem of analysis. In the program used, normalized intensity values are calculated as outlined above, and then the coefficients of the mathematical functions needed

---

* An IBM 360/65 computer was used for all calculations. Copies of the computer programmes used can be obtained from the authors.

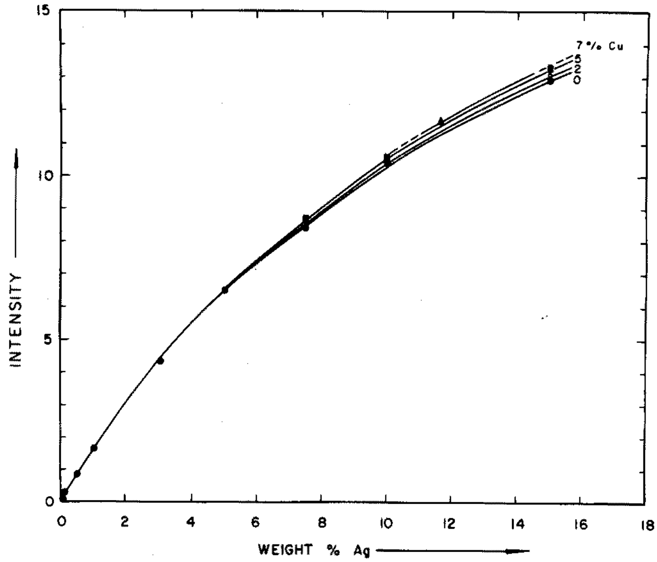

Fig. 3. Calibration curves for silver in Au–Ag–Cu alloys with the sputtering rate as reference (3 Torr).

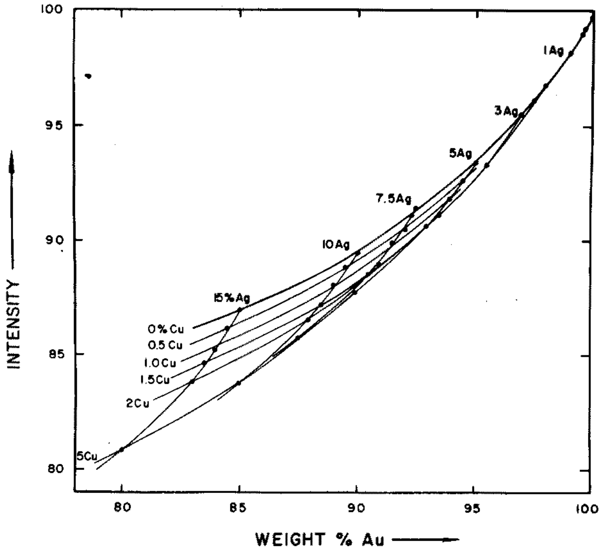

Fig. 4. Calibration curves for gold in Au–Ag–Cu alloys with the sputtering rate as reference (3 Torr).

to reproduce the calibration curves shown in Fig. 4 are calculated, using the line intensities and concentrations of gold standards; finally the concentrations of gold, silver and copper in unknown samples are calculated. The accuracy of this method is good (Table II).

Referring the data to the sputtering rate has the following advantages:

(*a*) because of the elimination of changes of the sputtering rate, the precision is very good (Table II);

TABLE II

PRECISION AND ACCURACY

Element	*Au*	*Ag*	*Cu*	
Relative standard deviation of single measurement	0.1 %	0.4 %	0.6 %	precision
Relative standard deviation of regression (variation from chemical value)	0.7%	0.5 %	0.5 %	accuracy

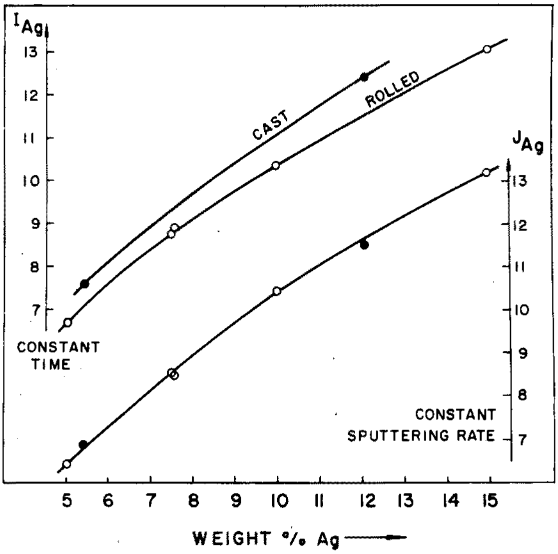

Fig. 5. Influence of the metallurgical history of the sample on the calibration curves of silver in Au–Ag–Cu alloys (3 Torr).

(*b*) the reproducibility of the whole analysis is excellent, as the conversion factors for the transformation of the intensities can be redetermined from a single standard sample as often as is required;

(*c*) the matrix element can be determined directly up to very high concentrations;

(*d*) metallurgical history effects (which will be dealt with later) can be eliminated.

It should further be mentioned that the same characteristic calibration curves also appear when other lamp conditions are used. The lamp was tested particularly at higher pressure (9 Torr), but the results were the same as at 3 Torr. The calibration curves were also calculated in atomic per cent. The curves showed neither a qualitative nor a quantitative difference and the accuracy of the analysis could not be improved. The use of atomic per cent has, therefore, been excluded.

Metallurgical history

The analysis of metals by the aid of the glow-discharge is influenced by the metallurgical history of the material. Samples of the same composition, but pretreated in different ways (orientation of the structure of a cast sample, *e.g.*, by rolling), have different barriers to removal by cathode sputtering.

This problem has been studied with cast and rolled gold samples of the same composition. Figure 5 shows calibration curves for silver in gold (copper concentration constant). At constant integration time the curves split since the rolled samples emit less radiation than the cast ones. Relating intensity values to the sputtering rate brings the intensities of all samples to a common calibration curve. The sputtering rate of a rolled sample is thus less than that of a cast one. The same result has been established for calibration curves for gold and copper.

Indeed, this effect can only be eliminated at low pressure (3 Torr) when reference is made to the sputtering rate; at high pressure (9 Torr) the results also improve, but less so than in the above case.

DISCUSSION

The discharge in the glow lamp used is a so-called abnormal one[6], distinguished by positive current–voltage characteristics. The variables, current, voltage, and pressure, are here determined by the type of sample and its composition. Figure 6 shows typical dependences of these variables on the gold content (and also on the content of impurities in the samples). In all cases and in every possible range of the variables, there are unambiguous functions which are very marked especially at

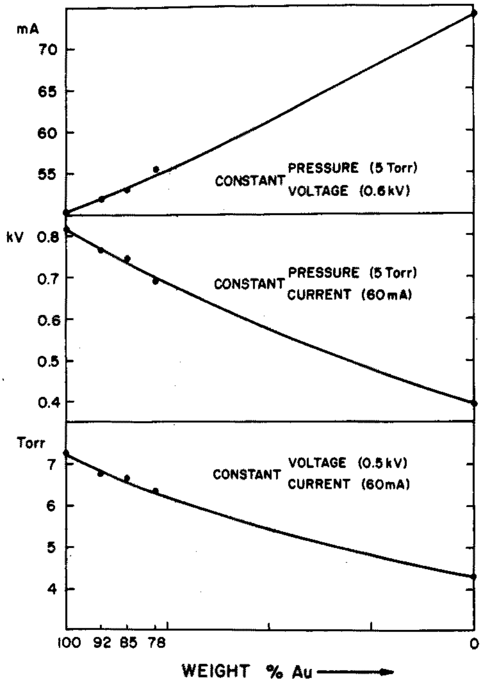

Fig. 6. Characteristic dependences of the discharge parameters on the composition of gold alloys (data of voltage and current are measured in pulse operation).

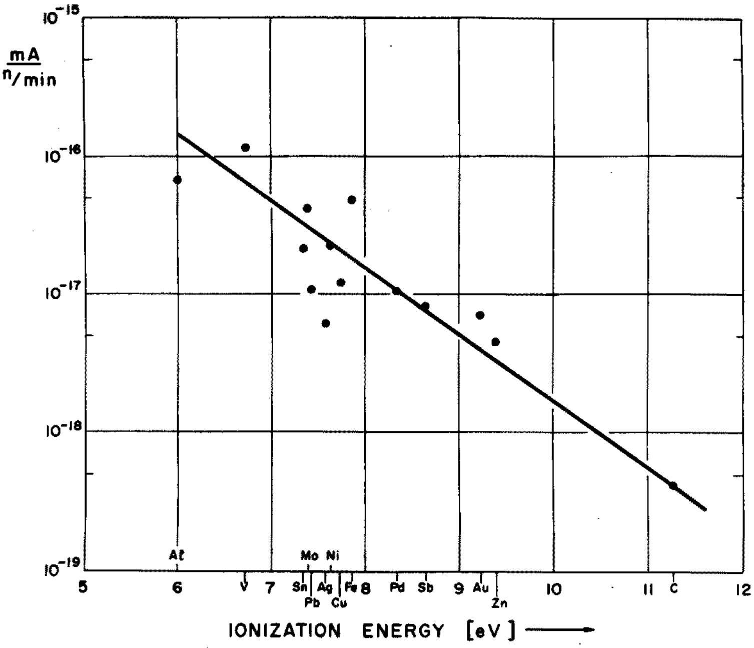

Fig. 7. Normalized discharge current as a function of the ionization energy of the sample element.

higher pressures, so that they are usable calibration curves for rough analyses. As the intensity of emission is a function of the discharge parameters, which are determined by the sample composition, the reason for non-linear and split calibration curves must be found in the changing discharge (third partner effect in the plasma).

To clarify this effect, the sputtering rates of pure elements were measured quantitatively by weighing (constant pressure and voltage). The loss of weight of the samples was converted to number of particles and the actual measured discharge current intensities were related to constant sputtering rate (particle/time). The current intensities normalized in this way are plotted in Fig. 7 against the ionization energies of the elements. A function linear over more than two decimals results. In detail, however, it shows relatively large variations. These are explained by the fact that the measured electron current is composed of both electrons released from the cathode and electrons originating in the plasma, the ratio differing from element to element. The electrons formed by impact ionization in the plasma come from argon and sample atoms. The higher the proportion of electrons from the sample material, the lower must be the ionization energy of the sample element, because the ionization energy of argon (15.74 eV) is relatively high. At constant voltage, therefore, the ionization energy of the sample element mainly determines the discharge current intensity

This result can also be applied to alloys. The components of gold alloys differ strongly in their ionization energies (Au 9.22 eV, Cu 7.72 eV, Ag 7.57 eV). At constant burning voltage the current thus increases with increasing copper and silver concentration in the gold sample.

The influence of changing discharge parameters on the emission will be the subject of further investigations.

The author would like to record his gratitude for the support received from the Rand Refinery of the Tvl. and O.F.S. Chamber of Mines (South Africa).

SUMMARY

A spectrographic method has been developed to analyse gold alloys with a glow-discharge lamp as a light source. The measured line intensities are referred to the constant sputtering rate of the sample. The method shows very good accuracy and reproducibility. Direct determination of all sample components including the matrix element, is possible. The effects of metallurgical history are suppressed. Calibration curves can be programmed in spite of a third partner effect. The reason for the third partner effect is investigated and the influence of the sample composition on the discharge is discussed.

RÉSUMÉ

On propose une méthode de dosage spectrographique pour l'analyse d'alliages d'or, à l'aide d'une lampe à décharge incandescente, comme source lumineuse. Les intensités de raies mesurées dépendent du degré de pulvérisation cathodique de l'échantillon. Cette méthode présente une très bonne exactitude et reproductibilité et permet le dosage direct de tous les constituants de l'échantillon, sans être influencé par le traitement métallurgique préliminaire. Les courbes d'étalonnage peuvent être transmises à un ordinateur.

ZUSAMMENFASSUNG

Die Glimmentladungslampe wird als Lichtquelle für die spektroskopische Analyse von Gold verwendet. Die gemessenen Linienintensitäten werden auf die Abbaurate der Probe als internen Standard bezogen. Diese Analysenmethode ist charakterisiert durch hohe Genauigkeit und Reproduzierbarkeit, direkte Bestimmung sämtlicher Probenkomponenten und durch die Unterdrückung von Einflüssen durch die metallurgische Vorbehandlung der Probe. Es ergeben sich programmierbare Eichkurven trotz eines Interelementseffektes, der diskutiert wird.

REFERENCES

1 A. Guentherschulze, *Vacuum*, 3 (1953) 360.
2 G. K. Wehner, *Proc. Fifth Conf. on Ionis. Phen. in Gases, Munich, 1961*, North-Holland, Amsterdam, 1962, p. 1141.
3 M. Kaminsky, *Atomic and Ionic Impact Phenomena on Metal Surfaces*, Springer Verlag, Berlin, Heidelberg, New York, 1965.
4 G. Knerr, J. Maierhofer and A. Reis, *Z. Anal. Chem.*, 229 (1967) 241.
5 W. Grimm, *Spectrochim. Acta*, 23 B (1968) 443.
6 G. Francis, *Handbuch der Physik*, Band XXII, Springer Verlag, Berlin, Göttingen, Heidelberg, 1956, p. 53.

Analytica Chimica Acta
Elsevier Publishing Company, Amsterdam
Printed in The Netherlands

ZUR BERECHNUNG VON INTERELEMENTEFFEKTEN BEI DER RÖNTGENFLUORESZENZSPEKTRALANALYSE

K. H. GROTHE UND H. RACKUR
Institut für Anorganische Chemie, TU Hannover (Deutschland)

(Eingegangen den 2. August 1971)

Bei der quantitativen Röntgenfluoreszenzanalyse nach dem üblichen Verfahren ist die Intensität der Röntgenfluoreszenzstrahlung eines Elementes im allgemeinen der Konzentration nicht direkt proportional sondern weicht durch Wechselwirkung mit anderen Elementen der Probe (Matrixeffekte) mehr oder weniger stark von der Linearität ab. Die Abweichung wird von folgenden Faktoren bestimmt: (a) Durch Absorptionseffekte innerhalb der Probe. Sie treten auf, wenn sich der Gesamtmassenschwächungskoeffizient mit der Zusammensetzung der Probe ändert. (b) Durch sogenannte Sekundäranregungseffekte. Sie treten auf, wenn die charakteristische Strahlung eines der Probenelemente ein anderes Probenelement zusätzlich zu der von aussen einfallenden Strahlung innerhalb der Probe anzuregen vermag.

Wir haben bereits früher dargelegt[1], dass die Bestimmung des Intesitätsanteils einer Röntgenfluoreszenzlinie, der durch Sekundäranregungseffekte hervorgerufen wird, sich auf experimentellem Wege allein nicht bestimmen lässt, und dass verschiedene Wege eingeschlagen worden sind, diesen Anteil rechnerisch zu bestimmen. Nach unseren ersten Vorschlägen zu einer vereinfachten Ermittlung dieses Anteils an der Sekundäranregung durch Vergleich von theoretischen Berechnungen mit experimentellen Ergebnissen soll in dieser Arbeit eine weitere Vereinfachung der mathematischen Behandlung des Problems beschrieben und die Brauchbarkeit dieser Methode gezeigt werden.

GRUNDLAGEN

Formeln für die Berechnung von Röntgenfluoreszenzintensitäten und die Voraussetzungen für die Gültigkeit dieser Formeln sind bereits früher ausführlich besprochen worden[2]. Es gilt folgende Beziehung für die als Bündel parallelen Lichts austretende Fluoreszenzintensität I_f des Elements x an der Probenoberfläche:

$$I_{fx} = \frac{I_e c_x \varepsilon_x (\mu/p)_{ex}/\cos\varphi_1}{(\mu/\rho)_e/\cos\varphi_1 + (\mu/\rho)_{fx}/\cos\varphi_2} \qquad (1)$$

Dabei ist:
c_x = Konzentration des Elements x in einer praktisch unendlich dicken Probe.
ε_x = der Emissionskoeffizient des Elements x.
I_e = Intensität einer als Bündel parallelen Lichts in die Probe einfallenden monochromatischen Strahlung.

μ/ρ = Massenschwächungskoeffizient der Probe, welcher sich additiv aus dem Massenschwächungskoeffizienten der Elemente der Probe zusammensetzt.
φ_1 = Einfallswinkel
φ_2 = Ausfallswinkel
e = Index für Grössen der einfallenden Strahlung
f = Index für Grössen der ausfallenden Strahlung
x = Index für Grössen, die sich auf das Element x beziehen.

Die in Gleichung (1) enthaltenen Grössen lassen sich in zwei Gruppen aufteilen:

1. Grössen, deren Wert unabhängig von der Konzentration des Elements x ist: I_e, ε_x und $(\mu/\rho)_{ex}$.

2. Grössen, deren Wert sich mit der Zusammensetzung der Probe ändert: c_x, $(\mu/\rho)_e/\cos\varphi_1$ und $(\mu/\rho)_{fx}/\cos\varphi_2$.

Bei der Anwendung der Gleichung (1) kommt es in dieser Arbeit nicht auf eine zahlenmässige Übereinstimmung zwischen berechneten und gemessenen Fluoreszenzintensitäten an. Es genügt vielmehr, wenn zwischen beiden konzentrationsunabhängige Proportionalität besteht. Deshalb können alle konzentrationsunabhängigen Glieder in einer Konstanten zusammengefasst werden:

$$K_x = I_e \varepsilon_x (\mu/\rho)_{ex}$$

Berücksichtigt man, dass bei der von uns für die Experimente benutzten Apparatur $\varphi_1 = \varphi_2$ ist, und setzt man

$$M_x = (\mu\rho)_e + (\mu/\rho)_{fx}, \tag{2}$$

so erhält Gleichung (1) folgende Form:

$$I_{fx} = \frac{K_x c_x}{M_x} \tag{3}$$

Methode zur Berechnung der Sekundäranregung

Eine wesentliche Voraussetzung für die Ableitung der Gleichung (1) besagt, dass keine Sekundäranregung stattfinden soll. In Wirklichkeit treten jedoch solche Sekundäranregungseffekte sehr häufig auf. Das ist z.B. bis zur Ordnungszahl 60 immer bei den K-Linien solcher Elementepaare der Fall, die sich nur um eine Ordnungszahl unterscheiden. Hier ist die Kβ-Linie des Elements mit der Ordnungszahl Z kürzerwellig als die K-Kante des Elements mit der Ordnungszahl $Z-1$ und vermag deshalb das letztere Element innerhalb der Probe anzuregen, also Sekundäranregungseffekte hervorzurufen. Am Beispiel solcher Zweikomponentenmischungen benachbarter Elemente soll gezeigt werden, wie die Bestimmung des relativen Anteils der Sekundäranregung an der Gesamtfluoreszenzintensität durchgeführt werden kann.

Werden bei der Methode des inneren Standards die Intensitätsverhältnisse $I_v = I_{fy}/I_{fx}$ der K$\alpha_{\frac{1}{2}}$-Linien experimentell bestimmt und theoretisch berechnet, so müssen die Ergebnisse Unterschiede aufweisen, da bei der Berechnung die Sekundäranregung nicht berücksichtigt wird. Auf Grund dieser Unterschiede lässt sich der relative Anteil der Sekundäranregung auf folgende Weise ermitteln.

Zum Vergleich des gemessenen Intensitätsverhältnisses ${}_gI_v$ mit dem berechneten ${}_bI_v$ bildet man zunächst den Quotienten Q aus beiden und bezieht ihn auf den gleichen Ort, nämlich die Probenoberfläche. Es gilt dann folgende Beziehung:

$$Q = L\,{}_gI_v \frac{K_x c_x M_y}{K_y c_y M_x} = \frac{L\,{}_gI_v}{K_v c_v M_v} = \frac{L}{K_v}\frac{{}_gI_v}{{}_bI_v} = \frac{L}{K_v} P \tag{4}$$

L ist ein konzentrationsunabhängiger Faktor, durch den die gemessene Fluoreszenzintensität auf die Probenoberfläche korrigiert wird.

Unter der Annahme, dass keine Anregung durch die Kβ-Strahlung des Elements x vorliegt, ist P konstant, da sich dann Zähler und Nenner mit wechselndem Mischungsverhältnis in gleichem Masse ändern. Für diesen Fall sollen die Quotienten Q_0 bzw. P_0 genannt werden.

Tatsächlich ist jedoch die Sekundäranregung der Kα_1-Linie des Elements Y von der Konzentration c_x abhängig. Daraus folgt, dass die Differenz $Q-Q_0$ ein Mass für diese Sekundäranregung ist. Für den relativen Anteil E (enhancement) der Sekundäranregung an der Gesamtanregung ergibt sich dann die Beziehung

$$E = \frac{Q-Q_0}{Q} = \frac{P-P_0}{P} \tag{5}$$

L und K_v entfallen durch Kürzen. P_0 erhält man durch Auftragen von P gegen c_x und Extrapolation auf $c_x=0$.

Vereinfachte Berücksichtigung der Massenschwächungskoeffizienten

Bei der Ermittlung der Grösse P ist die Berücksichtigung der darin enthaltenen Massenschwächungskoeffizienten, d.h. die Berechnung von M_v in Gleichung (4) am aufwendigsten, wie man mit Hilfe der Abb. (1) erkennen kann. Dort sind schematisch die Massenschwägungskoeffizienten der Elemente x und y im Bereich ihrer K-Kanten in Abhängigkeit von der Wellenlänge, die jeweilige Fluoreszenzstrahlung und eine anregende Wellenlänge aufgetragen. Für M_v erhält man dann mit den Bezeichnungen der Abb. (1)

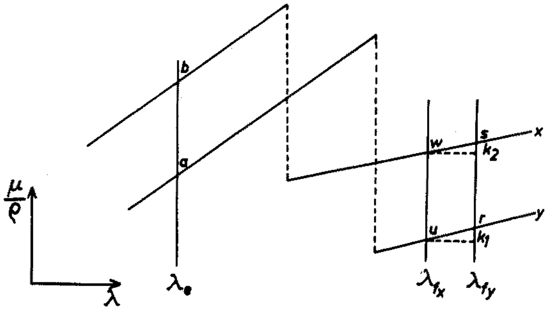

Abb. 1. Schematische Darstellung der Massenschwächungskoeffizienten μ/ρ, der anregenden Strahlung λ_e und der Fluoreszenzlinien λ_f in Abhängigkeit von der Wellenlänge im Bereich der K-Kanten für die Elemente x und y.

$$M_v = \frac{ac_y + bc_x + uc_y + wc_x}{ac_y + bc_x + rc_y + sc_x} \tag{6}$$

Diese Gleichung lässt sich unter bestimmten Voraussetzungen vereinfachen. In erster Näherung ist $k=k_1=k_2=r-u=s-w$. Kürzt man durch c_x und setzt für das Verhältnis $c_x/c_y=c_v$, dann ist:

$$M_v = \frac{c_v(a+u)+b+w}{c_v(a+u+k)+b+w+k}$$

Weiterhin gilt in erster Näherung, da a und b gross gegenüber $a-b$ sind, $a+u=b+w=A$. Kürzt man durch k und setzt $A/k=B$, so erhält man schliesslich

$$M_v = \frac{c_vB+B}{c_v(B+1)+(B+1)} = \frac{B}{B+1} \tag{7}$$

Das bedeutet, dass unter den angegebenen Voraussetzungen M_v vom Konzentrationsverhältnis unabhängig ist.

Für eine Serie von Mischungen zweier Elemente wird das Intensitätsverhältnis ${}_bI_v = c_vM_v$ berechnet, indem man nur einmal B bildet und aus einer für alle Fälle geltenden graphischen Darstellung, in der M_v gegen B aufgetragen ist (siehe Abb. 2), den zugehörigen M_v-Wert abliest. Dabei ist es zweckmässig, für A und k jeweils Mittelwerte ($A=(a+u+b+w)/2$; $k=(k_1+k_2)/2$) aus Tabellenwerten zu bilden, um den durch die Vereinfachungen verursachten Fehler gering zu halten.

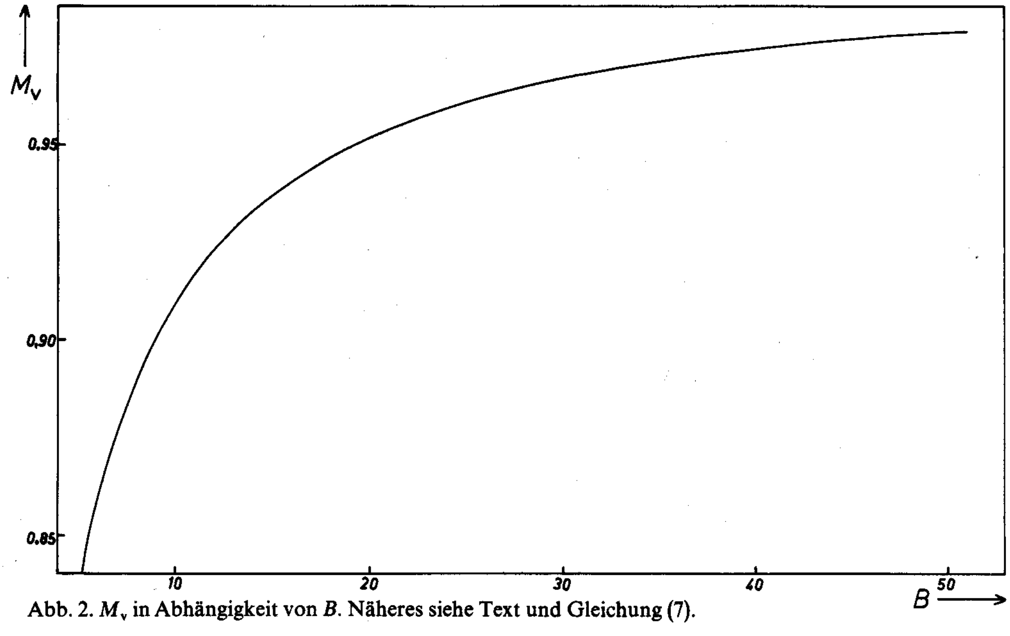

Abb. 2. M_v in Abhängigkeit von B. Näheres siehe Text und Gleichung (7).

Für die Elementepaare Co–Ni, Ni–Cu, Cu–Zn, Ga–Ge und Y–Zr und für die Konzentrationsbereiche von 1–99 Gew.-% für c_x, wurde M_v für verschiedene Wellenlängen λ_e mit Hilfe von Tabellen[3] einmal nach der Gleichung (6) und zum anderen nach Gleichung (7) bzw. mit der Abb. 2 ermittelt.

Es zeigte sich, dass die Abweichungen zwischen den graphisch ermittelten Werten mit denen nach Gleichung (6) berechneten in allen Fällen kleiner als 0.1% waren. Die Übereinstimmung ist besser als die Richtigkeit der in den Tabellen angegebenen Werte für die Massenschwächungskoeffizienten.

EXPERIMENTELLES

Die Proben wurden aus reinen Substanzen (99.9% Y_2O_3, 99.5% $ZrOCl_2$, 0.5% $HfOCl_2$) hergestellt, indem Lösungen unter Rühren in einem Guss (homogene Fällung) in überschüssige Ammoniak-Lösung gegeben wurden. Die gefällten Hydroxide wurden filtriert, bei 1000° verglüht und in einer Achatreibschale sorgfältig verrieben.

Die Metallkonzentrationen der oxidischen Mischungen werden in Gewichtsprozenten angegeben, wobei die Summe der Metalle gleich 100% gesetzt wird. Bei den Berechnungen wurde der Sauerstoff der oxidischen Mischungen nicht berücksichtigt, da sowohl wegen seines geringen Massenschwächungskoeffizienten als auch durch die Verwendung der Methode des inneren Standards hierdurch keine nennenswerten Fehler auftreten.

Es wurden folgende Geräte der Fa. Siemens und Halske, Karlsruhe, verwendet: Als Hochspannungserzeuger der Kristalloflex IV; eine Wolframröhre vom Typ AG W 60; ein Vakuum-Zählrohr-Goniometer mit LiF-Kristall und Ein- und Austrittswinkel an der Probe von je 45°; ein Scintillationszähler in Kombination mit einem Strahlungsmessgerät Typ GS.

Bei der Messung der Intensität der $K\alpha_{\frac{1}{2}}$-Fluoreszenzlinien wurden mit besonderer Sorgfalt folgende Punkte beachtet: (*a*) Die gemessene Untergrundsintensität muss der an der Stelle des Linienmaximums entsprechen. Fehler bei der Untergrundbestimmung wirken sich besonders im Bereich kleiner Konzentrationen auf die Berechnung von E aus. Die Bestimmung des Untergrunds ist dann richtig, wenn bei der Auftragung von I_v gegen c_v die Kurve durch den Koordinatenursprung verläuft. (*b*) Die Intensität im Linienmaximum muss der Fläche unter der Linie proportional sein.

Bestimmung der Sekundäranregung

Zur Bestimmung der Sekundäranregung wurde die experimentelle Bestimmung des Intensitätsverhältnisses $_gI_v$ (Gleichung 4) bei 25 und 50 kV Röhrenspannung

TABELLE I

GEMESSENE INTENSITÄTSVERHÄLTNISSE $_gI_v = I_{YK\alpha_{1/2}}/I_{ZrK\alpha_{1/2}}$ FÜR VERSCHIEDENE KONZENTRATIONSVERHÄLTNISSE $c_v = c_Y/c_{Zr}$ BEI UNTERSCHIEDLICHEN RÖHRENSPANNUNGEN

c_v	25 *kV*		50 *kV*	
	$_gI_v$	s_r[a] (%)	$_gI_v$	s_r[a] (%)
99.0	111	3.7	91.6	2.5
49.0	55.6	2.6	45.4	1.6
32.3	37.2	1.5	29.9	1.1
9.00	10.9	0.6	8.68	0.7
1.00	1.38	0.3	1.05	0.4
0.111	0.195	0.5	0.141	0.7
0.0309	0.0591	1.3	0.0417	1.1
0.0204	0.0399	1.8	0.0295	1.4
0.0101	0.0219	2.7	0.0167	2.1

[a] Relative Standardabweichung.

für das Elementepaar Y–Zr durchgeführt. In der Tabelle I sind die Ergebnisse für verschiedene Konzentrationsverhältnisse aufgeführt. Die Verringerung des Intensitätsverhältnisses ${}_{g}I_{v}$ bei verdoppelter Röhrenspannung U erscheint sinnvoll, da hierdurch eine Verschiebung der Grenzwellenlänge und der grössten spektralen Intensität des Bremsspektrums zu kürzeren Wellenlängen hin erfolgt und dadurch die ZrK$\alpha_{\frac{1}{2}}$-Linie relativ stärker angeregt wird (kürzere K-Kante) als die YK$\alpha_{\frac{1}{2}}$-Linie.

Die Berechnung der Intensitätsverhältnisse ${}_{b}I_{v}$ der in Tabelle I aufgeführten Proben erfolgte entsprechend Gleichung (4) nach der Beziehung ${}_{b}I_{v}=c_{v}\,M_{v}$ unter Zuhilfenahme der Abb. 2 für die Bestimmung von M_{v}. Der Faktor K_{v} brauchte nicht berücksichtigt zu werden, da er bei der Ermittlung von E fortfällt. Anstelle der in der Praxis anregenden polychromatischen Strahlung wurde bei der Berechnung (entsprechend den obigen Voraussetzungen) mit einer monochromatischen anregenden Strahlung einer sog. effektiven Wellenlänge gerechnet, die man sich als eine Art Schwerpunkt des gesamten anregenden Spektrums vorstellen kann. Als effektive Wellenlänge wurden 0.4 Å und 0.6 Å gewählt, die etwa den Maxima der Bremsspektren für 25 und 50 kV entsprechen. Die berechneten Werte sind in Tabelle II wiedergegeben.

Auch bei den theoretischen Berechnungen der Intensitätsverhältnisse tritt, wenn auch in geringerem Masse, der bereits beim experimentellen Bestimmen von Intensitätsverhältnissen beobachtete Effekt auf, dass beim Verschieben der anregenden Wellenlänge zu kürzeren Wellenlängen hin die ZrK$\alpha_{\frac{1}{2}}$-Linie relativ stärker angeregt wird als die YK$\alpha_{\frac{1}{2}}$-Linie. Der Effekt ist darauf zurückzuführen, dass mit kürzeren Wellenlängen (μ/ρ) kleiner wird und damit auch A bzw. B bzw. M_{v}.

TABELLE II

BERECHNETE INTENSITÄTSVERHÄLTNISSE ${}_{b}I_{v}=c_{v}\,M_{v}$ FÜR VERSCHIEDENE KONZENTRATIONSVERHÄLTNISSE $c_{v}=c_{Y}/c_{Zr}$ BEI UNTERSCHIEDLICHEN EFFEKTIVEN WELLENLÄNGEN

c_{v}	${}_{b}I_{v}$	
	$\lambda_{e}=0.6$ Å	$\lambda_{e}=0.4$ Å
99.0	95.5	92.2
49.0	47.3	45.6
32.3	31.2	30.1
9.00	8.68	8.38
1.00	0.964	0.931
0.111	0.107	0.103
0.0309	0.0298	0.0288
0.0204	0.0197	0.0190
0.0101	0.0097	0.0094

In der Abb. 3 sind die in den Tabellen I und II angegebenen bei 25 kV gemessenen und für $\lambda_{e}=0.6$ Å berechneten Intensitätsverhältnisse in doppelt logarithmischer Auftragung dargestellt. Nach der Gleichung ${}_{b}I_{v}=c_{v}\,M_{v}$ ergibt sich bei doppelt logarithmischer Auftragung für die berechneten Intensitätsverhältnisse eine Gerade mit der Steigung 1, da M_{v}, wie oben gezeigt wurde, von der Konzentration unabhängig ist.

Für die gemessenen Intensitätsverhältnisse findet man keine Gerade, da hier Sekundäranregungseffekte eingehen, die bei den berechneten Intensitätsverhältnissen

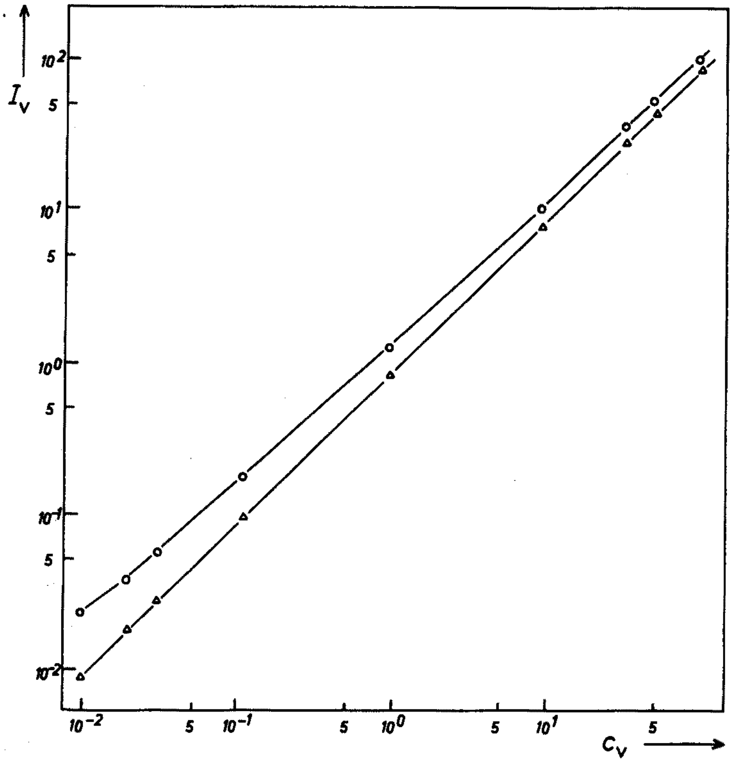

Abb. 3. Gemessene (○) und berechnete (△) Intensitätsverhältnisse I_v als Funktion des Konzentrationsverhältnisses c_v für 25 kV Röhrenspannung bzw. 0.6 Å effektiver Wellenlänge.

nicht berücksichtigt wurden. Eine zahlenmässige Übereinstimmung beider Geraden kann nicht erwartet werden, da K_v willkürlich gleich 1 gesetzt wurde.

Der Anteil der Sekundäranregung ergibt sich aus der Abweichung von der Parallelität beider Kurven. Diese Überlegungen sind auch Ausgangspunkt für die Entwicklung der Gleichung (5) zur Bestimmung des relativen Anteils E der Sekundäranregung an der Gesamtanregung.

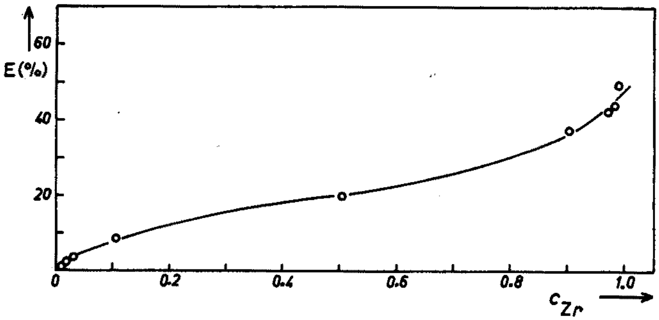

Abb. 4. Relativer Anteil E der Sekundäranregung (durch die ZrKβ-Strahlung hervorgerufen) an der Gesamtanregung der YKα_1-Fluoreszenzstrahlung in Abhängigkeit von der Zirkoniumkonzentration in Y–Zr-Mischungen bei 25 kV Röhrenspannung.

Bei hohen Zr-Konzentrationen weisen beide Kurven unterschiedliche Steigungen auf, während sie bei niedrigen Zr-Konzentrationen annähernd parallel verlaufen, da hier der Anteil der Sekundäranregung der $YK\alpha_{\frac{1}{2}}$-Linie durch die $ZrK\beta$-Fluoreszenzstrahlung nur noch gering ist.

Quantitative Werte für den relativen Anteil E der Sekundäranregung an der Gesamtanregung wurden mit Hilfe von Gleichungen (4) und (5) und den in Tabellen I und II angegebenen Werten für ${}_{g}I_{v}$ und ${}_{b}I_{v}$ ermittelt. Werte von E für 25 kV und für 50 kV sind in Tabelle III angegeben und in Abb. 4 für 25 kV graphisch dargestellt. Dem Kurvenverlauf ist zu entnehmen, in welchem Masse der relative Anteil der Sekundäranregung mit steigender Zr-Konzentration zunimmt. Wegen des steilen Anstiegs der Kurven bei hohen Zr-Konzentrationen ist eine graphische Extrapolation auf $c_{Zr}=1$ nicht vertretbar. E sollte jedoch nicht wesentlich grösser als 55% werden.

TABELLE III

RELATIVER ANTEIL E DER SEKUNDÄRANREGUNG AN DER GESAMTANREGUNG DER $YK\alpha_{\frac{1}{2}}$-FLUORESZENZSTRAHLUNG IN Y–Zr-MISCHUNGEN IN ABHÄNGIGKEIT VON DER ZIRKONIUMKONZENTRATION c_{Zr} FÜR UNTERSCHIEDLICHE RÖHRENSPANNUNGEN

c_{Zr} (*Gew.* %)	E (%)	
	25 *kV*	50 *kV*
1	1.2	0.1
2	2.3	0.2
3	3.8	0.3
10	8.5	4.1
50	19.6	11.5
90	36.9	27.0
97	42.1	31.4
98	43.5	36.1
99	49.1	43.9

DISKUSSION

Vergleicht man Ergebnisse dieser Arbeit mit früheren[1], die unter ähnlichen Bedingungen (18.5 kV Röhrenspannung), wenn auch mathematisch aufwendiger erhalten wurden, so fällt auf, dass bei Y–Zr-Mischungen der relative Anteil der Sekundäranregung an der Gesamtanregung gegenüber Co–Ni-Mischungen deutlich grösser ist. Bei $c_{v}=1$ beträgt z.B. E 20% bei Y–Zr-Mischungen und 10% bei Co–Ni-Mischungen. Die $ZrK\beta$-Strahlung muss demnach die YK-Kante relativ stärker anregen als die $NiK\beta$-Strahlung die CoK-Kante. Hierfür scheint der geringere Wellenlängenunterschied zwischen YK-Kante und $ZrK\beta_1$-Linie mit 0.026 Å gegenüber der vergleichbaren Differenz zwischen $NiK\beta_1$-Linie und CoK-Kante mit 0.106 Å verantwortlich zu sein, entsprechend der Regel: je näher die anregende Strahlung der Kante, desto grösser die Fluoreszenzintensität.

ZUSAMMENFASSUNG

Zur Berechnung von Interelementeffekten bei der Röntgenfluoreszenz-

spektralanalyse wird ein Verfahren beschrieben, bei dem mit einfachen mathematischen Mitteln sich der Anteil an der Gesamtanregung der Fluoreszenzstrahlung eines Elements errechnen lässt, der innerhalb der Probe durch Fluoreszenzstrahlung eines anderen Elements hervorgerufen wird. Das geschieht durch Vergleich von experimentellen Ergebnissen und theoretischen Berechnungen am Beispiel von Y–Zr-Mischungen, bei denen die $YK\alpha_{\frac{1}{2}}$-Linie durch die $ZrK\beta$-Strahlung angeregt wird. Der prozentuale Anteil dieser Anregung an der Gesamtanregung beträgt 9% bei 10 Gew.-% Zr, 20% bei 50 Gew.-% Zr und 40% bei 97 Gew.-% Zr.

SUMMARY

A method for the calculation of interelement effects in X-ray fluorescence spectroscopy is described. The percentage of the total excitation of the fluorescence of one element which is produced within the sample by fluorescence of another element, can be calculated by simple mathematical techniques. This is done by comparison of experimental results with theoretical calculations for the example of Y–Zr mixtures, in which the $YK\alpha_{\frac{1}{2}}$ line is excited by the Zr β radiation. The contribution of this excitation to the total excitation amounts to 9% for 10% Zr (by weight), 20% for 50% Zr and 40% for 97% Zr in the mixture.

RÉSUMÉ

Une méthode est proposée pour le calcul de l'influence d'interéléments en spectroscopie de fluorescence aux rayons-X. Le pourcentage d'excitation totale de fluorescence d'un élément, produit dans l'échantillon par fluorescence d'un autre élément, peut être calculé par simple formule mathématique. Les résultats expérimentaux concordent bien avec les calculs théoriques, pour les mélanges Y–Zr choisis comme exemples.

LITERATUR

1 K. H. GROTHE UND G. KRAUSE, *Z. Anal. Chem.*, 219 (1966) 54.
2 K. H. GROTHE UND G. KRAUSE, *Z. Anal. Chem.*, 216 (1966) 66.
3 R. THEISSEN UND D. VOLLATH, *Tabellen der Massenschwächungskoeffizienten von Röntgenstrahlen*, Verlag Stahleisen, Düsseldorf, 1967.

Analytica Chimica Acta
Elsevier Publishing Company, Amsterdam
Printed in The Netherlands

A SEMI-SOLID SURFACE FLUORESCENCE METHOD FOR THE DETERMINATION OF LACTATE DEHYDROGENASE

R. L. ZIMMERMAN, JR. AND G. G. GUILBAULT

Department of Chemistry, Louisiana State University in New Orleans, New Orleans, La. 70122 (U.S.A.)

(Received 30th June 1971)

Guilbault and Zimmerman[1] have reported the first successful solid-surface method for monitoring the rate of an enzyme reaction; the enzyme cholinesterase was determined. In the present paper a method for another clinically important enzyme, lactic dehydrogenase (LDH) is presented.

Before any serum samples were analyzed, the method was optimized for commercially available rabbit muscle LDH. The results of those experiments and the optimal conditions are reported.

Many authors have reported fluorimetric methods for the determination of both lactic acid[2], and LDH[3,4] by means of the enzyme-catalyzed reaction

$$\text{Li lactate} + \text{NAD} \xrightleftharpoons{\text{LDH}} \text{NADH} + \text{pyruvic acid} \tag{1}$$

or some variation of this reaction[5]. Bergmeyer *et al.*[6] have also described a method for the determination of serum LDH based on this equation; this method involves monitoring the disappearance of NADH at 340 nm. This standard assay procedure is compared to the method reported herein.

A technique described by Cabaud and Wroblewski[7] was used by the hospital from which the sera were obtained. The LDH values from this method were used as the "true" LDH content.

Vaughan and Guilbault[8] have developed a new and better cell design than that originally used by Guilbault and Zimmerman[1]. They also altered the pad design in order to enhance the reproducibility and accuracy of the semi-solid surface method. A third innovation they employed was the turning of the fluorimeter onto its side so that the pad, and drop of enzyme solution, would sit in a horizontal position in the fluorimeter. No adverse effects on the instrument were noted.

Normal ranges of the LDH content of healthy human blood serum have been reported by many authors to vary between 150 and 680 units per ml of serum[9-11]. Therefore, special attention was paid to samples possessing LDH values in this range. Sample values of LDH concentration were taken outside the above range in both directions for the commercial LDH, but the source of serum samples could not provide sera any lower than 160 units ml^{-1} at the time the analyses were performed. Sera with LDH values above 820 did not fit the linear calibration plot. Sera with LDH values between 620 and 820 were also not available.

EXPERIMENTAL

Instrumentation

All fluorescence measurements were made on an Aminco filter fluorimeter. The filter systems used were a Wratten 7-60 filter for the excitation wavelength and a Wratten 47B and 48 filter combination for the emission wavelength. A Heath Servo-Recorder (model EU-20B) was used to record all rates.

The fluorimeter was turned on its side for the reasons described above.

Syringes

Hamilton 50-μl syringes were used for all solution measurements. The syringe for the buffer solution was equipped with a Yale (regular point, 22G, 1″) luer-lok hypodermic needle; a Hamilton N72822 chromatographic hypodermic needle (luer-lok style) was used for all of the other solutions.

Fluorimeter cell holder

An Aminco-Bowman cell adapter (No. A6-63019), and the metal strip on which the pad was placed, was prepared as described by Vaughan and Guilbault[8].

Reagents for Bergmeyer's method

Phosphate–pyruvate solution. Dissolve 700 mg of dipotassium hydrogenphosphate and 3 mg of sodium pyruvate in 80 ml of triply distilled water (0.05 M phosphate, and $3.1 \cdot 10^{-4}$ M pyruvate at pH 7.5).

NADH solution. Dissolve 20 mg of NADH-Na_2 (Sigma Chemical Company) in 3.0 ml of the phosphate–pyruvate solution.

Reagents for fluorimetric method

NAD solution ($1 \cdot 10^{-3}$ M). Dissolve 6.6 mg of β-nicotinamide adenine dinucleotide (Sigma Chemical Company) in 10 ml of triply distilled water.

Lactate solution ($1 \cdot 10^{-3}$ M). Dissolve 1.0 mg of L (+)-lactic acid, lithium salt (Sigma Chemical Company) in 10 ml of triply distilled water.

Buffer. Loomis and Geho[12] have described a glycine buffer which not only gives the optimal pH for the reaction, pH 9.0, but also aids the progress of the reaction in the forward direction. Dissolve 18.77 g of glycine ethyl ester hydrochloride (Eastman Organic Chemicals) and 22.4 g of semicarbazide hydrochloride (Fisher Scientific Company) in *ca.* 400 ml of triply distilled water. Adjust to pH 9.0 with sodium hydroxide and dilute to 500 ml. The buffer was stable for about six weeks if kept refrigerated.

Enzyme solution. Lactate dehydrogenase (commercially available from Calbiochem; activity was 3850 I.U. ml^{-1}, as certified by the manufacturer, Lot No. 020066) standards were prepared by dissolving the appropriate volume of the LDH suspension in triply distilled water. Standards of 25, 100, 300, 500, 700, and 900 I.U. ml^{-1} were prepared.

Sera. All serum samples were obtained from Methodist Hospital, 5620 Read Road, New Orleans, La. No dilutions of the samples were made.

Preparation of silicone rubber pads

Vaughan and Guilbault[8] have described the physical structure of the pad. The same structure was used in this work.

Apply a 50-μl aliquot of the NAD solution to the pads, and evaporate over silica gel under reduced pressure, to produce a thin film of solid NAD on the surface of the pad. Then add a 20-μl aliquot of the lactate solution to the pad and evaporate similarly, to produce a thin film of solid lactate. Thus a thin film of solid NAD and lithium lactate on the silicone rubber surface was the final pad composition.

The pad can be stored over silica gel at atmospheric pressure, for over a month without any noticeable decomposition of the reactants.

PROCEDURES

The method of Bergmeyer *et al.* was applied as discussed previously[6]. The procedure for the new method was as follows.

Calibrate the fluorimeter daily by putting a 10-μl sample of a 10 μg ml^{-1} solution of quinine sulfate on a black pad and setting the sensitivity control of the instrument so that a reading of 57% transmittance on the 0.03 scale is obtained. The choice of this particular transmittance value is purely arbitrary. The pad should be permanently attached to one of the metal slides so that reproducible results are easier to obtain.

Place a pad in the proper position on the metal slide. Place a 10-μl aliquot of the buffer solution onto the pad, and spread it out so that the entire substrate film is dissolved in the drop of solution. Then set the metal slide in the fluorimeter, and record a background rate.

After recording the background for about 1 min, remove the slide from the instrument and place a 20-μl aliquot of either the commercially available enzyme solution or the serum solution, whichever is to be analyzed, onto the pad. Immediately place the slide back into the instrument, and record the fluorescence intensity.

Construct a calibration plot of the change in fluorescence units per min *versus* the enzyme concentration.

Analyze samples in a similar way.

RESULTS AND DISCUSSION

The results of the study on the commercially available LDH are shown in Table I. The slope of the line obtained from these data was $2.36 \cdot 10^{-2}$ ΔF min^{-1} c^{-1}, where c is the concentration expressed in terms of I.U. per ml. The results given by the commercially available LDH were considered excellent, and the adaptation of the method to the assay of LDH in blood serum was then studied. A standard assay as described by Bergmeyer *et al.*[6] was used to compare the quality of this method with that of an accepted method. The data and results of the Bergmeyer method and this method are given in Tables II and III, respectively.

The slopes of the lines obtained from the data for the Bergmeyer method and the proposed method are $5.64 \cdot 10^{-3}$ ΔF min^{-1} c^{-1} and $3.22 \cdot 10^{-2}$ ΔF min^{-1} c^{-1}, respectively.

Figure 1 shows clearly that the proposed method is more precise than the method proposed by Bergmeyer *et al.* The slopes of the lines show that the proposed method is over five times more sensitive than Bergmeyer's method, while the error is only one-eighth that of his method.

The pads could have been constructed of either translucent, black or grey silicone rubber. Therefore, a study was made as to which color would give the optimal

TABLE I

DATA[a] AND RESULTS OF THE ASSAY OF COMMERCIALLY AVAILABLE LDH (RABBIT MUSCLE) BY THE PROPOSED METHOD

Rate[b] (ΔF *min*$^{-1}$)	*Concentration taken* (*I.U. ml*$^{-1}$)	*Concentration found*[b] (*I.U. ml*$^{-1}$)	*Relative error* (%)
8.9	25	28	+13.0
10.5	100	107	+ 7.4
10.0[c]	100	86	−13.0
10.7	125	116	− 7.2
14.7	300	285	− 4.7
15.2[c]	300	306	+ 2.0
19.8	500	501	+ 0.1
20.2[c]	500	518	+ 3.4
24.3	700	691	− 1.3
	Average relative error		5.8%

[a] The data were submitted to a linear least-squares computer program in order to obtain these values.

[b] Represents an average of 4 or more determinations.

[c] These values were taken three days after the original analysis was performed in order to show the reproducibility of the method.

TABLE II

DATA[a] AND RESULTS OF THE ASSAY OF SERUM LDH BY THE METHOD OF BERGMEYER *et al.*

Rate[b] (ΔF *min*$^{-1}$)	*Concentration taken* (*I.U. ml*$^{-1}$)	*Concentration found*[b] (*I.U. ml*$^{-1}$)	*Relative error* (%)
1.2[c]	160	227	+41.3
1.4[d]	190	258	+35.8
1.5[d]	190	274	+43.7
1.5[d]	200	274	+36.5
1.3	280	243	−13.2
1.8[d]	320	320	+ 0.1
1.6	360	289	−19.4
2.3[c]	380	398	+ 4.5
2.2[c]	440	383	−13.0
2.7	460	460	0.0
1.9[c]	480	375	− 2.9
2.7	500	460	− 7.8
3.7[c]	630	615	− 0.7
5.3	820	864	+ 5.4
	Average relative error		16.0%

[a,b] See Table I.

[c] These values were taken one week after original analyses.

[d] These values were taken two weeks after original analyses.

TABLE III

DATA[a] AND RESULTS OF THE ASSAY OF SERUM LDH BY THE PROPOSED METHOD

Rate[b] (*ΔF min*$^{-1}$)	*Concentration taken* (*I.U. ml*$^{-1}$)	*Concentration found*[b] (*I.U. ml*$^{-1}$)	*Relative error* (%)
6.6[c]	160	168	+4.9
7.3[d]	190	189	−0.3
7.2[d]	200	186	−6.5
10.1	280	276	−1.3
13.2	360	372	+3.3
13.9[c]	380	394	+3.4
15.3[c]	440	437	−0.6
16.0[c]	460	459	−0.2
17.2	500	496	−0.8
18.8	560	546	−2.5
21.4[c]	620	626	+1.0
	Average relative error		2.3%

[a,b] See Table I.
[c,d] See Table II.

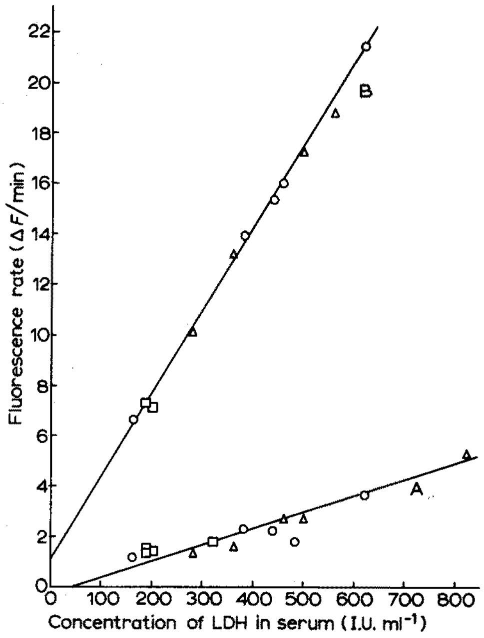

Fig. 1. Calibration graphs for the method of Bergmeyer *et al.*[6] (A) and the proposed method (B). (△) Original analysis; (○) 1 week later; (□) 2 weeks later.

conditions for the analysis. From Table IV it was concluded that the grey color would give closest to the optimal conditions, and grey pads were therefore used.

An investigation of the stability of the pads was conducted on both grey and

TABLE IV

COMPARISON OF PAD COLORS[a]

Color	*Background*	*Rate* (ΔF *min*$^{-1}$)
Translucent	1.29	4.6
Grey	0.30	4.3
Black	0.31	1.3

[a] Pad composition was 20 μl of both the β-NAD and the lithium lactate solution; also, 20 μl of the glycine buffer and 30 μl of the 3850 I.U. ml^{-1} commercially available enzyme solution were used in the analysis.

black pads. The grey pads were 10 days old and the black pads 30 days old. A 320 I.U. ml^{-1} serum sample was used for the determination on the grey pads. A 300 I.U. per ml solution of the commercially available enzyme was used for the assay on the black pads. (It should be stated here that black pads were used because, although they are not as sensitive as the grey pads, they also produce a linear calibration curve, and they were much older than the grey pads.)

The analysis on the 10-day old grey pads yielded a value of 326 I.U. ml^{-1}, which corresponds to an error of 2.0%. The 30-day old black pads also produced an excellent value, namely 305 I.U. ml^{-1}, which corresponds to an error of 1.6%. Both experimental values were above the taken values which strengthens the argument that the pads are stable for longer than a month if stored under silica gel desiccation at atmospheric pressure.

CONCLUSION

The proposed semi-solid surface method is more convenient than most normal solution methods because few solutions are required and there are fewer manipulations. Substrate solutions need be prepared only when the pads are made, which may be as seldom as once a month. The method is thus more economical than other techniques, especially since only small volumes are necessary.

Another advantage of this method is the time involved. The complete analysis, from the measurement of a volume of the buffer solution to the end of recording the rate, usually takes only 3–5 min. Many other methods have long incubation times or many difficult steps which require a significantly longer period.

SUMMARY

A semi-solid surface fluorescence method for the determination of lactic dehydrogenase (LDH) is reported. The commercially available enzyme in aqueous solution, and the enzyme in blood serum were studied. The serum analysis is compared to a method described by Bergmeyer *et al.* As little as 160 units of LDH per ml of blood serum can be determined with an accuracy of better than 3%. The reaction system used was:

$$\text{Li lactate} + \text{NAD} \overset{\text{LDH}}{\rightleftharpoons} \text{NADH} + \text{pyruvic acid}$$

The rate of production of the fluorescent product NADH was monitored. An investigation of pad color and pad stability was also performed.

RÉSUMÉ

On décrit une méthode de dosage de la déhydrogènase lactique (LDH) par fluorescence de surface semi-solide. On examine l'enzyme en solution aqueuse du commerce et l'enzyme du sérum sanguin. L'analyse du sérum est comparée à une méthode décrite par Bergmeyer *et al.* On peut doser une quantité minimum de 160 units LDH par ml de sérum sanguin, avec une exactitude supérieure à 3%. La réaction est la suivante:

$$\text{lactate Li} + \text{NAD} \overset{\text{LDH}}{\rightleftharpoons} \text{NADH} + \text{acide pyruvique.}$$

La vitesse de production du produit fluorescent NADH est contrôlée.

ZUSAMMENFASSUNG

Es wird eine Methode der Fluoreszenz halbfester Oberflächen für die Bestimmung von Milchsäuredehydrase (LDH) beschrieben. Das im Handel erhältliche Enzym in wässriger Lösung und das Enzym in Blutserum wurden untersucht. Die Enzymanalyse wird mit einer Methode verglichen, die von Bergmeyer *et al.* beschrieben worden ist. So geringe Gehalte wie 160 Einheiten LDH pro ml Blutserum können mit einer Genauigkeit von besser als 3% bestimmt werden. Es wurde folgendes Reaktionssystem verwendet:

$$\text{Li-Lactat} + \text{NAD} \overset{\text{LDH}}{\rightleftharpoons} \text{NADH} + \text{Brenztraubensäure.}$$

Die Bildungsgeschwindigkeit des fluoreszierenden Produktes NADH wurde gemessen. Färbung und Beständigkeit wurden ebenfalls untersucht.

REFERENCES

1 G. G. Guilbault and R. L. Zimmerman, Jr., *Anal. Letters*, 3 (1970) 133.
2 M. E. Loomis, *J. Lab. Clin. Med.*, 57 (1961) 966.
3 T. Laursen, *Scand. J. Clin. Lab. Invest.*, 11 (1959) 134.
4 F. Wroblewski and J. S. LaDue, *Proc. Soc. Exptl. Biol. Med.*, 90 (1955) 210.
5 E. Roabo, *Scand. J. Clin. Lab. Invest.*, 15 (1963) 233.
6 H.-U. Bergmeyer, E. Bernt and B. Hass, in H.-U. Bergmeyer, *Methods of Enzymatic Analysis*, Academic Press, New York, 1963, p. 736.
7 P. G. Cabaud and F. Wroblewski, *Amer. J. Clin. Pathol.*, 30 (1958) 234.
8 A. Vaughan and G. G. Guilbault, *Anal. Chim. Acta*, 55 (1971) 107.
9 F. Wroblewski, *Scand. J. Clin. Lab. Invest.*, 10 (1958) 230.
10 T. Jagt and O. A. Larsen, *Scand. J. Clin. Lab. Invest.*, 12 (1960) 200.
11 R. D. Rapp and E. R. Bell, *Amer. J. Clin. Pathol.*, 35 (1961) 116.
12 H. C. Damm, P. K. Besch, D. Couri and A. J. Goldwin (Editors), *Methods and References in Biochemistry and Biophysics*, The World Publishing Company, Cleveland, 1966, p. 119.

Analytica Chimica Acta
Elsevier Publishing Company, Amsterdam
Printed in The Netherlands

DETERMINATION OF TOTAL IODINE AND IODATE IN SEA WATER AND IN VARIOUS EVAPORITES

MARIAN M. SCHNEPFE
U.S. Geological Survey, Washington, D.C. 20242 (U.S.A.)

(Received 2nd August 1971)

Methods for the determination of iodine in sea water have been listed by Riley[1]. These methods include the titration of liberated iodine and photometric procedures involving: (*a*) the catalytic action of iodide on the oxidation of arsenic(III) by cerium(IV), (*b*) the color intensity of extracted iodine, and (*c*) the color intensity of the iodine–starch complex.

Many of the procedures require initial concentration and separation steps or a control of the chlorinity. Some of the procedures do not distinguish the iodine oxidation state. Matthews and Riley[2] have made a thorough study of the concentration steps and methods necessary to differentiate iodide and iodate, but their method is lengthy. The spectrophotometric procedure described here requires neither preliminary concentration nor separation of iodine, is applicable to water-soluble samples containing as little as 0.1 μg of iodine, either as total iodine or as iodate, and tolerates at least 500 mg of chloride and 5 mg of bromide.

The procedure involves adding sulfamic acid to destroy any nitrite, making the solution alkaline, oxidizing the iodine species to iodate with permanganate, reducing the excess of manganese(VII) with iron(II), acidifying, then treating with starch–iodide reagent and measuring the absorbance of the starch–iodine complex. The oxidation with permanganate is omitted when only the iodate is to be determined.

EXPERIMENTAL

Apparatus and reagents

A Beckman Model DU spectrophotometer with 5-cm cells was used.

Standard iodide solutions (0.1, 1, *and* 5 $\mu g\ ml^{-1}$). Prepare a stock solution from dry reagent-grade potassium iodide and from this prepare standards by successive dilution.

Standard iodate solution (0.1, 1, 5, *and* 10 $\mu g\ ml^{-1}$ *of iodine as iodate*). Prepare a stock solution from dry reagent-grade potassium iodate and by successive dilution prepare solutions containing iodine of the desired concentration.

Phosphate–iodate solution (0.25 *M phosphate containing* 0.3 $\mu g\ IO_3^-\text{-}I\ ml^{-1}$). Dissolve 57.1 g of dipotassium hydrogen orthophosphate trihydrate in water and dilute to 100 ml, filtering if necessary. Take 10 ml of this solution, add 30 μg of iodine as the iodate and dilute to 100 ml.

Iron(II) solution (0.1 *M*) *in* 0.2% (*v/v*) *sulfuric acid.* Dissolve 3.922 g of iron(II) ammonium sulfate hexahydrate in water. Add 0.4 ml of (1 + 1) sulfuric acid and dilute to 100 ml. Prepare a fresh solution each week. Cool in an ice bath to about 0° before using.

Sulfuric–phosphoric acid solution (10% (*v/v*) *in each*). Add 100 ml each of concentrated sulfuric acid and phosphoric acid to water and dilute to 1 l. Cool to about 0° before using.

Starch–iodide solution (0.5% (*w/v*) *starch and* 0.25 % (*w/v*) *cadmium iodide*). Boil about 1 l of water containing 2.5 g of cadmium iodide for about 10 min to remove any free iodine. Triturate 5 g of soluble starch with a little water. Add the resulting slurry with vigorous stirring to the boiling cadmium iodide solution and continue boiling for about 10 min. After cooling the solution, filter first through a "fast" filter paper and then through a coarse-sintered glass filter. The solution is stable for at least six weeks. Determine the wavelength of the starch–iodine complex absorption peak for each batch of starch solution by a spectral scan.

Procedure for the determination of total iodine

Dissolve 0.5 g of solid sample in 10 ml of water or take a 10-ml portion of sea water and filter initially if there is considerable insoluble material. Add 1 ml of aqueous 1% (w/v) sulfamic acid solution. The pH of the sample solution should be $\leqslant 2$; if necessary add dilute sulfuric acid. After 15 min, add 1 ml of 0.1 *M* sodium hydroxide solution (ascertaining afterwards that the pH is at least 7) and 0.5 ml of 0.1 *N* potassium permanganate. Cover the beaker and heat on a steam bath for 1 h. Cool the solution or slurry and filter through a 15-ml Gooch-type coarse-fritted glass crucible supported on a 30-ml beaker by a Teflon disc. No suction is required. Wash the residue and funnel with water bringing the volume to 16 ml. Prepare standards by heating iodide solutions with sodium hydroxide and potassium permanganate, filtering and proceeding as with the sample solutions.

Place the filtered sample and standard solutions in an ice bath and add, while stirring, 1.00 ml of the phosphate–iodate solution. Allow the solutions to attain a common temperature (0–5°). Then, while stirring, add 0.70 ml of the iron(II) solution followed within 1 min by 5.0 ml of the cold sulfuric–phosphoric acid mixture. Stir the resulting solution, ensuring that no manganese remains unreduced on the upper walls of the beaker. Without delay add, while stirring, 2.0 ml of the starch–iodide reagent. Adjust the volume to 25 ml. After 10–15 min, measure the absorbance at the starch–iodine absorption peak in a 5-cm cell with water as the reference.

Procedure for the determination of iodate

Filter the sea water or dissolved sample into a 30-ml beaker. Add 1 ml of aqueous 1% (w/v) sulfamic acid solution and after 15 min add 1 ml of the phosphate–iodate solution. Adjust the solution volumes to 17 ml. Prepare iodate standards similarly. Cool the solutions as described above and while stirring, add 0.2 ml of the iron(II) solution. Then proceed exactly as described above.

RESULTS AND DISCUSSION

Oxidation–reduction reactions and reagent concentrations

The presence of microgram quantities of nitrite will interfere with the determination of iodine when a starch–iodide indicator is used. The nitrite concentration in sea water is reported[3] to be as high as 50 μg l^{-1}. In an alkaline solution permanganate does not react with nitrite, therefore sulfamic acid is added. The sulfamic acid is generally sufficiently acidic to neutralize the mild alkalinity of most samples and to provide the low pH ($\leqslant 2$) required for its interaction with nitrite.

The essential difference between the procedures for determining total iodine and iodate is the omission of the permanganate in the latter. In an alkaline solution permanganate oxidizes iodide to the iodate without affecting chloride and bromide. The solution is made only mildly alkaline to avoid precipitation of substances such as magnesium hydroxide which would hamper the easy filtration of the permanganate-treated solution. Filtration is best made with Gooch-type crucibles with coarse-fritted glass discs, as various types of filter papers, pre-washed and otherwise, result in low and erratic iodine recoveries.

In alkaline solution in the presence of phosphate, permanganate and other oxidized states of manganese are destroyed by iron(II) without affecting iodate. In the absence of phosphate, manganese dioxide would form as one product of the reduction of permanganate. With no oxidized states of manganese present, oxidation of chloride and bromide on acidification of the solution is prevented. An excess of iron(II) prevents atmospheric oxidation of the starch–iodide reagent.

The alkaline solution is acidified with a solution containing both sulfuric and phosphoric acid. The sulfuric acid increases the rate of the color development and provides the desired acidity. The phosphoric acid serves to form a colorless iron(III) complex and also to stabilize the starch–iodine chromogen. No oil effects were observed when varying mixtures of the two acids were tested in which the concentration of each acid was increased or decreased individually or in combination by 50%. Similarly, no ill effects were observed when the concentration of other reagents were changed by this amount. However, enough iron(II) must be used to reduce the permanganate and to provide for a slight excess to prevent air-oxidation of the starch–iodide reagent.

The acid concentration can vary over a wide range for the reaction between the iodate and iodide ions. Lambert[4] states that the reaction works well from pH 7 to highly acidic solution and the pH must be below 0.5 before serious interference from dissolved oxygen occurs. With excess of iron(II), the pH of *ca.* 0.5 used in the proposed procedure yields no interference from air-oxidation in a 2-h period. This higher acidity was chosen to provide for the rapid reaction between the iodate and iodide and to increase the solubility of some of the salts.

Effect of time, excess of iron(II) and temperature

In the absence of high concentrations of chloride, at least a 30-min interval can be tolerated after each of the individual additions of the iron(II), the acid, and the starch–iodide reagent. In addition, the excess of iron(II) solution can be at least double the prescribed amount. The starch–iodine complex is stable for hours even at room temperature. In the presence of large amounts of chloride, both the time-lapse between the addition of the iron(II) solution and the starch–iodide solution, and the excess iron(II) must be restricted; also a lower temperature is required. Otherwise, there is a tendency for some of the iodate to be reduced by the iron(II) leading to low results.

Lowering the temperature to 0°–5° before the addition of the iron(II) solution serves to suppress the interference caused by chloride and to increase the absorbance of the starch–iodine chromogen. By placing all the solutions in an ice bath to produce a uniform temperature, excellent results can be obtained.

Wavelength of the starch–iodine absorption peak

A plot of the absorbance of the starch–iodine complex against the wavelength (400–700 nm) yields a bell-shaped curve with the wavelength of peak absorbance being determined by the particular starch used. This variation in the starch–iodine chromogen absorption peak is inferred from the literature[4-9], where wavelengths varying from 575 to 625 nm are recommended. Rundle *et al.*[10] state that the molecular absorptivity as well as the wavelength of maximum absorbance of the starch–iodine complex vary with the chain length of the starch, the chain length being characteristic of the plant source of the amylose.

A plot of the absorbance *versus* the concentration of iodine yields a non linear curve below a concentration of *ca.* 0.01 μg I ml^{-1}. When 0.3 μg of iodine as the iodate was added to each standard solution and absorbance measurements were made at the absorption maximum, the standard curve was found to conform to Beer's law up to an iodine concentration of 0.2 p.p.m., the maximum tested. With the starch used, the sensitivity according to Sandell's definition was 0.001 μg cm^{-2}.

Effects of diverse ions

As much as 5 mg of bromide, 500 mg of chloride or sulfate, 250 mg of nitrate and 5 μg of nitrite individually resulted in less than 5% error at the 1-μg iodine level. Doubling each of these quantities caused no more than a 10% deviation in the absorbances.

Where bromine is present as the bromate, its interference in the total iodine determination can be overcome by initially adding 0.5 ml of 1.0 *M* sodium sulfite followed by one drop of (1+1) sulfuric acid. (Sulfamic acid can be omitted when acidified sulfite is used.) After a 1–2 min wait for the reduction of the bromate, the solution is made slightly alkaline with sodium hydroxide and heated on a hot plate. Excess of sulfite is destroyed by the addition of 0.1 ml of 30% hydrogen peroxide and heating for an additional 15 min. Permanganate solution (1 drop) is added to achieve the decomposition of any residual peroxide. Permanganate is then added dropwise until a persistent purple remains. The prescribed 0.5-ml excess is added and the general procedure followed. Destruction of excess of sulfite with permanganate alone can result in the formation of large amounts of manganese dioxide.

The proposed procedure for the determination of total iodine is relatively free of interferences. In contrast, the procedure for the determination of iodate gives only a relative measure of the oxidizing power remaining after the addition of iron(II) solution. Some substances which interfere with the iodate determination could exist in alkaline solution with iodate. Examples might be bromate and sulfite which upon acidification would lead to high and low iodate values, respectively.

Test of the procedure

In preliminary experiments on a sea water sample collected from the mid-Atlantic Ocean, iodine was determined both by directly taking volumes varying from 2 to 20 ml and also by the method of addition. The total iodine content was found

TABLE I

DETERMINATION OF IODINE IN SEA WATER AND HALITE ROCKS. MEANS AND STANDARD DEVIATIONS

Sample	*No. of detns.*	*Mean (μg I)*	*Std. dev. (μg I)*
Procedural blank	10	0.00	0.01
Sea water (10 ml)	10	0.50	0.03
Sea water (10 ml) +1 $\mu g\ I^-$	10	1.50	0.03
Halite rock No. 1 (0.5 g)	4	0.00	0.05
Halite rock No. 1 (0.5 g) +1 $\mu g\ I^-$	4	0.90	0.03
Halite rock No. 2 (0.5 g)	4	0.00	0.02
Halite rock No. 2 (0.5 g) +1 $\mu g\ I^-$	4	0.97	0.02
Halite rock No. 3 (0.5 g)	4	0.00	0.02
Halite rock No. 3 (0.5 g) +1 $\mu g\ I^-$	4	1.02	0.02
Halite rock No. 4 (0.5 g)	4	0.00	0.01
Halite rock No. 4 (0.5 g) +1 $\mu g\ I^-$	4	0.98	0.02

TABLE II

TOTAL IODINE AND IODATE-IODINE IN SEA WATER

(Duplicate determinations)

Sample location			*Total iodine ($\mu g\ l^{-1}$)*	*Iodate-iodine ($\mu g\ l^{-1}$)*
Lat.	*Long.*	*Depth (m)*		
56° 26′ N	51° 03′ W	1485	55, 63	58, 64
56° 31′ N	51° 03′ W	1515	59, 61	59, 61
56° 25′ N	50° 35′ W	3068	58, 60	60, 64
56° 33′ N	50° 59′ W	3005	60, 66	63, 65
56° 30′ N	51° 00′ W	1501	57, 61	58, 62
21° 20′ N	38° 3′ E	853	78, 90	37, 43
Standard deviation (error)			4.7 $\mu g\ l^{-1}$	3.1 $\mu g\ l^{-1}$

to be 50±5 $\mu g\ l^{-1}$ by both methods. For 10 replicate determinations on 10-ml volumes, the total iodine and iodate-iodine concentrations were found to be 50±3 $\mu g\ l^{-1}$ and 27±1 $\mu g\ l^{-1}$, respectively. Total iodine was determined in four halite rock samples, three of which contained approximately 7% anhydrite which was filtered off initially. The results are listed in Table I.

Six additional sea-water samples were obtained from well-defined locations. The means and average deviations obtained from duplicate determinations of the total iodine and iodate are given in Table II. The range in iodine content of the sea water samples is consistent with the results of others. Barkley and Thompson[11] report that the total iodine content of sea water samples from the Northeast Pacific and Arctic Oceans varies from 45 to 70 $\mu g\ l^{-1}$. Thirty-three to 100% of the total iodine is present as the iodate which increases with depth in the Arctic Ocean. Evans[12] reports as much as 92 μg of iodine per l.

The author wishes to express her appreciation to Captain C. Buras of the Navy's Military Sea Transportation Service, R. O. Fournier of the U.S. Geological

Survey, M. C. Ingham of the Coast Guard Oceanographic Unit and Carmen Johnson of the National Oceanographic Data Center, for providing the sea water samples and for giving helpful suggestions.

SUMMARY

Iodine in sea water and evaporites is determined spectrophotometrically as the starch–iodine complex without prior separation or concentration of the iodine. In slightly alkaline solution, iodide is first oxidized to iodate with permanganate. Oxidized states of manganese are destroyed with iron(II) in phosphate medium without affecting the iodate. After acidification, iodide is added to react with the iodate in the presence of starch. The iodate content is determined by the same procedure, but without the addition of permanganate. As little as 0.1 μg of iodine is determinable in the presence of 500 mg of chloride and 5 mg of bromide. The total iodine concentration in seven samples of sea water was found to vary from 50 ± 3 to 84 ± 6 μg l^{-1} with 50–100% present as the iodate.

RÉSUMÉ

Une méthode est proposée pour le dosage de l'iode dans l'eau de mer par spectrophotométrie du complexe amidon–iode, sans séparation ou concentration préalable de l'iode. L'iodure est d'abord oxydé en iodate à l'aide de permanganate, en solution légèrement alcaline. Les formes oxydées du manganèse sont détruites par le fer(II) en milieu phosphate, sans toucher l'iodate. Après acidification, on ajoute de l'iodure, en présence d'amidon. On utilise le même procédé pour le dosage des iodates, mais sans addition de permanganate. On peut ainsi doser 0.1 μg d'iode en présence de 500 mg de chlorure et 5 mg de bromure. On a trouvé pour sept échantillons d'eau de mer des concentrations allant de 50 ± 3 à 84 ± 6 μg l^{-1} d'iode, dont 50 à 100% sous forme d'iodate.

ZUSAMMENFASSUNG

Jod in Meerwasser und eingedampften Proben wird spektrophotometrisch als Jod–Stärke-Komplex ohne vorhergehende Abtrennung oder Anreicherung des Jods bestimmt. In schwach alkalischer Lösung wird Jodid zunächst mit Permanganat zu Jodat oxidiert. Höhere Oxidationsstufen von Mangan werden mit Eisen(II) in Phosphatmedium ohne Einfluss auf das Jodat beseitigt. Nach Ansäuern wird Jodid für die Reaktion mit dem Jodat in Gegenwart von Stärke hinzugefügt. Jodat wird nach demselben Verfahren, jedoch ohne Permanganatzugabe, bestimmt. 0.1 μg Jod kann in Gegenwart von 500 mg Chlorid und 5 mg Bromid bestimmt werden. Die Gesamt-Jodkonzentration in sieben Meerwasserproben variierte zwischen 50 ± 3 und 84 ± 6 μg l^{-1} bei einem Jodatanteil von 50–100%.

REFERENCES

1 J. P. Riley, in J. P. Riley and G. Skirrow, *Chemical Oceanography*, Vol. 2, Academic Press, New York, 1965, pp. 349–350.
2 A. D. Matthews and J. P. Riley, *Anal. Chim. Acta*, 51 (1970) 295.

3 H. U. SVERDRUP, M. W. JOHNSON AND R. H. FLEMING, *The Oceans*, Prentice-Hall, Englewood Cliffs, N.J., 1942, p. 181.
4 J. L. LAMBERT, *Anal. Chem.*, 23 (1951) 1247.
5 F. G. HOUSTON, *Anal. Chem.*, 22 (1950) 493.
6 J. L. LAMBERT, P. ARTHUR AND T. E. MOORE, *Anal. Chem.*, 23 (1951) 1101.
7 J. L. LAMBERT, *Anal. Chem.*, 23 (1951) 1251.
8 K. SUGAWARA, T. KOYAMA AND K. TERADA, *Bull. Chem. Soc. Japan*, 28 (1955) 494.
9 W. H. CROUCH, JR., *Anal. Chem.*, 34 (1962) 1698.
10 R. E. RUNDLE, J. F. FOSTER AND R. R. BALDWIN, *J. Amer. Chem. Soc.*, 66 (1944) 2116.
11 R. A. BARKLEY AND T. G. THOMPSON, *Deep Sea Res.*, 7 (1960) 24.
12 L. H. EVANS, Doctoral Dissertation, Univ. of Washington, Seattle, 1932, pp. 38–86.

Analytica Chimica Acta
Elsevier Publishing Company, Amsterdam
Printed in The Netherlands

EXCITED STATE PROTOTROPISM AND SOLVENT DEPENDENCE OF THE FLUORESCENCE OF 3-AMINOQUINOLINE

S. G. SCHULMAN AND A. C. CAPOMACCHIA
College of Pharmacy, University of Florida, Gainesville, Fla. 32601 (U.S.A.)

(Received 29th June 1971)

3-Aminoquinoline fluoresces intensely in concentrated acid, dilute acid, neutral and dilute basic aqueous solutions as well as in a variety of organic solvents. However, in moderately concentrated alkaline solutions its fluorescence is quenched. The electronic absorption spectra of the various prototropic forms of 3-aminoquinoline have been studied[1,2] and the pK_a values for the various ground-state prototropic reactions have been determined[3]. In the range pH 14 to H_0 -10, three ground-state prototropic species, the neutral molecule, a monocation protonated at the ring nitrogen, and a doubly protonated cation have been observed (Fig. 1). It is of spectroscopic and photochemical interest to identify the fluorescing species derived from 3-aminoquinoline and to evaluate the nature of the excited state processes by which they are converted from one prototropic form to another. Since solvent shifts of electronic spectra, especially those related to hydrogen-bonding, differ from protonation shifts more in degree than in kind, comparison of protonation-induced shifts of absorption and fluorescence spectra with solvent shifts should yield clues about the nature of the interactions of the solute, in ground and electronically excited states, with the solvent.

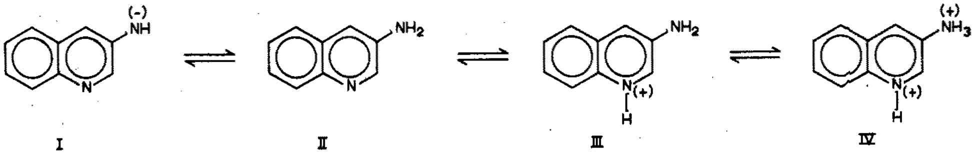

Fig. 1. Prototropic equilibria of 3-aminoquinoline. (I) Imino anion; (II) neutral species; (III) ring-protonated monocation; (IV) dication.

EXPERIMENTAL

3-Aminoquinoline (K&K Laboratories, Inc., Plainview, N.Y.) was purified by three recrystallizations from 50% ethanol–water. The purity was established by the agreement of the corrected excitation spectra with the electronic absorption spectra. Mallinckrodt reagent-grade sulfuric acid and Matheson, Coleman and Bell spectroquality chloroform, *p*-dioxane, *n*-heptane and acetonitrile were employed as solvents. Ethanol was distilled under low pressure to remove traces of benzene before use. Sodium hydroxide solutions were prepared from the carbonate-free solution by dilution with distilled deionized water. In the intermediate pH range, phosphate, acetate and borate buffers were employed.

Oxygen quenching was found to be unimportant as nitrogen purged solutions yielded essentially the same results as solutions containing dissolved oxygen at atmospheric pressure.

pH measurements were made on an Orion model 801 pH meter with a Beckman combination silver–silver chloride–glass electrode. Absorption spectra were taken on a Beckman DB-GT spectrophotometer. Fluorescence measurements were made on a Perkin-Elmer MPF-2A fluorescence spectrophotometer whose monochromators were calibrated against the line emission spectrum of xenon. Emission and excitation spectra were corrected for variability of response of monochromators and phototube to different wavelengths of light, by means of a Perkin-Elmer corrected spectra accessory, employing a rhodamine B quantum counter.

Quantum yields of fluorescence were calculated by the method of Parker and Rees[4] with quinine bisulfate in 0.10 *M* sulfuric acid as standard. All quantum yields determined by the latter method were multiplied by the ratio of the square of the refractive index of the test medium to that of the quinine bisulfate solution, to correct for differences in the light dispersion properties of the various solvents at the cell–solution interface.

RESULTS AND DISCUSSION

Room-temperature fluorescence spectra of 3-aminoquinoline in the various solvents are structureless. The maxima of these fluorescences as well as the long wavelength absorption maxima and fluorescence quantum yields are presented in Table I. In order to assign the fluorescences observed in acidic and aqueous solutions to the prototropic species from which they arise, fluorescence spectra were also taken in solutions of 3-aminoquinoline in 9 *M* sulfuric acid, $1 \cdot 10^{-3}$ *M* sulfuric acid and the pH 10.2 borate buffer (these media were dictated by the ground-state pK_a values) frozen in a dry ice–acetone bath. In these frozen media, the dication, ring-protonated monocation and neutral species, respectively, which are excited, are constrained to remain in the ground-state structural configurations (*i.e.* phototautomerism cannot occur). Thus the fluorescences which occur in the frozen solutions must correspond to the same species which were excited. Fluorescence maxima of the frozen solutions are presented in Table II. The data of Tables I and II show similar fluorescence

TABLE I

ROOM-TEMPERATURE FLUORESCENCE MAXIMA ($\bar{\nu}_f$), LONG-WAVELENGTH ABSORPTION MAXIMA ($\bar{\nu}_a$) AND QUANTUM YIELDS OF FLUORESCENCE (ϕ_f) OF 3-AMINOQUINOLINE IN SEVERAL SOLVENTS

(Excitation and fluorescence bandpasses were 5 nm. The excitation wavelength was 320 nm)

Solvent	$\bar{\nu}_a$ ($cm^{-1} \cdot 10^{-4}$)	$\bar{\nu}_f$ ($cm^{-1} \cdot 10^{-4}$)	ϕ_f
18 *M* H_2SO_4	3.16	2.39	0.22
$1 \cdot 10^{-3}$ *M* H_2SO_4	2.69	2.19	0.61
pH 10.2 borate buffer	2.92	2.32	0.48
Ethanol	2.84	2.40	0.08
Acetonitrile	2.81	2.51	0.10
Chloroform	2.84	2.56	0.10
p-Dioxane	2.87	2.51	0.09
n-Heptane	2.95	2.68	0.10

TABLE II

FLUORESCENCE MAXIMA OF 3-AMINOQUINOLINE IN DIFFERENT MEDIA

(Medium was frozen in dry ice-acetone. Excitation and fluorescence bandpasses were 5 nm. The excitation wavelength was 320 nm)

Solvent	$\bar{\nu}_f$ $(cm^{-1} \cdot 10^{-4})$
9 *M* H_2SO_4	2.32
$1 \cdot 10^{-3}$ *M* H_2SO_4	2.18
pH 10.2 borate buffer	2.40

maxima for solutions of comparable acidity. Moreover, the shifts of the maxima are the same in direction for successive protonations in both fluid and rigid media. These results indicate that in fluid solutions as well as rigid media, the doubly protonated cation, ring-protonated monocation and neutral species are responsible for the observed emissions in concentrated acid, dilute acid and dilute basic media, respectively. The differences between the fluorescence maxima in fluid and rigid solutions can be attributed to differences between the ground-state and excited-state equilibrium solvent configurations and differences in the distribution of vibrational energy in the ground state at room temperature and at the temperature of the dry ice–acetone bath. In the organic solvents employed, the neutral molecule is undoubtedly the fluorescing species.

Solvent dependences of electronic spectral maxima

In the series of solvents in which the fluorescence of neutral 3-aminoquinoline was studied, the fluorescence of the neutral species shows a continuous red shift with increasing solvent polarity and hydrogen-bonding capability. The long-wavelength absorption maxima of 3-aminoquinoline show a less regular solvent dependence, the absorption maxima in water and heptane, the most and least activating solvents, being comparable and higher in frequency than the spectra in solvents of intermediate to low polarity and hydrogen-bonding strength. These results can be explained as follows. Absorption occurs in 3-aminoquinoline as a transition from the ground-state molecule in a ground-state equilibrium solvent cage, to the excited molecule still in the ground-state equilibrium solvent configuration (the Franck–Condon excited state). The absorption frequency will be governed by the type and magnitude of interaction of the solvent with the ground and Franck–Condon excited molecules as well as by the difference in electronic energy between upper and lower states. For the present argument, the solvent effects on the solute may be considered to be of three types: (*a*) dispersive interaction—electrostatic energy produced by the interaction of permanent or induced solvent dipole moments with ground and excited state solvent dipoles; (*b*) hydrogen-bond donor interaction—chemical energy produced by a positively polarized hydrogen atom of the solvent electrostatically interacting with a lone pair of electrons on a basic atom in the solute in the ground or excited state; (*c*) hydrogen-bond acceptor interaction—chemical energy resulting from the interaction of a lone pair on a solvent atom with a positively polarized hydrogen atom of the solute in ground or excited state. The effect of the dispersive interaction on the absorption, depends upon whether the solute becomes more or less polar as a result of excitation. If the molecule becomes more polar, as is the case for most π–π^* transitions, dipole–dipole interaction lowers the energy of the Franck–Condon excited state relative to the ground state and the effect is a red shift of the absorption spectrum increasing with solvent polarity. The opposite is true if the polarity of the solute decreases upon excitation. Hydrogen-bonding donor solvents partially bind lone-pair electrons. As a result, if excitation results in charge-transfer away from the lone pair, the partial positive charge introduced into the atom bearing the hydrogen-bonded lone pair opposes the charge-transfer process so that the excited state is raised in energy relative to the ground state and a blue shift of the absorption spectrum results with increasing hydrogen-bond donor capacity of the solvent. On the other hand, if charge-transfer occurs to the H-bonded atom upon excitation, the positive charge introduced into that atom stabilizes the Franck–Condon excited state relative to the ground state, resulting in a red shift of the absorption spectrum with increasing solvent H-bond donor capacity. Correspondingly, H-bond acceptor solvents will cause red shifts when solvating solutes at atomic sites which lose charge in the Franck–Condon excited state, and will cause blue shifts when solvating solutes at atomic sites which gain charge in the Franck–Condon excited state. Of course, a combination of these effects is usually present, making it difficult to distinguish between them. If, however, it is considered that protonation and dissociation are extreme cases of hydrogen-bonding solvent donor and acceptor effects, respectively, the shifts of absorption spectra produced by protonation and dissociation at known acidic and basic sites, can be employed, to infer the shifts to be expected by the various H-bonding interactions and thereby to distinguish them, at least to some extent, from one another and from the dispersive types of solvent shifts.

The data of Table I indicate that upon protonation of the ring nitrogen, a red shift occurs, while protonation of the amino nitrogen results in a blue shift. These results imply that upon excitation from the ground to the Franck–Condon lowest singlet state of 3-aminoquinoline, electronic charge migrates away from the amino group and to the heterocyclic nitrogen atom[5]. Thus hydrogen-bond acceptors can only produce a red shift by interacting with the hydrogen atoms on the amino group of 3-aminoquinoline while hydrogen-bond donors can cause a red shift by interacting with the lone pair on the ring nitrogen or a blue shift by interacting with the lone pair on the amino group. In the series of hydrogen-bond acceptors, *p*-dioxane, chloroform, acetonitrile (in order of increasing polarity), a red shift of the 3-aminoquinoline absorption relative to that in hexane (a solvent with essentially no polarizing or hydrogen-bonding properties) is observed with the red shift increasing in magnitude with solvent polarity. These results indicate that 3-aminoquinoline is more polar in the Franck–Condon excited state, and hydrogen-bonds in the ground state, at least to some extent through the hydrogen atoms on the amino nitrogen. Water, which has hydrogen-bond donor properties in addition to acceptor properties, produces very little red shift in the 3-aminoquinoline absorption relative to that in heptane. This is in spite of the fact that water is the most polar solvent employed here. This suggests that the hydrogen-bond donor properties of water in the ground-state solvent cage, are more strongly manifested at the lone pair of the amino group than at the ring nitrogen and are more important than the dispersive stabilization of the excited state.

Because the lifetime of a fluorescing molecule, in the lowest excited singlet state, is long compared with the time required for reorientation of the solvent cage to the equilibrium excited-state configuration, emission in fluid solutions occurs from the molecule in the latter solvent cage. Emission terminates with the molecule in the ground electronic state but in the excited-state solvent cage (*i.e.* a Franck–Condon ground state). The arguments related to solvent shifts for absorption spectra also apply to fluorescence spectra except that solvent relaxation generally occurs in such a way as to stabilize the equilibrated excited state relative to the Franck–Condon excited state, and the Franck–Condon ground state is higher in energy than the thermalized ground state. As a result, not only is the fluorescence at frequencies lower than would be expected purely on the basis of vibrational relaxation after excitation, but the effects of solvent polarity and hydrogen-bonding upon fluorescence tend to be somewhat exaggerated relative to the effects upon absorption spectra. This is especially the case in polar solvents when the solute is more polar in the excited state and when there is considerable intramolecular charge-transfer accompanying excitation.

The fluorescence maxima of 3-aminoquinoline do indeed show more pronounced solvent-induced shifts (relative to the fluorescence in *n*-heptane), than do the corresponding absorption spectra. Moreover, the fluorescence shifts do not parallel the absorption shifts, especially in the case of water in which 3-aminoquinoline demonstrates its lowest frequency fluorescence maximum. The data of Table I suggest that while the hydrogen-bond acceptor solvents stabilize the charge-deficient amino group in the excited state, the hydrogen-bond donors play at least as important a role in the stabilization of the charge-enriched ring nitrogen atom of the excited molecule. The lower emission frequency in ethanol than in the more polar acetonitrile suggests that the hydrogen-donor effect at the ring nitrogen is more important than the electrostatic stabilization of the excited 3-aminoquinoline through dipole–dipole interaction. It is interesting that the change in fluorescence maximum on going from *n*-heptane to water or alcohol is greater than the fluorescence shift produced in water by protonation of the ring nitrogen. This suggests that the interaction between the solute and hydrogen-bonding solvent is very strong and may actually result in a stoichiometric complex (exciplex) between the excited molecule and the solvent. In support of the latter conclusion, in solutions of 3-aminoquinoline in *n*-heptane, addition of small amounts of ethanol (up to 2% v/v) results in a red shift of 1400 $\mathrm{cm^{-1}}$. Raising the ethanol content from 2 to 100% (v/v) results in a very gradual red shift of only another 1400 $\mathrm{cm^{-1}}$.

The quantum yield of 3-aminoquinoline fluorescence in all organic solvents was fairly constant. However, in water it is considerably greater. It is possible that the strong hydrogen-bonding of the ring nitrogen atom by water, in the lowest excited singlet state, interferes with a pathway for internal conversion or intersystem crossing from the excited singlet state.

Prototropic phenomena in the lowest excited singlet state

In aqueous solutions, the fluorescence of the neutral 3-aminoquinoline undergoes a red shift with decreasing pH. The midpoint of the red shift occurs at pH 5.0, coinciding with the ground-state pK_a for conversion of the neutral molecule to the ring nitrogen-protonated monocation. Consequently, it is concluded that the rates of protonation and dissociation in the lowest excited singlet state are too slow to compete with radiative deactivation of the excited singlet state. The conversion of fluorescence from that of the neutral form to that of the monocation occurs as a result of the ground-state prototropic reaction. Static protonation of heterocyclic nitrogen has also been observed, in the mid pH region, for all of the hydroxyquinolines[6-8], all of the aminopyridines, the aminoquinolines which have been studied to date[9], and in 1,10-phenanthroline[10]. In 1,10-phenanthroline, however, the second protonation occurs in perchloric acid media with equilibration of the singly and doubly protonated species occurring within the lifetime of the lowest excited singlet state.

It would appear that in the mid pH range, it is the low concentration of H^+ which limits the rate of excited state protonation and prevents equilibration. However, from the red shifts in both the absorption and fluorescence spectra, upon protonation, it is evident that 3-aminoquinoline is a stronger base in the excited state than in the ground state, with respect to dissociation from the ring nitrogen.

In moderately concentrated acid solutions, and with excitation at 320 nm, the intensity of the blue-green fluorescence of the 3-aminoquinoline monocation rises, reaching a maximum at $H_0 = -2.1$. The midpoint of this rise occurs at $H_0 = -0.4$. When the excitation wavelength is changed to 372 nm (the long-wavelength absorption band of the monocation) the blue-green fluorescence falls in intensity, vanishing at $H_0 = -2.1$. The midpoint of this quenching also occurs at $H_0 = -0.4$. In this region of acidity, the absorption spectrum blue shifts, corresponding to the conversion of the monocation to the dication in the ground state. The pK_a of the latter equilibrium is -0.4. Consequently, the variation of the fluorescence intensity of the 3-aminoquinoline monocation in the region pH 2 to $H_0 - 2$ is attributed to the ground-state equilibrium between the singly and doubly protonated species derived from 3-aminoquinoline.

In more concentrated acid solutions, the monocation fluorescence falls in intensity and blue shifts with no change in the absorption spectra. The midpoint of the blue shift of fluorescence occurs at $H_0 = -5.6$ and is assigned to the pK_a^* of the conversion between the excited monocation and excited dication derived from 3-aminoquinoline. The dication of 3-aminoquinoline is thus a stronger acid in the lowest excited singlet state. In support of the latter conclusion, calculation of pK_a^* for the equilibrium between the excited dication and monocation by the Förster cycle method[11], employing the corresponding ground-state pK_a value and the absorption or fluorescence maxima of dication and monocation, shows the dication to be a stronger acid in the excited state. However, Förster cycle calculations, employing fluorescence maxima, yield a value of -4.6 for pK_a^* while employment of the absorption shift upon protonation yields a value of -10.3 for pK_a^*. The value obtained from the fluorescence shift is in reasonably good agreement with the value obtained by fluorimetric titration. The discrepancy of one unit can be explained on the basis of the slight shifts observed for the fluorescences of substituted quinolines on going from aqueous sulfuric or perchloric acid media to almost pure acid media and to solvent relaxation in the ground state. The shifts are undoubtedly due to changes in dispersive or hydrogen-bonding properties of the solvent. Also, since fluorescence band maxima were employed in these calculations rather than 0–0 bands, differences in vibrational energy between the 0–0 band and the band maximum of one conjugate species which are not exactly compensated in the other conjugate species will produce errors in the calculation of pK_a^* by the Förster cycle method. However, judging from the agreement of the pK_a^* value obtained by fluorimetric titration with that obtained from the fluorescence shift, the latter sources of error are fairly small. It is thus significant that the value of pK_a^*, calculated from absorption shifts, indicates the excited dication to be far too acidic. The fluorescence shift in frozen aqueous and acidic media (Table II) gives results which are in better agreement with the fluorescence shifts in fluid solutions than with the absorption shifts. This is especially perplexing since solvent relaxation, which is supposed to provide the greatest source of discrepancy between the absorption and fluorescence shifts, should be virtually eliminated in frozen solutions[12].

In order to resolve this apparent dilemma the monoperchlorate and diperchlorate salts of 3-aminoquinoline were prepared. Attempts were made to extract these salts into *n*-heptane. However, while the monoperchlorate was extracted into *n*-heptane and fluoresced at $2.19 \cdot 10^4$ cm^{-1} in this medium, no fluorescence could be detected for the diperchlorate in *n*-heptane. Extraction of both salts into chloroform, however, was successful, with the singly protonated species fluorescing at $2.20 \cdot 10^4$ cm^{-1} (very close to the corresponding fluorescence in dilute aqueous acid) and the doubly protonated species fluorescing at $2.74 \cdot 10^4$ cm^{-1}, a considerably higher frequency than in concentrated acid. Apparently, solvent relaxation is unimportant for the monocation but is substantial in the case of the dication. It is interesting that in sulfuric acid the 3-aminoquinoline dication fluoresces at lower frequencies than does the quinolinium ion. This is anomalous for ammonium-substituted quinolinium ions[9] and suggests that in concentrated acid media, the dication of 3-aminoquinoline may form a hydrogen-bonded complex with the solvent which permits some degree of charge-transfer from the protonated amino group to the aromatic ring. In the chloroform media, which have low polarity and hydrogen-bonding strength, the fluorescence shifts resulting from protonation are thus in much better agreement, even in fluid solution, with the corresponding shifts in absorption maxima in aqueous and acidic media. These results indicate that solvent relaxation after excitation, especially in the case of the dication, is indeed responsible for the differences in the protonation shifts observed for absorption and fluorescence spectra. The failure of the fluorescence shifts in frozen media to reflect these differences can be explained as follows. In frozen media, the solvent cage is prevented from reorientating by rotations and translations of solvent molecules. However, some degree of hydrogen-bonding is already present in the ground-state solvent cage. Freezing a strongly hydrogen-bonding solvent to a rigid matrix probably does not prevent the hydrogen bridge between the solvent and solute from readjusting its equilibrium position, by vibrational means, to accord with the excited-state electronic configuration, within the lifetime of the excited state. If such a relaxation phenomenon does appreciably stabilize the excited molecule relative to the Franck–Condon excited state, motility of the entire solvent molecule may not be necessary to produce an appreciable solvent relaxation shift. However, in a solvent of low polarity and of poor hydrogen bonding capability, such as chloroform, even in fluid solutions the thermally relaxed excited molecule may not be very different in energy, from the unrelaxed excited molecule. Solvent relaxation effects upon the fluorescing molecule will then be rather small and fluorescence shifts should then parallel absorption shifts produced by protonation. It is thus apparent that studies of gross solvent relaxation effects upon fluorescence are better studied by comparison of fluorescence spectra in nonpolar, non-hydrogen bonding media with those in polar hydrogen bonding media, whenever possible, than by comparison of fluorescence spectra taken in activating media alone, under fluid and rigid conditions, respectively. However, fluorescence studies in all three types of media do serve to differentiate, to some degree, between the various processes involved in solvent relaxation.

In moderately basic solutions the fluorescence of the neutral 3-aminoquinoline is quenched, with half-quenching occurring at pH 12.1. No change in the absorption spectrum accompanies this quenching. A similar quenching was observed for 3-aminopyridine[13] and was attributed to equilibrium, in the lowest excited singlet state, between the neutral species and the imino anion. Presumably, the corresponding process is seen here with the excited imino anion of 3-aminoquinoline being the conjugate base (Fig. 1) and responsible for the quenching of the fluorescence of the neutral species. The pK_a^* of this equilibrium is 12.1 and suggests that with respect to abstraction of a proton from the amino group, 3-aminoquinoline is a much stronger acid in the excited state than in the ground state.

SUMMARY

The effects of solvent polarity and hydrogen-bonding capability on the fluorescence of 3-aminoquinoline have been studied. The failure of the solvent dependence of the absorption spectrum to parallel that of the fluorescence spectrum is attributed to differences in hydrogen bonding in ground and lowest excited singlet states. The large Stokes shifts produced by addition of small amounts of hydrogen-bonding solvents to solutions of 3-aminoquinoline in non-activating solvents suggest the formation of a well defined solute–solvent complex in the excited state. 3-Aminoquinoline is a stronger acid in the excited state than in the ground state with respect to dissociation from the amino group. The same is true for the dication. Förster cycle calculations, however, indicate that dissociation from the heterocyclic nitrogen is more difficult in the excited state. It is shown that when hydrogen-bonding interactions are present, solvent relaxation effects after excitation are best studied in non-activating solvents rather than in rigid hydrogen-bonding solvents.

RÉSUMÉ

Une étude est effectuée sur l'influence de la polarité d'un solvant et de la possibilité de liaison hydrogène sur la fluorescence de l'amino-3-quinoléine. A l'état excité, l'amino-3-quinoléine est un acide plus fort d'après la dissociation du groupe amino. Il en est de même pour le "dication". Cependant, Förster indique que la dissociation d'un azote hétérocyclique est plus difficile, à l'état excité. On constate que lorsqu'il y a interactions de liaison hydrogène, les effets de relaxation du solvant sont mieux étudiés en solvants non-activants qu'en solvants à liaison hydrogène rigide.

ZUSAMMENFASSUNG

Die Einflüsse der Polarität und der Fähigkeit des Lösungsmittels zur Wasserstoffbindung auf die Fluoreszenz von 3-Aminochinolin wurden untersucht. Das Fehlen der Lösungsmittelabhängigkeit des Absorptionsspektrums entsprechend der

des Fluoreszenzspektrums wird Unterschieden in der Wasserstoffbindung im Grund- und niedrigstem angeregtem Singulettzustand zugeschrieben. Die starken Stokes-Verschiebungen, die durch Zugabe kleiner Mengen von wasserstoffbindenden Lösungsmitteln zu 3-Aminochinolin-Lösungen in nichtaktivierenden Lösungsmitteln hervorgerufen werden, deuten die Bildung eines wohldefinierten Komplexes des gelösten Stoffes mit dem Lösungsmittel im angeregten Zustand an. 3-Aminochinolin ist hinsichtlich der Dissoziation an der Aminogruppe im angeregten Zustand eine stärkere Säure als im Grundzustand. Dasselbe gilt für das Dikation. Förster-Cyclus-Berechnungen zeigen jedoch an, dass die Dissoziation am heterocyclischen Stickstoff im angeregten Zustand schwieriger ist. Es wird gezeigt, dass beim Vorliegen wasserstoffbindender Wechselwirkungen Lösungsmittel-Relaxationseffekte nach Anregung am besten in nichtaktivierenden Lösungsmitteln untersucht werden und nicht in stark wasserstoffbindenden Lösungsmitteln.

REFERENCES

1 E. A. STECK AND F. C. NACHOD, *Z. Phys. Chem.*, 15 (1958) 372.
2 S. G. SCHULMAN, *J. Pharm. Sci.*, 60 (1971) 371.
3 E. V. BROWN AND A. C. PLASZ, *J. Heterocyclic Chem.*, 7 (1970) 335.
4 C. A. PARKER AND W. T. REES, *Analyst*, 85 (1960) 587.
5 A. WELLER, *Progress in Reaction Kinetics*, 1 (1961) 187.
6 R. E. BALLARD AND J. W. EDWARDS, *J. Chem. Soc.*, (1964) 4868.
7 S. F. MASON, J. PHILP AND B. E. SMITH, *J. Chem. Soc.*, (1968) 3051.
8 S. G. SCHULMAN, A. C. CAPOMACCHIA AND B. TUSSEY, *Photochem. Photobiol.*, 14 (1971) 733.
9 S. G. SCHULMAN AND L. B. SANDERS, *Anal. Chim. Acta*, 56 (1971) 83.
10 S. G. SCHULMAN, P. T. TIDWELL, J. J. CETORELLI AND J. D. WINEFORDNER, *J. Amer. Chem. Soc.*, 93 (1971) 3179.
11 T. FÖRSTER, *Z. Elektrochem.*, 54 (1950) 42.
12 E. L. WEHRY AND L. B. ROGERS, *Spectrochim. Acta*, 21 (1965) 1976.
13 S. G. SCHULMAN, A. C. CAPOMACCHIA AND M. S. RIETTA, *Anal. Chim. Acta*, 56 (1971) 91.

Analytica Chimica Acta
Elsevier Publishing Company, Amsterdam
Printed in The Netherlands

LIGAND STRUCTURE AND FLUORESCENCE OF METAL CHELATES; N-HETEROCYCLIC HYDRAZONES WITH ZINC

D. E. RYAN, F. SNAPE AND M. WINPE
Department of Chemistry, Dalhousie University, Halifax, Nova Scotia (Canada)

(Received 26th July 1971)

The factors affecting the fluorescence of metal chelate compounds are basically no different from those which influence other systems and these have been defined and discussed in detail[1,2]. Although many factors are operative, it is evident that rigid, uncrowded, planar structures are conducive to fluorescence production; reaction of a metal ion with a chelating agent induces rigidity into the overall molecule and promotes fluorescence.

Modifications of the ligand structure or a change in metal ion may markedly affect the fluorescence intensity by changing the efficiency of certain energy transfer steps. The present work was undertaken to find some correlation of ligand structure of N-heterocyclic hydrazones (R–CH=N–NH–R′) with the fluorescence intensity of their zinc chelates. These compounds were chosen because extensive spectrophotometric studies have been done in this laboratory[3-8] and, with N-heterocyclic groups as the R and R′ substituents, these hydrazones behave as planar tridentate chelating agents on reaction with zinc.

EXPERIMENTAL

Apparatus

An Amino-Bowman spectrofluorimeter was used for obtaining excitation and emission spectra and for intensity measurements at a particular wavelength; a Xenon arc lamp was the excitation source.

A Radiometer PHM4c meter, calibrated with NBS pH standards at 25 ± 2°, was used for pH measurements. Radiometer electrodes G200C and K100 were used.

A Unicam SP 8000 recording spectrophotometer and a Unicam SP 500 spectrophotometer were used for absorptiometric measurements in matched 1.00-cm silica cells.

Melting points were obtained with a Kofler melting point block (Reichert, Vienna).

Mass spectra and infrared spectra were done on all compounds.

Reagents

The N-heterocyclic hydrazones were prepared as previously described[8] by condensation of equimolar proportions of the particular aldehyde or ketone and hydrazine. All starting chemicals were commercial products (Aldrich and Eastman) with the exceptions of phenanthridine-6-carboxaldehyde, 6-hydrazinophenanthridine and benzimidazole-2-aldehyde; the phenanthridine-6-carboxaldehyde was prepared as described previously[8-10]. The benzimidazole derivative was prepared by the method of Link *et al.*[11,12]; this involved reacting hydrated calcium gluconate with σ-phenylenediamine at $135 \pm 5°$ to form the D-glucobenzimidazole; cleavage of the latter with sodium metaperiodate yielded the aldehyde (m.p. 233°). 6-Hydrazinophenanthridine (m.p. 170–2°) was prepared from the 6-chloro derivative by heating for 1 h at 90° with hydrazine hydrate; the chloro compound was obtained by reacting phosphorus oxychloride with commercial phenanthradinone (Pfaltz and Bauer).

The hydrazones were recrystallised from ethanol or benzene. A list of the hydrazones examined in this paper together with their melting points and abbreviated names is shown in Table I.

The reagents were dissolved in absolute ethanol.

TABLE I

ABBREVIATED AND FULL NAMES FOR HYDRAZONES

Full name	*Abbreviated form*	*M.p. (°)*
Pyridine-2-aldehyde-2-pyridylhydrazone	PAPH	181–184
Quinoline-2-aldehyde-2-pyridylhydrazone	QAPH	209
Phenanthridine-2-aldehyde-2-pyridylhydrazone	PDAPH	222–223
Pyridine-2-aldehyde-2-quinolylhydrazone	PAQH	197
Quinoline-2-aldehyde-2-quinolylhydrazone	QAQH	264
Phenanthridine-2-aldehyde-2-quinolylhydrazone	PDAQH	174–176
Pyridine-2-aldehyde-2-phenanthridylhydrazone	PAPDH	183–185
Quinoline-2-aldehyde-2-phenanthridylhydrazone	QAPDH	192–195
Phenanthridine-2-aldehyde-2-phenanthridylhydrazone	PDAPDH	178–182
Benzimidazole-2-aldehyde-2-pyridylhydrazone	BAPH	199–204
Benzimidazole-2-aldehyde-2-quinolylhydrazone	BAQH	283–284
Benzimidazole-2-aldehyde-2-phenanthridylhydrazone	BAPDH	245–248
Phenyl-2-pyridylketone-2-pyridylhydrazone	PP'KPH	148
Phenyl-2-pyridylketone-2-quinolylhydrazone	PP'KQH	186–187
Phenyl-2-pyridylketone-2-phenanthridylhydrazone	PP'KPDH	168–169

Solutions

Standard zinc solutions (1000 p.p.m.) were prepared by dissolving pure zinc metal (99.99%) in a small volume of perchloric acid and also by dissolving AnalaR grade zinc nitrate in doubly distilled water. The solutions were standardised by titration with EDTA and Eriochrome black T indicator[13]. The stock solutions were diluted as required immediately before use.

Buffer solutions were prepared by addition of AnalaR concentrated nitric acid to 0.5 *F* tris(hydroxymethylamino)methane solution.

Procedure

Add 8 ml of a $4 \cdot 10^{-5}$ *F* solution of reagent in absolute alcohol to a 10-ml volumetric flask containing 1 ml of a 1 p.p.m. zinc solution and 1 ml of buffer of pH 8.0. Measure the fluorescence at the emission maximum in a 1.00-cm cell against a reagent blank.

The fluorescence characteristics of the reagents were studied by the above procedure because preliminary experiments showed that optimal results were obtained in 80%(v/v) ethanol–water systems containing a twenty-fold molar excess of reagent over zinc.

RESULTS

The relative fluorescence intensities and excitation and emission wavelength maxima are shown in Table II; the instrument was calibrated before all measurements by adjusting to a fluorescence reading of 40 for 1 p.p.m. of quinine sulphate at a meter multiplier setting (MM) of 1.0 and sensitivity (S) 0.0. The results in Table II are for solutions containing 0.1 p.p.m. of zinc and a 20-fold molar excess of reagent in 80% ethanol compared to reagent blank (MM, 0.01; S, 0.0); the comparative relative fluorescence for 0.1 p.p.m. of quinine sulphate is 400.

TABLE II

FLUORIMETRIC DATA FOR ZINC CHELATES

Reagent	$\lambda_{\text{excitation}}$ (*nm*)	$\lambda_{\text{emission}}$ (*nm*)	*Relative fluorescence*
PAPH	455	515	1
QAPH	490	540	2
PDAPH	490	545	7
PAQH	470	535	660
QAQH	495	595	20
PDAQH	525	610	16
PAPDH	450	540	100
QAPDH	510	600	110
PDAPDH	580	620	230
BAPH	440	510	140
BAQH	470	520	2000
BAPDH	480	530	440
PP'KPH	420	470	8
PP'KQH	470	550	450
PP'KPDH	490	575	1520

The molar absorptivities, determined at the wavelength of maximum absorption, assuming that 1 mole of complex is formed for every g-ion of metal present, are shown in Table III. Efficiency ratios (ER), determined by dividing the relative fluorescence intensities by the molar absorptivities, are also given in Table III.

Since the molar absorptivity is a measure of the transition probability, the efficiency ratio serves as an indicator of the effect of non-radiative processes (internal conversion, intersystem crossing, chemical reaction, etc.) which compete with fluorescence from the excited state; the higher the efficiency ratio the smaller the effect of competing processes and the better the fluorescence efficiency. The reagents in Table III are arranged in increasing order of efficiency ratio; the fluorescence efficiency is maximal with BAQH. For greatest sensitivity in analytical work the chelate showing the highest efficiency ratio need not necessarily be the best to use; a high transition probability and a lesser efficiency ratio could, of course, still result in high sensitivity.

TABLE III

MOLAR ABSORPTIVITIES AND EFFICIENCY RATIOS FOR ZINC CHELATES[a]

Reagent	*Chelate*		*Efficiency ratio* $\cdot 10^4$
	λ_{max}	$\varepsilon \cdot 10^{-4}$	
PAPH	455	2.7	0.4
QAPH	475	3.2	0.6
PDAPH	510	5.4	1.3
PDAQH	515	3.9	4.1
QAQH	505	3.8	5.3
PDAPDH	580	8.5	27.1
QAPDH	525	2.9	37.9
BAPH	460	2.8	50.0
BAPDH	480	4.4	100.0
PAQH	500	4.2	157
PP'KQH	485	2.1	214
PP'KPDH	495	5.7	266
BAQH	485	1.3	1538

[a] PAPDH and PP'KPH are not listed because absorption wavelength maxima for reagent and chelate were not sufficiently different.

DISCUSSION

Except for the phenylketone derivatives, where the phenyl group cannot lie in the same plane as the rest of the molecule, no significant steric differences exist between the different hydrazones. The hydrazones, on reacting with a metal ion, behave as planar tridentate chelating agents; the resulting complexes are sufficiently fluorescent, in some cases, to permit analysis for zinc at the p.p.b. level. Since no significant steric differences exist between the different hydrazones, the wide variation in the efficiency ratios of their zinc complexes cannot be attributed to the effect of steric factors on the efficiency of non-radiative processes from the excited state.

Except for the benzimidazole derivative, the fluorescence intensity with all hydrazinopyridine derivatives is slight. There is a large difference in the fluorescence behaviour of QAPH and PAQH with zinc; it would appear, on initial consideration, that these molecules have the same extended π system after proton removal and differ only in the interchange of substituent groups. However, two resonance forms for the zinc chelate can be written when deprotonation takes place at the imino group; for PAQH these are

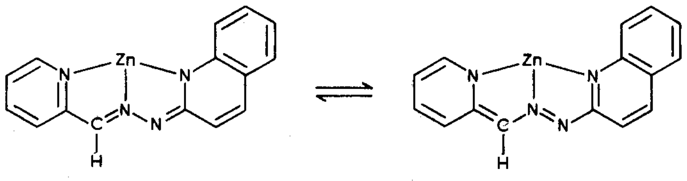

I II

It is evident that structure I will be favored energetically since the decrease in resonance energy caused by the loss of the aromaticity of one ring of a multiring system is less than that for a single aromatic ring; in other words, the form having the

–C=N– rather than the –N=N– structure is preferred. Similar consideration of the other compounds studied shows that high fluorescence was obtained for those compounds for which a –C=N– structure is energetically favored and low fluorescence was observed both where neither –C=N– nor –N=N– structures are preferred (PAPH, QAQH) and where –N=N– is energetically more favorable (QAPH, PDAPH). These observations suggest that fluorescence of the zinc hydrazones depends upon their preference for the –C=N– structural form. The benzimidazole derivatives were synthesized to test this premise because only one structural form, the –C=N–, would maintain the conjugation of the aromatic rings. The high fluorescence intensity and efficiency ratio for BAQH seem to support the argument; BAQH is the most sensitive reagent of those tested for zinc, and < 1 p.p.b. can be determined.

Photochromism in hydrazones in the solid state is well documented and certain quinolylhydrazones are photochromic in solution[14]. Salicylaldehyde-2-quinolylhydrazone is photochromic and the presence of the *o*-hydroxyl group, the N-proton and the quinoline ring are essential features for photochromism. Intramolecular hydrogen bonding of the *o*-hydroxyl group is claimed to facilitate the photochromic change and irradiation results in proton transfer from the exocyclic nitrogen to the ring nitrogen as shown in IV.

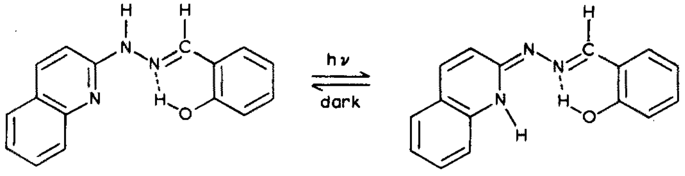

III IV

The N-heterocyclic hydrazones may be considered to behave similarly on reacting with zinc ion to promote formation of the longer conjugated chromophore I which is similar to IV. It is interesting to note that salicylaldehyde-2-pyridylhydrazone is not photochromic whilst the 2-quinolyl moiety is; this is similar to the fluorescence behaviour of PAPH (very slightly fluorescent) compared to PAQH (strongly fluorescent) on reaction with zinc ion and the difference in photochromism of the compounds studied by Wong and Bruscato[14] may also be accounted for by a comparison of the energy changes caused by loss of aromaticity of ring systems.

This work was supported by grants from the National Research Council and Defence Research Board of Canada.

SUMMARY

Benzimidazole-2-aldehyde-2-quinolylhydrazone is the most sensitive reagent of 15 N-heterocyclic hydrazones studied for the fluorimetric determination of zinc; < 1 p.p.b. of zinc can be determined (λ_{ex} 470 nm, λ_{em} 520 nm). Efficiency ratios (ER), which are a measure of the effect of non-radiative processes which compete with fluorescence from the excited state, are given; pyridine-2-aldehyde-2-pyridylhydrazone, which shows slight fluorescence with zinc, has an ER of $0.4 \cdot 10^{-4}$ whilst benzimidazole-2-aldehyde-2-quinolylhydrazone, which fluoresces strongly on reacting with zinc, has an ER of $1538 \cdot 10^{-4}$. Fluorescence intensity is greatest for those compounds which energetically prefer a –C=N– structural form.

RÉSUMÉ

La benzimidazole-2-aldéhyde-2-quinolylhydrazone constitue le réactif le plus sensible parmi les 15 hydrazones N-hétérocycliques examinées pour le dosage fluorimétrique du zinc; elle permet de doser des quantités inférieures à 1 p.p.b. de zinc (λ_{ex} 470 nm, λ_{em} 520 nm). L'intensité de fluorescence est fonction de la structure du ligand. Elle est la plus forte pour les composés qui énergétiquement préfèrent la forme –C=N–.

ZUSAMMENFASSUNG

Benzimidazol-2-aldehyd-2-chinolylhydrazon ist das empfindlichste Reagenz von 15 N-heterocyclischen Hydrazonen, die für die fluorimetrische Bestimmung von Zink untersucht worden sind; < 1 p.p.b. Zink kann bestimmt werden (λ_{ex} 470 nm, λ_{em} 520 nm). Die Wirkungsverhältnisse (ER), die ein Mass für den Einfluss strahlungsloser Prozesse sind, welche mit der Fluoreszenz vom angeregten Zustand konkurrieren, werden angegeben; Pyridin-2-aldehyd-2-pyridylhydrazon, das mit Zink eine schwache Fluoreszenz ergibt, hat ein ER von $0.4 \cdot 10^{-4}$, während Benzimidazol-2-aldehyd-2-chinolylhydrazon, welches nach der Reaktion mit Zink stark fluoresziert, ein ER von $1538 \cdot 10^{-4}$ hat. Die Fluoreszenzintensität ist bei jenen Verbindungen am grössten, die energetisch eine –C=N– Strukturform bevorzugen.

REFERENCES

1 W. E. Ohnesorge, in D. M. Hercules, *Fluorescence and Phosphorescence Analysis*, Interscience, New York, 1966, Ch. 4.
2 C. E. White, in G. G. Guilbault, *Fluorescence, Theory, Instrumentation and Practice*, M. Dekker, New York, 1967, Ch. 7.
3 M. L. Heit and D. E. Ryan, *Anal. Chim. Acta*, 32 (1965) 448.
4 M. L. Heit and D. E. Ryan, *Anal. Chim. Acta*, 34 (1966) 407.
5 S. P. Singhal and D. E. Ryan, *Anal. Chim. Acta*, 37 (1967) 91.
6 B. K. Afghan and D. E. Ryan, *Anal. Chim. Acta*, 41 (1968) 167.
7 D. E. Ryan and M. Katyal, *Anal. Letters*, 2 (1969) 515.
8 V. Zatka, J. Abraham, J. Holzbecher and D. E. Ryan, *Anal. Chim. Acta*, 54 (1971) 65.
9 G. T. Morgan and L. P. Walls, *J. Chem. Soc.*, (1931) 2447.
10 E. Ritchie, *J. Proc. Roy. Soc. N. S. Wales*, 78 (1945) 164; *Chem. Abstr.*, 40 (1946) 879^7.
11 S. Moore and K. P. Link, *J. Biol. Chem.*, 133 (1940) 293.
12 C. H. Heubner, R. Lohmar, R. J. Dimler, S. Moore and K. P. Link, *J. Biol. Chem.*, 159 (1945) 503.
13 T. S. West and A. S. Sykes, *Analytical Applications of EDTA*, BDH Ltd., Poole, England.
14 J. L. Wong and F. Bruscato, *Tetrahedron Letters*, (1968) 4593.

Analytica Chimica Acta
Elsevier Publishing Company, Amsterdam
Printed in The Netherlands

A NEW SENSITIVE METHOD FOR THE EXTRACTIVE–SPECTROPHOTOMETRIC DETERMINATION OF NICKEL

R. S. BARRATT, R. BELCHER, W. I. STEPHEN AND P. C. UDEN*
Department of Chemistry, The University of Birmingham, P.O.Box 363, Birmingham B15 2TT (England)

(Received 20th July 1971)

Thio-derivatives of β-diketones have received considerable attention in recent years and particular significance has been attached to the monothio-derivatives because of their ability to form chelates readily with certain divalent metals which show little or no reaction with the β-diketones themselves[1,2]. The analytical utility of these chelates has not been fully exploited, although Berg and Reed[3] have examined thiothenoyltrifluoroacetone as a possible colorimetric reagent for zinc, cadmium, mercury(II), and lead. The volatility of the chelates of fluorinated monothio-β-diketones has been utilized in gas chromatography[4] and separations of nickel, cobalt, and palladium[5], and nickel, palladium, and platinum[6] have been reported.

Studies[3,7,8] of the visible and ultraviolet spectra of some metal monothio-β-diketonates have provided spectrophotometric data of considerable analytical significance, and recently some favourable solvent extraction properties have been described[9] which reinforce the general analytical potentialities of these ligands as useful analytical reagents.

Earlier investigations[4], particularly of the Group VIII metal chelates of these monothio-β-diketones, indicated that bis(monothiotrifluoroacetylacetonato)nickel(II) showed great analytical potential from its spectrophotometric data, and the present paper describes a new and sensitive method for the determination of nickel with monothiotrifluoroacetylacetone which is superior to most of the recognised methods for this metal.

EXPERIMENTAL

Instrumentation and techniques

Reactions were generally carried out on a small scale in 2-dram vials which were thoroughly cleaned with chromic acid and distilled water, the caps being cleaned with acetone. Larger volumes were accommodated in either narrow-mouthed glass-stoppered bottles or separating funnels which were similarly cleaned.

A Griffin & George "Microid" shaker was used for equilibrating the two-phase extraction systems.

Equilibrium pH measurements were made with a Pye "Dynacap" pH meter

---

* Present address: Department of Chemistry, The University of Massachusetts, Amherst, Mass. 01002, U.S.A.

and a single combination electrode.

Absorbance measurements were made with a Unicam SP 800 recording spectrophotometer in 10-mm silica cells.

Materials

Monothiotrifluoroacetylacetone (1,1,1-trifluoro-4-mercaptopent-3-en-2-one; H(T-TFA)) was prepared in a manner similar to that reported in the literature[10]; trifluoroacetylacetone in ethanolic solution was treated at $-70°$ with hydrogen sulphide and hydrogen chloride. The crude H(T-TFA) was isolated and purified as the lead chelate[5] from which it was generated as required by the passage of hydrogen sulphide through a suspension of the chelate in diethyl ether. Solutions of the ligand were prepared by removing the ether from the filtered solution by distillation, and dissolving the dark red H(T-TFA) in the required solvent.

Trifluoroacetylacetone was prepared by the condensation of ethyl trifluoroacetate with acetone in the presence of sodium hydride.

Bis(monothiotrifluoroacetylacetonato)nickel(II), $Ni(T\text{-}TFA)_2$, was prepared by shaking an aqueous solution of a nickel salt with a solution of the ligand in *n*-hexane. Separation and evaporation of the organic extract gave brown crystals which were purified by sublimation at 120° (0.6 mm Hg). The product was characterised by its melting point of 155° (reported: 153° [10]), and by elemental analysis (found 30.5% C, 2.1% H, 29.1% F; $Ni(CF_3COCHCSCH_3)_2$ requires 30.3% C, 2.02% H, 28.8% F). Standard solutions of $Ni(T\text{-}TFA)_2$ were freshly prepared as required.

Hydrogen sulphide (99.5%, B.O.C.) and hydrogen chloride generated by dropping concentrated sulphuric acid on solid ammonium chloride, were used.

Laboratory-grade solvents were used throughout.

Standard aqueous solutions of nickel were prepared from AnalaR nickel nitrate hexahydrate.

Buffer solutions were prepared from AnalaR reagents according to the formulae of Clark and Lubs[11]

RESULTS AND DISCUSSION

The spectrum of $Ni(T\text{-}TFA)_2$

Freshly prepared solutions of $Ni(T\text{-}TFA)_2$ in various solvents gave the ultraviolet spectral characteristics shown in Table I.

The molar absorptivities may be compared with some reported values for reagents which already find widespread use in the determination of nickel (Table II). It was considered that the potential analytical applications of $Ni(T\text{-}TFA)_2$ surpassed those of many of the standard spectrophotometric methods for the determination of trace amounts of nickel.

Although chloroform offered maximal sensitivity by means of the absorption at 256 nm, *n*-hexane was preferred as solvent because it was more suitable for gas-chromatographic studies which were carried out simultaneously. Figure 1 shows that all the absorbances in this solvent conform to Beer's law over the range 0–4 p.p.m. of nickel (0–27 p.p.m. of chelate), but for maximal sensitivity and accuracy the absorption at 251 nm was selected, as this was not present in the spectrum of the ligand, unlike the absorption at 314 nm.

TABLE I

ABSORPTION BANDS OF $Ni(T\text{-}TFA)_2$

Solvent	*Wavelength (nm)*	*Molar absorptivity*
Ethanol	382	$7.6 \cdot 10^3$
	315	$2.1 \cdot 10^4$
	250	$2.4 \cdot 10^4$
	222	$1.9 \cdot 10^4$
Chloroform	400	$4.4 \cdot 10^3$
	316	$2.9 \cdot 10^4$
	256	$3.4 \cdot 10^4$
n-Hexane	396	$3.8 \cdot 10^3$
	314	$2.4 \cdot 10^4$
	251	$2.8 \cdot 10^4$
	225	$2.0 \cdot 10^4$

TABLE II

REAGENTS FOR THE COLORIMETRIC DETERMINATION OF NICKEL[12]

Reagent	*Wavelength (nm)*	*Molar absorptivity*
Dimethylglyoxime in an oxidizing medium	465	$1.5 \cdot 10^4$
Dimethylglyoxime in chloroform	375	$3.5 \cdot 10^3$
	325	$5.0 \cdot 10^3$
α-Furildioxime in dichlorobenzene	438	$1.7 \cdot 10^4$
Sodium diethyldithiocarbamate	325	$3.7 \cdot 10^4$
	385	$6.0 \cdot 10^4$

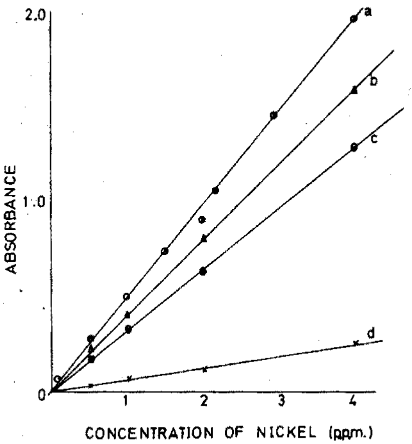

Fig. 1. Calibration graph for nickel as $Ni(T\text{-}TFA)_2$. (a) 251 nm, (b) 314 nm, (c) 225 nm, (d) 396 nm.

Factors influencing the extraction of nickel

The optimal conditions for the chelation and extraction of nickel from an aqueous solution were determined by considering the variation of the equilibrium pH of the aqueous phase and the variation of the equilibration time. All reactions were carried out at ambient temperature, and as the change in phase volumes was found to be negligible on partition, analyses were carried out on aliquots of the organic phase which were withdrawn with a syringe.

To investigate the effect of changing the pH of the aqueous phase on the extraction of the chelate, the following procedure was adopted. To a 2-dram vial was added 1.0 ml of ligand solution ($7 \cdot 10^{-3}$ *M*), 1.0 ml of nickel solution, and 1.0 ml of the appropriate buffer solution. The nickel solution was of a concentration such that an excess of nickel was present to remove as much of the ligand as possible. The mixture was shaken mechanically for 5 min after which it was allowed to stand for a few minutes to allow the phases to separate. The organic phase was removed with a syringe and its absorbance was measured at 251 nm. The equilibrium pH of the aqueous phase was measured. The results are represented graphically in Fig. 2, which shows that the formation and extraction of nickel as Ni(T-TFA)$_2$ is greatest in the range pH 4.4–5.0.

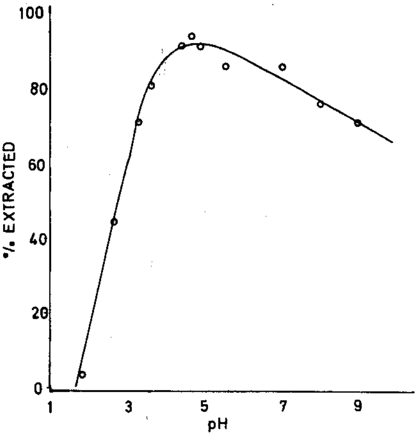

Fig. 2. Effect of pH on the distribution of nickel between water and *n*-hexane containing H(T-TFA).

The effect of the reaction time on the system was determined in a manner similar to that described above; a pH 4.6 buffer solution was used and the vials were equilibrated mechanically at the same rate for various times before the phases were separated. The results are shown in Fig. 3. The equilibrium seems to be reached quite rapidly, and 5 min was more than sufficient for complete reaction. Subsequent extractions were standardized on a 5-min extraction time.

Recovery of nickel

The systematic investigation of the extraction of nickel as Ni(T-TFA)$_2$ showed that virtually quantitative chelation and extraction were possible in the presence of an excess of nickel ions. Essentially quantitative extraction was also obtained under typical analytical conditions in which the ligand was in excess; some typical values of the yields of Ni(T-TFA)$_2$ are given in Table III.

TABLE III

THE RECOVERY OF NICKEL FROM AQUEOUS SOLUTION

Amount of Ni taken (g per 50 ml)	*Yield of Ni(T-TFA)₂*		*Recovery (%)*
	Theoretical	*Found*	
$2.499 \cdot 10^{-4}$	$1.693 \cdot 10^{-3}$	$1.70 \cdot 10^{-3}$	100.3
$4.998 \cdot 10^{-5}$	$3.386 \cdot 10^{-4}$	$3.10 \cdot 10^{-4}$	91.6
$2.499 \cdot 10^{-5}$	$1.693 \cdot 10^{-4}$	$1.608 \cdot 10^{-4}$	95.0

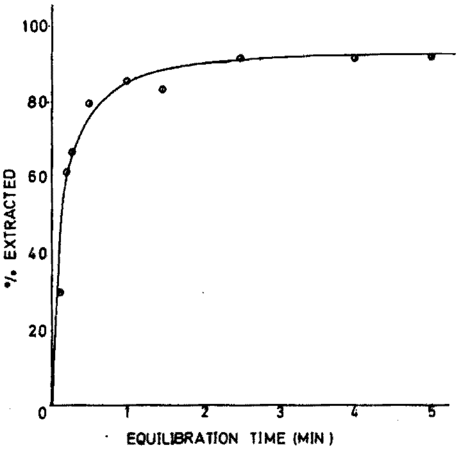

Fig. 3. Effect of equilibration time on the distribution of nickel.

Lower limits of detection

The determination of lower levels of nickel in standard aqueous solutions was easily and quickly achieved at the 0.1-p.p.m. level by extracting 10 ml of the aqueous solution with 1.0 ml of the ligand solution. The phases separated without any difficulty, and high recoveries were once again obtained; some typical data are presented in Table IV.

The determination of nickel at the 0.01-p.p.m. level was possible by extracting 250 ml of the aqueous phase with 2.0 ml of the ligand solution, and once again a clean

TABLE IV

THE DETERMINATION OF TRACE AMOUNTS OF NICKEL IN AQUEOUS MEDIUM

Nickel concentration (p.p.m.)		*No. of detns.*	*Std. devn.*
Taken	*Found*		
1.0	0.975	7	±0.078
0.1	0.081	5	±0.006
0.01	0.0095	—	—

phase separation was obtained. These results demonstrate the excellent solvent extraction properties of these chelates. No advantage was obtained by using a second extraction in which no chelate was detected.

Interfering elements

In order to verify that the method would not be impaired by the presence of other elements which might be present with nickel, an investigation was made into the recovery of nickel at the 1.0-p.p.m. level in the presence of 100-fold amounts (by weight) of other elements. The results are shown in Table V.

Significant interferences were obtained in the presence of Hg(I), Hg(II), Cu(II), and Co(II), where the chelates were apparently formed in preference to the nickel chelate and so masked its spectrum. Even when mercury(I) and mercury(II) were present in amounts equivalent to 1 p.p.m. of nickel, low recoveries of nickel were obtained. Cobalt also presented difficulties, giving a high recovery (*ca.* 121%) when present at the same concentration as the nickel, but a low recovery (*ca.* 77%) when present in a 5-fold amount. The interference of copper(II) could be reduced quite dramatically by treating the copper(II)/nickel(II) solution with hydrogen sulphide in acidic medium, expelling excess of hydrogen sulphide by warming and adjusting the solution to pH 4.6 for the extraction of the nickel. Recoveries of 1 p.p.m. of nickel in the presence of 100 p.p.m. of copper(II) were about 80%, whereas no determination was possible without this treatment. With a 10-fold amount of copper(II), a recovery of 90.6% was obtained.

TABLE V

THE INFLUENCE OF VARIOUS METAL IONS ON THE RECOVERY OF NICKEL

Metal ion	*Recovery of nickel relative to control* (%)	*Metal ion*	*Recovery of nickel relative to control* (%)
Cd(II)	94	V(V)	94.8
Zn(II)	84	Ca(II)	92.3
Mn(II)	96	Ba(II)	89.4
Pb(II)	100	Mg(II)	92.3
Pt(II)	112	Hg(I)	41.7
Fe(III)	106	Hg(II)	Indeterminable
Cr(III)	95.2	Cu(II)	Indeterminable
Al(III)	100	Co(II)	Indeterminable
Sn(IV)	95.8		

The application of the method to an alloy

The method was applied to a standard nickel–steel alloy (Sample No. 22a, Bureau of Analysed Samples Ltd., Newham Hall, Middlesbrough), which although containing 2.89% nickel would serve as a suitable sample after dilution of the solution to a manageable concentration. The following method was used.

A sample of the alloy (0.2480 g) was dissolved in 10 ml of 1 + 1 hydrochloric acid and then 2.0 ml of concentrated nitric acid was added, the mixture being boiled until no solid residue remained, and nitrous fumes were no longer evolved. The product was diluted to 250 ml with distilled water and a 2.5-ml aliquot was further diluted to 250 ml to give the working solution. Aliquot samples (50 ml) of this solution were extracted with 5.0 ml of the ligand solution in the presence of 10 ml of a pH 4.6 buffer. After extraction the organic phase was washed for 30 sec with 0.01 *M* sodium hydroxide solution which removed some of the remaining ligand and also served to break the emulsion formed in the presence of the precipitate formed in the aqueous phase. A blank value was obtained by taking a sample of distilled water through the procedure. Several determinations gave an average value of 2.83 ± 0.15% as the nickel content of the alloy.

CONCLUSIONS

The combination of solvent extraction with spectrophotometry offers a rapid and sensitive method for the determination of nickel over a wide range of concentrations. The values previously described indicate that 0.1 p.p.m. of nickel can easily be determined, and under ideal conditions 0.01 p.p.m. of nickel could be determined. Further work may lower this detection limit.

The interferences of cobalt and copper are inconvenient, but nickel can also be determined by gas chromatography, and this may afford a separation of these interfering chelates; the details of the gas chromatographic method will be reported in the near future.

One of us (R.S.B.) thanks the University of Birmingham for the provision of a research grant.

SUMMARY

A new method is presented for the determination of nickel in aqueous solution by extraction of its complex with monothiotrifluoroacetylacetone in *n*-hexane solution at pH 4.6. The complex has a molar absorptivity of $2.80 \cdot 10^4$ at 251 nm, as little as 0.01 p.p.m. of nickel being determinable. The method is suitable for 0–4.0 p.p.m. of nickel. Mercury(I), mercury(II), cobalt(II), and copper(II) are serious interferences, but the deleterious effect of copper can be readily eliminated by previous treatment with hydrogen sulphide.

RÉSUMÉ

Une nouvelle méthode est proposée pour le dosage du nickel en solution aqueuse, par extraction de son complexe avec la monothiotrifluoracétylacétone dans le *n*-hexane, à pH 4.6. Le coefficient d'absorption molaire est de $2.80 \cdot 10^4$ à 251 nm; la concentration limite inférieure pour ce dosage est de 0.01 p.p.m. Cette méthode convient de 0 à 4.0 p.p.m. de nickel. Le mercure(I) et (II), le cobalt(II) et le cuivre(II) présentent de sérieuses interférences; le cuivre peut être facilement éliminé par traitement préalable à l'hydrogène sulfuré.

ZUSAMMENFASSUNG

Es wird eine neue Methode zur Bestimmung von Nickel in wässriger Lösung

vorgeschlagen. Sie beruht auf der Extraktion mit Monothiotrifluoracetylaceton in *n*-Hexan-Lösung bei pH 4.6. Der Komplex hat bei 251 nm einen molaren dekadischen Extinktionskoeffizienten von $2.80 \cdot 10^4$; so geringe Gehalte wie 0.01 p.p.m. Nickel können bestimmt werden. Die Methode eignet sich für 0–4.0 p.p.m. Nickel. Quecksilber(I), Quecksilber(II), Cobalt(II) und Kupfer(II) stören ernsthaft; der Einfluss von Kupfer kann durch vorhergehende Behandlung mit Schwefelwasserstoff eliminiert werden.

REFERENCES

1 S. H. H. Chaston, S. E. Livingstone, T. N. Lockyer, V. A. Pickles and J. S. Shannon, *Australian J. Chem.*, 18 (1965) 673.
2 R. Belcher, W. I. Stephen, I. J. Thomson and P. C. Uden, *J. Inorg. Nucl. Chem.*, 33 (1971) 1851.
3 E. W. Berg and K. P. Reed, *Anal. Chim. Acta*, 36 (1966) 372.
4 R. Belcher, W. I. Stephen, I. J. Thomson and P. C. Uden, *J. Inorg. Nucl. Chem.*, (1972) in press.
5 R. Belcher, W. I. Stephen, I. J. Thomson and P. C. Uden, *Chem. Commun.*, (1970) 1019.
6 W. I. Stephen, I. J. Thomson and P. C. Uden, *Chem. Commun.*, (1969) 269.
7 S. H. H. Chaston and S. E. Livingstone, *Australian J. Chem.*, 20 (1967) 1079.
8 I. J. Thomson, *Ph.D. Thesis*, University of Birmingham, 1970.
9 M. Leban, O. Siimann and J. Fresco, *160th A.C.S. Meeting, Chicago, Ill., Sept. 1970, Abstract Anal.*, 81.
10 R. K. Y. Ho, S. E. Livingstone and T. N. Lockyer, *Australian J. Chem.*, 19 (1966) 1179.
11 *pH Values and their Determination*, B. D. H. Chemicals Ltd., Poole, England, 1970.
12 G. Charlot (Editor), *Colorimetric Determination of Elements*, Elsevier, Amsterdam, 1964.

Analytica Chimica Acta
Elsevier Publishing Company, Amsterdam
Printed in The Netherlands

SPECTROPHOTOMETRIC DETERMINATION OF SMALL AMOUNTS OF REAGENTS USED IN SOLVENT EXTRACTION PROCESSES

PART I. α-HYDROXYOXIMES

A. W. ASHBROOK

Chemical Analysis Section, Extraction Metallurgy Division, Mines Branch, Department of Energy, Mines and Resources, Ottawa (Canada)

(Received 12th July 1971)

The use of substituted oximes as commercial reagents for the separation of copper from leach liquors was first introduced by General Mills Inc. in 1963, the first reagent being LIX-63[1]. Since that time, two more reagents of a similar nature have become available[2,3], LIX-64 and LIX-64N. The latter are more stable towards acids and more selective for copper than is LIX-63.

The general structure of these reagents is given as[1]

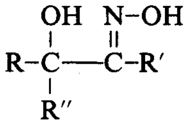

$$\begin{array}{ccc} & \mathrm{OH} & \mathrm{N{-}OH} \\ & | & \| \\ \mathrm{R{-}} & \mathrm{C}{-\!\!-} & \mathrm{C{-}R'} \\ & | & \\ & \mathrm{R''} & \end{array}$$

where R, R′, R″ are various aliphatic hydrocarbon radicals. Also, either R or R″ may be H.

All three reagents have been, or are being, used in investigations into solvent extraction processes being carried on by this Extraction Metallurgy Division[4]. A search of the literature failed to reveal a method suitable for the determination of small quantities of the LIX reagents in aqueous solutions. Losses of LIX-64 and -64N have been reported to be less than 0.1 lb/1000 gal of solution (100 p.p.m.) in a liquid–liquid extraction process from acidic solution[5]. This result was obtained by inventory. The application of these reagents to solvent-in-pulp processes could result in much higher losses, *e.g.*, by adsorption on the solid phase. Consequently, a method was required in order to determine such losses, since in small pilot-plant runs an accurate determination of losses cannot readily be obtained by inventory.

Attempts to use a complex formed between the extractant and iron(III) thiocyanate[6] showed that only LIX-63 formed such an extractable complex. However, all three extractants form extractable yellow or yellow/green copper(II) complexes which though not highly colored, absorb sufficiently strongly in the 350–450 nm range to allow their determination in the p.p.m. range. A rapid and accurate method has thus been developed by which all three reagents can be determined in both slurries and aqueous solution in the p.p.m. range.

EXPERIMENTAL

Reagents

Copper nitrate solution. For the stock solution prepare a 25% (w/v) copper nitrate trihydrate solution in water. For the reagent solution, adjust the stock solution to pH 3.75 by the addition of a saturated solution of ammonium acetate. Prepare just before use.

Standard solutions of LIX-63, -64 and -64N. Prepare solutions of the extractants by dissolving weighed amounts in methanol to give about 200 μg ml^{-1}.

Recommended procedure for solutions

Transfer an aliquot of up to 25 ml of the sample solution to a Teflon beaker and adjust to about pH 3.8 with either dilute sulphuric acid or saturated ammonium acetate solution. Transfer to a 125-ml separatory funnel and rinse the beaker into the funnel with a minimum amount of methanol. Add 25 ml of copper reagent solution (pH 3.75) and 10.0 ml of carbon tetrachloride. Shake vigorously for 2 min, and allow the phases to separate. Filter the organic phase through a Whatman phase separating paper (1PS) and measure the absorbance in a 1-cm cell, at the appropriate wavelength, against a carbon tetrachloride blank. The optimal wavelengths are: LIX-63, 425 nm; LIX-64, 365 nm; LIX-64N, 380 nm.

Recommended procedure for slurries

(*a*) *Determination of LIX reagents in aqueous plus solid phases.* Weigh the sample and container. Adjust the pH to about 3.8 and transfer to a 125-ml separatory funnel with a minimal amount of methanol. Add 25 ml of copper reagent solution, 10.0 ml of toluene, and shake for 2 min. Allow the phases to separate, drain the solids and aqueous phase, and either filter the organic phase through a Whatman phase separating paper, or centrifuge. Measure the absorbance at the appropriate wavelength against a sample blank carried through the procedure but without the addition of copper solution.

(*b*) *Separate determination of LIX reagents in the aqueous and solid phases.* Transfer the sample to a centrifuge tube or bottle and centrifuge to separate the solid and aqueous phases. If the volume of liquid is less than about 25 ml, decant into a 125-ml separatory funnel, adjust the pH, and determine the extractant as described for *Solutions.* Alternatively, the solution may be transferred to a suitable volumetric flask, diluted to volume and an aliquot taken for analysis.

Repulp the solids four times with sufficient methanol to provide about 50% solids. Centrifuge after each repulp, and combine the methanol solutions. Dilute to a suitable volume with methanol and take an aliquot for analysis.

Spectra of the extracted species

Spectra of the copper(II)–LIX-63, -64 and -64N species in carbon tetrachloride are shown in Fig. 1. The wavelengths at which maximum absorption occurs in the visible range are: LIX-63, 425 nm; LIX-64, 365 nm; LIX-64N, 380 nm. Similar absorption maxima are given in chloroform and toluene.

Optimal pH and time of extraction

The pH at which maximal extraction of the copper–oxime species occurs was

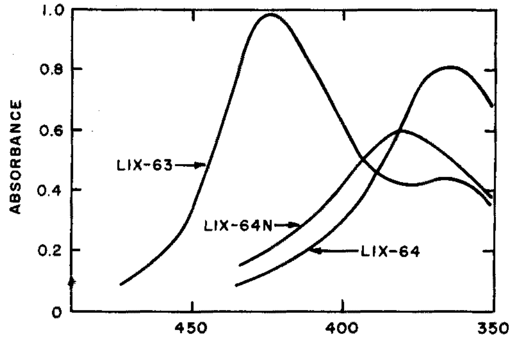

Fig. 1. Spectra of the extracted species.

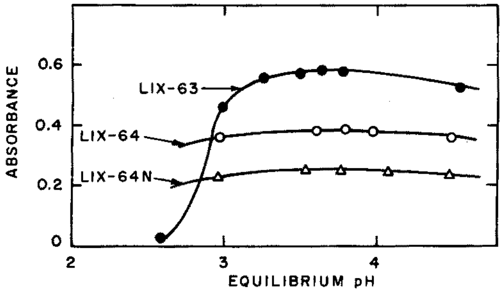

Fig. 2. Effect of pH on the extraction of LIX-63, -64 and -64N.

found to be 3.75 in each case. This was determined by contacting fixed amounts of oxime with the copper nitrate reagent, at various equilibrium pH values obtained by the addition of ammonium acetate. After extraction with carbon tetrachloride, the phases were separated and filtered. The absorbance of the organic phase was measured at the appropriate wavelength and the equilibrium pH of the aqueous phase determined. The effect of pH on the extraction of the copper complexes is shown in Fig. 2.

Shaking fixed amounts of oxime and the copper reagent solution with carbon tetrachloride, for periods up to 30 min, showed that the absorbance of the organic phase remained constant between about 1 min and 30 min for all three oximes. A 2-min shaking period was selected to ensure complete formation and extraction of the complexes. The color of the extract is stable for at least 30 min.

Concentration of the reagent

The concentration of copper necessary for complete formation of the complexes

TABLE I

EFFECT OF COPPER CONCENTRATION ON THE DETERMINATION OF LIX-63, LIX-64 AND LIX-64N

Vol. water (ml)	*Vol. Cu soln.*[c] *(ml)*	*[Cu] (M)*	*Absorbance of extract*[a,b]		
			LIX-63	*LIX-64*	*LIX-64N*
0	25	1.99	0.361	0.265	0.192
5	25	1.67	0.360	0.263	0.193
10	25	1.44	0.362	0.265	0.190
15	25	1.26	0.362	0.266	0.191
20	25	1.13	0.360	0.265	0.191
25	25	1.01	0.362	0.264	0.193
30	25	0.92	0.362	0.263	0.192
50	25	0.68	0.342	0.252	0.180
100	25	0.41	0.318	0.242	0.167

[a] 1.0 ml each of a methanol solution of LIX-63, LIX-64 and LIX-64N added, containing respectively, 1128, 795, and 1025 μg of extractant.

[b] 10.0 ml CCl_4, 1.0-cm cells.

[c] 2.07 *M* Cu(II).

was determined by taking fixed amounts of oxime and copper nitrate solution and diluting with water to various volumes, before extraction of the complexes with carbon tetrachloride. The results are shown in Table I for all three reagents and indicate that a minimal concentration of about 0.9 *M* copper(II) is necessary to ensure complete formation of the copper–oxime complexes, for up to *ca.* 1000 μg of each extractant.

Effect of diverse ions

No interference in the determination of LIX-63, -64 or -64N was found in the presence of up to 0.5 g of each of the following ions: Fe(III), Co(II), Ni(II), Zn(II), Mn(II), Cr(III), V(V), SO_4^{2-}, Cl^-. If the anion concentration is high, pH adjustment may cause some precipitation, but this does not appear to affect the determination.

Determination of extractants

Recovery from aqueous solution. A 10% (v/v) solution of LIX-63 in kerosene solution was contacted with water (aqueous/organic ratio of 200/1) at pH 4.8 for 15 min. After the phases had been allowed to separate, the organic phase was discarded. Aliquots of the aqueous phase were taken for determination of the soluble LIX-63. Similar solutions were prepared with LIX-64 and LIX-64N.

The results of these determinations, and statistical analyses of the results, are given in Table II.

TABLE II

DETERMINATION OF LIX-63, LIX-64 AND LIX-64N FROM AQUEOUS SOLUTION[a]

	LIX-63[b] (*p.p.m.*)	*LIX-64*[c] (*p.p.m.*)	*LIX-64N*[d] (*p.p.m.*)
Average	5.8	4.3	6.2
% Rel. std. dev.	±2.1	±2.9	±2.2

[a] 25.0-ml aliquots taken for analysis in each case. The average values given refer to 15 determinations. Aqueous pH values were: [b]4.8, [c]3.7, [d]4.7.

Recovery from slurries. Solids from a slurry obtained by a sulphuric acid leach of a uranium-containing ore (Rio Algom Mines, Ltd., Ontario) were separated and dried at room temperature. To a weighed portion of the solid material contained in a Teflon beaker was added a known amount of LIX-63, followed by sufficient methanol to bring the liquid:solid (L:S) ratio to about 1:1. The reagent added was approximately equivalent to 0.1 lb/ton of solids. The mixture was agitated for 15 min and then the methanol was evaporated at room temperature.

Weighed portions of the treated solid material were transferred to separatory funnels and water, previously adjusted to about pH 3.8 with acetic acid, was added to bring the L:S ratio to about 1:1. After the addition of 25 ml of copper nitrate reagent solution and 10.0 ml of toluene, the funnel was shaken for 2 min. The solids and aqueous phase were drained, the organic phase filtered (or centrifuged) and its absorbance measured in 1-cm cells. Similar experiments were carried out with LIX-64 and LIX-64N. The results are given in Table III.

TABLE III

RECOVERY OF LIX-63, LIX-64 AND LIX-64N ABSORBED ON SOLID MATERIAL

	Sample wt. (g)	*p.p.m. recovered*		
		LIX-63[a]	*LIX-64*[b]	*LIX-64N*[c]
	5.0	47	52	57
	5.0	45	51	57
	10.0	46	52	58
	10.0	47	50	57
	20.0	44	53	55
	20.0	46	52	58
	25.0	46	51	58
	25.0	—	53	57
Average		46	52	57
% Rel. std. dev.		±2.3	±2.0	±1.7

[a] 49 p.p.m. added

[b] 55 p.p.m. added.

[c] 60 p.p.m. added.

To a weighed portion of the treated solids material contained in a 100-ml polypropylene centrifuge tube was added an equal volume of methanol. The tube was stoppered and shaken vigorously for 2 min. After centrifuging, the methanol was poured off into a separatory funnel, and the extractant determined. This procedure was carried out a further 4 times on the residue from the first extraction, and the extractant in the methanol determined. The results are plotted in Fig. 3 and show that 4 extractions are required to extract 99% of the LIX reagents from the treated solid material.

Another series of experiments was carried out on the original slurry. After

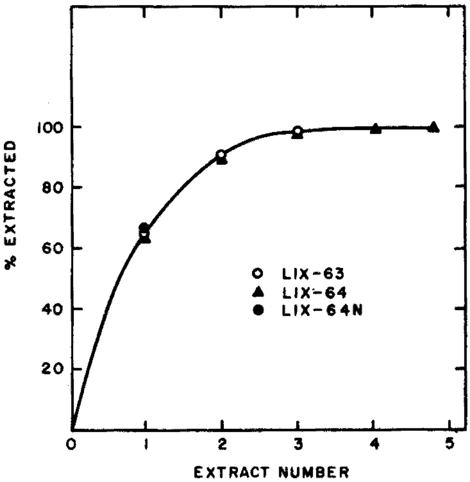

Fig. 3. Recovery of LIX reagents from treated solids by methanol extraction. (○) LIX-63, (▲) LIX-64; (●) LIX-64N.

the pH of the slurry had been adjusted to about 3.8, portions were transferred to separatory funnels. Known amounts of oxime were added and determined as described previously. Recoveries of added oximes are given in Table IV.

TABLE IV

RECOVERY OF LIX-63, LIX-64 AND LIX-64N FROM A SLURRY[a]

Approx. vol. of slurry (ml)	*μg LIX-63*		*μg LIX-64*		*μg LIX-64N*	
	Added	*Found*	*Added*	*Found*	*Added*	*Found*
10	56	57	40	38	52	51
10	112	115	80	81	104	101
20	56	54	40	38	104	103
20	224	221	120	118	208	208
30	56	56	80	81	104	103
30	224	220	240	238	208	206

[a] Approximately 50% solids.

SUMMARY

A rapid spectrophotometric method for the determination of small amounts of a-hydroxyoximes (liquid ion-exchange reagents LIX-63, -64 and -64N) in aqueous solution is described. The method utilizes the selectivity of these reagents for copper to form yellow/green complexes in acidic solution, which are quantitatively extracted into a non-polar solvent and determined spectrophotometrically. None of the metal ions expected to be present in feed solutions to solvent extraction processes with these reagents interferes. The method is suitable for the determination of the three reagents in the p.p.m. range in both aqueous solutions and slurries, with a relative standard deviation of ± 2–3%.

RÉSUMÉ

On décrit une méthode spectrophotométrique rapide pour le dosage de faibles quantités d'α-hydroxyoximes en solution aqueuse. Elle est basée sur la sélectivité de ces réactifs pour le cuivre, formant des complexes vert jaune en solution acide. Ces complexes sont extraits quantitativement dans un solvant non polaire et dosés spectrophotométriquement. Cette méthode convient pour le dosage des trois réactifs en quantité de l'ordre du p.p.m. soit en solutions aqueuses, soit dans des boues, avec une déviation standard relative de ± 2–3%.

ZUSAMMENFASSUNG

Es wird eine schnelle spektrophotometrische Methode für die Bestimmung kleiner Mengen α-Hydroxyoxime (flüssige Ionenaustausch-Reagenzien LIX-63, -64 und -64N) in wässriger Lösung beschrieben. Die Methode beruht auf der Selektivität dieser Reagenzien für Kupfer unter Bildung gelber/grüner Komplexe in saurer Lösung, die mit einem unpolaren Lösungsmittel quantitativ extrahiert und spektro-

photometrisch bestimmt werden. Es stört keines der Metallionen, mit deren Gegenwart in Lösungen gerechnet werden muss, die Lösungsmittelextraktionsprozessen unter Verwendung dieser Reagenzien zugeführt werden. Die Methode eignet sich für die Bestimmung der drei Reagenzien im p.p.m.-Bereich sowohl in wässrigen Lösungen als auch in breiigen Massen; die relative Standardabweichung ist ±2–3%.

REFERENCES

1 D. W. Agers and R. R. Swanson, A New Reagent for the Extraction of Copper, *Annual Meeting of the AIMM, Feb., 1964.*
2 D. W. Agers, J. E. House, R. R. Swanson and J. L. Drobnick, *Copper Recovery from Acid Solutions Using Liquid Ion Exchange*, General Mills, Inc., Minneapolis, Minn.
3 E. R. DeMent and C. R. Merigold, LIX-64N, A Progress Report on the Liquid Ion Exchange of Copper, *99th Annual Meeting of the AIME, Denver, Colo., Feb., 1970.*
4 G. M. Ritcey and B. H. Lucas, Separation of Copper from Nickel and Cobalt by Liquid–Liquid Extraction from Ammoniacal Solutions, *Annual Meeting of the CIMM, Quebec City, April, 1971.*
5 K. R. Rawling, *World Mining*, December, 1969, p. 34–37.
6 A. W. Ashbrook, *Anal. Chim. Acta*, 58 (1972)

Analytica Chimica Acta
Elsevier Publishing Company, Amsterdam
Printed in The Netherlands

SPECTROPHOTOMETRIC DETERMINATION OF SMALL AMOUNTS OF REAGENTS USED IN SOLVENT EXTRACTION PROCESSES

PART II. BIS(2-ETHYLHEXYL)PHOSPHORIC ACID

A. W. ASHBROOK

Chemical Analysis Section, Extraction Metallurgy Division, Mines Branch, Department of Energy, Mines and Resources, Ottawa (Canada)

(Received 12th July 1971)

The use of bis(2-ethylhexyl)phosphoric acid (EHPA) in liquid–liquid and liquid–pulp extraction processes has created a need for accurate and rapid determination of losses of this reagent. This has arisen not only from an economic point of view but also from a need to control problems of environmental pollution caused by organic reagents.

Although EHPA has been used frequently in solvent extraction processes[1], a review of the literature failed to reveal a rapid and accurate method for its determination in aqueous solution and in slurries. It is generally assumed that the solubility of this reagent is sufficiently low to make it economically useful for solvent extraction processes. This assumption appears to be based on the often quoted solubility of 20 p.p.m. given by Blake *et al.*[2].

The use of a colored complex formed between an extractant and a metal thiocyanate in aqueous solution, which is quantitatively extracted into an inert organic phase, was first reported by Ashbrook[3] for the determination of triisooctylamine in aqueous solution. It appeared likely that this approach could result in a method for the rapid determination of small amounts of EHPA in solvent extraction raffinates.

In considering the metal thiocyanate most likely to be applicable, iron(III) thiocyanate appeared to offer the greatest possibilities for several reasons. First, iron(III) is almost always present to some extent in liquors obtained on leaching ores. Secondly, with almost all general or unspecific extractants such as EHPA, iron(III) is extracted at low pH values. This could result in interference if other metal thiocyanates were used (see, for example, ref. 3). Of the metal ions which form colored thiocyanates, iron(III) thiocyanate probably has the greatest stability constant ($\log K \simeq 2.3$)[4]. Finally, iron(III) thiocyanate is not extracted by non-polar solvents such as carbon tetrachloride and toluene over the pH range 1–6.

For these reasons, the use of iron(III) thiocyanate as a reagent for the determination of small amounts of EHPA in aqueous solution and slurries was studied.

EXPERIMENTAL

Reagents

Iron(III) thiocyanate solution, ca. 0.4 M. Dissolve 15 g of iron(III) nitrate nonahydrate and 6 g of ammonium thiocyanate in about 80 ml of water. Adjust to pH 2.9 with a saturated aqueous solution of ammonium acetate and dilute to 100 ml. Prepare fresh daily.

Recommended procedure for solutions.

Adjust an aliquot of up to 25 ml of the sample solution to about pH 2.9 by the addition of dilute sulphuric acid or saturated ammonium acetate solution, and transfer quantitatively to a 125-ml separatory funnel. The aliquot taken for analysis should contain less than 0.1 g of copper(II). Alternatively, the sample aliquot may be transferred to the separatory funnel, and the pH adjusted in the funnel with the aid of a combination electrode.

Add 25 ml of the iron(III) thiocyanate solution and mix thoroughly. By pipette add 15.0 ml of carbon tetrachloride, stopper the funnel and shake vigorously for 2 min. Allow the phases to separate and filter the lower (organic) phase through a Whatman No. 1 PS phase separating paper. Measure the absorbance at 430 nm in a 5-cm cell, with the spectrophotometer zeroed on a blank carried through the procedure on 20 ml of water.

Determine the amount of EHPA from a calibration curve, obtained with known amounts of EHPA as described above.

Recommended procedure for slurries

Treatment of slurry samples is carried out in a manner similar to that described previously for the determination of α-hydroxyoximes in slurries[5], and the EHPA determined as described above under *Solutions.*

Spectrum of the extracted species

The spectrum of the iron(III) thiocyanate–EHPA complex in carbon tetrachloride is shown in Fig. 1. Maximum absorption occurs at 430 nm. The same maximum is obtained for toluene as the solvent.

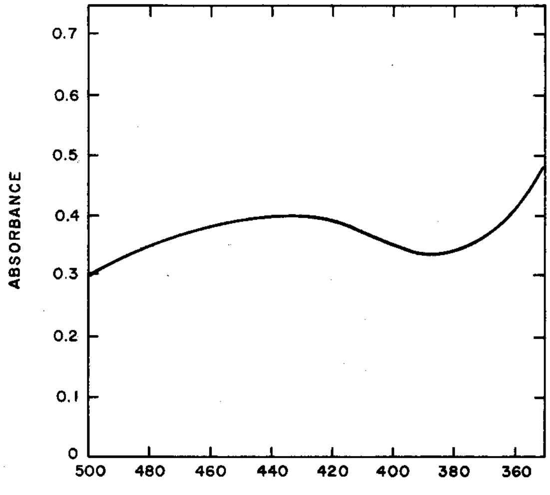

Fig. 1. Spectrum of the Fe(SCN)–EHPA complex in carbon tetrachloride.

Optimal pH and time of extraction

Fixed amounts of EHPA were reacted with iron(III) thiocyanate solution at various pH values obtained by the addition of a saturated solution of ammonium acetate. After extraction with carbon tetrachloride the phases were separated and filtered. The absorbance of the organic phase was measured at 430 nm, and the pH of the aqueous phase was determined. Formation and extraction of the extractable species as a function of pH is shown in Fig. 2. Maximal extraction of the complex occurs at pH 2.9.

Shaking fixed amounts of EHPA and iron(III) thiocyanate solution, at pH 2.9, for 1–30 min showed that maximal extraction was achieved after 1 min. A 2-min shaking period was selected to ensure complete formation and extraction of the complex. The color of the extract is stable for at least 30 min.

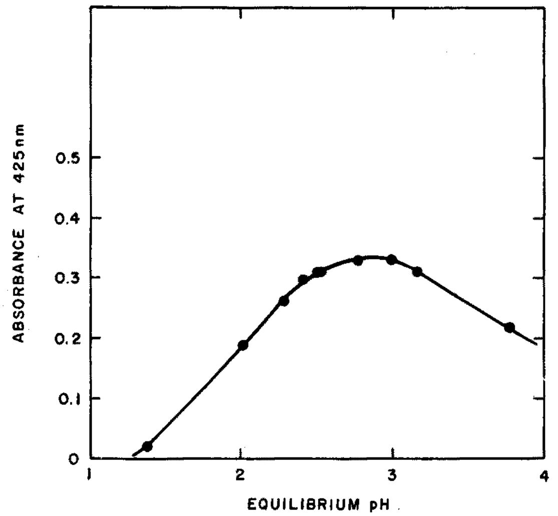

Fig. 2. Effect of pH on the extraction of the Fe(SCN)–EHPA complex.

Concentration of the iron(III) thiocyanate reagent

The concentration of iron(III) thiocyanate required for complete formation of the Fe(SCN)–EHPA species was determined as follows. Fixed amounts of EHPA and reagent solution were placed in separatory funnels and volumes of water, previously adjusted to pH 2.9 with sulphuric acid, were added. The aqueous solutions were shaken with carbon tetrachloride, the organic phases were separated and filtered, and the absorbance of each was determined at 430 nm. The results (Table I) indicate that a minimal concentration of 0.16 *M* iron(III) thiocyanate is required to ensure complete formation and extraction of the extractable species with up to 1000 μg of EHPA.

Effects of diverse ions

No interference in the determination of EHPA was found in the presence of up to 0.5 g of each of the following ions: Fe(III), Co(II), Ni(II), Zn(II), Mn(II), Ca(II), Mg(II), V(V), SO_4^{2-}, Cl^-, and NO_3^-. Copper(II) interferes if more than 0.1 g is present in the sample aliquot, giving low recoveries. This interference is a result of the

TABLE I

EFFECT OF IRON(III) THIOCYANATE CONCENTRATION ON THE DETERMINATION OF EHPA

Vol. H_2O[a] added (ml)	*$FeSCN^{2+}$ ($M\ l^{-1}$)[b]*	*Absorbance of extract at 430 nm*
0	0.35	0.360
5	0.28	0.360
10	0.24	0.361
15	0.20	0.358
20	0.18	0.359
25	0.16	0.355
30	0.14	0.345
50	0.10	0.316
100	0.06	0.272

[a] 1.0 ml EHPA solution in methanol added, containing 966 μg EHPA.
[b] 20.0 ml of a 0.37 *M* $FeSCN^{2+}$ solution added.

TABLE II

DETERMINATION OF EHPA IN AQUEOUS SOLUTION

Amount of EHPA added (μg)	*Amount of EHPA found (μg)*
49	49, 48, 49, 47
100	98, 101, 99, 98
299	298, 298, 296, 299
Sat. aqueous soln. at pH 2.3	16, 16, 15, 16, 15, 14, p.p.m. 17, 15, 16

TABLE III

RECOVERY OF EHPA FROM SOLID MATERIAL[a]

Wt. solid (g)	*EHPA*	
	Found (p.p.m.)	*Recovery (%)*
5.0	48	96.0
	49	98.0
10.0	48	96.0
	48	96.0
25.0	49	98.0
	48	96.0

[a] EHPA added to give 50 p.p.m.

formation of insoluble copper(II) thiocyanate, which is presumably formed at the expense of the iron(III) thiocyanate. The addition of a large excess of thiocyanate ion, however, did not compensate for this.

Effects of other reagents

The use of EHPA/kerosene mixtures as solvents in solvent extraction processes requires the addition of third-phase and emulsion suppressors (modifiers). One of the following is usually used for this purpose: tri-*n*-butyl phosphate, isodecanol, 2-ethylhexanol. No interference was found in the determination of EHPA in the presence of up to 10 mg of each of these modifiers. Kerosene was also found not to interfere.

Determination of EHPA

Recovery from aqueous solution. A solution containing 10% (v/v) of EHPA and 5% isodecanol in kerosene was contacted for 15 min with water at pH 2.3. The water contained 10 g of sodium sulphate per liter to aid in phase separation, and the aqueous/organic ratio was about 200/1. After the phases had been separated, aliquots of the aqueous phase were taken for the determination of EHPA. Results are given in Table II.

Recovery from slurries. The preparation of slurry solids containing a known amount of EHPA was carried out in a manner similar to that described previously[5]. Weighed portions of this material were transferred to separatory funnels and water, previously adjusted to pH 2.9 with sulphuric acid, was added to give a slurry containing about 50% solids. The EHPA was determined as described above. Recovery of the added EHPA is shown in Table III.

Extraction of EHPA from the solid material by methanol was also studied. A sample of the material was shaken in a stoppered 100-ml polypropylene centrifuge tube for 2 min. After centrifugation, the methanol was poured into a separatory

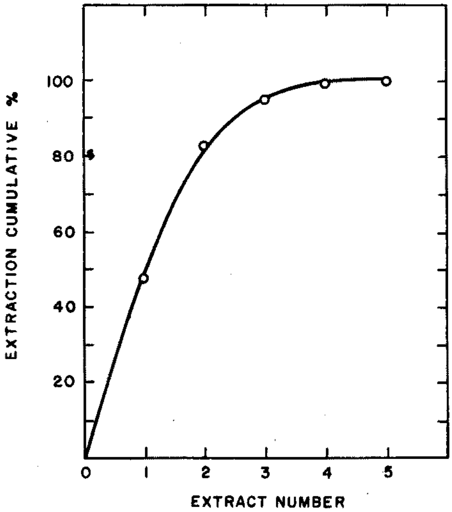

Fig. 3. Extraction of EHPA from solid material with methanol.

funnel and the EHPA determined. The residue was repulped with methanol a further 4 times and the EHPA determined on the methanol extracts.

The results are illustrated in Fig. 3 and show that a minimum of 4 extractions with methanol are required to recover at least 99% of EHPA from the solid material.

TABLE IV

RECOVERY OF EHPA FROM SLURRIES

Vol. slurry[a] *(ml)*	*EHPA* *Added* *(μg)*	*EHPA* *Recovered* *(μg)*
10	100	98
	299	292
20	100	97
	299	293
30	100	97
	299	296
	398	391

[a] Slurry contained about 50% solids.

Recovery of EHPA from an actual slurry was next investigated. The slurry, containing about 50% solids, was adjusted to pH 2.9 by the addition of a saturated solution of ammonium acetate. Portions of the slurry were then transferred to separatory funnels and known amounts of EHPA added. After shaking thoroughly the EHPA was determined as described previously. The results of these experiments are given in Table IV.

DISCUSSION

At an iron(III)/thiocyanate ratio of about 1 the iron(III) thiocyanate species present in acidic solution is probably[6]* $FeSCN^{2+}$.

Above this ratio there is evidence[6] for the formation of $Fe(SCN)_2^+$. The strong color of iron(III) thiocyanate solutions is attributed[7-9] to the species $FeSCN^{2+}$. If this species is assumed to be the one which reacts with EHPA, then the extracted complex is probably $((RO)_2PO_2)_2FeSCN$, where R is the ethylhexyl group.

$FeSCN^{2+}$ absorbs at 460 nm in aqueous solution[9], whereas the EHPA–FeSCN species absorbs at 430 nm in carbon tetrachloride. The effect of the thiocyanate/iron(III) ratio on the formation and extraction of the EHPA–FeSCN complex was found to be constant over the range 1–3. As this ratio was decreased below 1 recovery of EHPA decreased slightly. An arbitrary ratio of 2 was chosen to ensure complete formation of the extractable species.

Autoreduction of iron(III) by thiocyanate ion[9] did not present any apparent problems when the iron(III) thiocyanate solution was prepared just before use.

---

* Coordinated water has been omitted for clarity.

SUMMARY

A rapid spectrophotometric method for the determination of small amounts of bis(2-ethylhexyl)phosphoric acid (EHPA) in aqueous solution and in slurries is described. The method is based on the formation of a yellow complex formed between iron(III) thiocyanate and EHPA, which is extracted into a non-polar solvent such as carbon tetrachloride or toluene and determined spectrophotometrically. Of the metal ions usually found in solutions obtained from the processing of ores only copper(II) interferes. Kerosene and modifiers such as isodecanol, 2-ethylhexanol and tri-*n*-butyl phosphate do not interfere The method is suitable for the determination of 1–500 p.p.m. of EHPA in aqueous solutions and in slurries. Beer's law is obeyed up to 1000 μg of EHPA.

RÉSUMÉ

On décrit une méthode spectrophotométrique rapide pour le dosage de faibles quantités d'acide bis-(éthylhexyl-2)phosphorique (EHPA) en solution aqueuse et dans des boues. Elle est basée sur la formation d'un complexe jaune, formé entre le thiocyanate de fer(III) et EHPA ; ce complexe est extrait dans un solvant non-polaire tel que tétrachlorure de carbone ou toluène et dosé par spectrophotométrie. Parmi les métaux généralement rencontrés dans le traitement des minerais, seul le cuivre(II) gêne. Le kérosène et d'autres agents tels que isodécanol, éthyl-2-hexanol et tri-*n*-butylphosphate n'interfèrent pas.

ZUSAMMENFASSUNG

Es wird eine schnelle spektrophotometrische Methode für die Bestimmung kleiner Mengen Bis(2-äthylhexyl)phosphorsäure (EHPA) in wässriger Lösung und in breiigen Massen beschrieben. Die Methode beruht auf der Bildung eines gelben Komplexes zwischen Eisen(III)-thiocyanat und EHPA, der mit einem unpolaren Lösungsmittel wie Tetrachlorkohlenstoff oder Toluol extrahiert und spektrophotometrisch bestimmt wird. Von den Metallionen, die gewöhnlich in Lösungen aus der Erzaufbereitung gefunden werden, stört nur Kupfer. Kerosin und Zusatzmittel wie Isodecanol, 2-Äthylhexanol und Tri-*n*-butylphosphat stören nicht.

REFERENCES

1 G. M. Ritcey, *Dept. of Energy, Mines and Resources, Mines Branch, Canada, Inf. Circular IC 213*, 1969.
2 C. A. Blake, K. B. Brown and C. F. Coleman, *ORNL-1903*, 1955.
3 A. W. Ashbrook, *Analyst*, 84 (1959) 177.
4 *Stability Constants*, Spec. Publ. No. 7, The Chemical Society, London, 1958.
5 A. W. Ashbrook, *Anal. Chim. Acta*, 58 (1972) 115.
6 S. E. Polchlopek and J. H. Smith, *J. Amer. Chem. Soc.*, 71 (1949) 3280.
7 R. K. Gould and W. C. Vosburgh, *J. Amer. Chem. Soc.*, 64 (1942) 1630.
8 J. F. Below, R. E. Connick and C. P. Coppel, *J. Amer. Chem. Soc.*, 80 (1958) 2961.
9 R. H. Betts and F. S. Dainton, *J. Amer. Chem. Soc.*, 75 (1953) 5721.

Analytica Chimica Acta
Elsevier Publishing Company, Amsterdam
Printed in The Netherlands

STUDIES OF SUBSTITUTED DIHYDROXY-*p*-BENZOQUINONES AS PRECIPITATE-EXCHANGE REAGENTS

J. E. BARNEY II* AND D. D. ROSEBROOK
Midwest Research Institute, Kansas City, Mo. 64110 (U.S.A.)

(Received 21st May 1971)

The introduction of salts of chloranilic acid (2,5-dichloro-3,6-dihydroxy-*p*-benzoquinone) as precipitate-exchange reagents for determining anions[1-9] has led to their subsequent increasingly widespread usage[10] in spectrophotometric methods. Successful application of these salts to the determination of a particular anion is dependent upon the judicious choice of the cation, the solvent, the pH, and the wavelength of absorption.

Another useful parameter is the absorbing anion, in this case chloranilate or acid chloranilate. Other anions such as chromate and oxalate[11] have been used in precipitate-exchange reactions. However, these ions do not have large molar absorptivities, so either sensitivity must be sacrificed or the ions must be converted to a more strongly absorbing species.

Other substituted dihydroxy-*p*-benzoquinones were proposed for use as analytical reagents during the development of the chloranilates[3]. Although several of these compounds, including bromanilic acid (2,5-dibromo-3,6-dihydroxy-*p*-benzoquinone), iodanilic acid (2,5-dihydroxy-3,6-diiodo-*p*-benzoquinone), and nitranilic acid (2,5-dihydroxy-3,6-dinitro-*p*-benzoquinone), have been evaluated for determining cations by spectrophotometric methods[11-16], salts of these and related compounds such as polyporic acid (2,5-dihydroxy-3,6-diphenyl-*p*-benzoquinone) and atromentin (2,5-dihydroxy-3,6-bis(dihydroxyphenyl)-*p*-benzoquinone), have not been systematically studied for use as precipitate-exchange reagents for anions.

This report describes the preparation of the barium salts of bromanilic acid, nitranilic acid, polyporic acid and atromentin, and the study of their application as reagents for the determination of sulfate. Although these studies did not produce a significantly better reagent than barium chloranilate, new syntheses of barium bromoanilate, barium nitranilate and barium polyporate were developed, and some new information was obtained from the ultraviolet absorption spectrum of polyporic acid.

EXPERIMENTAL

Preparation of reagents

Because of commercial availability or relative ease of synthesis, bromanilic acid, nitranilic acid, polyporic acid and atromentin were selected for this study.

---

* Present address: Stauffer Chemical Company, Western Research Center, 1200 South 47th Street, Richmond, Calif. 94804, U.S.A.

Bromanilic acid (Chemical Procurement Laboratories, College Point, N.Y. 11356) was purified by recrystallization from acetic acid. The purified acid was bright orange.

Nitranilic acid (Nutritional Biochemicals Corporation, Cleveland, Ohio 44128) was purified by leaching out the impurities with acetone; recrystallization from common organic solvents was not possible because of low solubility of the acid in the solvents tested.

Polyporic acid was prepared by a modification of Adams' method[17]. 2,5-Diphenyl-*p*-benzoquinone (6.6 g) was dissolved in 450 ml of anhydrous acetic acid, and the solution was heated to 100°; 10.7 ml of bromine were added with vigorous stirring, and the solution was heated at 100° for 80 min. The reaction mixture was poured into 1.5 l of water, and the resulting mixture was boiled for 90 min. The orange-yellow precipitate of 2,5-dibromo-3,6-diphenyl-*p*-benzoquinone was removed by filtration and was washed with 150 ml of cold water. This compound was dissolved in 900 ml of (1 + 1) methanol–aqueous 10% sodium hydroxide at 45°, and this solution was held at 45° for 2 h. The reddish-brown precipitate was removed by filtration and washed with cold water. The washings were added to the filtrate, and the precipitate was discarded. Additional cold water was added to the filtrate until its volume was 1,350 ml, after which it was acidified with concentrated hydrochloric acid. This solution was evaporated to about 700 ml, and the precipitate of polyporic acid was removed by filtration. The latter was washed with cold water and dried at 100° for 100 min. The yield of deep brown polyporic acid was 88%.

Atromentin was synthesized by an extension of the method of Plummerer and Prell[18]. *p*-Benzoquinone (16.7 g) was suspended in 200 ml of carbon disulfide at 0°, 60 g of anhydrous aluminum chloride were added, and the mixture was stirred for 1 h. Phenol (35 g) in 60 ml of carbon disulfide at 0° was added, and the mixture was stirred continuously for 4 h while being maintained at 0°. The reaction mixture was poured over a mixture of ice and concentrated hydrochloric acid. After the ice had melted, the solution was filtered, and the black precipitate of 2,5-bis(*p*-hydroxyphenyl)-*p*-hydroquinone was washed alternately with three 150-ml portions each of water and carbon disulfide. The moist precipitate was suspended in 150 ml of 5% acetic acid, excess of iron(III) chloride hexahydrate was added, and this mixture was boiled for 15 min. Reddish-brown 2,5-bis(*p*-hydroxyphenyl)-*p*-benzoquinone was removed by filtration, washed with 5% acetic acid, and air-dried. A portion (7 g) of this intermediate was dissolved in 450 ml of anhydrous acetic acid, the solution was heated to 100°, 10.7 g of bromine were added, and the solution was heated to 100° for 90 min. The mixture was then poured into 2.5 l of water and this mixture was heated under reflux for 1 h. 2,5-Dibromo-3,6-bis(*p*-hydroxyphenyl)-*p*-benzoquinone was removed by filtration, and was washed with cold water followed by 10 ml of methanol. The moist precipitate was dissolved in 900 ml of (1 + 1) methyl alcohol–aqueous 10% sodium hydroxide at 42°, and the solution was held at 42° for 2.5 h. The resulting mixture was filtered, the precipitate was discarded, and aqueous 25% hydrochloric acid was added to the filtrate. The latter was evaporated to about 300 ml, and atromentin was removed by filtration, washed with 500 ml of cold water, and dried at 110° for 3 h. The yield of chocolate-colored atromentin was 28%. A portion (1 g) of this product was purified for further use by recrystallizing it from (20 + 80) acetonitrile–toluene.

Barium bromanilate was prepared by two methods. In one, it was prepared from barium chloride dihydrate and bromanilic acid by precipitation from (30 + 70) methanol–water, similarly to a method used to prepare barium chloranilate[19]. In the other method, 1 g of bromanilic acid was dissolved in 1 l of methyl Cellosolve, 500 ml of an aqueous 5% (w/v) solution of barium chloride dihydrate were added with stirring, and the mixture was digested for 3 days at 40°. The purple salt was removed by filtration, and was washed twice with 75 ml of (40 + 60) methyl Cellosolve–water, three times with 45 ml of methyl Cellosolve, and twice with diethyl ether. It was purified by adding it to boiling methyl Cellosolve, filtering the resulting mixture at 70° to recover the undissolved salt, washing the precipitate three times with diethyl ether, and drying it at 70° for 1 h. Part of the first preparation was equilibrated with absolute ethanol for 11 days, while part of the second preparation was equilibrated with acetonitrile for 11 days.

Barium nitranilate was prepared from barium chloride dihydrate and nitranilic acid. Nitranilic acid (1 g) was dissolved in 500 ml of ethanol, 500 ml of an aqueous 5% (w/v) solution of barium chloride dihydrate were added with stirring, and the mixture was digested for 24 h at room temperature with stirring. The yellow salt was separated from the mixture by filtration, washed with (50 + 50) ethanol–water, and dried at 70° for 1 h.

Barium polyporate was prepared from barium chloride dihydrate and polyporic acid. Polyporic acid (0.5 g) was dissolved in 400 ml of acetone and heated to 40°, and 200 ml of an aqueous 5% (w/v) solution of barium chloride dihydrate were added slowly with stirring. The polyporic acid solution was maintained at a pH just sufficient to prevent precipitation of barium hydroxide by occasionally adding aqueous 0.1 *M* hydrochloric acid, and a constant volume was maintained by occasionally adding small amounts of acetone.

Barium polyporate was removed by filtration. Unreacted polyporic acid was leached from the salt with hot acetone, and unreacted barium chloride was leached with water. The remaining barium polyporate was vacuum-dried for 2 h at 80°.

The barium salt of atromentin could not be prepared because of the extremely low solubility of atromentin in acidic solutions.

Absorption spectra

All absorption spectra were obtained on the highest purity reagents with a Beckman Model DU spectrophotometer except as noted in Table I. Buffers used were: *pH 1.99*, 50 ml of 1 *M* sodium acetate plus 116.7 ml of 0.450 *M* hydrochloric acid, diluted to 250 ml; *pH 4.63*, equal parts of 0.2 *M* acetic acid and 0.2 *M* sodium acetate; *pH 5.89*, five parts of 0.2 *M* acetic acid plus 95 parts of 0.2 *M* sodium acetate; *pH 9.0*, 0.75 g of potassium chloride plus 0.62 g of boric acid plus 14.7 ml of 0.291 *M* sodium hydroxide, diluted to 200 ml.

The pertinent information about the absorption spectra is shown in Table I.

Studies with barium bromanilate

The usefulness of any precipitate-exchange reagent depends upon finding a suitable solvent for the exchange reaction. The solubility and reactivity of barium bromanilate prepared by the first method were studied in many solvents. About 25 mg of barium bromanilate was added to about 10 ml of the solvent, and the mix-

TABLE I

SPECTRAL DATA FOR VARIOUS DIHYDROXY-*p*-BENZOQUINONES

Compound	*Solvent*	*pH*	*Wavelengths of maximum absorbance (nm)*		*Molar absorptivity at λ_{max}*	
			Visible	*U.v.*	*Visible*	*U.v.*
Bromanilic acid	Water	1.99	522	322	520	18,400
Bromanilic acid	Water	4.63	518	331	200	24,800
Bromanilic acid	Water	5.89	—	331	—	30,760
Bromanilic acid	Water	9.0	515	330	165	22,800
Bromanilic acid	(40+60) Methyl Cellosolve–water	4.63	517	331	260	20,550
Bromanilic acid	(40+60) Methyl Cellosolve–water	5.89	513	331	260	24,700
Bromanilic acid	(60+40) Methyl Cellosolve–water	4.63	514	330	275	20,200
Bromanilic acid	(60+40) Methyl Cellosolve–water	5.89	512	331	260	23,300
Bromanilic acid	(70+30) Methyl Cellosolve–water	4.63	514	330	275	19,650
Bromanilic acid	(70+30) Methyl Cellosolve–water	5.89	510	331	260	23,800
Bromanilic acid	(80+20) Methyl Cellosolve–water	4.63	510	329	280	19,500
Bromanilic acid	(80+20) Methyl Cellosolve–water	5.89	508	330	260	23,000
Nitranilic acid	Water	1.99	—	360; 292.5	—	5,920; 13,900
Nitranilic acid	Water	5.89	—	360; 292.5	—	5,870; 14,180
Nitranilic acid	Water	9.0	—	360; 292.5	—	5,510; 14,600
Polyporic acid	Water	9.0	530	331; 286	155	18,500; 14,400
Polyporic acid	(60+40) Methyl Cellosolve–water	9.0	520	320	150	18,800
Polyporic acid	(60+40) Methyl Cellosolve–water	4.63	525	289	1,200	20,000
Polyporic acid	(60+40) Methyl Cellosolve–water	1.99	525	287	1,200	19,580
Polyporic acid	Abs. ethanol[a]	—	520	(325)[c]; 262	465	(~7,000); 21,800
Polyporic acid	Abs. ethanol[b]	—	450	—	383	—
Atromentin	Water	9.0	530	303; 213	185	16,080; 32,950
Atromentin	(60+40) Methyl Cellosolve–water	9.0	535	307; 213	185	16,350; 29,600
Atromentin	(60+40) Methyl Cellosolve–water	4.63	530	298	665	14,600
Atromentin	(60+40) Methyl Cellosolve–water	1.99	530	295	670	14,560

[a] Recorded with a Beckman DK; concn. $=3\cdot10^{-5}$ *M*.
[b] Recorded with a Beckman DK; concn. $=3\cdot10^{-4}$ *M*.
[c] ( ) Designates shoulder

TABLE II

OBSERVATIONS ON SOLUBILITY OF BARIUM BROMANILATE AND ITS REACTIVITY WITH SULFATE

Solvent	*Observations*	
	Solvent alone	*Solvent containing sulfate*
Distilled water	No color	White precipitate, pale purple solution
pH 2, water	All dissolved, dark purple color	White precipitate only
pH 4.6, water	All dissolved, pale purple color	(Not studied)
pH 9, water	All dissolved, pale purple color	(Not studied)
pH 4.6, (50+50) *n*-propanol–water	Partially dissolved, pale purple color	White precipitate, dark purple solution
pH 9.0, (50+50) *n*-propanol–water	Partially dissolved, pale purple color	Completely dissolved, pale purple solution
pH 4.6, (50+50) methyl Cellosolve–water	Partially dissolved, pale purple color	White precipitate only
pH 9.0, (50+50) methyl Cellosolve–water	No color	Slow color development
pH 9.0, (50+50) methanol–water	No color	Pale purple color
(50+50) dioxane–water	Partially dissolved, pale purple color	Pale purple color
pH 9.0, (50+50) acetone–water	No color	Pale purple color

TABLE III

SOLUBILITY OF BARIUM BROMANILATE AS INDICATED BY ABSORBANCE OF SOLUTIONS

Solvent	*Absorbance*
pH 7.2, (30+70) ethanol–water	1.555[a]
pH 7.5, (50+50) ethanol–water	0.820[a]
pH 8.0, (30+70) ethanol–water	0.388[a]
pH 7.2, (50+50) acetonitrile–water	1.000
pH 7.2, (70+30) acetonitrile–water	0.452
pH 2.9, (50+50) methyl Cellosolve–water	Very high
pH 5.1, (50+50) methyl Cellosolve–water	0.252
pH 5.0, (60+40) methyl Cellosolve–water	0.204
pH 5.0, (70+30) methyl Cellosolve–water	0.158
pH 9.1, (50+50) methyl Cellosolve–water	0.494
pH 9.1, (60+40) methyl Cellosolve–water	0.291
pH 9.2, (70+30) methyl Cellosolve–water	0.199
pH 4.0, (50+50) ethanol–water	0.205
pH 7.5, (50+50) ethanol–water	0.796
pH 7.9, (60+40) ethanol–water	0.520
pH 8.1, (70+30) ethanol–water	0.201
pH 5.2, (70+30) ethanol–water	0.204
pH 4.8, (60+40) ethanol–water	0.444
pH 7.8, (50+50) acetone–water	Very high

[a] Determined on barium bromanilate aged in ethanol; all others, on barium bromanilate aged in acetonitrile.

ture was shaken. These results are shown in Table II. Sodium sulfate was used to provide the sulfate ion.

The effect of pH and the nature of the solvent on the solubility of barium bromanilate, produced by the second method of synthesis, as indicated by the absorbance of the solution, was studied in several solvents. Results are shown in Table III. All measurements were made at 330 nm in 1-cm cells on solutions in equilibrium with solid barium bromanilate. The solutions were not buffered, but the pH was adjusted to the values shown with dilute hydrochloric acid or sodium hydroxide solution.

Studies of barium polyporate

The solubility of barium polyporate was studied by measuring the absorbance of solutions in acetone and water buffered at pH 5.89 with the acetic acid–sodium acetate buffer. Absorbances were measured in 1-cm cells at several wavelengths because the λ_{max} shifted with the solvent. Results are shown in Table IV.

TABLE IV

SOLUBILITY OF BARIUM POLYPORATE AS INDICATED BY ABSORBANCE OF SOLUTIONS

Solvent	*Wavelength (nm)*	*Absorbance*
(25+75) acetone–water	332	0.582
(40+60) acetone–water	332	0.791
(55+45) acetone–water	325	0.960
(70+30) acetone–water	323	1.17

DISCUSSION

In evaluating the potential usefulness of these substituted dihydroxy-*p*-benzoquinones as precipitate-exchange reagents for determining sulfate, they were compared to the established reagent, barium chloranilate.

Bromanilic acid and barium bromanilate

The data in Tables I, II, and III show that the best solvent is (70+30) methyl Cellosolve–water (low solubility, some reaction with sulfate) and the best pH is near 5.89 (highest λ_{max}). However, despite repeated attempts to prepare a calibration curve for the determination of sulfate with barium bromanilate with this solvent, the blank solutions were always darker than the solutions containing added sulfate ion. This phenomenon persisted even when large proportions of water were used in the solvent, when the pH was varied from 2.9 to 9.2, and when either ethanol or acetonitrile were used as solvent. Furthermore, the absorbance of the blank solutions increased after standing for a few hours. A possible explanation for this effect is the decomposition of barium bromanilate in aqueous solutions, which is retarded by the presence of sulfate.

A discouraging result of the studies with barium bromanilate is that it is more soluble than barium chloranilate in the same solvent[3] ($9\cdot10^{-5}$ *vs.* $5.2\cdot10^{-6}$ mole l^{-1} in (50+50) ethanol–water at pH 4). Although this comparison cannot be extended directly to other solvents, it does suggest that barium bromanilate solutions will usually produce more strongly absorbing blank solutions than will barium chloranilate.

Nitranilic acid and barium nitranilate

Although barium nitranilate was synthesized and used for a few studies, they are not reported because this reagent is probably no more useful than barium chloranilate for determining sulfate. The following argument shows why.

Because nitranilic acid is a fairly strong acid[20] the nitranilate ion is the absorbing species in the pH range 2–9, and the absorption spectrum does not change. Thus, from a spectral point of view, nitranilic acid is potentially more useful than chloranilic acid because there is no preferred pH for its use as a precipitate-exchange reagent.

One important factor that can affect the usefulness of a reagent is the molar absorptivity of the absorbing species. Table I shows that the molar absorptivity of nitranilic acid is around 14,000 at the λ_{max} in the ultraviolet region, while that for chloranilic acid is 13,200[3]. Thus, under identical reaction conditions, the two barium salts would give about the same limit of detection for sulfate.

The only possibility of lowering the detection limit for sulfate for the barium nitranilate reagent relative to the barium chloranilate reagent would be to find a solvent in which the ratio of the solubility of barium nitranilate to barium sulfate is much smaller than the ratio of barium chloranilate to barium sulfate. This event is unlikely because the two reagents are of such similar chemical structure that the solubilities of their barium salts should be similar in all solvents.

Polyporic acid and barium polyporate

Acetone was selected as a possible solvent for effecting the reaction between barium polyporate and sulfate ion because this solvent was the only one in which the former could be prepared. The most satisfactory metal chloranilates for precipitate-exchange reactions are precipitated from the solvent in which the reagent will be used[19]. However, no increase in absorbance was observed when sodium sulfate was added to suspensions of barium polyporate in various acetone solutions, so this reagent shows little promise for determining sulfate.

Spectral shifts in polyporic acid solutions

During these studies, the spectrum of polyporic acid in dimethylsulfoxide and several other solvents was observed to change greatly with the concentration of polyporic acid. This effect for dimethylsulfoxide is clearly shown in Fig. 1. The shift of the long wavelength absorption band from 520 nm to a shoulder at 450 nm with a 30-fold increase in concentration is indicative of dimer formation. The dimer in this system could be one that forms through strong intermolecular hydrogen bonds between the hydrogen of a hydroxyl group and the oxygen in a quinone group. This type of interaction tends to make all eight oxygens equivalent. Equivalence of the oxygens lessens or destroys the quinoid structure and hence causes the hypsochromic shift of the absorption band.

The main absorption band of polyporic acid shifts from 260 nm at $6.5 \cdot 10^{-4}$ mole l^{-1} to 307 nm at $2.34 \cdot 10^{-6}$ mole l^{-1}. This is equivalent to an energy of 14.8 kcal mole^{-1}, which is a measure of the strength of the dimer.

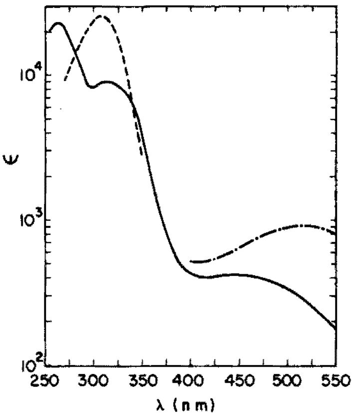

Fig. 1. Polyporic acid in dimethylsulfoxide. (——) $6.50 \cdot 10^{-4}$ mole l^{-1}, (–·–·–) $1.95 \cdot 10^{-5}$ mole l^{-1}, (----) $2.34 \cdot 10^{-6}$ mole l^{-1}.

Atromentin

The adsorption spectrum of atromentin in various solvents was not studied in detail. Such studies could provide more information about the proposed dimer formation and large hypsochromic and bathochromic shifts observed in solutions of polyporic acid.

CONCLUSION

These studies have shown that the barium salts of bromanilic acid, nitranilic acid, and polyporic acid offer little promise for replacing barium chloranilate for determining sulfate. Other salts of bromanilic acid may be useful as precipitate-exchange reagents if the observed high blanks can be avoided. Studies with other salts of nitranilic and polyporic acid might prove useful for developing improved precipitate-exchange reagents for determining fluoride, chloride, and phosphate. Atromentin is not useful for preparing precipitate-exchange reagents because it is too insoluble to permit preparation of metal salts.

SUMMARY

Studies of the barium salts of bromanilic acid, nitranilic acid and polyporic acid show that they are not superior to barium chloranilate as reagents for determining sulfate. Improved syntheses of polyporic acid and atromentin are presented; two new syntheses of barium bromanilate, and one new synthesis of barium nitranilate and of barium polyporate are also presented. Ultraviolet absorption spectra show that polyporic acid forms a dimer in dimethylsulfoxide solution.

RÉSUMÉ

Une étude est effectuée sur l'utilisation des sels de baryum des acides bromanilique, nitranilique, et polyporique, comme réactifs pour le dosage des sulfates; on constate qu'ils ne sont pas supérieurs au chloranilate de baryum. On propose de nouvelles synthèses de ces réactifs. Les spectres d'absorption obtenus dans l'ultraviolet montrent que l'acide polyporique forme un dimère dans le diméthylsulfoxyde.

ZUSAMMENFASSUNG

Untersuchungen der Bariumsalze von Bromanilsäure, Nitranilsäure und Polyporsäure ergeben, dass sie als Reagenzien für die Sulfatbestimmung dem Bariumchloranilat nicht überlegen sind. Es werden verbesserte Synthesen von Polyporsäure und Atromentin beschrieben; zwei neue Synthesen von Bariumbromanilat und eine neue Synthese von Bariumnitranilat und von Bariumpolyporat werden ebenfalls dargelegt. Die Ultraviolett-Absorptionsspektren zeigen, dass Polyporsäure in Dimethylsulfoxid-Lösung ein Dimeres bildet.

REFERENCES

1 R. J. Bertolacini and J. E. Barney ii, *Anal. Chem.*, 29 (1957) 281.
2 J. E. Barney ii and R. J. Bertolacini, *Anal. Chem.*, 28 (1957) 1187.
3 R. J. Bertolacini and J. E. Barney ii, *Anal. Chem.*, 30 (1958) 202.
4 L. Fine and E. A. Wynne, *Microchem. J.*, 3 (1959) 515.
5 A. L. Hensley and J. E. Barney ii, *Anal. Chem.*, 32 (1960) 828.
6 K. Hayashi, T. Danzuka and K. Ueno, *Talanta*, 4 (1960) 126.
7 K. Hayashi, T. Danzuka and K. Ueno, *Talanta*, 4 (1960) 244.
8 E. Hoffmann and A. Saracz, *Z. Anal. Chem.*, 190 (1962) 326.
9 E. Hoffmann, *Z. Anal. Chem.*, 185 (1962) 372.
10 Fisher Scientific Company, *Technical Data TD-178.*
11 T. E. Banyai and L. Erdey, *Acta Chim. Acad. Sci. Hung.*, 8 (1956) 383.
12 A. D. Marenzi and F. Vilallonga, *Anales Farm. Bioquim. (Buenos Aires)*, 11 (1940) 105.
13 E. Mueller, *Z. Physiol. Chem.*, 268 (1941) 245.
14 S. Kubo and C. Tsutsumi, *Rept. Food Res. Inst. (Tokyo)*, 2 (1949) 145.
15 L. Erdey and L. Jankovits, *Acta Chim. Acad. Sci. Hung.*, 4 (1954) 245.
16 I. S. Mustafin, L. D. Matneev and E. A. Kashkovskaya, *Inst. Geokhim. Analit. Khim*, 11 (1960) 87.
17 P. R. Shildneck and R. Adams, *J. Amer. Chem. Soc.*, 53 (1931) 2373.
18 R. Plummerer and E. Prell, *Ber.*, 55 (1922) 3105.
19 J. E. Barney to L. Fine, private communication, 1957.
20 K. Wallenfels and K. Friedrich, *Chem. Ber.*, 93 (1960) 3070.

Analytica Chimica Acta
Elsevier Publishing Company, Amsterdam
Printed in The Netherlands

SPECIFIC METHOD FOR THE DETERMINATION OF OZONE IN THE ATMOSPHERE

SHAM L. SACHDEV*, J. P. LODGE, JR.** AND PHILIP W. WEST
Coates Chemical Laboratories, Louisiana State University, Baton Rouge, La. 70803 (U.S.A.)

(Received 23rd August 1971)

Ozone is the principal oxidant in the photochemical smog and a detailed study of ozone toxicity in man has been reported[1]. It is also considered to be the most damaging of all air pollutants affecting vegetation[2]. The natural occurrence of ozone and its formation in the urban atmospheres is well known[3].

Published methods for the determination of ozone involve a variety of analytical techniques such as chemical oxidation[4-7], absorption of ultraviolet light[8-10], catalytic decomposition[11,12], chemiluminescence or fluorescence[13,14], and cleavage of an olefinic bond[15-18]. Most of these methods are not specific for ozone, and they are generally used for determinations of total oxidants. Others which are specific suffer from the disadvantage that they are complicated or require frequent calibration. Obviously the need for a simple, specific and reliable method for ozone is becoming critical.

The method presented here is based on the reaction of ozone with 4-allyl-2-methoxyphenol (eugenol). This reaction has been found to be specific. Ozone preferentially attacks the olefinic bond in allyl groups and releases formaldehyde. Formaldehyde formed is determined by a slight modification of the West-Gaeke procedure[19] for sulfur dioxide.

EXPERIMENTAL

Apparatus

Gas samplers[20], midget impingers (MSA Catalog No. 46984). Air flow meters (Fisher and Porter Co., Catalog No. 450-015). Dyna-vac pump (Cole-Parmer, Catalog No. 7064). Beckman DB spectrophotometer.

Reagents

Sodium tetrachloromercurate(II) solution. Dissolve 13.6 g of mercury(II) chloride and 5.8 g of sodium chloride per l of distilled water.

Sodium dichloro-sulfito mercurate(II) solution. Dissolve 0.25 g of sodium sulfite in 50 ml of sodium tetrachloromercurate(II) solution. (This reagent is unstable and should not be used over 24 h.)

Para-rosaniline reagent. Dissolve 0.16 g of para-rosaniline hydrochloride

---

* Present address: Kem-Tech Laboratories, Inc., 16550 Highland Road, Baton Rouge, La. 70808, U.S.A.
** National Center for Atmospheric Research, Boulder, Colo. 80302, U.S.A.

(Fisher Scientific Co., Catalog No. 42500) in 24 ml of concentrated hydrochloric acid, and dilute to 100 ml with distilled water.

Alkaline iodide solution. Dissolve 10 g of potassium iodide and 40 g of sodium hydroxide per 1 of water.

Acidifying reagent. Dissolve 5 g of sulfamic acid in 100 ml of water, add 84 ml of 85% phosphoric acid and dilute the mixture to 200 ml with water.

Preparation of ozonized air

Samples of ozonized air were prepared by passing prepurified air through a brown glass 5-l aspirator bottle in which a germicidal lamp (4 W, GE OZ4S11) was fixed. The mouth of the bottle was sealed with a cork through which passed the leads of the lamp and an outlet tube as shown in Fig. 1. After initial assembly of the ozonation apparatus, the lamp was kept on for a week so that it could generate enough ozone to react with any of the organic matter that might be present in the aspirator. Subsequently, before analyses, the lamp was turned on every morning at least an hour before any samples were ozonized. Ozone concentrations could be established at any desired concentration between 0.5 and 10 p.p.m. by adjusting the flow of air through the aspirator. Lower concentrations (down to 0.05 p.p.m. ozone) were obtained by partially covering the lamp with aluminum foil and equilibrating the system for 10 days to allow for any reaction of ozone with aluminum foil.

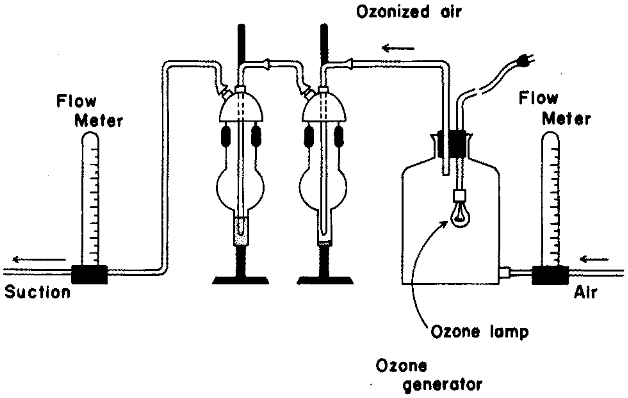

Fig. 1. Sampling equipment.

Purification of eugenol

Eugenol, as well as other 1-alkenes tried, were found to contain formaldehyde as an impurity; probably this results from the exposure of the compounds to atmospheric ozone. Each olefin was purified just before use, by passing it through a 3-in column of pure, dry sodium sulfite crystals.

Recommended procedures

Sampling procedure. The sampling equipment was set up as shown in Fig. 1. The gas samplers shown were obtained from the National Center for Atmospheric Research, Boulder, Colo. Alternatively, midget impingers were also found to be satisfactory. Two sampling bubblers were used in series. One was used as an impinger in which air containing ozone was directed upon the surface of eugenol placed in the container; the second, containing 10 ml of distilled water, was used as an absorber for formaldehyde. Air in the first impinger was passed through an orifice of 1 mm diameter at a rate of 2 l min^{-1}. The jet velocity has been estimated to be 44 m sec^{-1}. With 1 ml of eugenol in the tube, the spacing between the orifice tip and the surface of the eugenol was 5 mm. In the second bubbler, the orifice may be replaced by a frit which must be completely immersed in the water used for absorbing the formaldehyde. Slower sampling rates at 1 l min^{-1} and 0.5 l min^{-1} showed no significant effects on the reaction of ozone with eugenol or the recovery of formaldehyde formed.

Determination of formaldehyde. To 10 ml of the aqueous solution of formaldehyde add 1 ml of sodium dichloro-sulfitomercurate(II) solution and mix thoroughly. Add 1 ml of para-rosaniline solution, mix and allow to stand for 20 min. Determine the absorbance at 560 nm, and by means of a calibration curve in the range 1–10 μg per 10 ml, determine the total amount of formaldehyde in 10 ml of the sample solution.

Calculations

Convert the volume of air sampled to the volume at standard conditions of 25° and 760 mm Hg:

$$V_R = V \cdot \frac{P}{760} \cdot \frac{298}{(t+273)}$$

where V_R = volume of air at 25° and 1 atmosphere, V = volume of air sampled (l), P = barometric pressure (mm Hg), and t = temperature of air sampled (°).

Ordinarily, the correction for pressure is slight and may be neglected.

If we assume 1:1 stoichiometry for the 1% neutral buffered potassium iodide method[6] for ozone, the following expression should be used for determining ozone concentrations.

$$\text{p.p.m. ozone} = \frac{\mu\text{g HCHO found} \cdot 22.4}{30 \cdot \text{volume of air sampled (l)}} \cdot 1.54$$

or

$$(\mu\text{g m}^{-3})\text{ ozone} = \frac{\mu\text{g HCHO found} \cdot 48}{30 \cdot \text{volume of air sampled (l)}} \cdot 1000 \cdot 1.54$$

RESULTS AND DISCUSSION

A study of ozonolysis of various 1-alkenes was undertaken to develop a reliable method for the determination of ozone. A similar attempt was made by Hauser and Bradley[18] who reacted ozone with various 1-alkenes directly in solvents such as ethyl acetate, acetic acid, dimethylsulfoxide, etc. They found formaldehyde in some of the ozonized mixtures but discontinued studies along this line because of the water insolubility of 1-alkenes and a high degree of color formed in the blank determinations.

Because of the high reactivity of ozone, it was decided that the direct passage of ozone-containing air samples into 1-alkenes and then through a second bubbler containing 10 ml of distilled water would be the most reliable approach. The formaldedehyde, which has a low boiling point (−21°) and a very low solubility in alkenes, was expected to be collected in the second bubbler. Air containing known concentrations of ozone was reacted with several organic compounds containing the $-CH=CH_2$ group and the formaldehyde formed was collected and determined by the method of Lyles *et al.*[19]. The results are shown in Table I. Impinging of air on the alkene was found to be as effective as bubbling for the production of formaldehyde. In the case of bubbling, however, more alkenes were carried over to the second container and had to be removed before taking final spectrophotometric readings.

TABLE I

STUDY OF OZONOLYSIS OF VARIOUS 1-ALKENES

(Sampling rate: 2 l min^{-1}; sampling time: 5 min. Ozone concentration determined by neutral iodide method: 2.2 p.p.m.; ozone concentration determined by alkaline iodide method: 1.5 p.p.m.)

Compound used	*HCHO obtained (μg)*	*Ozone concentration (proposed method, p.p.m.)*
1-Octene	9	0.67
1-Decene	9	0.67
1-Dodecene	8	0.60
Eugenol	20	1.5
3, 4-Dimethoxyallyl benzene	6	0.45
Diallyl phthalate	6	0.45
Diallyl isophthalate	6.5	0.49

Determination of formaldehyde

Two reliable methods are available for the determination of formaldehyde: (*a*) the method developed by Lyles *et al.*[19] and (*b*) the chromotropic acid method[21]. The chromotropic acid method was tried, but some vapors of eugenol were carried into the air along with the formaldehyde formed, and interfered with the determination of formaldehyde. Moreover, the sampling solution used in the latter method (0.1% chromotropic acid in concentrated sulfuric acid) is certainly not a desirable one to work with. The method of Lyles *et al.*, which is based on the reverse of the West-Gaeke method for sulfur dioxide, was found to be simple, reliable, and satisfactory for the determination of formaldehyde formed by the ozonolysis of eugenol.

Stoichiometry of the eugenol reaction

The ozone concentration in an air containing about 2 p.p.m. of ozone was determined by the formaldehyde method, the neutral iodide method and the alkaline iodide method. The same ozonized air under exactly similar conditions was used in all three determinations. The following results were obtained:

Method	*Ozone concentration (p.p.m.)*
Neutral iodide	2.3
Alkaline iodide	1.55
Eugenol–formaldehyde	1.50

A recent report on the stoichiometry of the iodide method[22] indicated that the alkaline iodide method yields one iodine molecule for every molecule of ozone reacted, whereas the neutral iodide method actually yields 1.54 molecules of iodine per molecule of ozone reacted. On the contrary, results obtained by Kopczynski and Bufalini[23] show that in neutral buffered iodide method one mole of iodine is released per mole of ozone. Because of unavailability of standard ozone concentrations, it is difficult to decide which method yields the true results. Results of the present study are in complete agreement with results obtained by alkaline iodide method[5].

Determinations of ozone at different concentration levels

Ozone was determined in several samples of air containing ozone in the range 0.05–2.0 p.p.m. Each concentration level was determined three times by the alkaline iodide method as well as by the eugenol–formaldehyde procedure. Results are given in Table II.

TABLE II

COMPARATIVE STUDY OF EUGENOL–FORMALDEHYDE METHOD AND ALKALINE IODIDE METHOD

Ozone concentration (p.p.m.)[a]	
Alkaline iodide method	*Eugenol–formaldehyde method*
0.045	0.050
0.11	0.10
0.18	0.17
0.25	0.25
0.99	0.92
1.20	1.15
1.50	1.45
1.90	1.80

[a] Results tabulated are averages of three determinations.

The eugenol–formaldehyde method yields results similar to those obtained by the alkaline iodide method of Byers and Saltzman[5] at all concentrations within the range 0.05–2 p.p.m. Since it is unlikely that ozone will exist in ordinary atmospheres at concentrations greater than 2.0 p.p.m., determinations of higher concentrations were not extensively investigated. A few concentrations in the range of 2–5 p.p.m. of ozone were determined by the eugenol–formaldehyde procedure, but no comparison was made with the iodide method.

Sensitivity of the method

The sensitivity of the method is exactly the same as that for the formaldehyde method of Lyles *et al.*[19], since ozone reacts to produce formaldehyde. An ozone concentration of 0.02 p.p.m. can be easily determined by sampling the air for 40 min at a rate of 2 l min^{-1}.

Selectivity of the method

The eugenol–formaldehyde method described seems to be specific for ozone.

However, it is important that appropriate correction be made for the formaldehyde present in the ambient atmosphere. This presents no problem because the formaldehyde background level can be determined as a check by simply by-passing the first (eugenol) impinger and collecting and determining the formaldehyde in a separate bubbler.

Interference effects of hydrogen peroxide (3%) and peracetic acid were examined by spraying the two solutions into the air being sampled. Neither of these compounds produced any formaldehyde when reacted with eugenol. Sulfur dioxide and other reducing agents present in the air were not observed to interfere with the ozone determination.

Field studies

The method has been tested for on-site determinations of ozone. These studies indicate that the method would be quite suitable for field studies. Any formaldehyde monitoring equipment can be easily adapted for monitoring ozone. One need only connect to the formaldehyde monitor a midget impinger containing 1 ml of eugenol to convert to an ozone monitor.

The work on which this publication is based was done under Contract No. CPA 22-69-100 with the National Air Pollution Control Administration, CPE, Public Health Service, Department of Health, Education and Welfare.

SUMMARY

A simple, sensitive and specific method for the determination of ozone in the atmosphere is described. Reactions of ozone with several 1-alkenes were studied at room temperature (25°). Eugenol (4-allyl-2-methoxyphenol), when reacted with ozone, was found to produce relatively large amounts of formaldehyde compared to other 1-alkenes tested. The method described was compared with alkaline iodide method for the determination of various concentrations of ozone in the range 0.05–2.0 p.p.m. Hydrogen peroxide, peracetic acid, sulfur dioxide and various reducing agents commonly present in the air, do not interfere. Formaldehyde when present in the air, must be determined simultaneously and the concentration of formaldehyde subtracted from that of the ozone. Any formaldehyde monitoring equipment can be easily adapted for the determination of ozone.

RÉSUMÉ

On décrit une méthode simple, sensible et spécifique pour le dosage de l'ozone dans l'atmosphère. On examine les réactions de l'ozone avec plusieurs alcènes-1. L'eugénol (allyl-4-méthoxy-2-phénol) donne avec l'ozone de relativement grandes quantités de formaldéhyde, comparativement aux autres alcènes-1 essayés. La méthode décrite est comparée à la méthode à l'iodure alcalin pour des concentrations en ozone de 0.05–2.0 p.p.m. Peroxyde d'hydrogène, acide peracétique, anhydride sulfureux et divers réducteurs généralement présents dans l'air, ne gênent pas. Le formaldéhyde, lorsqu'il est présent dans l'air, doit être dosé simultanément; la concentration de formaldéhyde est soustraite de celle de l'ozone.

ZUSAMMENFASSUNG

Es wird eine einfache, empfindliche und spezifische Methode für die Bestimmung von Ozon in der Atmosphäre beschrieben. Die Reaktionen von Ozon mit verschiedenen 1-Alkenen wurden bei Raumtemperatur (25°) untersucht. Eugenol (4-Allyl-2-methoxyphenol) ergibt bei der Reaktion mit Ozon relativ grosse Mengen an Formaldehyd im Vergleich zu den anderen untersuchten 1-Alkenen. Die beschriebene Methode wurde mit der Alkalijodid-Methode für die Bestimmung verschiedener Ozonkonzentrationen im Bereich 0.05–2.0 p.p.m. verglichen. Wasserstoffperoxid, Peressigsäure, Schwefeldioxid und verschiedene gewöhnlich in der Luft vorhandene Reduktionsmittel stören nicht. In der Luft enthaltener Formaldehyd muss gegebenenfalls simultan bestimmt und die Formaldehydkonzentration von der des Ozons abgezogen werden. Jede Einrichtung für die Überwachung von Formaldehyd kann leicht auf die Bestimmung von Ozon angewendet werden.

REFERENCES

1 S. S. Griswold, L. A. Chambers and H. L. Motley, *A.M.A. Arch. Ind. Health*, 15 (1957) 108.
2 H. E. Heggestad, *J. Air Pollution Control Assoc.*, 19 (1969) 424.
3 N. A. Renzetti, *Advan. Chem. Ser.*, 21 (1959) 230.
4 A. W. Brewer and J. R. Milford, *Proc. Roy. Soc. (London), Ser. A*, 256 (1960) 470.
5 D. H. Byers and B. E. Saltzman, *Advan. Chem. Ser.*, 21 (1959) 93.
6 A. J. Haagen-Smit and M. F. Burnelle, *Intern. J. Air Water Pollution*, 1 (1958) 59.
7 B. E. Saltzman and N. Gilbert, *Amer. Ind. Hyg. Assoc. J.*, 20 (1959) 319.
8 I. R. Cohen, T. C. Purcell and A. P. Altshuller, *Env. Sci. Tech.*, 1 (1967) 247.
9 N. A. Renzetti and J. C. Romanowsky, *J. Air Pollution Control Assoc.*, 6 (1959) 379.
10 R. Stair, T. C. Bagg and R. G. Johnston, *J. Res. Natl. Bur. Std.*, 52 (1954) 133.
11 C. R. McCully, J. E. Roester, E. S. Gordon, J. N. Van Scoyoc and R. A. Carrigan, *IRE Trans. Instr.*, 1–10 (1961) 89.
12 F. J. Olmer, *Advan. Chem. Ser.*, 21 (1959) 87.
13 V. H. Regner, *J. Geophys. Res.*, 65 (1960) 3975.
14 H. Watanabe and T. Nakodoi, *J. Air Pollution Control Assoc.*, 16 (1966) 614.
15 C. E. Bradley and A. J. Haagen-Smit, *Rubber Chem. Technol.*, 24 (1951) 750.
16 H. A. Bravo and J. P. Lodge, Jr., *Anal. Chem.*, 36 (1964) 761.
17 J. J. Bufalini, *Env. Sci. Tech.*, 2 (1968) 703.
18 T. A. Hauser and D. W. Bradley, *Anal. Chem.*, 38 (1966) 1529.
19 G. R. Lyles, F. B. Dowling and V. Blanchard, *J. Air Pollution Control Assoc.*, 15 (1965) 106.
20 A. F. Wartburg, J. B. Pate and J. P. Lodge, Jr., *Env. Sci. Tech.*, 3 (1969) 767.
21 A. P. Altshuller, D. L. Miller and S. F. Sleva, *Anal. Chem.*, 33 (1961) 621.
22 A. W. Boyd, C. Willis and R. Cyr, *Anal. Chem.*, 42 (1970) 670.
23 S. L. Kopczynski and J. J. Bufalini, *Anal. Chem.*, 43 (1971) 1126.

Analytica Chimica Acta
Elsevier Publishing Company, Amsterdam
Printed in The Netherlands

THE DISTRIBUTION OF SALTS OF LARGE CATIONS BETWEEN WATER AND ORGANIC SOLVENTS*

PART I. STUDIES ON THE EXTRACTION OF QUATERNARY PHOSPHONIUM AND ARSONIUM SALTS OVER A RANGE OF CATION AND ANION CONCENTRATIONS

N. A. GIBSON AND D. C. WEATHERBURN**
Chemistry School, Sydney University, Sydney, N.S.W. 2006 (Australia)

(Received 13th August 1971)

In recent years an increasing interest has been shown in extraction systems involving quaternary ammonium, phosphonium, arsonium and stibonium salts. These investigations have been largely concerned with the use of the quaternary cations to extract anionic metal complexes[1-5], but some work has been reported on the extraction of simple inorganic anions[6-9]. The factors which influence the extraction into the organic solvent have however received scant attention. The purpose of the work reported in this and the following paper was to investigate the extraction behaviour of a series of quaternary salts in order to elucidate these factors. This paper reports the results of the effect of changing concentrations of cation and/or anion on the extraction behaviour and the results are interpreted as indicative of the nature of the species in the two phases. The following paper is concerned with the factors which influence the magnitude of the distribution ratio.

EXPERIMENTAL

Reagents

Many of the quaternary phosphonium cations studied are available commercially (Fluka A. G.). These salts were recrystallized from ethanol before use. The preparation of the quaternary arsonium salts has been described elsewhere[10]; phosphonium salts not available commercially were prepared and purified as for the arsonium salts. Aqueous stock solutions of the quaternary salts were prepared by direct weighing; the ionic strength was adjusted to 0.1 with sodium sulphate. In some cases the solubility of the quaternary salt in water was not sufficient to prepare solutions of the desired concentration; solutions of the quaternary salt in the organic solvent were then used. For some studies aqueous stock solutions of the quaternary sulphate were prepared by dissolving the quaternary halides in hot water, adding an excess of finely divided silver oxide and boiling the mixture for about 10 min. This treatment resulted in the decomposition of all phosphonium salts containing benzyl groups but little or no decomposition was observed with the other cations studied. The solution was cooled, filtered and neutralized with sulphuric acid, and the ionic strength adjusted to 0.1

---

* Based on the Ph.D. thesis of D. C. Weatherburn, Sydney University, 1968.

** Present address: Chemistry Department, University of Queensland, St. Lucia, Qld. 4067, Australia.

with sodium sulphate. The stock solution was standardised spectrophotometrically.

The variation of the distribution ratio with the pH of the aqueous phase was not investigated as previous work has shown that the distribution is generally independent of pH[6,7]. The pH of a few of the aqueous phases were measured, however, and were found to be in the range pH 3–5.

Apparatus

Equal volumes of the aqueous and organic phases were equilibrated in rotating glass containers immersed in a thermostated water bath maintained at 25.0+0.5°. Equilibration time was generally overnight but times as short as 2 h were used without obtaining significantly different results. Results obtained with the quaternary salt initially present in the organic phase were identical with the results obtained when the salt was in the aqueous phase. The concentration of the quaternary salt in the aqueous phase was determined spectrophotometrically on a Hilger Uvispec single-beam spectrophotometer. All the cations studied contained at least one aromatic ring and the absorption at *ca.* 260 nm due to the aromatic rings was measured. The aqueous solution in most of the systems studied contained a large excess of sulphate in addition to the anion of interest. In the absence of all anions except sulphate, the concentration of the quaternary cation in the aqueous phase after equilibration with organic solvent was slightly less than the initial concentration. This effect increased as the size of the cation increased. The distribution ratios have been corrected for this effect by assuming that the distribution ratio of the quaternary sulphate was independent of the cation concentration. This assumption was found to be true for the distribution of $[(C_6H_5)_4As]_2SO_4$ between chloroform and water over a wide concentration range (Table I).

TABLE I

DISTRIBUTION RATIOS FOR $((C_6H_5)_4As)_2SO_4$ BETWEEN CHLOROFORM AND SODIUM SULPHATE SOLUTION (0.03 *M*) OVER A RANGE OF CONCENTRATIONS OF $(C_6H_5)_4As^+$

$[(C_6H_5)_4As^+] \cdot 10^4 M$	D
114.5	0.08
57.3	0.10
22.9	0.07
11.5	0.07
5.73	0.10
2.29	0.08
0.57	0.11
0.23	0.09

RESULTS AND DISCUSSION

Extraction of quaternary salts over a range of cation concentrations with the anion concentration constant

The theory of the extraction of quaternary salts over a range of cation concentration with the anion concentration held constant has been developed by Krasnov *et al.*[11]. The theory predicts that if ion pairs are the only significant species present in the organic phase then the distribution ratio is independent of the cation concentration and directly proportional to the anion concentration.

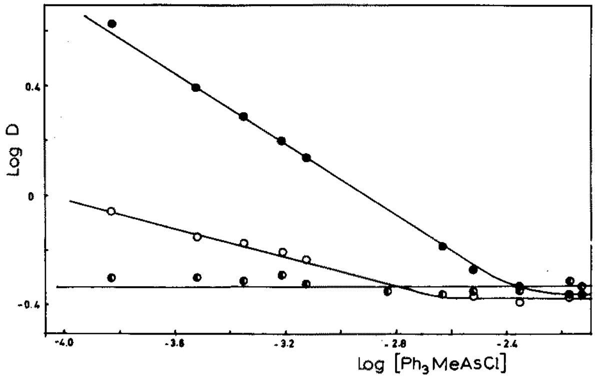

Fig. 1. Plot of log D against log [$(C_6H_5)_3CH_3AsCl$]. The extraction is from 0.5 M potassium chloride into (◐) chloroform; (○) 1,2-dichloroethane and (●) 2,2′-dichlorodiethylether. Temp. 25°.

The distribution of triphenylmethylarsonium chloride between three organic solvents (chloroform, 1,2-dichloroethane and 2,2′-dichlorodiethylether) and an aqueous solution of 0.5 M potassium chloride over a range of $(C_6H_5)_3CH_3AsCl$ concentrations is illustrated in Fig. 1.

The constant value of the distribution ratio into chloroform over the entire concentration range studied indicates that ion pairs are the only significant species in the chloroform phase. It has been shown that at higher concentrations than studied here, tetraphenylarsonium chloride can form higher aggregates (dimer and tetramer)[9,12]. The dissociation of ion pairs of triphenylmethylarsonium chloride in the other two solvents is indicated by the results in Fig. 1. This dissociation gives rise to an increase in the distribution ratio when the concentration of the quaternary salt in the organic solvent is less than 2.5×10^{-3} M in 1,2-dichloroethane and 6×10^{-3} M in 2,2′-dichlorodiethylether. If the quaternary salt were completely dissociated in the organic phase, then theory[11] predicts that the distribution ratio is inversely proportional to the concentration of the quaternary salt in the organic solvent. No such relationship was observed in the concentration range studied in the present work with any of the organic solvents.

The distribution ratios of $(C_6H_5)_3CH_3AsCl$ have very similar values for the three solvents at the highest concentrations measured. This is somewhat surprising in view of the large differences in the dielectric constants of these solvents. Possible reasons for this behaviour are considered in the following paper[13].

Extraction over a range of concentrations of the quaternary salt from aqueous sulphate media

Theory. The extraction of R_4PX into the organic phase from an aqueous solution which contains sodium sulphate may be described in the following reactions*.
(a) Association of the salt R_4PX in the aqueous phase

---

* The salt R_4PX is used to represent the quaternary salt, R may be either an alkyl or an aryl group, P may be replaced by N, As or Sb, X is a univalent anion. In the discussion to follow o refers to the organic phase, concentrations without subscripts to the aqueous phase. Charges have been omitted for the sake of clarity in the expressions; for the equillibrium constants and distribution ratios, concentrations have been used in place of activities.

$$R_4P^+ + X^- \rightleftarrows (R_4P^+, X^-)$$

$$K_1 = \frac{[R_4PX]}{[R_4P]\,[X]} \tag{1}$$

(b) Extraction of the ion pair into the organic solvent

$$(R_4P^+, X^-) \rightleftarrows (R_4P^+, X^-)_o$$

$$K_2 = \frac{[R_4PX]_o}{[R_4PX]} \tag{2}$$

(c) Dissociation of the ion pair in the organic phase

$$(R_4P^+, X^-)_o \rightleftarrows (R_4P^+)_o + (X^-)_o$$

$$K_3 = \frac{[R_4P]_o\,[X]_o}{[R_4PX]_o} \tag{3}$$

(d) Association of $(R_4P)_2SO_4$ in the aqueous phase

$$2R_4P^+ + SO_4^{2-} \rightleftarrows (R_4P^+)_2, SO_4^{2-})$$

$$K_4 = \frac{[(R_4P)_2SO_4]}{[R_4P]^2[SO_4]} \tag{4}$$

(e) Extraction of $(R_4P)_2\ SO_4$ into the organic phase

$$((R_4P^+)_2, SO_4^{2-} \rightleftarrows ((R_4P^+)_2, SO_4^{2-})_o$$

$$K_5 = \frac{[(R_4P)_2SO_4]_o}{[(R_4P)_2SO_4]} \tag{5}$$

It is possible to envisage association of ion pairs to higher aggregates but under the conditions used this is not important. The distribution ratio D of the salt R_4PX is given by the expression:

$$D = \frac{\text{Total concentration of } R_4PX \text{ in the organic phase}}{\text{Total concentration of } R_4PX \text{ in the aqueous phase}}$$

The concentration of the ion pair in the aqueous phase will in general be very small compared to the concentration of the dissociated ions, therefore

$$D = \frac{[X]_o}{[X]} + \frac{[R_4PX]_o}{[X]} \tag{6}$$

Substituting eqns.(1), (2), (4) and (5) in eqn. (6):

$$D = \frac{[X]_o}{[X]} + \frac{K_1K_2[(R_4P)_2SO_4]_o^{\frac{1}{2}}}{K_4^{\frac{1}{2}}K_5^{\frac{1}{2}}[SO_4]^{\frac{1}{2}}} \tag{7}$$

The distribution ratio of the salt $(R_4P)_2SO_4$ from aqueous solutions containing a large excess of sulphate is independent of the initial concentration of R_4P^+ in the aqueous phase (Table I). Therefore:

$$[(R_4P)_2SO_4]_o = k[R_4P]_T$$

where $[R_4P]_T$ represents the initial concentration of the R_4P^+ ion in the aqueous phase and k is a constant.

Substituting in eqn. (7):

$$D = \frac{[X]_o}{[X]} + \frac{K_1K_2k^{\frac{1}{2}}[R_4P]_T^{\frac{1}{2}}}{K_4^{\frac{1}{2}}K_5^{\frac{1}{2}}[SO_4]^{\frac{1}{2}}} \tag{8}$$

If little or no dissociation occurs in the organic phase then

$$D = K'[R_4P]_T^{\frac{1}{2}} \tag{9}$$

where

$$K' = \frac{K_1K_2k^{\frac{1}{2}}}{K_4^{\frac{1}{2}}K_5^{\frac{1}{2}}[SO_4]^{\frac{1}{2}}}$$

It should be pointed out that a model which assumes that (*a*) free ions extract into the organic phase and then associate to ion pairs, or (*b*) ion pairs are formed at the interface of the two solvents, leads to equations that are formally similar to those derived above. There is some evidence, however, which suggests that ion pairing occurs in aqueous solution of quaternary salts especially when cation and anion are large[14] and this supports the model used.

In Fig. 2 the logarithm of the distribution ratio of a number of different salts extracting into chloroform is plotted against the logarithm of the initial concentration of the quaternary salts in the aqueous phase. The results for triphenyl-*n*-amylphos-

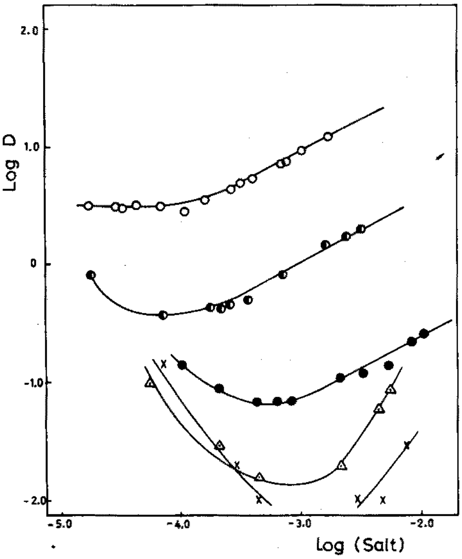

Fig. 2. Plot of log *D* for chloroform against log $[R_4PX]_T$, which is the total concentration of quaternary salt in the system. (○) $(C_6H_5)_3CH_3AsClO_4$; (◐) $(C_6H_5)_3CH_3AsI$; (●) $(C_6H_5)_3CH_3AsNO_3$; (△) $(C_6H_5)_3CH_3$-$AsBr$; (×) $(C_6H_5)_3CH_3AsCl$.

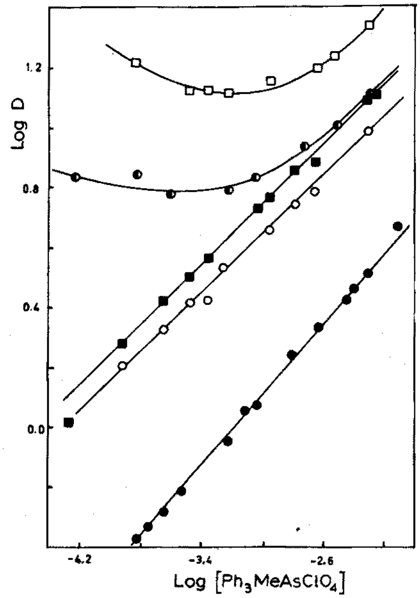

Fig. 3. Plot of log *D* against log $[(C_6H_5)_3CH_3AsClO_4]$. (□) 2,2'-Dichlorodiethylether at 25°; (◐) 1,2-dichloroethane at 25°; (■) dichloromethane at 25°; (○) dichloromethane at 35°; (●) chloroform at 25°.

phonium iodide, triphenylmethylarsonium iodide and triphenylmethylarsonium nitrate at high concentrations fall on straight lines with slopes of 0.50±0.05 in very good agreement with theory. At low concentrations the distribution ratio is higher than the value predicted by this linear relationship, indicating that dissociation of the ion pairs is occurring. This behaviour is first observed when the concentration of the salt in the chloroform falls below 10^{-4} *M*. The results for $(C_6H_5)_3CH_3AsBr$ and $(C_6H_5)_3CH_3AsCl$, also given in Fig. 2, do not obey the theoretical relationship. With these salts under the experimental conditions used the concentration in the organic phase is always less than 10^{-4} *M* even at the highest initial concentrations used.

Results for $(C_6H_5)_3CH_3AsClO_4$ in the four different solvents are presented in Fig. 3. The results indicate essentially no dissociation in chloroform at 25° and in dichloromethane at 25° and 35°. Extensive dissociation occurs in the solvents 1,2-dichloroethane and 2,2′-dichlorodiethylether under the same conditions, but the results approach a linear relationship at the highest concentrations measured. The large difference in the extraction behaviour of dichloromethane and 1,2-dichlorethane is somewhat surprising in view of the relatively small differences in their dielectric constants (9.1 and 10.4, respectively).

Extraction of quaternary salts over a range of anion concentrations with the cation concentration constant

The theory developed by Krasnov *et al.*[11] predicts that under conditions such that ion pairs are the only important species in the organic phase then the distribution ratio is proportional to the concentration of the anion in the aqueous phase.

Results obtained for $(C_6H_5)_3CH_3AsCl$, $(C_6H_5)_3CH_3AsBr$, $(C_6H_5)_3(n\text{-}C_5H_{11})PCl$ and $(C_6H_5)_4AsCl$ extracting into chloroform are presented in Fig. 4. The distribution ratio is directly proportional to the halide concentration from $5 \cdot 10^{-3}$ *M* to 1 *M* chloride. Above 1 *M* halide the linear relationship breaks down, probably because of activity effects. Similar results to these have been reported previously for $(C_6H_5)_4AsCl$[15,9] and the results obtained are in excellent agreement. The slope of the line in the plot of *D* against the chloride ion concentration was reported to be 30[15], in very good agreement with the value of 32 from Fig. 4.

The values of *D* for $(C_6H_5)_3(n\text{-}C_5H_{11})PBr$ and $(C_6H_5)_4AsBr$ also given in Fig. 4 show a linear relationship with bromide concentration over the small concentration range shown in the figure. At higher bromide concentrations the values of *D* obtained are lower than those predicted by this linear relationship. This behaviour cannot be explained by association to higher aggregates in the organic phase, for this would be expected to result in an increase not a decrease in the distribution ratio. However, the determination of distribution ratios at high values of *D* is difficult with the techniques used in this study and the effect may not be real.

The results presented in Fig. 4 were obtained with potassium chloride as the source of chloride ions. The use of lithium, sodium and cesium chlorides produced identical results to those obtained with potassium chloride. Hydrochloric acid gave identical results to potassium chloride for the extraction of $(C_6H_5)_3CH_3AsCl$ into chloroform, dichloromethane and 1,2-dichloroethane up to concentrations of 0.4 *M* chloride. Above this concentration very pronounced differences in behaviour were observed as illustrated in Fig. 5. Similar behaviour has been reported for $(C_6H_5)_4AsCl$

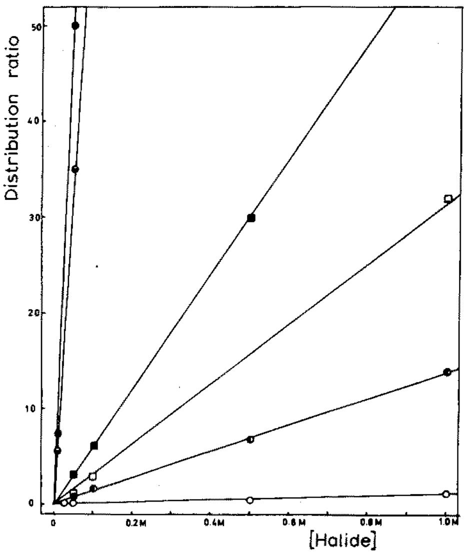

Fig. 4. Plot of the distribution ratio against the halide concentration. Temp. 25°. $[R_4PX]_T = 5 \cdot 10^{-3}$ *M*. (●) $(C_6H_5)_3(n\text{-}C_5H_{11})PBr$; (◒) $(C_6H_5)_4AsBr$; (■) $(C_6H_5)_3(n\text{-}C_5H_{11})PCl$; (□) $(C_6H_5)_4AsCl$; (◐) $(C_6H_5)_3CH_3AsBr$; (○) $(C_6H_5)_3CH_3AsCl$.

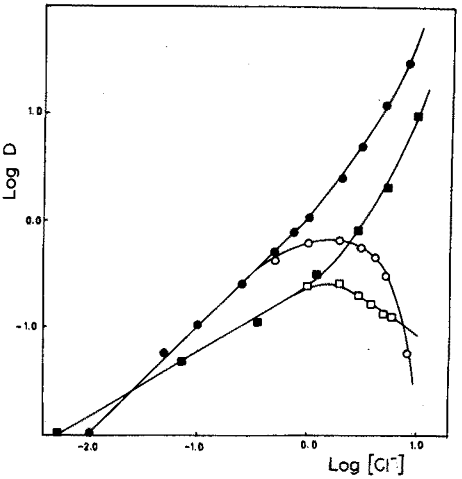

Fig. 5. Plot of log *D* against log $[Cl^-]$ for the extraction of $(C_6H_5)_3CH_3AsCl$ from LiCl or HCl solutions into chloroform or 1,2-dichloroethane. (●) Chloroform/LiCl; (○) chloroform/HCl; (■) 1,2-dichloroethane/LiCl; (□) 1,2-dichloroethane/HCl.

extracted from hydrochloric acid solution into chloroform[15,9], and for the extraction of metal chloro complexes with quaternary ammonium cations[3,4]. Explanations which have been advanced to explain the behaviour of the metal chloro complex anions[16,17] do not explain why the quaternary cation does not extract into the organic solvent. Titration of the separated organic layer indicated that in the presence of the triphenylmethylarsonium cation there was no significant extraction of hydrochloric acid into the organic solvent. It is therefore difficult to imagine any interactions in the organic solvent which would explain the anomalous behaviour and so the explanation probably lies in the properties of the hydrochloric acid solution. Sandell *et al.*[9] have asserted that this behaviour is the result of the formation of $R_4PCl \cdot H^+$ and $R_4PCl \cdot HCl$ in the aqueous phase but do not cite any evidence to support this conclusion, or to prove the existence of these species in the aqueous phase. The explanation here advanced for this behaviour differs from that of Sandell *et al.* although the possibility that such species do exist in hydrochloric acid solutions cannot be excluded.

The dielectric constant of solutions of electrolytes decreases with increasing electrolyte concentration[18,19], and the decrease is greater for hydrochloric acid solutions than for alkali metal chlorides. Unfortunately the dielectric constants of hydrochloric acid solutions have been measured only up to concentrations of 0.5 *M* but if the empirical relationship derived by Hasted *et al.*[18] is obeyed by hydrochloric acid solutions then the dielectric constant of a 2 *M* hydrochloric acid solution is less than 40. In a solution with such a low dielectric constant a significant amount of the quaternary salt could be associated as ion pairs.

When the ions of quaternary salt are transferred from the aqueous solution to an organic solvent of low dielectric constant they lose most, if not all, of their hydration energy[20] and this energy loss is then compensated for by the energy of ion-pair formation in the organic solvent. If, however, the quaternary salt exists as ion pairs in the aqueous phase, then it has lost one of the factors which favours extraction into the organic solvent, and the extraction may become energetically unfavourable.

The formation of ion pairs of quaternary salts in aqueous solution has been postulated by a number of authors. Diamond[21] has pointed out that because of their large size and hydrophobic nature there will be a tendency for the water structure to force quaternary cations to form ion pairs. Kay and Evans[22,23] have found evidence for a small amount of ion-pair formation in solutions of tetra-*n*-butylammonium iodide in D_2O and H_2O from conductivity measurements. The ion pairing of the quaternary salts postulated here in hydrochloric acid solution would be primarily electrostatic in character, favoured by low dielectric constant in the aqueous phase and by ions with small radii and high charges.

The maximum in the distribution ratio for $(C_6H_5)_4AsCl$ from hydrochloric acid solutions was observed at hydrochloric acid concentrations of 2.5 *M* when $(C_6H_5)_4AsCl$ was $5 \cdot 10^{-4}$ *M*[15] and at hydrochloric acid concentrations of *ca.* 2 *M* when $(C_6H_5)_4AsCl$ was $1 \cdot 10^{-2}$ *M*[9]. In the present study the maximum distribution ratio is observed around 2 *M* (Fig. 5). This behaviour is consistent with ion-pair formation; the higher concentration of $(C_6H_5)_4AsCl$ and smaller size of $(C_6H_5)_3CH_3$-AsCl favour ion-pair formation and the effect of the ion-pair formation is observed at lower hydrochloric acid concentrations. It should also be pointed out that it has been suggested that ion association of hydrochloric acid itself becomes important at concentrations greater than 4 *M*[24]. If this is the case then it would not be surprising if quaternary cations became associated at lower concentrations.

The anomalous extraction behaviour of quaternary chlorides from hydrochloric acid solution is therefore adequately explained by the postulate of ion-pair formation in the aqueous phase. Species such as $R_4PCl \cdot H^+$ or $R_4PCl \cdot HX$ cannot be excluded but their formation is not necessary to explain the observed behaviour.

SUMMARY

The results of the extraction of quaternary phosphonium and arsonium salts from aqueous solution into the organic solvents, chloroform, dichloromethane, 1,2-dichloroethane and 2,2′-dichlorodiethylether over a range of cation and anion concentrations are reported. The results are interpreted as indicating that under the conditions studied the quaternary salts exist as ion pairs or as dissociated ions in the organic phase. The extraction of triphenylmethylarsonium chloride from hydrochloric acid solution is anomalous; the distribution ratio reaches a maximum at about 2.0 *M* hydrochloric acid and then decreases rapidly with increasing acid concentration. This behaviour is attributed to the formation of ion pairs of the quaternary salt in the aqueous phase.

RÉSUMÉ

Une étude sur l'extraction de sels de phosphonium et d'arsonium quaternaires d'une solution aqueuse dans des solvants organiques: chloroforme, dichlorométhane, dichloro-1,2-éthane et dichloro-2,2′-diéthyléther, pour diverses concentrations en cations et anions. Dans les conditions examinées, les sels quaternaires existent comme paires ioniques ou comme ions dissociés, dans la phase organique. L'extraction du chlorure de triphénylméthylarsonium d'une solution acide chlorhydrique fait exception: il y a formation de paires ioniques du sel quaternaire dans la phase aqueuse.

ZUSAMMENFASSUNG

Es wird über die Verteilung quaternärer Phosphonium- und Arsoniumsalze zwischen wässriger Lösung und organischen Lösungsmitteln wie Chloroform, Dichlormethan, 1,2-Dichloräthan und 2,2′-Dichlordiäthyläther bei unterschiedlichen Kation- und Anionkonzentrationen berichtet. Die Ergebnisse werden als Hinweis darauf gedeutet, dass unter den untersuchten Bedingungen die quaternären Salze in der organischen Phase als Ionenpaare oder als dissoziierte Ionen vorliegen. Die Extraktion von Triphenylmethylarsoniumchlorid aus salzsaurer Lösung ist anormal; das Verteilungsverhältnis erreicht bei etwa 2.0 *M* Salzsäure ein Maximum und nimmt dann mit zunehmender Säurekonzentration stark ab. Dieses Verhalten wird auf die Bildung von Ionenpaaren des quaternären Salzes in der wässrigen Phase zurückgeführt.

REFERENCES

1 J. Yoshimura and K. Ueno, *Mem. Fac. Sci. Kyushu Univ., Ser. C Chem.*, 4 (1961) 152.
2 W. J. Maeck, G. L. Booman, M. E. Kussy and J. E. Rein, *Anal. Chem.*, 33 (1961) 1775.
3 A. M. Wilson, L. Churchill, K. Kiluk and P. Hovespian, *Anal. Chem.*, 34 (1962) 203.
4 M. L. Good, S. C. Srivastava and F. F. Holland, *Anal. Chim. Acta*, 31 (1964) 534.
5 T. Sato and M. L. Good, in D. Dyrssen, J. O. Liljenzin and J. Rydberg, *Solvent Extraction Chemistry, Proc. Int. Conf., Gothenburg, Sweden*, 1966, North-Holland, Amsterdam, 1967, p. 477.
6 R. Bock and G. M. Beilstein, *Z. Anal. Chem.*, 192 (1963) 44.
7 R. Bock and J. Jainz, *Z. Anal. Chem.*, 198 (1963) 315.
8 R. Bock and E. Grallath, *Z. Anal. Chem.*, 222 (1966) 283.
9 J. S. Fok, ZZ. Hugus and E. B. Sandell, *Anal. Chim. Acta*, 48 (1969) 243.
10 R. Armstrong, N. A. Gibson, J. W. Hosking and D. C. Weatherburn, *Aust. J. Chem.*, 20 (1967) 2771.
11 K. S. Krasnov, F. D. Kashirna and K. B. Yatsimirskii, *Tr. Kom. Anal. Khim.*, 14 (1963) 59.
12 S. Tribalat, *Anal. Chim. Acta*, 4 (1950) 228.
13 N. A. Gibson and D. C. Weatherburn, *Anal. Chim. Acta*, 58 (1972) 159.
14 D. F. Evans and R. F. Kay, *J. Phys. Chem.*, 70 (1966) 366.
15 I. P. Alimarin and C. A. Perezhagin, *Talanta*, 14 (1967) 109.
16 M. L. Good, S. E. Bryan, F. F. Holland and G. J. Mans, *J. Inorg. Nucl. Chem.*, 25 (1963) 1167.
17 M. L. Good and S. C. Srivastava, *J. Inorg. Nucl. Chem.*, 27 (1965) 2429.
18 J. B. Hasted, D. M. Ritson and C. H. Collie, *J. Chem. Phys.*, 16 (1948) 1.
19 G. H. Haggis, J. B. Hasted and T. J. Buchanan, *J. Chem. Phys.*, 20 (1952) 1452.
20 R. M. Diamond and D. G. Tuck, *Prog. Inorg. Chem.*, 2 (1960) 109.
21 R. M. Diamond, *J. Phys. Chem.*, 67 (1963) 2513.
22 R. L. Kay and D. F. Evans, *J. Phys. Chem.*, 69 (1965) 4216
23 D. F. Evans and R. L. Kay, *J. Phys. Chem.*, 70 (1966) 366.
24 H. M. Widmer, *J. Phys. Chem.*, 74 (1970) 3251.

Analytica Chimica Acta
Elsevier Publishing Company, Amsterdam
Printed in The Netherlands

THE DISTRIBUTION OF SALTS OF LARGE CATIONS BETWEEN WATER AND ORGANIC SOLVENTS*

PART II. FACTORS AFFECTING THE MAGNITUDE OF THE DISTRIBUTION RATIO

N. A. GIBSON AND D. C. WEATHERBURN**
Chemistry School, Sydney University, Sydney, N.S.W. 2006 (Australia)

(Received 13th August 1971)

In Part I[1] the extraction of quaternary phosphonium and arsonium salts from water into organic solvents was described under conditions where the concentrations of either the cation or the anion were varied. The results obtained were interpreted as indicating that under the conditions used, ion pairs and dissociated ions were the only important species present in the organic phase. In this paper are reported the results of the extraction of quaternary salts at a 1:1 mole ratio of cation to anion under conditions where ion pairs are thought to be the only important species present in the organic phase. Under these conditions comparisons between the various cations and anions are valid.

Irving and Damodaran[2] have recently discussed the present state in our knowledge of the extraction of quaternary salts and have pointed out that it is not possible to predict which anions will be extracted, or to guess at the size of the distribution ratio. The results presented here are discussed in terms of the various factors which influence the extraction and a basis for making predictions as to the order of extraction and even to guess at the size of the distribution ratio is suggested.

EXPERIMENTAL

The experimental procedures and the general method of preparation of the quaternary salts have been described elsewhere[1,3]. The results reported here were obtained at an initial concentration of quaternary salt in the aqueous phase of $5 \cdot 10^{-3}$ *M*. The aqueous phase was maintained at a constant ionic strength of 0.1 by addition of sodium sulphate. Changes in the ionic strength of the aqueous solution from $\mu = 0.02$ to 0.5 were shown to have no effect on the distribution ratios.

An initial aqueous phase concentration of $5 \cdot 10^{-3}$ *M* was chosen because the results reported in Part I indicate that at this concentration ion pairs are the predominant species in the organic phase for most of the salts and solvents studied. The exceptions to this statement were those salts which had low distribution ratios, and here the concentration of the quaternary salt in the organic phase was so low that dissociation of the ion pairs occurred to an appreciable extent. In all, the distribution

---

* Based on the Ph. D. thesis of D. C. Weatherburn, Sydney University, 1968.
** Present address: Chemistry Department, University of Queensland, St. Lucia, Qld. 4067, Australia.

behaviour of some fourteen quaternary cations with eighteen different anions was investigated with four different solvents (chloroform, dichloromethane, 1,2-dichloroethane and 2,2'-dichlorodiethylether).

RESULTS AND DISCUSSION

The results of the distribution studies are presented in Tables I–IV. Those anions and cations which failed to extract are not given in the tables. The anions sulphate, sulphite, fluoride, iodate, phosphate, hydroxide, thiosulphate, acetate, oxalate and carbonate, did not extract (with one exception, see below) under the conditions used into any of the solvents with any of the cations studied. The benzyltriethylammonium, phenyltrimethylarsonium and phenyltrimethylammonium cations did not

TABLE I

DISTRIBUTION RATIOS OF VARIOUS QUATERNARY SALTS BETWEEN CHLOROFORM AND AQUEOUS SOLUTION (Temperature 25°. Ionic strength 0.1. Concentration of quaternary salt initially in the aqueous phase, $5 \cdot 10^{-3}$ *M*)

Cation	*Anions*							
	ClO_4^-	SCN^-	I^-	ClO_3^-	NO_3^-	Br^-	BrO_3^-	Cl^-
$(C_6H_5)_3C_5H_{11}P^+$	27.0	16.0	9.5	3.0	2.2	1.7	0.51	0.18
$(C_6H_5)_4As^+$	—[a]	25.0	8.5	2.7	2.2	1.6	0.38	0.16
$(C_6H_5)_4P^+$	—[a]	26.0	9.0	2.9	2.0	1.7	0.40	0.14
$(C_6H_5)_3n\text{-}C_3H_7P^+$	12.0	6.3	6.9	0.84	0.53	0.52	0.11	0.04
$(C_6H_5)_3\text{iso-}C_3H_7P^+$	13.7	6.5	7.3	1.0	0.62	0.72	0.12	0.06
$(C_6H_5)_3C_2H_5P^+$	6.5	3.1	3.6	0.40	0.25	0.17	0.05	0.02
$(C_6H_5)_3C_3H_5P^+$	4.1	2.6	2.0	0.38	0.23	0.19	0.04	0.02
$(C_6H_5)_3CH_3As^+$	3.2	1.6	1.8	0.19	0.14	0.12	0.03	0.01
$(C_6H_5)_3CH_3P^+$	2.7	1.5	1.7	0.18	0.11	0.10	0.03	0.01
$(C_6H_5)_2(CH_3)_2As^+$	0.15	0.05	0.09	0	0	0	0	0

[a] Not measured because perchlorate salt is insoluble in both phases at the concentrations used.

TABLE II

DISTRIBUTION RATIOS OF VARIOUS QUATERNARY SALTS BETWEEN DICHLOROMETHANE AND AQUEOUS SOLUTION (Temperature 25°. Ionic strength 0.1. Concentration of quaternary salt initially in aqueous phase, $5 \cdot 10^{-3}$ *M*)

Cation	*Anion*							
	ClO_4^-	SCN^-	I^-	ClO_3^-	NO_3^-	Br^-	BrO_3^-	Cl^-
$(C_6H_5)_3C_5H_{11}P^+$	70	40	8.5	5.6	4.6	2.3	1.0	0.22
$(C_6H_5)_4P^+$	110	75	15	14	10.0	3.5	1.5	0.33
$(C_6H_5)_3n\text{-}C_3H_7P^+$	60	10	4.3	2.1	1.4	0.68	0.22	0.03
$(C_6H_5)_3\text{iso-}C_3H_7P^+$	65	8.7	3.9	1.8	1.3	0.57	0.21	0.02
$(C_6H_5)_3C_2H_5P^+$	40	5.3	4.9	0.90	0.62	0.25	0.08	0.01
$(C_6H_5)_3C_3H_5P^+$	11.5	4.3	2.0	0.75	0.46	0.24	0.04	0.01
$(C_6H_5)_3CH_3As^+$	11.0	2.4	1.9	0.53	0.43	0.24	0.04	0.02
$(C_6H_5)_3CH_3P^+$	9.5	2.2	1.7	0.40	0.26	0.08	0.04	0.02

TABLE III

DISTRIBUTION RATIOS OF VARIOUS QUATERNARY SALTS BETWEEN 1,2-DICHLOROETHANE AND AQUEOUS SOLUTION
(Temperature 25°. Ionic strength 0.1. Concentration of quaternary salt initially in aqueous phase, $5 \cdot 10^{-3}$ *M*)

Cation	*Anion*							
	ClO_4^-	SCN^-	I^-	ClO_3^-	NO_3^-	Br^-	BrO_3^-	Cl^-
$(C_6H_5)_3C_5H_{11}P^+$	50	16.0	9.5	3.5	2.5	0.79	0.44	0.08
$(C_6H_5)_3n\text{-}C_3H_7P^+$	55	7.5	3.2	1.2	0.77	0.23	0.10	0.02
$(C_6H_5)_3\text{iso-}C_3H_7P^+$	50	7.1	2.9	1.0	0.64	0.20	0.10	0.02
$(C_6H_5)_3C_2H_5P^+$	27	3.7	1.7	0.58	0.39	0.11	0.02	0.01
$(C_6H_5)_3C_3H_5P^+$	6.5	2.2	0.71	0.45	0.23	0.08	0.04	0.01
$(C_6H_5)_3CH_3As^+$	10.6	1.7	0.60	0.30	0.18	0.05	0.02	0.01
$(C_6H_5)_3CH_3P^+$	8.2	1.5	0.60	0.26	0.15	0.05	0.01	0

TABLE IV

DISTRIBUTION RATIOS OF VARIOUS QUATERNARY SALTS BETWEEN 2,2'-DICHLORODIETHYLETHER AND AQUEOUS SOLUTION

(Temperature 25°. Ionic strength 0.1. Concentration of quaternary salt initially present in aqueous phase, $5 \cdot 10^{-3}$ *M*)

Cation	*Anion*							
	ClO_4^-	SCN^-	I^-	ClO_3^-	NO_3^-	Br^-	BrO_3^-	Cl^-
$(C_6H_5)_3C_5H_{11}P^+$	90	4.7	6.8	4.0	3.1	0.85	0.64	0.17
$(C_6H_5)_3n\text{-}C_3H_7P^+$	65	2.9	3.1	1.6	1.2	0.35	0.20	0.04
$(C_6H_5)_3\text{iso-}C_3H_7P^+$	45	2.7	3.0	1.4	1.0	0.27	0.19	0.04
$(C_6H_5)_3CH_3As^+$	21	2.4	1.1	0.53	0.37	0.13	0.03	0.02
$(C_6H_5)_3CH_3P^+$	15	2.3	1.0	0.49	0.35	0.10	0.04	0.02

extract any of the anions studied into chloroform. The largest cation studied, benzylhexadecyldimethylammonium, was found to be completely extracted into chloroform from aqueous sodium sulphate solution and so no comparison between the different anions could be made for this cation.

The effect of the cation on the distribution ratio

The results presented in Tables I–IV show that for a majority of anions the distribution ratio increases in general with the size of the cation. Reasons for this behaviour have been discussed by Agarwal and Diamond[4]. The results obtained in this work show that in the series $(C_6H_5)_3CH_3P^+$, $(C_6H_5)_3C_2H_5P^+$, $(C_6H_5)_3n\text{-}C_3H_7P^+$, $(C_6H_5)_3n\text{-}C_5H_{11}P^+$ the value of the distribution ratio increases in general by a factor of about two for each additional CH_2 group in the alkyl chain. These results are in fair agreement with the results of Agarwal and Diamond[4], Collander[5] and Senise[6] for the increase in the distribution ratios with increasing chain length. Senise[6] has reported that with seven carbon atoms in the alkyl chain, a high value of the distribution ratio is reached which remains constant with further increases in the alkyl chain length. This effect may also be seen for alkyl chain lengths of less than 7 in the results in Tables

I–IV where for the perchlorate, thiocyanate and iodide ions which have high distribution ratios the increase in the value of the distribution ratio of each additional CH_2 group is less than 2.

The results reported in Table I for the distribution ratios of the $(C_6H_5)_4As^+$ and $(C_6H_5)_4P^+$ salts are identical within experimental error, indicating that very little difference is caused by the difference in size between these cations. The results reported by Bock *et al.*[7,8] and Orenberg and Morris[9] also indicate very little difference between these cations; Tribalat and Beydon[10] have reported the distribution ratios for $(C_6H_5)_4AsCl$ and $(C_6H_5)_4PCl$ between chloroform and water, under different experimental conditions from those used in the above studies, to be 200 and 25, respectively, and these figures have been quoted as indicating the effect of ion size on the distribution ratio.

Whilst no significant differences in the distribution ratios were observed for $(C_6H_5)_4As^+$ and $(C_6H_5)_4P^+$ salts, slight but significant differences may be observed for the salts of the $(C_6H_5)_3CH_3As^+$ and $(C_6H_5)_3CH_3P^+$ cations. In all four solvents studied the phosphonium salts had the smaller distribution ratio.

Similar differences, which may be due to ion size are observed between the salts of the $(C_6H_5)_3n\text{-}C_3H_7P^+$ and $(C_6H_5)_3C_3H_5P^+$ cations. The allyl group is smaller than the propyl group and the distribution ratios of the salts of the $(C_6H_5)_3C_3H_5P^+$ are always smaller than those of the salts of the $(C_6H_5)_3n\text{-}C_3H_7P^+$ cation. The effect seems, however, to be much larger than would be expected for the small difference in the size of these cations and the increased hydration of the $(C_6H_5)_3C_3H_5P^+$ cation compared to the $(C_6H_5)_3n\text{-}C_3H_7P^+$, owing to the presence of the double bond in the allyl group, is probably the most important effect. This dependence of the distribution ratio on the hydration energy of the ions being extracted has been mentioned in Part I[1] and will be discussed more fully below.

The distribution behaviour reported here for the triphenyl-*n*-propylphosphonium and triphenyl-isopropylphosphonium cations calls for some detailed comment. Senise[6,11] has reported remarkable differences in the extraction of a number of metal complexes with these cations. The results presented here indicate that there is a difference in the extraction behaviour of these cations but the effect observed is much smaller than that reported by Senise for metal complex salts. The larger triphenyl-*n*-propylphosphonium cation would be expected to extract anions better than the triphenyl-isopropylphosphonium cation and this is indeed observed for extraction into dichloromethane, 1,2-dichloroethane and 2,2′-dichlorodiethylether. However, the distribution ratios for triphenyl-isopropylphosphonium salts between chloroform and water are greater than the distribution ratios of the triphenyl-*n*-propylphosphonium salts. This increase in the extraction of the triphenyl-isopropylphosphonium salt must be due to increased solvation of ion pairs of the $(C_6H_5)_3iso\text{-}C_3H_7P^+$ cation relative to the $(C_6H_5)_3n\text{-}C_3H_7P^+$ cation in chloroform.

The effect of solvent on the distribution ratio

The solvent used to extract quaternary salts may affect the extraction in a number of different ways and some of these have been discussed recently elsewhere[2,12]. It was shown in Part I[1] that the extraction behaviour was strongly influenced by the state of aggregation of the quaternary salt in the organic solvent; dissociation of ion pairs in the organic solvent leads to an increase in the extraction over that expected for the ion pair alone. For this reason the conditions for the experiments described here were carefully chosen to ensure that the quaternary salt existed predominantly as ion pairs in the organic phase. The extraction of quaternary salts with distribution ratios less than 0.05 may be affected by dissociation in the organic phase but for most results reported here, this solvent effect has been eliminated.

Inspection of the results in Tables I–IV indicates that (at least for the four solvents studied) the effect of the solvent on the extraction is quite small, very much smaller than the effects of the cation discussed above, and the anion discussed below. However, definite solvent effects on the extraction may be seen, although there is little correlation between extracting ability and bulk properties such as dielectric constant. The extraction of the halide ions and thiocyanate into chloroform in particular is anomalous, and this may be attributed to specific interactions (hydrogen bonding) between the chloroform and the ion pairs, which results in small increases in the distribution ratios.

The effect of the anion on the distribution ratio

The order of extraction of the anions into the organic solvents was the same for all cations *viz.*

$ClO_4^- > SCN^- > I^- > ClO_3^- > NO_3^- > Br^- > BrO_3^- > Cl^-$ with the exception that for some cations the orders for nitrate and bromide, and thiocyanate and iodide, were reversed. The distribution ratios for the permanganate anion with the cations $(C_6H_5)_4As^+$, $(C_6H_5)_3CH_3As^+$, $(C_6H_5)_2(CH_3)_2As^+$, $C_6H_5(CH_3)_3As^+$ have been measured[13] and the results indicate that this anion has higher distribution ratios than the perchlorate anion. No divalent anions were found to extract and the monovalent anions, fluoride, hydroxide, iodate and acetate also failed to extract under the conditions used. Diamond and Tuck[14] have emphasized the importance of the change in the solvation energy of the solute on passing from the aqueous to the organic phase as the major factor governing the size of the distribution ratio. In the aqueous phase the total hydration energy of the quaternary salts will be dominated by the hydration energy of the anion unless this is large and hydrophobic like the cation. Differences in the free energy of the extraction process are determined by differences in the enthalpy and not by differences in the entropy of the extraction process[15]. The enthalpies of solvation of the anions in organic solvents are not known, but it has been suggested that the enthalpies of solvation of anions in aprotic solvents are in the reverse order to the enthalpies of hydration[16]; The enthalpy of hydration of the anion should therefore be the major factor determining the distribution ratio of the quaternary salt. In Fig. 1 the percentage extractions of triphenyl-*n*-amylphosphonium salts into dichloromethane and triphenylmethylphosphonium salts into chloroform are plotted against the enthalpies of hydration of the anion. Similar plots are obtained with all the cations and anions studied. The shape of the curve drawn in Fig. 1 was calculated from an equation derived by Ionin and Kurina[17] by making the additional assumptions that the distribution ratio is determined solely by changes in the enthalpies of hydration of the anion and that the activities of the salt in both phases are unity. The values of the enthalpy of hydration of the anions were taken from several sources[18–20]. It is worthwhile to point out that the two examples chosen for Fig. 1 were selected because they are representative of a large cation extracting into a relatively good solvent and a smaller cation extracting into a much poorer solvent. However, as shown in the

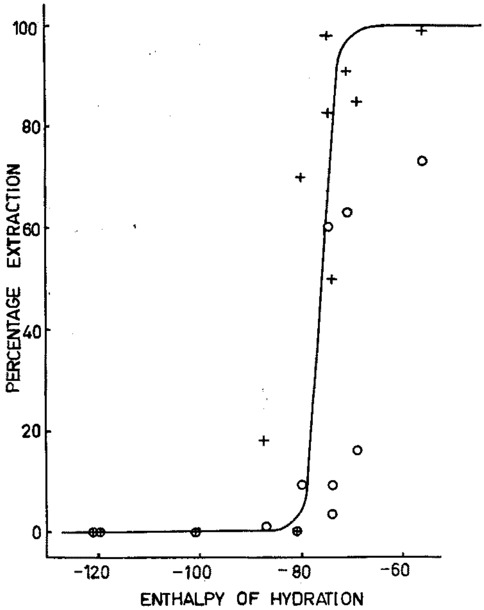

Fig. 1. Plot of percentage extraction against the enthalpy of hydration of the anion. (+) $(C_6H_5)_3C_5H_{11}P^+$ into CH_2Cl_2; (○) $(C_6H_5)_3CH_3P^+$ into $CHCl_3$. The enthalpies of hydration used in the plot are (in kcal mole^{-1}): ClO_4^- 56, SCN^- 75, I^- 71, NO_3^- 74, Br^- 80, ClO_3^- 69, BrO_3^- 74, Cl^- 87, F^- 121, OH^- 120, IO_3^- 81, OAc^- 101.

Figure one theoretical line can be drawn so that it is a good approximation to a best fit for both sets of data.

A similar explanation to the one outlined above has been proposed to explain anion-exchange resin selectivities[21], but in that explanation no attempt was made to compare resin selectivities with the known values of the enthalpy of hydration of the anion.

Irving and Damodaran have recently[2] measured the tendency of quaternary ammonium complex metal cyanides to extract into organic solvents and have explained the sequences observed on the basis of a "hole-theory". Unfortunately, the enthalpies of hydration of the complex cyanides studied have never been measured but the order of extraction of these anions is certainly consistent with their expected order of enthalpies of hydration.

Figure 1 suggests that predictions for a particular solvent extraction system both as to the order of extraction of different anions and even the magnitude of the distribution ratio may be made, provided that the enthalpy of hydration of the anions and some reference point are known. Other factors, such as the size of the cation, and the solvating properties of the organic solvent influence the extraction, and in favourable cases could be exploited to effect separations, but the dominant factor appears to be the enthalpy of hydration of the anion.

SUMMARY

The extraction of salts of fourteen different quaternary cations with nineteen different anions into four different solvents was measured. The results obtained are discussed in terms of the effects of the cation, the anion and the organic solvent on the distribution ratio. The extraction is found to depend on the size of the quaternary cation and the solvating properties of the organic solvent. A good correlation is obtained between percentage extraction of the quaternary salt and the enthalpy of hydration of the anion.

RÉSUMÉ

Une étude est effectuée sur l'extraction de sels de quatorze cations quaternaires différents avec dix-neuf anions, dans quatre solvants différents. On constate que l'extraction est fonction de la dimension du cation quaternaire et des propriétés de solvatation du solvant organique. Le pourcentage d'extraction du sel quaternaire correspond bien avec l'enthalpie d'hydratation de l'anion.

ZUSAMMENFASSUNG

Die Extraktion der Salze von vierzehn verschiedenen quaternären Kationen mit neunzehn verschiedenen Anionen mittels vier verschiedener Lösungsmittel wurde untersucht. Die erhaltenen Ergebnisse werden hinsichtlich des Einflusses des Kations, des Anions und des organischen Lösungsmittels auf das Verteilungsverhältnis diskutiert. Die Extraktion hängt von der Grösse des quaternären Kations und von den Solvatisierungseigenschaften des organischen Lösungsmittels ab. Es wird eine gute Wechselbeziehung zwischen der prozentualen Extraktion des quaternären Salzes und der Hydratationsenthalpie des Anions erhalten.

REFERENCES

1 D. C. WEATHERBURN AND N. A. GIBSON, *Anal. Chim. Acta*, 58 (1972) 149.
2 H. M. N. H. IRVING AND A. D. DAMODARAN, *Anal. Chim. Acta*, 53 (1971) 267, 277.
3 R. ARMSTRONG, N. A. GIBSON, J. W. HOSKING AND D. C. WEATHERBURN, *Aust. J. Chem.*, 20 (1967) 2771.
4 B. R. AGARWAL AND R. M. DIAMOND, *J. Phys. Chem.*, 67 (1963) 2785.
5 R. COLLANDER, *Acta Chem. Scand.*, 3 (1949) 717.
6 P. SENISE, in P. W. WEST, A. M. G. MACDONALD AND T. W. WEST, *Analytical Chemistry 1962*, Elsevier, Amsterdam, 1963, p. 171.
7 R. BOCK AND G. M. BEILSTEIN, *Z. Anal. Chem.*, 192 (1963) 44.
8 R. BOCK AND J. JAINZ, *Z. Anal. Chem.*, 198 (1963) 315.
9 J. B. ORENBERG AND M. D. MORRIS, *Anal. Chem.*, 39 (1967) 1776.
10 S. TRIBALAT AND J. BEYDON, *Anal. Chim. Acta*, 6 (1952) 96.
11 P. SENISE AND L. R. M. PITOMBO, *Anal. Chim. Acta*, 26 (1962) 85.
12 T. HIGUCHI, A. MICHAELIS AND J. H. RYTTING, *Anal. Chem.*, 43 (1971) 287.
13 E. GUYMER, *B. Sc. (Hons) Thesis*, University of Sydney, 1965.
14 R. M. DIAMOND AND D. G. TUCK, *Prog. Inorg. Chem.*, 2 (1960) 109.
15 K. S. KRASNOV, F. D. KASHIRINA AND K. B. YATSIMIRSKII, *Tr. Kom. Anal. Khim.*, 14 (1963) 59.
16 J. MILLER AND A. J. PARKER, *J. Am. Chem. Soc.*, 83 (1961) 117.
17 M. V. IONIN AND N. V. KURINA, *Tr. Kom. Anal. Khim.*, 14 (1963) 87.
18 H. F. HALLIWELL AND S. C. NYBURG, *Trans. Faraday Soc.*, 59 (1963) 1126.
19 K. B. YATSIMIRSKII, *Izv. Akad. Nauk SSSR, Otd. Khim. Nauk*, (1948) 398; *Chem. Abstr.*, 42 (1948) 8604.
20 V. P. VASIL'EV, E. K. ZOLOTAREV, A. F. KAPUSTINSKII, K. P. MISHCHONKO, E. A. PODGORNAYA AND K. B. YATSIMIRSKII, *Russ. J. Phys. Chem.*, 34 (1960) 840.
21 B. CHU, D. C. WHITNEY AND R. M. DIAMOND, *J. Inorg. Nucl. Chem.*, 24 (1962) 1405.

Analytica Chimica Acta
Elsevier Publishing Company, Amsterdam
Printed in The Netherlands

THE DIRECT GAS-CHROMATOGRAPHIC SEPARATION AND DETERMINATION OF IMPURITIES IN TEREPHTHALIC ACID

JACKSON E. HICKS AND RUTH S. JESSEE

Acid Division, Analytical Development Laboratory, Tennessee Eastman Company, Kingsport, Tenn. 37662 (U.S.A.)

(Received 5th August 1971)

In the production of terephthalic acid by the oxidation of *p*-xylene, a number of by-products are possible. Even under the most carefully controlled conditions these impurities will be produced in small amounts. The principal impurities that might be found in the final product are *p*-toluic acid, benzoic acid, 4-carboxybenzaldehyde, *p*-(hydroxymethyl)benzoic acid and isophthalic acid. There are numerous publications[1-6] describing separation or determination of one or more of these products from terephthalic acid. A method of separating and quantitatively determining the concentration of all these impurities is highly desirable. These analytical requirements are often satisfied by gas-chromatographic techniques. However, the separation of aromatic carboxylic acids by gas chromatography usually requires the preparation of a suitable derivative which increases the volatility and reduces the polarity of the substrate.

One of the most commonly used procedures converts the free acids to their methyl esters either by reaction with diazomethane or methanol and a suitable catalyst[7]. Baumann and Lavigne[8] have described a method for the gas-chromatographic analysis of xylene oxidation products after esterification with methanol. Another approach that has gained much popularity is the conversion of the carboxylic acids to their corresponding trimethylsilyl esters[9]. The production of a derivative of the free acid is not only a time-consuming step, but also is a source of error which may result from modifications that can take place during conversion of the free acids to their respective derivatives. The separation of the free acids by gas chromatography is quite difficult because of their high boiling or sublimation points.

Several alkylbenzoic acids have been successfully separated in their free state by Hill and Hill[10]. This procedure, however, fails to give separation when a second polar substituent is placed on the benzoic acid nucleus. The method is, therefore, limited to monobasic acids.

Witte and Rasse[11] have described a method that is capable of separating free mono and dicarboxylic aromatic acids. Their method uses a liquid phase of polyester (LAC-446) and phosphoric acid on Chromosorb W. The major point in their method is the use of an all-glass injector and column system. Witte and Rasse point out that any contact of the substrates with hot metal surfaces must be avoided. The work described in this report utilized the findings of Witte and Rasse and shows that small amounts of impurities in terephthalic acid can be separated and their concentrations determined with no pretreatment of the initial sample.

EXPERIMENTAL

Apparatus

All gas-chromatography experiments were performed on a Varian-Aerograph Model 1520 chromatograph equipped with a flame ionization detector. The injection port was equipped with a glass insert which was directly connected to a 3-mm o.d. Teflon column, 30 mm in length. The column was packed with 15% LAC-446 and 3% phosphoric acid on 80–100 mesh Chromosorb AW-DMCS. The column outlet was connected directly to the flame ionization detector block to eliminate all contact with hot metal surfaces except for the short distance between the Teflon column and the quartz tip of the flame ionization detector.

The chromatograph was operated in the linear programmed-temperature mode with an initial temperature of 145° and a final temperature of 225°. The programmed rate was 8° min^{-1}. The carrier gas was helium, and the flow rate was 70 cm^{3} min^{-1}. The injection port temperature was held at 330° and the flame ionization detector was operated at 220°.

All samples were injected by means of a Hamilton syringe. A sample size of 0.6 μl of a 4% solution in N,N-dimethylformamide (DMF) was used.

Column packing procedure

Dissolve 1.5 g of LAC-446 and 0.3 g of phosphoric acid (85%) in *ca.* 20 ml of acetone. Transfer 8.2 g of Chromosorb AW-DMCS and the dissolved liquid phase into a 250-ml fluted round-bottom flask. Connect the flask and contents to a Rinco evaporator, attach to a vacuum system that is capable of maintaining a vacuum of at least 100 mm Hg, and start the evaporator rotating slowly. Continue this rotary evaporation until all the solvent is gone, and a free-flowing material is obtained.

Prepare the column for packing by placing a small piece of glass wool in one end of the column and connecting this end to a vacuum source. Slowly pour the coated packing in the column while gently tapping the column. Leave about 1 cm unfilled and place a small piece of glass wool in this end to complete the column.

The column is conditioned before use by heating to 235° in a conventional gas-chromatography unit for *ca.* 24 h.

Sample preparation

Accurately weigh a 1.0-g sample (±0.0002 g) of terephthalic acid into a 25-ml volumetric flask. Add 1 ml of a 1% solution of suberic acid in DMF as an internal standard, and dilute to the mark with DMF.

Procedure

Inject 0.6 μl of the sample solution and record the chromatogram. Calculate the peak area for each component and determine the ratio of the component area to internal standard area. Calculate the concentration from the above ratio by use of a calibration factor obtained by determining the ratio for standards of known concentration.

RESULTS AND DISCUSSION

Figure 1 shows a chromatographic curve obtained from a mixture of the pro-

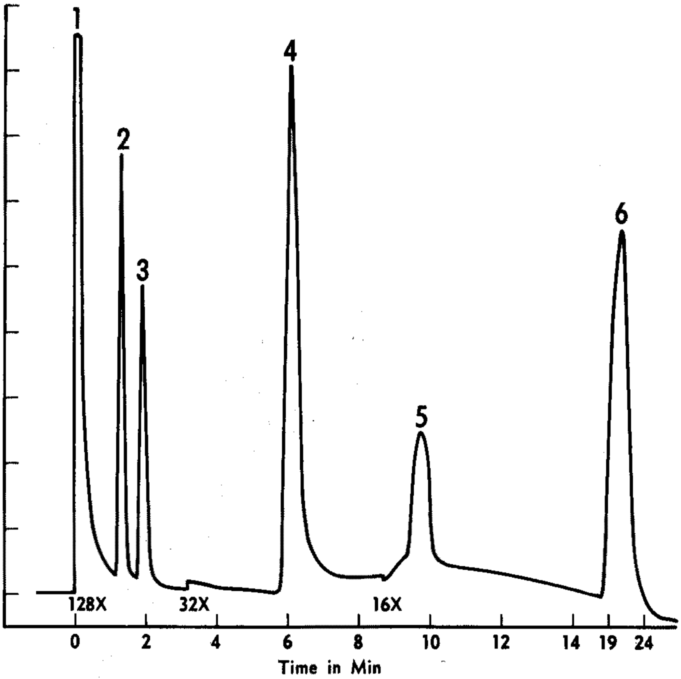

Fig. 1. Chromatographic separation of compounds known to be present in terephthalic acid. (1) Dimethylformamide; (2) benzoic acid; (3) *p*-toluic acid; (4) 4-carboxybenzaldehyde; (5) *p*-(hydroxymethyl)benzoic acid; (6) terephthalic acid.

bable components that would be found in a terephthalic acid sample. Isophthalic acid is not separated from terephthalic acid by this column. It should also be noted that the recorder chart speed was slowed by a factor of 5 after 14 min. The elution data obtained for these compounds are given in Table I. Suberic acid was chosen for use as an internal standard and its retention time was used to obtain the relative retention data given in Table I.

Figure 2 shows a synthetic terephthalic acid sample containing three impurities. This is a typical curve used to obtain the precision data reported for benzoic acid, *p*-toluic acid and 4-carboxybenzaldehyde. Again, it should be noted that the recorder

TABLE I

RETENTION DATA

Compound	*Retention time (min)*	*Relative retention*
Benzoic acid	1.25	0.15
Toluic acid	2	0.24
4-Carboxybenzaldehyde	6	0.71
Suberic acid	8.5	1.00
p-(Hydroxymethyl)benzoic acid	9.5	1.12
Terephthalic acid	21	2.47

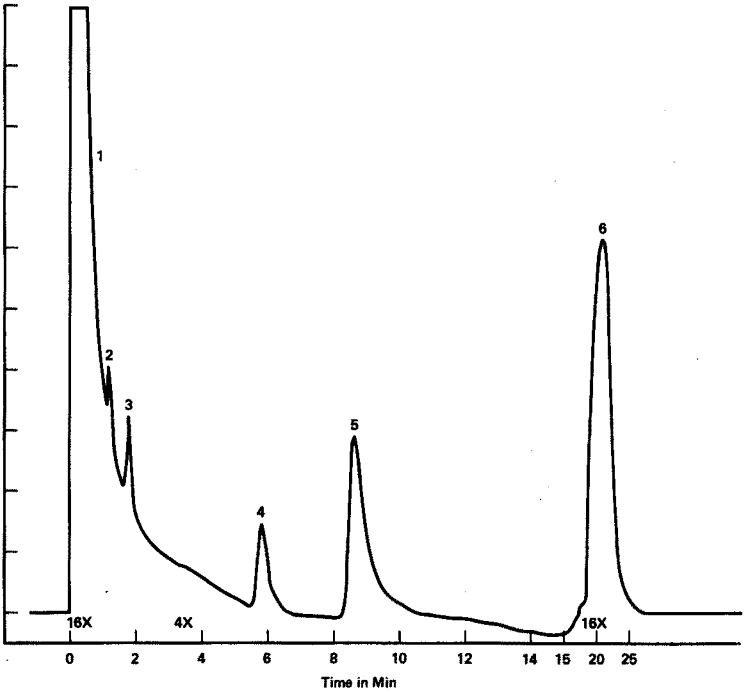

Fig. 2. Chromatographic curve of a synthetic terephthalic acid mixture. (1) DMF; (2) benzoic acid; (3) *p*-toluic acid; (4) 4-carboxybenzaldehyde; (5) suberic acid; (6) terephthalic acid.

chart speed was slowed by a factor of 5 after 15 min. The benzoic and *p*-toluic acid concentrations were 0.15% while the 4-carboxybenzaldehyde concentration was 0.41%.

Suberic acid was chosen for the internal standard because of its elution time and stability. Standards were prepared by adding known amounts of each component to a sample of pure terephthalic acid dissolved in dimethylformamide. The area of each peak was then used to determine the ratio of component peak to internal standard peak. A plot of peak ratios *versus* concentration produced a straight line. Calibration factors were obtained and used for all analytical determinations.

Witte and Rasse[11] clearly stated that the key to successful separations of aromatic acids with additional polar substituents was the use of an all-glass system. Contact of the acids with hot metal surfaces causes serious decomposition problems. This was again shown to be true during the preliminary experimental work reported here. The standard Varian-Aerograph Model 1520 chromatograph utilizes a short (*ca.* 150 cm) metal tube to connect the end of the chromatographic column to the base of the detector block. This tube was not removed in the early part of this work and although the chromatographic data obtained indicated satisfactory separations, the quantitative results were very erratic and the precision was unsatisfactory. The metal tube connector was removed from the system and the Teflon column was connected directly to the detector block, thus eliminating contact with any hot metal surfaces except for the short distance between the end of the Teflon column and the quartz tip of the flame ionization detector. Precision data were again obtained by repeatedly analyzing a single sample of terephthalic acid. Data collected during a series of measurements conducted on the same day gave a very satisfactory precision. In the case of 4-carboxybenzaldehyde, an average value of 0.39% and a standard deviation of 0.011% were obtained on a sample known to contain 0.41% of the aldehyde. However, when an attempt was made to reproduce these data from measurements taken on different

TABLE II

EFFECT OF DETECTOR TEMPERATURE ON DETERMINATION OF 4-CARBOXYBENZALDEHYDE

Detector temperature (°)	*% 4-Carboxybenzaldehyde found*
215	0.41
220	0.41
230	0.40
250	0.19
275	0.18
280	0.20
285	0.16

TABLE III

PRECISION DATA FOR 4-CARBOXYBENZALDEHYDE

Day	*Test*	*% 4-Carboxybenzaldehyde*
1	1	0.46
	2	0.50
	3	0.46
	4	0.41
2	1	0.47
	2	0.45
	3	0.44
	4	0.42
	5	0.48
3	1	0.40
	2	0.42
	3	0.46
	4	0.44
	5	0.39
4	1	0.39
	2	0.37
	3	0.41
	4	0.41
	5	0.34
	6	0.44
	7	0.45
5	1	0.44
	2	0.42
	3	0.41
	4	0.42
Standard deviation		0.036
Coefficient of variation		8.4%
$\bar{X}$		0.43

days, it was found that the precision was very poor. The only instrumental parameter that might cause such effects, and which had been changed during the period over which the measurements were made, was the temperature of the flame ionization detector block. Several detector temperatures were investigated and the results are shown in Table II. From these data, it can be seen that as the temperature of the detector increases, low results were obtained. Since little effect could be seen over the range 215–230°, an intermediate temperature, 220°, was chosen for all subsequent measurements.

Tables III and IV show the precision data obtained when a sample of terephthalic acid was analyzed a number of times over a period of several days. The results for benzoic and *p*-toluic acids could be improved considerably by optimizing the conditions to provide better separation of the two peaks from that of the DMF solvent. Figure 2 is a typical example of the chromatographic curve from which these data were taken. The precision data for determination of 4-carboxybenzaldehyde are quite satisfactory. The results obtained agreed very well with the amount of aldehyde known to be present, that is 0.41 %. Because of its extreme susceptibility to oxidation, it is quite difficult to determine the concentration of 4-carboxybenzaldehyde by a gas-chromatographic method that requires esterification before separation. Dimethylformamide solutions of terephthalic acid containing small amounts of 4-carboxybenzaldehyde were found to be stable for several hours. The procedure is rapid and the chromatographic column is quite stable.

TABLE IV

PRECISION DATA FOR BENZOIC AND *p*-TOLUIC ACIDS

Day	*Test*	*% Benzoic*	*% Toluic*
1	1	0.14	0.15
	2	0.16	0.14
	3	0.14	0.15
	4	0.12	0.16
2	1	0.18	0.17
	2	0.14	0.16
	3	0.16	0.16
3	1	0.12	0.13
	2	0.12	0.14
	3	0.16	0.14
	4	0.16	0.15
	5	0.16	0.15
	6	0.14	0.15
Standard deviation		0.018	0.011
Coefficient of variation		12.9%	7.2%
$\bar{X}$		0.15	0.15

The authors are grateful to Mr. Ralph T. McPherson for his helpful suggestions and to the Tennessee Eastman Company for permission to publish this work.

SUMMARY

A direct gas-chromatographic separation of impurities likely to be present in commercial terephthalic acid is described. The separation requires no chemical modification of the sample and utilizes commercially available gas-chromatographic equipment. The only instrumental modifications required are the use of a glass injector lining and a Teflon column to prevent contact with hot metal surfaces. Precision data are reported for benzoic acid, *p*-toluic acid and 4-carboxybenzaldehyde.

RÉSUMÉ

On décrit une méthode de séparation par chromatographie gazeuse directe pour l'analyse des impuretés d'un acide téréphtalique commercial. Ce procédé ne nécessite aucun traitement chimique de l'échantillon et aucun équipement particulier. Il faut cependant utiliser un injecteur de verre et une colonne de Teflon pour éviter tout contact sur des surfaces métalliques chaudes. On indique la précision obtenue pour l'acide benzoïque, l'acide *p*-toluique et le carboxy-4-benzaldéhyde.

ZUSAMMENFASSUNG

Es wird eine direkte gaschromatographische Trennung von Verunreinigungen beschrieben, die in handelsüblicher Terephthalsäure vorliegen können. Die Trennung erfordert keine chemische Umwandlung der Probe und ist mit im Handel erhältlicher gaschromatographischer Ausrüstung durchführbar. Die einzigen erforderlichen instrumentellen Abwandlungen sind die Anwendung einer gläsernen Injektorbeschichtung und einer Teflonsäule, damit der Kontakt mit heissen Metalloberflächen vermieden wird. Die Reproduzierbarkeit bei Benzoesäure, *p*-Toluylsäure und 4-Carboxybenzaldehyd wird angegeben.

REFERENCES

1 J. Kulicka, R. Baranowski, Z. Gregorowicz and Z. Kulicki, *Chem. Anal. (Warsaw)*, 12 (1) (1967) 171.
2 R. Baranowski, Z. Gregorowicz and J. Kulicka, *Mikrochim. Acta*, 4 (1968) 806.
3 J. W. Frankenfeld, *J. Chromatogr.*, 18 (1965) 179.
4 W. Funasaka, T. Kojima, G. Takeshima and J. Kimoto, *Bunseki Kagaku*, 11 (1962) 434.
5 F. C. Taussell and R. E. Lewis, *Anal. Chim. Acta*, 34 (1966) 243.
6 W. Czerwinski and J. Gruberska, *Chem. Anal. (Warsaw)*, 13 (1968) 101.
7 M. Schmitzer and J. G. Desjordino, *J. Gas Chromatogr.*, 2 (1964) 270.
8 F. Baumann and J. B. Lavigne, *Gas Chromatogr., Intern. Symp.*, 4 (1963) 139.
9 M. L. Kaufmann, S. Friedman and I. Wender, *Anal. Chem.*, 39 (1967) 1011.
10 J. T. Hill and J. D. Hill, *Anal. Chem.*, 36 (1964) 2504.
11 K. Witte and H. Rasse, *Chromatographia*, 1 (1968) 32.

Analytica Chimica Acta
Elsevier Publishing Company, Amsterdam
Printed in The Netherlands

THERMAL PROPERTIES OF SOME COMPOUNDS OF LUTIDINIC ACID WITH DIVALENT METALS

G. D'ASCENZO, U. BIADER CEIPIDOR AND G. DE ANGELIS
Istituto di Chimica Analitica, Università degli di Roma, 00100 Rome (Italy)

(Received 16th July 1971)

In a continuation of a systematic study on the behaviour of compounds obtained by reaction between metal ions and heterocyclic ligands[1-4], the complexes of lutidinic acid (pyridine-2,4-dicarboxylic; 2,4-H_2PC) with manganese(II), iron(II), cobalt(II), nickel(II), copper(II) and zinc(II) were examined by thermal analysis (TG) and differential thermal analysis (DTA). Only fragmentary data concerning these compounds have previously been discussed[5].

EXPERIMENTAL

Instrumentation

The instruments used were those previously described[3]. A heating rate of 10° min^{-1} was employed.

Preparation of compounds

Lutidinic acid (Aldrich Chemical Co, Inc, Milwaukee, Wisc.) was used. Other chemicals employed were of reagent grade.

The compounds were prepared by adding a 0.1 *M* solution of lutidinic acid at pH to a 0.1 *M* solution of the metal chloride until an initial ligand–metal molar ratio of 1.5:1 was obtained. With larger ligand–metal molar ratios, a mixture of solid compounds was obtained and the separation of these compounds from the mixture was impossible. Only for copper was it possible to isolate species having ligand–metal molar ratios of 1:1 and 2:1.

The solution obtained was mechanically stirred for about 1 h. The precipitate, if present, was filtered off, washed with a 1:1 water–ethanol mixture and then with 95% ethanol, and dried *in vacuo* for 48 h at room temperature. If precipitation did not occur from aqueous solution, the medium was suitably adjusted by adding ethanol or acetone until a precipitate was obtained.

Thermogravimetry was used in order to determine the water content and the residual metal oxide; the metal content was also established by complexometric titration of the anhydrous compound (Table I).

RESULTS

Each compound is discussed briefly. The temperatures referred to are the procedural decomposition temperatures at the heating rate indicated. The data ob-

TABLE I

COMPLEXOMETRIC DETERMINATION OF METAL CONTENT IN ANHYDROUS COMPOUNDS

Compound	*Metal (%)*	
	Found	*Theor.*
Mn(2,4-PC)	24.8	24.85
Fe(2,4-PC)	25.4	25.16
Co(2,4-PC)	26.5	26.18
Ni(2,4-PC)	25.8	26.11
Cu(2,4-PC)	27.3	27.66
Zn(2,4-PC)	28.3	28.24

TABLE II

DECOMPOSITION TEMPERATURES FROM TGA AND DTA CURVES OF METAL–PYRIDINE-2,4-CARBOXYLATES

Metal		*TG*				*DTA*			
		H_2O I	*H_2O II*	*Decomp. I*	*Decomp. II*	*H_2O I*	*H_2O II*	*Peak I*	*Peak II*
Mn(II)	N_2	85[a]		465		70[b]	120	460	
		30–140[c]		400–510	510→	30–90	90–145	400–510	510→
	Air	90		475					
		30–150		400–515					
Fe(II)	N_2	90		450		90	115	445	
		30–125		380–505	505→	30–100	100–135	390–500	500→
	Air	90		390	475				
		35–130		370–405	405–510				
Co(II)	N_2	80	120	435		85	120	430	
		30–95	95–140	370–495	495→	30–100	100–140	360–490	490→
	Air	85	130	407					
		30–110	110–155	370–435					
Ni(II)	N_2	90		435		75	120	425	
		30–150		350–500	500→	30–100	100–150	345–500	500→
	Air	95		435	620				
		30–150		350–500	500–700				
Cu(II)	N_2	100		310		100		315	
		30–150		295–340	340→	30–150		290–345	345→
	Air	105		300					
		30–155		295–320					
Zn(II)	N_2	75		430		80		430	
		30–110		375–500	500→	30–110		380–490	490→
	Air	85		440	650				
		30–125		375–500	500–740				

[a] Maximum rate.
[b] Peak minimum.
[c] Temperatures in ° at beginning and end of reaction.

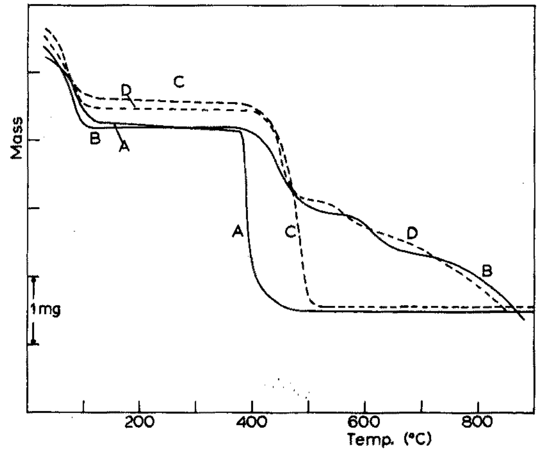

Fig. 1. Weight loss curves of manganese(II) and iron(II) pyridine-2,4-dicarboxylates. Heating rate 10° min^{-1}. (——) Fe; (– – –) Mn. Curves A and C were obtained in air and curves B and D in nitrogen.

tained by TG in nitrogen or air and by DTA in nitrogen are summarized in Table II. Thermogravimetry was done up to 900°. DTA in nitrogen was done only up to 500° and only endothermic processes were found.

Manganese(II)–pyridine-2,4-dicarboxylate

A white compound precipitates from aqueous solution. The simplest formula is $Mn(2,4\text{-}PC)2H_2O$, which agrees with the metal determination (Table I) and with the thermogravimetric data.

Thermogravimetry shows that in nitrogen or air, water is evolved in a single step (19.5% found; theor. 19.72%) (Fig. 1). The anhydrous compound is stable up to 400°, above which decomposition starts. In a nitrogen atmosphere (curve D) decomposition occurs in two successive steps, the second of which does not reach constant weight; in air (curve C) only one process is involved and the oxide Mn_3O_4 (found 27.9%; theor. 27.82%) is formed.

The DTA curve in a nitrogen atmosphere shows two endothermic peaks for the water loss and confirms decomposition by an endothermic peak (Fig. 2).

Iron(II)–pyridine-2,4-dicarboxylate

A red-brown compound is obtained from water–ethanol solution. The simplest formula $Fe(2,4\text{-}PC)3H_2O$ agrees with the metal determination (Table I) and with thermogravimetric data.

According to thermogravimetry this compound loses its water molecules in one step (20.0% found; 19.65% theor.) (Fig. 1). The anhydrous compound in a nitrogen atmosphere (curve B), begins to decompose at 380°; decomposition occurs in two steps, the second of which does not reach constant weight. In air (curve A) the decomposition is very fast and gives the oxide Fe_2O_3 (28.6% found; 29.03% theor.).

The DTA curve in a nitrogen atmosphere (Fig. 2) shows two partially overlapped endothermic peaks for the water loss, while for the decomposition there is an endothermic peak up to 500°.

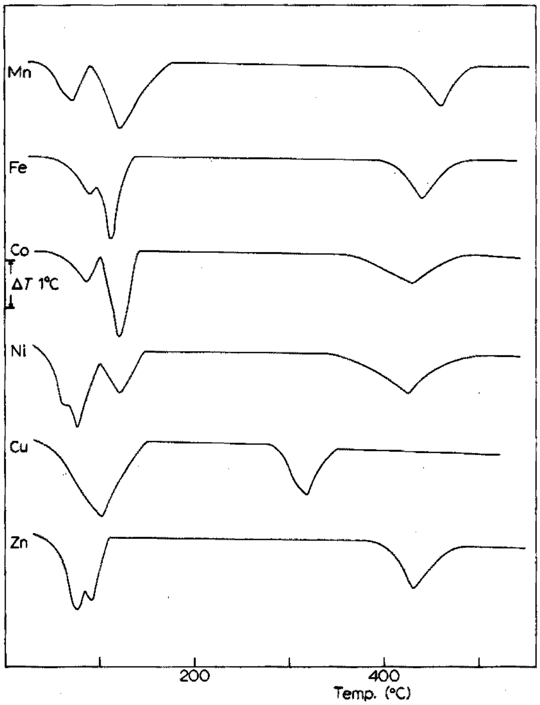

Fig. 2. DTA curves of manganese(II), iron(II), cobalt(II), nickel(II), copper(II) and zinc(II) pyridine-2,4-dicarboxylates. Heating rate 10° min^{-1}; N_2 atmosphere.

Cobalt(II)-pyridine-2,4-dicarboxylate

The compound precipitates from water–ethanol solution as a pink solid. The metal determination (Table I) and thermogravimetric data agree with the simplest formula $Co(2,4\text{-}PC)5H_2O$.

Thermogravimetry shows that three molecules of water are evolved (Fig. 3) between 30 and 95° (17.2% found; 17.14% theor.), while the remaining two are evolved in the temperature range 95–140° (28.8% found; 28.56% theor.).

The decomposition of the anhydrous compound starts at 370°; in nitrogen it does not reach a constant weight (Fig. 3, curve D) while in air it decomposes abruptly to give the oxide Co_3O_4 (25.7% found; 25.48% theor.) (Fig. 3, curve C).

The DTA curve in nitrogen (Fig. 2) gives two incompletely resolved endothermic peaks for the dehydration, followed by another peak caused by the decomposition reaction.

Nickel(II)-pyridine-2,4-dicarboxylate

A blue compound precipitates from water–ethanol solution. The simplest formula is $Ni(2,4\text{-}PC)3H_2O$ which is in accord with the metal determination (Table I) and thermogravimetric data. Thermogravimetry shows a single step corresponding to the loss of the three water molecules (Fig. 3) (19.2% found; 19.45% theor.). The DTA curve (Fig. 2) gives three incompletely resolved endothermic peaks for this phenomenon.

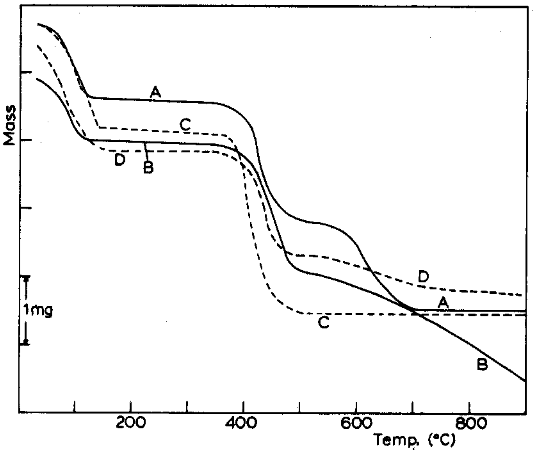

Fig. 3. Weight loss curves of cobalt(II) and nickel(II) pyridine-2,4-dicarboxylates. Heating rate 10° min^{-1}. (——) Ni; (- - -) Co. Curves A and C were obtained in air, and curves B and D in nitrogen.

The decomposition begins at 350°; in nitrogen (Fig. 3, curve B) there is only one step after which there is a slow weight loss, while in air (curve A) nickel oxide, NiO (26.7% found; 26.88% theor.) is formed through two steps.

In a nitrogen atmosphere the decomposition reaction shows only a broad peak in the DTA curve (Fig. 2), corresponding to the first step observed in the TG curve.

Copper(II)-pyridine-2,4-dicarboxylate

A blue-violet compound precipitates from aqueous solution with the simplest formula Cu(2,4-PC)2.5H_2O, according with the metal determination (Table I) and thermogravimetric data. It loses its water molecules in one step (Fig. 4) (16.7% found; 16.46% theor.). The DTA curve (Fig. 2) shows just one asymmetric endothermic peak corresponding to this phenomenon.

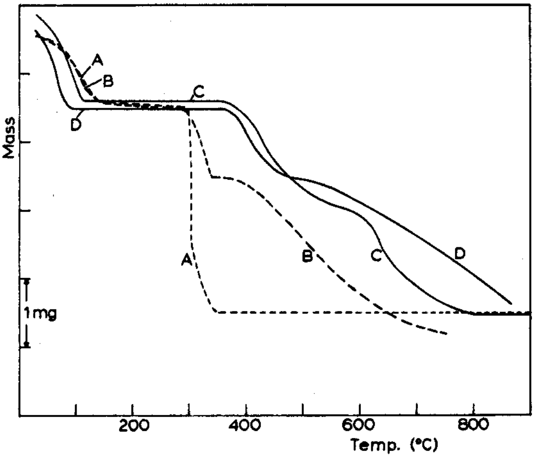

Fig. 4. Weight loss curves of copper(II) and zinc(II) pyridine-2,4-dicarboxylates. Heating rate 10° min^{-1}. (——) Zinc; (- - -) copper. Curves A and C were obtained in air, and curves B and D in nitrogen.

The anhydrous form is stable up to 295°. Thermogravimetry in a nitrogen atmosphere (Fig. 4, curve B) shows two decomposition steps, but constant weight is not attained.

In air (Fig. 4, curve A), there is an almost explosive reaction to give the oxide CuO (28.9% found; 29.06% theor.).

The DTA curve in nitrogen (Fig. 2) shows only overlapped peaks below 350° and a slight base-line deviation.

Zinc(II)–pyridine-2,4-dicarboxylate

A white compound is obtained from water–acetone solution. The simplest formula $Zn(2,4\text{-}PC)3.5H_2O$ agrees with the metal determination (Table I) and with the thermogravimetric data. The compound loses its water molecules in only one step (Fig. 4)(21.4% found; 21.48% theor.). Contrarily, the DTA curve (Fig. 2) shows a two-step endothermic peak for the dehydration.

After the water loss, the TG curve does not show any weight change until 375° where the anhydrous form begins to decompose. This decomposition occurs in two steps. In nitrogen (Fig. 4, curve D) constant weight is not achieved, whereas in air (curve C) the second step gives the metal oxide (27.8% found; 27.72% theor.). The DTA curve in nitrogen (Fig. 2) shows an endothermic phenomenon for the decomposition below 500°.

DISCUSSION

The thermal stability order for the examined divalent metal ions shown by the experimental data is:

$$Mn(II) > Fe(II) > Co(II) \cong Zn(II) > Ni(II) > Cu(II)$$

Wendlandt *et al.*[6,7] found the same sequence for the thermal stability of other compounds of the same metal ions. The general series found by Irving and Williams for the stability of complexes in solution[8] is practically the reverse of the above series for the thermal stability. This behaviour can be explained on the basis that the strength of intermolecular bonds plays a notable part in the thermal stability of solid compounds. It seems probable that the intermolecular bonds of the solid lattice of complexes having strong covalent metal–ligand bonds are weaker than those existing in the case of complexes in which the metal–ligand bond has a higher ionic character.

The compounds studied show different water contents. From the DTA curves, it is possible to see that the dehydration peaks result as a superimposition of at least two unresolved peaks. This behaviour can be explained either by the presence of two different kinds of water (crystallization and coordination) and/or by a configurational change involving the loss of water molecules from the hydration sphere of the metal. All the dehydration temperature ranges of these compounds lie between 80 and 150°, where the thermal contribution of water evaporation is always prevalent, with a global endothermic character.

The decomposition of the anhydrous compounds can be explained by the mechanism suggested by Kaneda and Hara[5], *i.e.* release of free pyridine radicals, carbon dioxide and/or carbon monoxide. The radicals then form pyridine and/or bipyridine. Only in air, is a definite metal oxide obtained.

When the ligand and metal are mixed in a molar ratio of 1.5 : 1, solid compounds with a 1 : 1 molar ratio are obtained, whereas if the molar ratio of the reagents is 4 : 1, a mixture of solid 1 : 1 and 2 : 1 ligand/metal complexes is obtained. The isocinchomeronic acid (2,5-H_2PC) complexes of these divalent metal ions were readily obtained under the same conditions with a 1 : 4 metal/ligand molar ratio in the initial solution, pure solid compounds with a 1 : 2 metal/ligand molar ratio being formed[4].

The difference in behaviour of the lutidinates and isocinchomeronates could be explained by a difference in the basic strengths of the two 1 : 1 complexes. When each mole of these two pyridinecarboxylic acids is bound to one mole of metal ion, the different contribution to the normal state of a resonance form which localizes a positive charge near the nonchelating carboxylic group, decreasing its basic strength, can be examined.

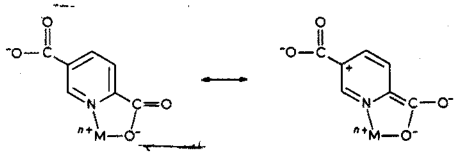

II_a, I_b

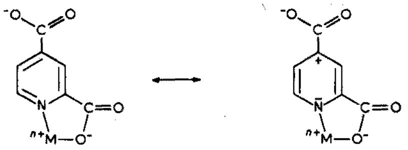

II_b

In the II_b form, the negative charge localization is nearer to the metal ion and is more symmetrically distributed than in the II_a form. It is likely, therefore, that the contribution to the normal state of the II_b form is bigger than that of the II_a form. If this is true, the $Me(2,4\text{-}PC)^{(n-2)+}$ complex is, on the whole, less basic than the $Me(2,5\text{-}PC)^{(n-2)+}$ complex, and under the same conditions

$$\frac{Me(2,4\text{-}HPC)^{(n-1)+}}{Me(2,4\text{-}PC)^{(n-2)+}} < \frac{Me(2,5\text{-}HPC)^{(n-1)+}}{Me(2,5\text{-}PC)^{(n-2)+}}$$

When the 1 : 1 forms for the complexes of the two pyridinecarboxylic acids with the divalent metal ions ($n = 2$) are considered, the following points are important. Protonation of the free carboxylic group, which is higher in the case of isocinchomeronic than of lutidinic complexes, increases the total positive charge of the former compared to the latter, favoring electrostatic attraction of another ionized ligand molecule. The negative charge localization near the complexed metal ion, is lower in the isocinchomeronic than in the lutidinic complexes, hence the metal acidity of the former is increased, again favoring the formation of a 2 : 1 complex.

The 1 : 1 complex formation gives a zero-charged (as a whole) compound more readily with lutidinic acid than with isocinchomeronic acid; precipitation of the 1 : 1 lutidinate is more probable.

In the series studied, the 2 : 1 copper–lutidinate complex is the only one which can be isolated, probably because of its very high metal–ligand affinity.

The authors wish to thank the C.N.R. for financial support.

SUMMARY

The thermal properties of the complexes of lutidinic acid with several divalent metal ions were determined by thermogravimetry (TG) and differential thermal analysis (DTA). The complexes precipitate from aqueous solution as hydrated 1 : 1

complexes. On heating in air, hydrate water is lost first, followed by total disruption of the anhydrous complex to yield the metal oxide; in a nitrogen atmosphere, the pattern is similar, but final weight constancy is not achieved. The thermal stability of the metal complexes is in the order:

$$\mathrm{Mn(II)} > \mathrm{Fe(II)} > \mathrm{Co(II)} \cong \mathrm{Zn(II)} > \mathrm{Ni(II)} > \mathrm{Cu(II)}$$

The different metal–ligand ratio in the solid state for analogous compounds with isocinchomeronic acid is discussed.

RÉSUMÉ

Les propriétés thermiques des complexes de l'acide lutidinique avec certains métaux bivalents ont été examinées par TG et DTA. D'une solution aqueuse on obtient la précipitation de ces composés sous la forme de complexes hydrate avec un rapport 1:1 entre metal et ligand. La décomposition commence par la perte de l'eau et se termine dans l'air avec la formation de l'oxyde du métal. L'échelle de stabilité thermique déterminée est la suivante:

$$\mathrm{Mn(II)} > \mathrm{Fe(II)} > \mathrm{Co(II)} \cong \mathrm{Zn(II)} > \mathrm{Ni(II)} > \mathrm{Cu(II)}$$

On a même essayé d'expliquer la différence entre les rapports molaires obtenus dans ces composés et ceux des homologues avec l'acide isocincoméronique à travers des phénomènes de résonance.

ZUSAMMENFASSUNG

Die thermischen Eigenschaften der Komplexe von Lutidinsäure mit verschiedenen zweiwertigen Metallionen wurden durch Thermogravimetrie (TG) und Differentialthermoanalyse (DTA) ermittelt. Die Komplexe fallen aus wässriger Lösung als hydratisierte 1:1-Komplexe aus. Beim Erhitzen in Luft wird zuerst Hydratwasser abgegeben, danach erfolgt die vollständige Zersetzung des wasserfreien Komplexes unter Bildung des Metalloxides. In Stickstoffatmosphäre ist das Verhalten ähnlich, jedoch wird zum Schluss keine Gewichtskonstanz erreicht. Für die thermische Stabilität der Metallkomplexe gilt folgende Reihenfolge:

$$\mathrm{Mn(II)} > \mathrm{Fe(II)} > \mathrm{Co(II)} \cong \mathrm{Zn(II)} > \mathrm{Ni(II)} > \mathrm{Cu(II)}.$$

Das unterschiedliche Metall–Ligand-Verhältnis im festen Zustand für analoge Verbindungen mit Isocinchomeronsäure wird diskutiert.

REFERENCES

1 G. DE ANGELIS, E. CHIACCHIERINI AND G. D'ASCENZO, *Gazz. Chim. Ital.*, 96 (1966) 39.
2 G. DE ANGELIS, G. D'ASCENZO AND E. CHIACCHIERINI, *C.N.R. Meeting, Rome, Italy, 12–14 January 1967*, p. 82.
3 G. D'ASCENZO AND W. W. WENDLANDT, *Anal. Chim. Acta*, 50 (1970) 79.
4 G. D'ASCENZO AND W. W. WENDLANDT, *Gazz. Chim. Ital.*, 100 (1970) 371.
5 A. KANEDA AND T. HARA, *Doshisha Daigaku Rikogaku Kenkyu Hokoku*, 7 (1967) 172.
6 W. W. WENDLANDT AND G. R. HORTON, *Anal. Chem.*, 34 (1962) 1098.
7 W. W. WENDLANDT, J. H. VAN TOSSEL AND G. R. HORTON, *Anal. Chim. Acta*, 23 (1960) 332.
8 H. IRVING AND R. J. P. WILLIAMS, *J. Chem. Soc.*, (1953) 3192.

Analytica Chimica Acta
Elsevier Publishing Company, Amsterdam
Printed in The Netherlands

A DIRECT ELECTROCHEMICAL METHOD FOR THE DETERMINATION OF ALLOPURINOL AND URIC ACID MIXTURES

ADSORPTION OF URIC ACID AT THE PYROLYTIC GRAPHITE ELECTRODE

GLENN DRYHURST AND P. K. DE
Department of Chemistry, University of Oklahoma, Norman, Okla. 73069 (U.S.A.)

(Received 1st September 1971)

Allopurinol (4-oxypyrazolo[3,4-d]pyrimidine) is used extensively as a drug for the treatment of gout[1]. It functions by inhibiting the enzyme xanthine oxidase, which is responsible for oxidizing purines to uric acid which in gouty patients precipitates in joints. Allopurinol has also been characterized as a metabolite of 4-aminopyrazolo[3,4-d]pyrimidine, a compound also employed in the treatment of gout[2]. Allopurinol is also used to reduce the toxicity of the anti-viral drug N^6-(hydroxymethyl)adenine.

In order to be able to understand the effectiveness of allopurinol in gout therapy, it is of course desirable to have a simple and direct method for monitoring the concentration of allopurinol and uric acid in body fluids. Allopurinol in body fluids is normally estimated clinically by spectrophotometric methods based on its characteristic ultraviolet absorption spectrum, after it has been separated from interfering materials by use of various ion-exchange resins[3,4]. Uric acid also has a characteristic ultraviolet absorption spectrum which is different to that of allopurinol. However, because of the presence of other purines, *e.g.*, xanthines, in biological fluids, which absorb in the same spectral regions, more specific clinical analyses are usually performed. Benedict and Franke[5] have described a spectrophotometric method where the uric acid in, *e.g.*, urine, is treated directly with tungstoarsenophosphoric acid and sodium cyanide. The resultant blue color is directly proportional to the uric acid concentration. Buchanan *et al.*[6] have described a more selective method based on the enzyme uricase which specifically oxidizes uric acid. However, both these methods for uric acid are time-consuming. We have recently reported the mechanism of the electrochemical reduction of allopurinol at the dropping mercury electrode (D.M.E.)[7]. At the D.M.E., allopurinol exhibits a well-defined diffusion-controlled polarographic wave. Uric acid, however, is not reducible electrochemically, yet is very readily oxidized at the pyrolytic graphite electrode (P.G.E.)[8,9], giving rise to a well-formed voltammetric peak at the stationary P.G.E. In the present work, it was found that allopurinol also gives a voltammetric oxidation peak at the P.G.E. but at much more positive potential than that of uric acid, so that there is no interference. Although many xanthines and other purines encountered in biological fluids are electrochemically oxidizable[10-12], they are all more difficultly oxidized than uric acid. None of the xanthines or other oxidized purines expected in biological fluids are electrochemically reducible.

In view of the electrochemistry of uric acid and allopurinol, it appeared that a simple, rapid and direct method could be developed for analysis of mixtures of these compounds.

The work reported here characterizes the adsorption of uric acid at the P.G.E. and the effect of allopurinol on this adsorption. Very satisfactory methods for analysis of mixtures of millimolar and lower concentrations of allopurinol and uric acid have been developed.

EXPERIMENTAL

Chemicals

Allopurinol (Calbiochem) was found to be chromatographically homogeneous. Uric acid (Nutritional Biochemicals Corp.) was used as received. Other chemicals were of reagent grade.

Buffer solutions were all 0.5 in ionic strength except sulfuric acid and acetic acid which were 1 *M*.

Water-saturated argon was employed for deoxygenating solutions.

Apparatus

A Sargent Model XV Polarograph was used for recording both d.c. polarograms at the D.M.E. and d.c. voltammograms at the stationary P.G.E. A voltage scan rate of 3.3 mV sec^{-1} was employed. The D.M.E. had normal m and t values.

Alternating current voltammograms at the P.G.E. were obtained with an operational amplifier instrument[13] combined with a Princeton Applied Research Model 121 Lock-in Amplifier/Phase Detector. For a.c. voltammetry, a d.c. ramp of 5 mV sec^{-1} and a sinusoidal signal of 100 Hz and 10 mV peak-to-peak, was employed for all experiments. All a.c. voltammograms were recorded on a Hewlett-Packard Model 7001A X-Y recorder.

A three-compartment cell maintained at $25 \pm 0.1°$ was employed for all experiments and contained a saturated calomel reference electrode (S.C.E.) and a platinum gauze counter electrode. All potentials are referred to the S.C.E. at 25°.

Preparation of the P.G.E. for d.c. and a.c. voltammetry has been described in detail previously[14].

Procedure for determination of allopurinol and uric acid

For determination of allopurinol the test solution containing allopurinol and uric acid was diluted with the desired supporting electrolyte. (1 *M* Sulfuric acid, acetate buffer pH 4.7 or McIlvaine buffer pH 6 were used. No doubt other buffer systems of different pH could be utilized if necessary.) The resultant solution should preferably be between 0.1–*ca.* 1 m*M* in allopurinol. After about 5 min deaeration a d.c. polarogram was recorded on an aliquot of this solution.

At least three replicate polarograms were always recorded. A background polarogram was recorded in exactly the same way, except that the allopurinol–uric acid test sample was omitted. The mean background current at the potential of the limiting current plateau of the test sample was subtracted from the mean allopurinol limiting current. The concentration of allopurinol was then determined from a calibration curve prepared for known allopurinol concentrations (between 0.1–1 m*M*) in the appropriate supporting electrolyte.

A second aliquot of the test solution diluted in the appropriate supporting electrolyte and containing 0.05–0.5 m*M* uric acid was then treated with sufficient solid allopurinol to make the solution *ca.* 7 m*M* with respect to allopurinol. The solution was stirred on a hot plate for about 10 min at *ca.* 40°. All of the allopurinol does not dissolve and after cooling the solution to 25° the test solution is saturated with this compound. Three replicate d.c. voltammograms of the resultant solution were then recorded. A background voltammogram was recorded with a saturated solution of allopurinol in the appropriate supporting electrolyte. The uric acid peak current was obtained by subtracting the mean background current at the uric acid peak potential from the mean current for the uric acid voltammogram. The concentration of uric acid was determined from a calibration curve prepared for known uric acid concentrations (0.05–0.5 m*M*) in the appropriate supporting electrolyte saturated with allopurinol.

RESULTS AND DISCUSSION

D.C. polarography of allopurinol

Allopurinol exhibits a well-defined polarographic wave between pH 0 and 8. At pH 0 this wave is due to the 4-electron reduction of allopurinol to 2, 3, 6, 7-tetrahydroallopurinol. At higher pH the electrode reaction involves only two electrons and is due to reduction of protonated allopurinol to 6,7-dihydroallopurinol. The mechanism of these reactions and certain follow-up processes that occur under conditions of prolonged electrolysis have been described elsewhere[7]. The polarographic wave rapidly decreases in height above pH 6 and disappears above pH 8. At pH 6–8 the wave is under kinetic control. Accordingly, the useful analytical range for polarography of allopurinol is pH 0–6. The half-wave potential for allopurinol shifts linearly more negative with increasing pH according to the equation $E_{\frac{1}{2}} = -1.118 - 0.067$ pH.

Three supporting electrolyte systems were employed to examine the analytical relationship of the polarographic diffusion current to the concentration of allopurinol, namely 1 *M* sulfuric acid, acetate buffer pH 4.7 and McIlvaine buffer pH 6.0.In each supporting electrolyte system a linear diffusion current *versus* concentration relationship was observed (Fig. 1). The greater slope of the relationship in 1 *M* sulfuric acid is simply due to the 4-electron nature of the polarographic process at this pH compared to the 2-electron process at higher pH.

D.C. voltammetry of allopurinol

Allopurinol exhibits a single voltammetric oxidation peak at the P.G.E. over the entire normal pH range (0–14). This peak occurs close to background discharge potentials and its peak potential is described by the equation $E_p = 1.405 - 0.051$ pH. The reactions responsible for this peak are presently under investigation. In view of the better resolution of the polarographic reduction wave of allopurinol and the rather greater precision of polarographic waves at the D.M.E. compared to voltammetric peaks at stationary solid electrodes, the analytical utility of this peak was not investigated further. In addition, the purpose of this work was to develop a method for the determination of allopurinol and uric acid in mixtures. Uric acid can only be determined electrochemically via its voltammetric oxidation peak at the P.G.E. If allopurinol was determined in mixtures with uric acid by means of its oxidation peak,

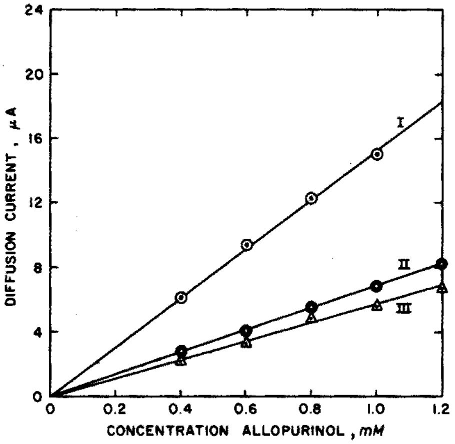

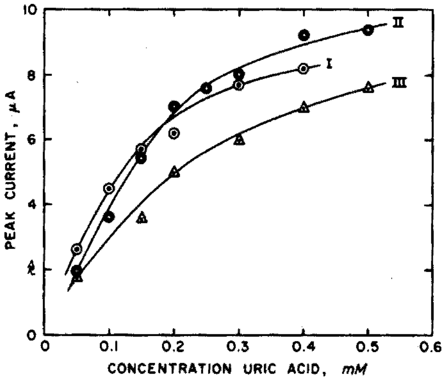

Fig. 1. Linear current–concentration curves for the polarographic reduction of allopurinol at the D.M.E. in (I) 1 *M* sulfuric acid, (II) acetate buffer pH 4.7 and (III) McIlvaine buffer pH 6.

Fig. 2. Peak current-concentration curves for the voltammetric oxidation of uric acid at the P.G.E. in (I) 1 *M* sulfuric acid, (II) acetate buffer pH 4.7, and (III) McIlvaine buffer pH 6.0. Geometric area of P.G.E. 12.5 mm^2.

which occurs at more positive potentials than that of uric acid, considerable error could be expected because of the well known difficulty in estimating the peak current for the second of two consecutive voltammetric peaks[15].

D.C. voltammetry of uric acid

Uric acid gives a very well-formed anodic oxidation peak at the stationary P.G.E. The electrode mechanism responsible for this peak has been discussed extensively elsewhere[8,9]. The peak potential shifts linearly more negative with increasing pH according to the equation $E_p = 0.71 - 0.052$ pH for data between pH 0–6.

In all the supporting electrolyte systems uric acid shows non-linear anodic peak current *versus* concentration relationships (Fig. 2); for many analytical purposes such curves, if reproducible, could be utilized satisfactorily. However, investigation of the determination of uric acid in mixtures with allopurinol showed that the results for uric acid were always low. Allopurinol was found to have a pronounced effect on the voltammetric oxidation peak of uric acid. This is shown clearly in Fig. 3 where the effect of increasing the allopurinol concentration on the peak current for a fixed concentration of uric acid is presented.

The non-linear peak current–concentration curves of uric acid clearly indicate that adsorption of uric acid or its oxidation products takes place at the P.G.E. The fact that addition of allopurinol to uric acid solutions reduces the anodic peak current for uric acid suggests that some type of competitive adsorption takes place, with adsorbed uric acid being partially displaced from the electrode surface in the presence of allopurinol. Quite variable relative concentrations of uric acid and allopurinol are expected in clinical and other samples; accordingly, in order to maintain a constant solution composition of allopurinol it was decided to saturate the test solutions with this compound. A saturated solution of allopurinol in the background solutions employed here corresponds to a concentration between 6–7 m*M*. It was

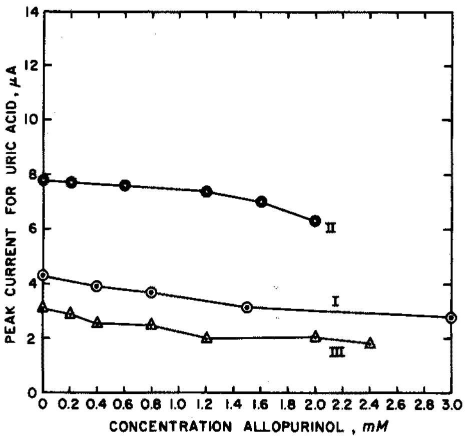

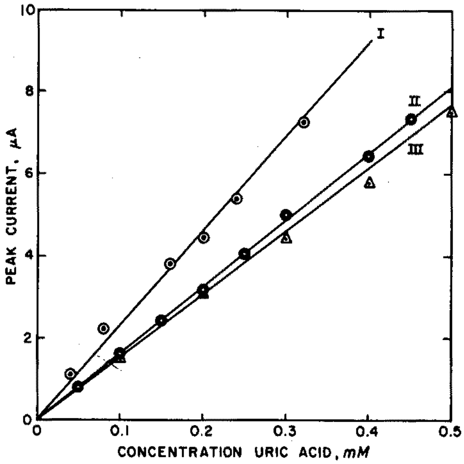

Fig. 3. Variation of uric acid anodic peak current with increasing amounts of allopurinol. (I) 0.1 m m*M* uric acid in 1 *M* sulfuric acid, (II) 0.25 m*M* uric acid in acetate buffer pH 4.7, and (III) 0.063 m*M* uric acid in McIlvaine buffer pH 6. Geometric area of P.G.E. 12.5 mm^2.

Fig. 4. Linear peak current–concentration curves for the voltammetric oxidation peak of uric acid at the P.G.E. in solutions saturated with allopurinol in (I) 1 *M* sulfuric acid, (II) acetate buffer pH 4.7, and (III) McIlvaine buffer pH 6.0.

found that, in a solution saturated with allopurinol, the peak current for uric acid at the P.G.E. became linearly proportional to concentration (Fig. 4). The differences in the slope of the latter curves in the various supporting electrolytes probably result from changes in the diffusion coefficient of uric acid.

Scan rate studies

In order to study further the adsorption of uric acid at the P.G.E., the effect of voltage scan rate on the peak currents of the two compounds was examined. According to Nicholson and Shain[16], the theoretical peak current (in μA) for reversible peak voltammograms at a plane electrode is given by eqn. (1):

$$(i_p)_{\text{rev}} = 2.69 \cdot 10^5 n^{\frac{3}{2}} A D^{\frac{1}{2}} V^{\frac{1}{2}} C \qquad (1)$$

where n is the number of electrons involved in the electrode reaction, A the electrode area in cm^2, D the diffusion coefficient (cm^2 sec^{-1}), V the voltage scan rate (V sec^{-1}) and C the bulk concentration of the electroactive species (mM l^{-1}). The primary electrochemical oxidation of uric acid is essentially reversible as evidenced by fast sweep cyclic voltammetry and a.c. voltammetry (*vide infra*) although it is complicated by irreversible follow-up chemical reactions[9]. According to eqn. (1) the peak current function, $i_p/ACV^{\frac{1}{2}}$, should be a constant independent of the scan rate, but for uric acid this function markedly increases with increasing scan rate (Table I). This behavior is typical of an electrode process where the reactant is adsorbed at the electrode[17]. In a solution saturated with allopurinol, the function for uric acid is much smaller and increases much less rapidly than in the absence of allopurinol (Table I).

A.C. voltammetry

A.C. voltammetry at the P.G.E. has previously been shown to be an excellent

TABLE I

VARIATION OF THE PEAK CURRENT FUNCTION[a] OF URIC ACID[b] AS A FUNCTION OF VOLTAGE SCAN RATE

Scan rate ($mV\ sec^{-1}$)	*Peak current function* ($\mu A\ mm^{-2}\ mM^{-1}\ (mV/sec)^{-\frac{1}{2}}$)	
	Uric acid	*Uric acid in solutions saturated with allopurinol*
1 *M* H_2SO_4		
5	1.30	0.90
20	2.10	1.05
50	2.70	1.40
100	2.85	1.60
200	3.40	1.75
500	3.50	2.40
Acetate buffer pH 4.7		
5	1.18	0.91
20	1.41	0.92
50	2.04	1.25
100	2.07	1.31
200	2.32	1.43
500	2.81	1.95
McIlvaine buffer pH 6.0		
5	0.77	0.60
20	1.14	0.76
50	1.47	0.85
100	1.81	0.94
200	2.01	1.30
500	2.31	1.82

[a] $i_p/ACV^{\frac{1}{2}}$; for definition of terms see text.

[b] Uric acid concentration for all studies 0.2 m*M*.

qualitative technique for the detection of adsorption phenomena[14]. Voltammograms of uric acid in acetate buffer pH 4.7 (Fig. 5A) and in McIlvaine buffer pH 6.0 (Fig. 5B) clearly indicate that uric acid, and possibly an oxidation product, are adsorbed at the P.G.E., for the alternating base current is depressed at potentials negative and to a lesser extent positive of the faradaic a.c. peak. Formation of a well formed a.c. peak at about the same peak potential as the d.c. peak clearly establishes the reversible nature of the electrochemical oxidation of uric acid. When any of the background solutions were saturated with allopurinol, the alternating base current was depressed very considerably (Fig. 6A, B). However, addition of uric acid to the latter solutions resulted in only a very slight further base current depression, indicating that uric acid is considerably less extensively adsorbed in the presence of a large excess of allopurinol than in the absence of allopurinol. The a.c. data all confirmed the qualitative findings from the scan rate studies of uric acid in the presence and absence of allopurinol.

Effect of uric acid on the polarographic reduction of allopurinol

In view of the fact that allopurinol has a marked effect on the anodic peak current for uric acid at the P.G.E., the effect of uric acid on the cathodic polarographic limiting current of allopurinol was investigated. It was found that solutions of uric acid ranging

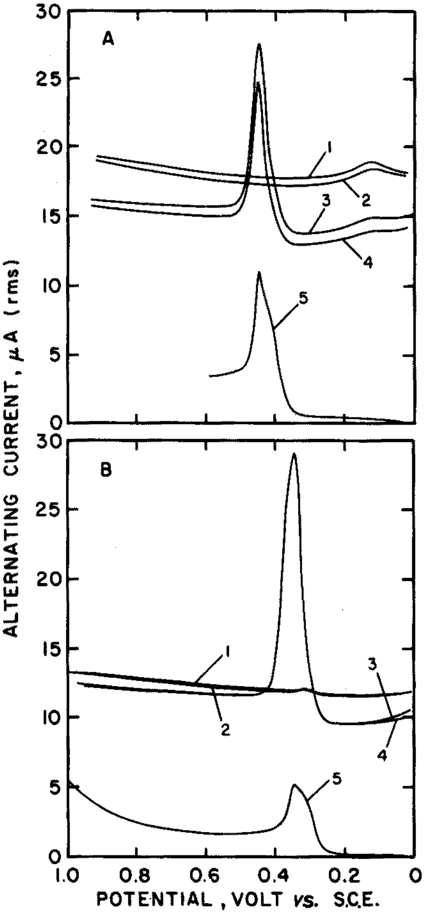

Fig. 5. A.c. voltammograms of 0.5 m*M* uric acid in (A) acetate buffer pH 4.7 and (B) McIlvaine buffer pH 6.0. Scans 1 and 2 are background traces, scans 3 and 4 are for uric acid in the same background, and scan 5 is a d.c. voltammogram. Alternating voltage: 100 Hz and 10 mV peak-to-peak.

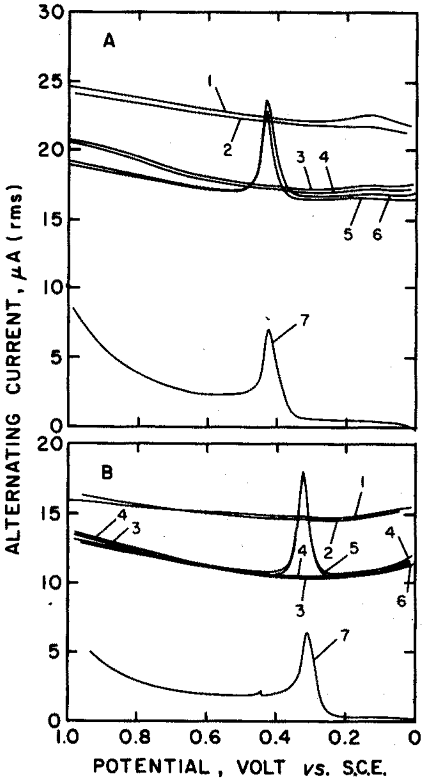

Fig. 6. A.c. voltammograms of 0.5 m*M* uric acid in (A) acetate buffer pH 4.7 and (B) McIlvaine buffer pH 6.0 saturated with allopurinol. Scans 1 and 2 are background traces, scans 3 and 4 are traces of background saturated with allopurinol, scans 5 and 6 are of 0.5 m*M* uric acid in background saturated with allopurinol and scan 7 is a d.c. voltammogram in the latter solution. Alternating voltage: 100 Hz and 10 mV peak-to-peak.

from 0.01 to *ca.* 0.5 m*M* (saturated) had no effect on the polarographic limiting current of allopurinol.

Development of analytical methods

Concentration and scan rate studies and a.c. voltammetry of uric acid prove that this compound is strongly adsorbed at the P.G.E.; in solutions saturated with allopurinol, this adsorption is considerably decreased. From an analytical viewpoint, the most important factor is that the normally non-linear peak current–concentration curves for uric acid become linear and very reproducible in solutions saturated with allopurinol. Uric acid is not polarographically reducible at the D.M.E. whereas allopurinol is, and uric acid has no effect on the polarographic wave of allopurinol. Accordingly, a very straightforward analytical method was possible (see *Experimental*). The allopurinol in the mixtures is determined via its polarographic reduction wave at the D.M.E. at pH 0–6; the solution is then saturated with allopurinol and the uric acid concentration is determined via its voltammetric oxidation peak at the P.G.E. Calibration curves were prepared and were essentially identical to those shown earlier in Figs. 1 and 4. Some typical analytical data obtained on uric acid–allopurinol mixtures at pH 0, 4.7 and 6.0 (Table II) show that this method is very accurate and rapid for these analyses.

TABLE II

DETERMINATION OF MIXTURES OF ALLOPURINOL AND URIC ACID

Allopurinol taken (mM)	*Uric acid taken (mM)*	*Allopurinol found (mM)*	*Uric acid found (mM)*
1 M H_2SO_4			
0.40	0.32	0.40	0.31
0.60	0.28	0.61	0.28
0.80	0.24	0.80	0.23
1.00	0.20	0.99	0.21
1.20	0.16	—	0.16
Acetate buffer pH 4.7			
0.40	0.40	0.40	0.39
0.60	0.35	0.59	0.35
0.80	0.30	0.80	0.30
1.00	0.25	0.99	0.27
1.20	0.20	1.20	0.20
McIlvaine buffer pH 6.0			
0.40	0.25	0.40	0.27
0.60	0.30	0.58	0.29
0.80	0.35	0.82	0.36
1.00	0.40	0.99	0.39
1.20	0.20	1.18	0.19

The authors would like to acknowledge financial support for this study from the National Science Foundation and from the Graduate College of the University of Oklahoma.

SUMMARY

Uric acid and allopurinol are both electrochemically oxidized at the pyrolytic graphite electrode (P.G.E.) in aqueous solution, the oxidation of allopurinol occurring at more positive potentials. Allopurinol is polarographically reducible at the dropping mercury electrode, and the wave is not affected by uric acid. Uric acid is strongly adsorbed at the P.G.E., so that concentration *vs.* anodic peak current curves are not linear, but when the solution is saturated with allopurinol, these plots become linear. and changes in scan rate have less effect. It is shown that allopurinol is adsorbed at the P.G.E., and in saturated solutions, displaces adsorbed uric acid from the electrode surface. Allopurinol (0.1–1 m*M*) can be determined via its polarographic reduction wave at the D.M.E.; the solution is then saturated with allopurinol and uric acid (0.05–0.5 m*M*) is determined via its anodic peak at the P.G.E. The procedure is satisfactory in supporting electrolyte systems of pH 0–6.

RÉSUMÉ

L'acide urique et l'allopurinol sont oxydés tous deux électrochimiquement à l'électrode de graphite pyrolytique, en solution aqueuse; l'oxydation de l'allopurinol se produit à des potentiels plus positifs que l'acide urique. L'allopurinol est réductible polarographiquement à l'électrode à gouttes de mercure; sa vague n'est pas affectée par l'acide urique. L'acide urique (0.05–0.5 m*M*) peut être dosé également par polarographie par mesure de son pic anodique, après saturation de la solution avec l'allopurinol.

ZUSAMMENFASSUNG

Harnsäure und Allopurinol werden in wässriger Lösung beide elektrochemisch an der pyrolytischen Graphitelektrode (P.G.E.) oxidiert, wobei die Oxidation des Allopurinols bei positiveren Potentialen erfolgt. Allopurinol ist an der tropfenden Quecksilberelektrode (D.M.E.) polarographisch reduzierbar, und die Stufe wird durch Harnsäure nicht beeinflusst. Harnsäure wird an der P.G.E. stark adsorbiert, so dass keine lineare Beziehung zwischen Konzentration und anodischem Spitzenstrom erhalten wird. Wenn jedoch die Lösung an Allopurinol gesättigt ist, wird diese Beziehung linear, und Änderungen der Scan-Geschwindigkeit haben geringeren Einfluss. Es wird gezeigt, dass Allopurinol an der P.G.E. adsorbiert wird und in gesättigten Lösungen adsorbierte Harnsäure von der Elektrodenoberfläche verdrängt. Allopurinol (0.1–1 m*M*) kann über seine polarographische Reduktionsstufe an der D.M.E. bestimmt werden. Die Lösung wird dann mit Allopurinol gesättigt und Harnsäure (0.05–0.5 m*M*) mittels ihres anodischen Spitzenstromes an der P.G.E. bestimmt. Das Verfahren ist in Trägerelektrolytsystemen von pH 0–6 befriedigend.

REFERENCES

1 W. N. Kelly, J. B. Wyngaarden, G. H. Hitchings, G. B. Elion and H. R. Silberman, *Trans. Assoc. Am. Physicians*, 76 (1963) 126.
2 J. F. Henderson, *Cancer Res.*, 21 (1961) 118.
3 E. F. Salim and J. E. Murphy, *J. Pharm. Sci.*, 57 (1968) 649.
4 P. D. Gressel and J. F. Galleli, *J. Pharm. Sci.*, 57 (1968) 335.
5 S. R. Benedict and E. Franke, *J. Biol. Chem.*, 52 (1922) 387.
6 O. H. Buchanan, W. D. Block and A. A. Christman, *J. Biol. Chem.*, 157 (1945) 181.
7 P. K. De and G. Dryhurst, *J. Electrochem. Soc.*, submitted for publication.
8 W. L. Struck and P. J. Elving, *Biochem.*, 4 (1965) 1343.
9 G. Dryhurst, *J. Electrochem. Soc.*, 116 (1969) 1411; 118 (1971) 699.
10 G. Dryhurst and P. J. Elving, *J. Electrochem. Soc.*, 115 (1968) 1014.
11 G. Dryhurst and G. F. Pace, *J. Electrochem. Soc.*, 117 (1970) 1259.
12 B. H. Hansen and G. Dryhurst, *J. Electroanal. Chem.*, 30 (1971) 407; 30 (1971) 417.
13 G. Dryhurst, M. Rosen and P. J. Elving, *Anal. Chim. Acta*, 42 (1968) 143.
14 G. Dryhurst, *Anal. Chim. Acta*, 57 (1971) 137.
15 P. Delahay, *New Instrumental Methods in Electrochemistry*, Interscience, New York, 1954, pp. 129–130.
16 R. S. Nicholson and I. Shain, *Anal. Chem.*, 36 (1964) 706.
17 R. H. Wopschall and I. Shain, *Anal. Chem.*, 39 (1967) 1514.

Analytica Chimica Acta
Elsevier Publishing Company, Amsterdam
Printed in The Netherlands

ELECTROCHEMICAL STUDIES OF THE URANIUM(VI)–DIETHYLENETRIAMINEPENTAACETIC ACID COMPLEXES

E. JACOBSEN, G. O. KALLAND* AND O. LYKKJEN
Department of Chemistry, University of Oslo, Blindern, Oslo 3 (Norway)

(Received 31st August 1971)

Chelate formation between the uranyl ion (UO_2^{2+}) and various complexing agents (EDTA, NTA, DCTA, IDA, HEDTA) has been the subject of numerous investigations[1-14], but, surprisingly, work on the diethylenetriaminepentaacetic acid (DTPA) complexes has been very limited. Razbitnaya and Korovina[15,16] claim that the reaction between uranium(VI) and DTPA is very fast and that only one complex with cation–ligand ratio 1 : 1 is formed. This conclusion has not been confirmed by other investigators although various workers[3,5,7,10,13] have concluded that EDTA can react with uranyl ions to form both 2 : 1 and 1 : 1 complexes.

The present work was undertaken to investigate the electrochemical reduction of the uranyl–DTPA system and to establish the composition of the complexes formed.

EXPERIMENTAL

Apparatus

Polarograms were recorded with a Metrohm E 261 R Polarecord connected to a Metrohm E 393 a.c. modulator. An Ag/AgCl/saturated KCl electrode served as reference electrode and a tungsten electrode was employed as auxiliary electrode. All a.c. polarograms were obtained with an amplitude of 10 mV r.m.s. The capillary characteristics of the dropping mercury electrode, measured in 0.1 *M* potassium nitrate (open circuit) at a mercury height of 45.5 cm, were $m = 3.280$ mg sec^{-1} and $t = 2.99$ sec. All experiments were performed at 25 ± 0.1°. Dissolved air was removed from the solutions by bubbling oxygen-free nitrogen through the cell for 10 min and passing it over the solution during the electrolysis.

Cyclic voltammetry and coulometric experiments were performed with a versatile solid-state instrument constructed in this laboratory following the design of Goolsby and Sawyer[17]. A Mosely 7030 AM X-Y recorder and a Honeywell Electronic 194 strip-chart recorder were used in conjunction with the instrument. A three-electrode assembly was used for all measurements. A Metrohm E410 hanging mercury drop was used as working electrode for the cyclic voltammetric experiments and a mercury pool was employed for the controlled-potential coulometric measurements. The reference electrode was an aqueous Ag/AgCl wire and a platinum coil wire served as auxiliary electrode. These electrodes were isolated in glass tubes with fine-

---

* Present address: Nordisk Husholdshøgskole, Ernaeringslinjen, University of Oslo, Blindern, Oslo 3, Norway.

porosity fritted-glass discs. The shield tubes were filled with the supporting electrolyte used in the sample solution. The solution was stirred with a magnetic stirrer and a Teflon-covered stirring bar.

Reagents

Diethylenetriamine pentaacetic acid (DTPA) was obtained from Geigy Chemical Corp., New York. A 0.05 *M* stock solution was prepared and standardized as described previously[18]. A 0.01 *M* uranium(VI) solution was prepared by dissolving 2.8603 g of UO_3 (K. and K. Laboratories, Inc., New York) in perchloric acid and diluting to 1 l with distilled water. The molarity was checked gravimetrically. Dodecylamine (Armour Industrial Chemical Co., Chicago, Ill.) was used as maximum suppressor. A 1% stock solution was prepared as described previously[19]. The remaining chemicals were of reagent-grade and were used without further purification.

RESULTS AND DISCUSSION

Polarography

On addition of DTPA to an acidic solution of uranium(VI) the intensity of the yellow colour increases and the half-wave potential is shifted to more negative values indicating complex formation. In the presence of excess of DTPA, uranium(VI) produces a single well-defined wave at the dropping mercury electrode. In acidic solutions the polarographic wave exhibits a maximum which is easily suppressed in the presence of dodecylamine. In the following experiments 0.002% dodecylamine was added to all solutions of pH less than 5. At higher pH values no maximum was observed and no surfactant was added.

The effect of pH on the polarographic wave was investigated with acetate and borate buffers as supporting electrolytes. When the pH of the electrolyte was increased above 8 a precipitate was formed. This precipitate is probably the result of hydrolysis of the uranium(VI) complex and the following experiments were restricted to lower pH values.

As indicated in Fig. 1 the limiting current of the d.c. wave is very dependent on pH of the supporting electrolyte. Below pH 4.5 and above pH 6 the current is fairly constant but the great difference in the limiting currents indicates the existence of different uranium–DTPA complexes in acidic and in neutral solutions. Hence, two series of experiments (at pH 4.5 and pH 6.5) were performed.

The reversibility of the electrode reaction was tested by plotting $\log i/(i_d - i)$ *vs.* the potential. The plots yield straight lines of slopes −72 mV and −65 mV per log unit at pH 4.5 and pH 6.5, respectively. The electron transfer parameter, αn_a, calculated from

$$E = E_{\frac{1}{2}} - \frac{0.059}{\alpha n_a} \log i/(i_d - i)$$

were 0.82 and 0.91 at pH 4.5 and pH 6.5, respectively, indicating an irreversible one-electron reduction.

The d.c. polarographic step was followed by an a.c. polarographic wave. The height of the a.c. wave increased with increasing pH (Fig. 1) indicating an increased reversibility at higher pH values. At pH 6.5 the width of the a.c. wave at half height

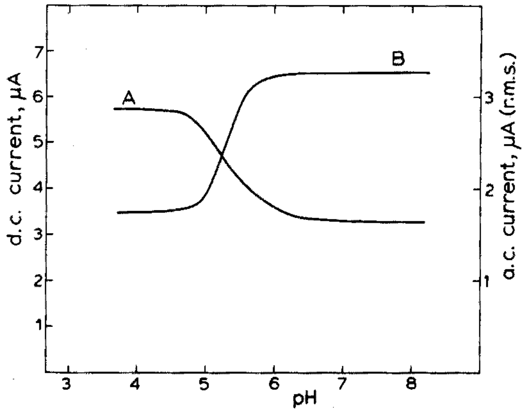

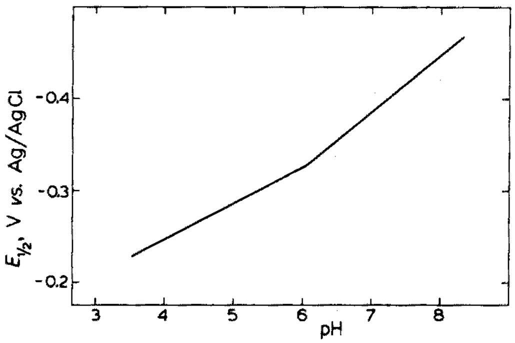

Fig. 1. Limiting current of 10^{-3} *M* uranium(VI) in the presence of 10^{-2} *M* DTPA in 0.1 *M* acetate and borate buffers at various pH values. (A) D.c. current, (B) a.c. current.

Fig. 2. Half-wave potentials of 10^{-3} *M* uranium(VI) in the presence of 10^{-2} *M* DTPA at various pH values.

was 100 mV which is close to the theoretical value for a reversible one-electron process.

The half-wave potential was shifted to more negative values with increasing pH of the electrolyte as shown in Fig. 2. The slopes of the lines were −40 mV per pH unit at pH values below 6, and −65 mV per pH unit at higher pH values. The number of hydrogen ions, Z, involved in the electrode reaction was calculated from the equation

$$\Delta E_{\frac{1}{2}}/\Delta\,\mathrm{pH} = -0.059\cdot Z/\alpha n_a$$

The values $Z=0.55$ at pH 4.5 and $Z=1.00$ at pH 6.5 were obtained; these imply that one hydrogen ion is involved in the reduction of two uranium(VI) at pH 4.5, but above pH 6 one hydrogen ion is consumed in the reduction of one uranium(VI).

The effect of drop-time was investigated by recording polarograms at various heights of the mercury column. At pH 4.5 the limiting current increased with the height of the column and the value $i/\sqrt{h}$, where h is the height of the column after correction for the "back pressure", was constant, indicating that the limiting current

TABLE I

EFFECT OF PRESSURE OF MERCURY ON THE POLAROGRAPHIC WAVE OF 10^{-3} *M* URANIUM(VI) AND 10^{-2} *M* DTPA AT pH 6.5

h_{corr} (*cm*)	*Current* (*μA*)	$i_d/\sqrt{h}$ (*μA* $cm^{-\frac{1}{2}}$)
37.5	3.10	0.506
42.5	3.25	0.499
47.5	3.45	0.501
52.5	3.55	0.490
57.5	3.70	0.488
62.5	3.85	0.487
65.5	3.95	0.488

is diffusion-controlled. Moreover, the height of the a.c. wave was independent of the height of the column. The temperature coefficient of the limiting current (determined in the range 25–55°) was +1.3% per degree, which also indicates that the current is controlled essentially by diffusion. At pH 6.5 the value $i/\sqrt{h}$ decreased slightly with increasing height of the column (Table I). Moreover, the temperature coefficient of the limiting current was +2.6% per degree (Table II), implying that the current is partly controlled by a kinetic or catalytic process.

The diffusion current constant, I, was determined by recording polarograms of various amounts of uranium(VI) in the presence of 10^{-2} M DTPA. The diffusion current constant at pH 6.5 calculated from the data in Table III was $I = 1.41$ and the diffusion coefficient $D = 5.4 \cdot 10^{-6}$ cm^2 sec^{-1}. This value is close to that for the mononuclear uranyl–EDTA complex[12] ($D = 5.5 \cdot 10^{-6}$ cm^2 sec^{-1}) and indicates that the

TABLE II

EFFECT OF TEMPERATURE ON THE POLAROGRAPHIC WAVE OF 10^{-3} M URANIUM(VI) AND 10^{-2} M DTPA AT pH 6.3

Temp. (°)	$-E_{\frac{1}{2}}$ (*V*)	$-E_s$ (*V*)	i_d (*μA*)	i_s (*μA*)
24.9	0.358	0.384	3.20	3.67
30.3	0.360	0.382	3.72	4.20
34.8	0.361	0.380	4.22	4.72
39.7	0.360	0.376	4.80	4.94
45.0	0.362	0.377	5.43	5.14
		Temp. coeff.:	+2.6%/°	+1.7%/°

TABLE III

POLAROGRAPHIC DATA FOR THE REDUCTION OF VARIOUS AMOUNTS OF URANIUM(VI) IN THE PRESENCE OF 10^{-2} M DTPA

(Capillary characteristics, $m^{\frac{2}{3}}t^{\frac{1}{6}} = 2.49$ and 2.65 at pH 4.5 and pH 6.5, respectively)

pH	*Concn.* (*mM*)	i_d (*μA*)	i_d/C (*μA mM*$^{-1}$)	i_s (μA (*r.m.s.*))	i_s/C (*μA* (*r.m.s.*)*mM*$^{-1}$)
4.5	0.01	0.050	5.00	0.048	4.80
4.5	0.05	0.248	4.96	0.240	4.80
4.5	0.10	0.497	4.97	0.460	4.60
4.5	0.20	0.980	4.90	0.760	3.80
4.5	0.50	2.48	4.96	1.53	3.06
4.5	1.00	4.95	4.95	1.92	1.92
		Mean	4.96		
6.5	0.025	0.093	3.72	0.225	9.00
6.5	0.050	0.188	3.76	0.450	9.00
6.5	0.10	0.376	3.76	0.890	8.90
6.5	0.20	0.755	3.77	1.58	7.90
6.5	0.50	1.85	3.70	3.12	6.24
6.5	1.00	3.65	3.65	3.44	3.44
6.5	2.00	7.45	3.72	2.80	1.40
		Mean	3.73		

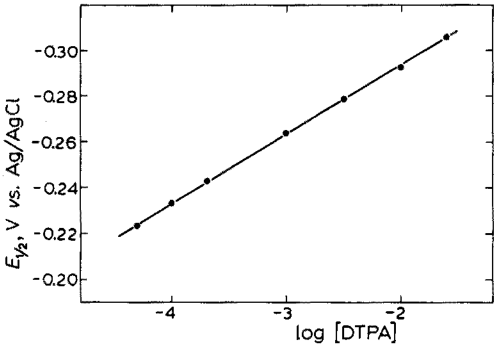

Fig. 3. Effect of excess DTPA on the half-wave potential of 10^{-4} M uranium(VI), at pH 4.5. Supporting electrolyte: 0.2 M sodium perchlorate, 0.01 M acetate buffer and 0.002% dodecylamine.

uranyl–DTPA wave is caused by a one-electron reduction to uranium(V). However, at pH 4.5 the diffusion current is considerably higher (Table III) implying that this wave must be due to the reduction of a different DTPA complex.

The effect of the concentration of DTPA on the half-wave potential was studied by varying the concentration of DTPA and keeping the concentration of uranium(VI) constant at 10^{-4} M. In order to avoid complex formation between uranium(VI) and the supporting electrolyte, the concentration of the acetate buffer was kept as low as possible. The result of one series of polarograms recorded at pH 4.5 is shown in Fig. 3, in which the half-wave potential is plotted against the logarithm of the DTPA concentration. The slope of the straight line is −30 mV per log unit which implies that one ligand is liberated in the reduction of two uranyl ions. On the other hand, at pH 6.5 the half-wave potential was found to be independent of the DTPA concentration in the range $5 \cdot 10^{-4}$ to $2.5 \cdot 10^{-2}$ M DTPA, indicating that the same number of ligands are attached to the oxidized and the reduced form of the depolarizer.

The polarographic data indicate that the wave observed at pH values above 6 is due to a slightly irreversible one-electron reduction to uranium(V). One hydrogen ion is consumed in the electrode process which may be represented by

$$UO_2HY^{2-} + H^+ + e \rightleftharpoons UO_2H_2Y^{2-} \quad \text{where } H_5Y \text{ denotes DTPA.}$$

At pH values below 5 the diffusion current is considerably higher and the electrode reaction more irreversible. Only one hydrogen ion is consumed and only one ligand is liberated in the reduction of two uranium(VI) ions. Hence, the complex species at pH less than 5 is probably composed of two uranyl ions for each molecule of DTPA and the electrode reaction at these pH values is probably

$$(UO_2)_2HY + 2e + H^+ \rightarrow 2UO_2^+ + H_2Y^{3-}$$

The high temperature coefficient and the drop-time dependence of the limiting current observed at pH values above 6 imply that the current is partly controlled by the rate of a kinetic or catalytic reaction. Hence, this electrode reaction was further investigated by other techniques.

Cyclic voltammetry

Voltammetric experiments were performed at a hanging mercury drop electrode. Reproducible results were obtained, provided that the mercury drop was exchanged between each potential sweep.

The data obtained at pH 6.5 are given in Table IV. At fast scan rates well defined cathodic and anodic waves were obtained. At the scan rate 0.1 V sec^{-1} the peak separation, ΔE_p, was 80 mV, indicating an almost reversible one-electron transfer process. However, the peak separation increased at faster scan rates. Moreover, when the scan rate was decreased below 0.05 V sec^{-1} the anodic wave disappeared and only the cathodic wave was observed on the voltammogram (Fig. 4).

The data given in Table IV were perfectly reproducible, provided that the voltammograms were recorded shortly after mixing the solution. Voltammograms recorded a few days later showed that the cathodic peak current decreased with time and that a new wave appeared at more negative potentials (Fig. 5). No anodic wave

TABLE IV

VOLTAMMETRIC DATA FOR THE REDUCTION OF 10^{-3} *M* URANIUM(VI) AND 10^{-2} *M* DTPA AT pH 6.5

Scan rate (*V* sec^{-1})	$(i_p)_c$ (μA)	$(i_p)_a$ (μA)	$(i_p)_c/Cv^{\frac{1}{2}}$ (μA mM^{-1} $V^{-\frac{1}{2}}$ $sec^{\frac{1}{2}}$)	$-(E_p)_c$ (*V*)	$-(E_p)_a$ (*V*)
1.0	22.3	21.1	22.3	0.480	0.30
0.5	15.9	13.3	22.5	0.445	0.31
0.2	10.3	7.3	22.8	0.425	0.33
0.1	7.36	4.4	23.2	0.420	0.34
0.033	4.50		24.6	0.415	
0.0166	3.50		27.2	0.412	
0.0083	2.78		30.5	0.410	
0.0033	1.95		34.2	0.405	

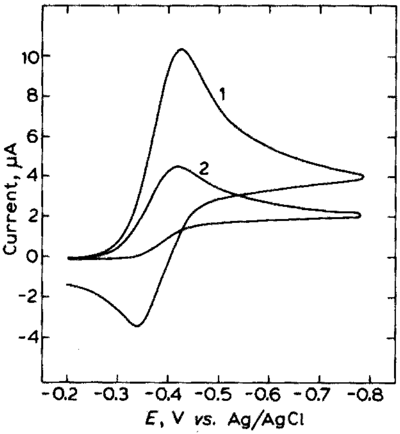

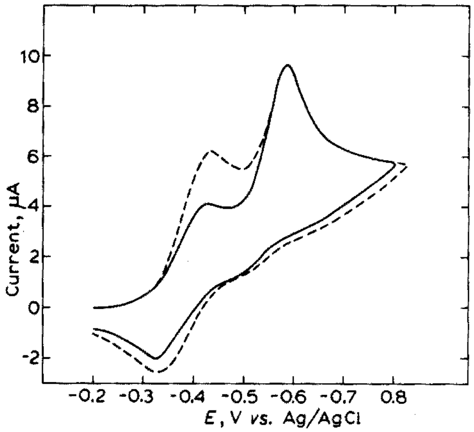

Fig. 4. Cyclic voltammograms of 10^{-3} *M* uranium(VI) and 10^{-2} *M* DTPA at pH 6.5. Scan rate 0.2 V sec^{-1} (curve 1) and 0.033 V sec^{-1} (curve 2).

Fig. 5. Cyclic voltammograms of 10^{-3} *M* uranium(VI) and 10^{-2} *M* DTPA at pH 6.5 recorded 4 days (dashed line) and 8 days (solid line) after mixing the solution. Scan rate 0.2 V sec^{-1}.

resulting from reoxidation of the reduction product of the second cathodic wave was observed at any scan rate, indicating a highly irreversible process. The decrease in the cathodic peak current and the appearance of a new wave is probably the result of a slow hydrolysis or polymerization of the complex. Hence, the following experiments were performed as soon as possible after mixing the solution.

The current function, $i_p/Cv^{\frac{1}{2}}$, of the cathodic peak increased rapidly at low scan rates (Fig. 6). Moreover, the ratio of the anodic peak current to the cathodic peak current approached unity at high scan rates (Fig. 7). These diagnostic criteria clearly demonstrate a reversible charge transfer followed by a catalytic reaction[20]. The experiments were repeated at various concentrations of uranium(VI). Exactly the same results were obtained for $5 \cdot 10^{-4}$ *M* uranium(VI) in the presence of 10^{-2} *M* DTPA. However, when the concentration of uranium(VI) was decreased below 10^{-4} *M* the current function became fairly constant and almost independent of the scan rate, indicating that the catalytic contribution to the current decreased with decreasing concentration of the depolarizer.

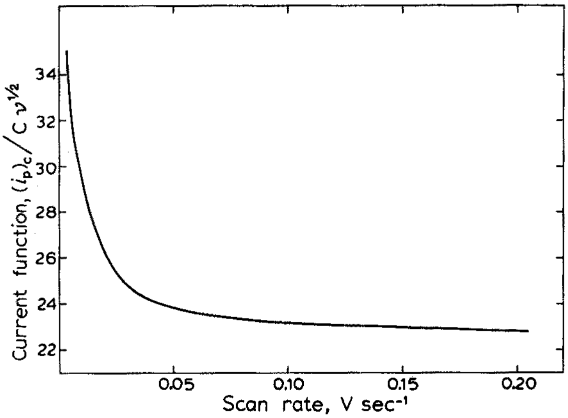

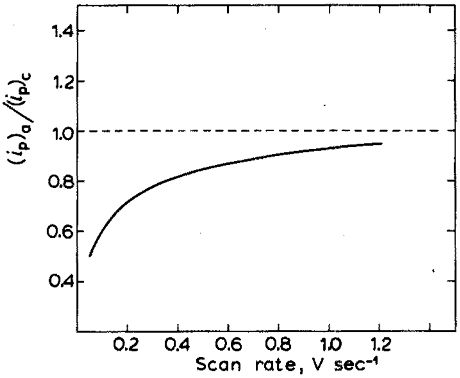

Fig. 6. Variation of cathodic peak current function with rate of voltage scan. 10^{-3} *M* uranium(VI) and 10^{-2} *M* DTPA at pH 6.5.

Fig. 7. Ratio of anodic to cathodic peak currents as a function of rate of voltage scan. 10^{-3} *M* uranium(VI) and 10^{-2} *M* DTPA at pH 6.5.

Voltammograms of the uranium complex recorded at pH 4.2 showed no anodic peak at any scan rate, indicating a highly irreversible reduction. Reproducible data were hard to obtain, but the cathodic peak current function seemed to increase slightly with decreasing scan rate. Hence, a small catalytic contribution to the current might occur also at lower pH values.

Coulometry

Coulometric reductions at controlled potential were performed to determine the number of electrons involved in the overall electrode process. The experiments were carried out in the absence of air in a small electrolysis cell with a mercury pool as the cathode; the potential was controlled slightly cathodic of the peak potential observed in cyclic voltammetry.

In acetate medium of pH 6 with excess of DTPA present, 3.3 C were consumed in the reduction of $2.0 \cdot 10^{-5}$ mole uranium(VI). The coulomb integral was obtained after 50 min of electrolysis and corresponds to an *n* value of 1.75. Obviously, more than one electron and most probably two electrons are consumed in the overall electrode process.

CONCLUSION

The polarographic and cyclic voltammetric data obtained at pH values above 6 imply that the uranium(VI)–DTPA complex undergoes an almost reversible one-electron reduction to a uranium(V) complex. However, the coulometric data indicate that 2 electrons are involved in the overall electrode process. Hence, the uranium(V)–DTPA complex must be unstable and disproportionate to uranium(VI) and uranium(IV). Evidently, the rate of the disproportionation is slow but is easily observed on cyclic voltammograms. Although the electron-transfer reaction involves only one electron, the overall reduction of the complex involves 2 electrons from uranium(VI) to uranium(IV), which was indicated by the coulometric measurements. Voltammograms recorded at pH 4.5 indicate that a disproportionation of the reduction product might occur also at lower pH values. However, the rate of this reaction must be very slow and does not affect the reduction at the dropping mercury electrode. Hence, reduction mechanism at low pH values was not investigated further.

SUMMARY

The electrochemical reduction of uranium(VI) in the presence of excess of DTPA has been studied by polarography, cyclic voltammetry and coulometry at controlled potential. Above pH 6 a complex with cation–ligand ratio 1 : 1 is formed. At mercury electrodes the complex is reversibly reduced to a uranium(V)–DTPA complex. The reduction product is unstable and disproportionates to uranium(VI) and uranium(IV). At pH values below 5 a complex with a cation–ligand ratio 2 : 1 is formed. This complex is irreversibly reduced to uranium(V). The diffusion current constants and polarographic behaviour of the two complexes are described.

RÉSUMÉ

Une étude est effectuée sur la réduction électrochimique de l'uranium(VI), en présence d'un excès de DTPA, par polarographie, voltammétrie cyclique et coulométrie à potentiel contrôlé. On observe la formation de deux complexes différents, suivant le pH. On examine leur comportement polarographique et leurs constantes de courant de diffusion.

ZUSAMMENFASSUNG

Die elektrochemische Reduktion von Uran(VI) in Gegenwart von überschüssigem DTPA wurde durch Polarographie, cyclische Voltammetrie und Coulometrie bei kontrolliertem Potential untersucht. Oberhalb pH 6 wird ein Komplex mit einem Kation–Ligand-Verhältnis 1 : 1 gebildet. An Quecksilberelektroden wird der Komplex reversibel zu einem Uran(V)–DTPA-Komplex reduziert. Das Reduktionsprodukt ist instabil und disproportioniert zu Uran(VI) und Uran(IV). Bei pH-Werten unterhalb 5 wird ein Komplex mit einem Kation–Ligand-Verhältnis 2:1 gebildet. Dieser Komplex wird irreversibel zu Uran(V) reduziert. Die Diffusionsstromkonstanten und das polarographische Verhalten der beiden Komplexe werden beschrieben.

REFERENCES

1 M. J. Cabell, *Analyst*, 77 (1952) 859.
2 R. Hara and P. W. West, *Anal. Chim. Acta*, 12 (1955) 285.
3 G. G. Rao and G. Somidevamma, *Z. Anal. Chem.*, 157 (1957) 27.
4 J. Stary and J. Pasilova, *J. Inorg.Nucl. Chem.*, 17 (1961) 361.
5 D. G. Davis, *Anal. Chem.*, 33 (1961) 492.
6 T. Lai and T. Chang, *Anal. Chem.*, 33 (1961) 1193.
7 T. R. Bhat and M. Krishnamurthy, *J. Inorg. Nucl. Chem.*, 26 (1964) 587.
8 T. Lai and T. Chen, *J. Inorg. Nucl. Chem.*, 29 (1967) 2975.
9 T. Lai and J. Chen, *Anal. Chim. Acta*, 37 (1967) 253.
10 J. J. R. Frausto DaSilva and M. L. S. Simoes, *Talanta*, 15 (1968) 609.
11 T. Lai and S. Lee, *Anal. Chem.*, 41 (1969) 1316.
12 B. C. Baker and D. T. Sawyer, *Inorg. Chem.*, 9 (1970) 197.
13 M. Krishnamurthy and K. B. Morris, *Inorg. Chem.*, 8 (1969) 2620.
14 T. T. Lai and C. Kao, *Anal. Chim. Acta*, 54 (1971) 521.
15 L. M. Razbitnaya and I. A. Korovina, *Radiokhim.*, 3 (1961) 593.
16 L. M. Razbitnaya, *Radiokhim.*, 6 (1964) 202.
17 A. D. Goolsby and D. T. Sawyer, *Anal. Chem.*, 39 (1967) 411.
18 E. Jacobsen and G. Kalland, *Talanta*, 11 (1964) 139.
19 E. Jacobsen and G. Kalland, *Anal. Chim. Acta*, 30 (1964) 240.
20 R. S. Nicholson and I. Shain, *Anal. Chem.*, 36 (1964) 706.

Analytica Chimica Acta
Elsevier Publishing Company, Amsterdam
Printed in The Netherlands

POLAROGRAPHIC MAXIMA OF THE FIRST KIND: CHARACTERISTICS IN ABSENCE OF RESISTANCE-CONTROLLED CURRENTS

F. M. HAWKRIDGE*, T. W. HOLT** AND H. H. BAUER
Department of Chemistry, University of Kentucky, Lexington, Ky. 40506 (U.S.A.)

(Received 22nd July 1971)

A large part of the polarographic literature is devoted to, or mentions, the phenomena described as polarographic maxima. In the case of maxima of the first kind, it has long been recognized that the resistance of the polarographic circuit has a profound effect on the nature of the results; the current on the rising portion of the wave is, in fact, limited by this resistance and not by the electrode process[1]. Consequently, in order to study the electrode process and how this gives rise to a maximum, one needs to counteract the effect of the circuit resistance. The present note describes some salient features of polarographic maxima of the first kind, observed by means of three-electrode circuitry, under conditions where the current is not resistance-controlled; no previous studies of this sort seem to have appeared in the literature***.

The system for which results are reported here consists of copper(II) in 1 M supporting electrolyte. The two-electrode measurements were made with an external reference electrode and H-type salt bridges, giving a total circuit resistance of the order of 1000 ohms. It is this total resistance (salt bridges, galvanometer and shunt, mercury thread in the capillary) that limited the magnitude of the current, and resistances of this magnitude are commonly present in two-electrode polarographic measurements. Use of a three-electrode arrangement compensates for the circuit resistance with the exception of that due to the mercury thread and to the electrolyte between mercury drop and reference electrode. This residual resistance was not high enough to be current-limiting in the case reported here, as evidenced by the absence of a current region showing Ohm's law behavior. In other cases, however, it might be necessary to use additional positive feedback to overcome the uncompensated resistance: *e.g.*, in studies of maxima in dilute electrolytes (for example, the oxygen maximum is most pronounced in dilute electrolytes—less than 10^{-2} M potassium chloride—and here the electrolyte resistance can become significant; work on the latter system is in progress).

EXPERIMENTAL

Apparatus

The potentiostat used for the work done in lithium nitrate was constructed in

---

* Present address: Department of Chemistry, Case Western Reserve University, Cleveland, Ohio 44106, U.S.A.

** Present address: Tobacco and Health Research Institute, University of Kentucky, Lexington, Ky. 40506, U.S.A.

*** However, such observations have certainly been made, albeit not reported[2,3].

this laboratory, the design being based on that of Brown *et al.*[4]. A Hewlett Packard/ Moseley Division Model 7001AM X-Y Recorder was used to record polarograms. A Princeton Applied Research Model 170 Electrochemistry System was used in the work done in sodium sulfate and the current *vs.* time curves were photographed with a Tektronix Inc. Oscilloscope Camera C-12 from a Tektronix Inc. Type 502A Dual-Beam Oscilloscope. The current *vs.* E(measured) polarograms were obtained with a Ballantine Model 355 a.c.–d.c. Digital Voltmeter.

Procedure

All solutions were de-aerated with prepurified nitrogen for 15 min before measurement and were thermostated at $25 \pm 0.1°$. Temperature control was accomplished by circulating water from a temperature bath through a jacketed cell. Two salt bridges, made from the supporting electrolyte and either a 4% agar solution or paper pulp, were used with an intermediate cell containing the electrolyte to isolate the SCE from the electrochemical cell. A platinum gauze electrode and a mercury pool were used as the auxiliary electrode for the lithium nitrate and sodium sulfate systems, respectively. The half-cell potential values were obtained by measuring the potential difference between the working electrode and a second reference electrode.

Reagents

Reagent-grade chemicals were used in all cases without further purification; mercury used in the dropping mercury electrode was triply distilled (Bethlehem Instrument Co.).

Shape of the maximum

Maxima of the first kind are said to be typically acute[5], the current increasing linearly with applied potential until at a certain value the current decreases sharply to its diffusion-controlled value (*cf.* Fig. 1, curve A). The magnitude of the current on the rising part of the maximum is limited by the resistance of the circuit. Thus, the increasing voltage applied between the working and reference electrodes in a two-electrode system produces an increase in the ohmic drop in the circuit, but almost no change in the half-cell potential of the working electrode. This fact can be demonstrated by using a second reference electrode and monitoring the voltage between this electrode and the working electrode; a plot of current as a function of the half-cell potential of the working electrode then has the form shown in Fig. 1 (curve B). (The fact that the electrode potential changes but little during the rising portion of an acute maximum was inferred originally by Heyrovsky[6] on the basis of measurements of interfacial tension.)

It can be seen that no information has been obtained regarding the current at potentials of the working electrode over a range of about 370 mV (from *ca.* -80 mV to -450 mV). This results from the use of two-electrode apparatus; during the rise of the maximum, most of the applied voltage appears as ohmic drop. When the current falls to the diffusion-controlled value, the ohmic drop decreases and most of the applied voltage is effective in controlling the potential of the working electrode. Thus, as the current falls abruptly at a certain value of the applied voltage, the potential of the working electrode jumps, by about 400 mV in the system shown in Fig. 1.

The system can, however, be studied at all potentials if an instrument is used

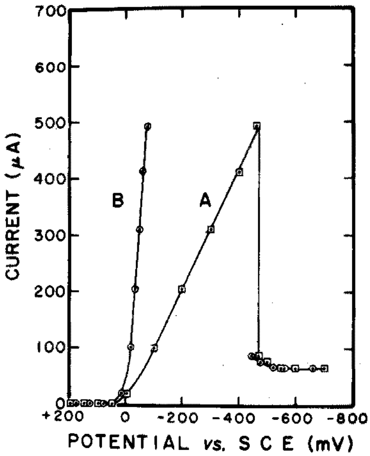

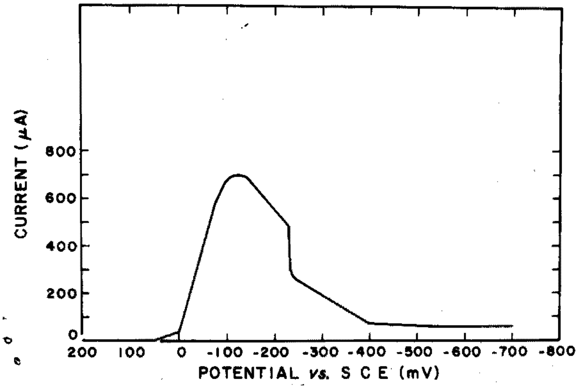

Fig. 1. Acute maximum obtained with two-electrode apparatus. (A) Current *vs.* applied potential (□); (B) current *vs.* electrode potential measured against a separate reference electrode (SCE) (⊙). Reduction of copper (II) ($8\cdot10^{-3}$ *M*) in 1 *M* Na_2SO_4; $m^{2/3}t^{1/6}=2.592$ mg$^{2/3}$sec$^{1/6}$, $t=2.72$ sec.

Fig. 2. Maximum obtained with three-electrode circuit (automatic compensation for ohmic drop) for same system as in Fig. 1.

that makes the ohmic drop sufficiently small. Figure 2 shows the polarographic wave obtained with such an instrument, again for the same system as described by Fig. 1. It is evident that the current is not resistance-controlled; the maximum is rounded, not acute, although the current does drop abruptly on the cathodic side of the maximum. Obviously, information is available about the magnitude of the current at all potentials of the working electrode.

Thus, the criterion that maxima of the first kind are typically acute in shape is based on observations that actually describe only an experimental artefact, *viz.* that circuit resistance is large enough to limit the flow of current and to obscure the nature of the electrode reaction.

Current-vs.-time behavior

On acute maxima (Fig. 1, curve A), the current varies with time in a characteristic manner (Fig. 3) that has been reported by a number of workers. With three-electrode circuitry, the curves do not have the shape of Fig. 3; rather, they are as shown in Fig. 4. The curves previously reported (*cf.* Fig. 3) reflect the changing ohmic drop. (A comprehensive discussion of current-*vs.*-time behavior at polarographic maxima will be published elsewhere.)

Onset of the maximum

It is usually said that maxima of the first kind appear on the rising portion of the polarographic wave. It is not easy to determine from curves such as Fig. 1, however, where the curve begins to change from diffusion-controlled to resistance-controlled. On the other hand, polarograms obtained with a three-electrode potentiostat circuit show, at least under some conditions, a segment of a diffusion-controlled polarographic step (anodic to *ca.* +0.005 V, Fig. 5), followed by maximum formation

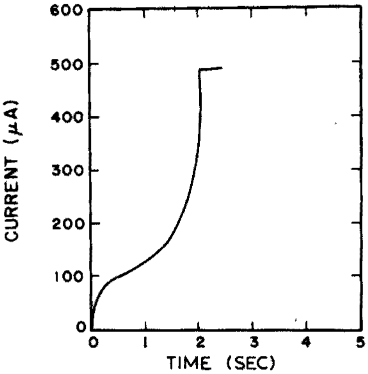

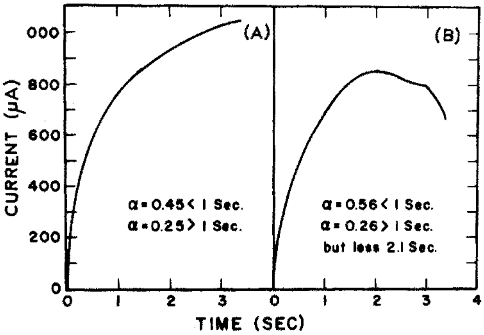

Fig. 3. Current *vs.* time curve for same system as in Fig. 1 at applied potential of −460 mV *vs.* SCE (on the peak of the maximum; measured electrode potential, −28.2 mV).

Fig. 4. Current *vs.* time curves corresponding to polarogram in Fig. 2. (A) On the anodic rise of the maximum (−200 mV), (B) on the cathodic side (−300 mV). In the early part of drop life, current increases with time to the power of 0.4–0.6 under various conditions, and the current increases more slowly later in drop growth.

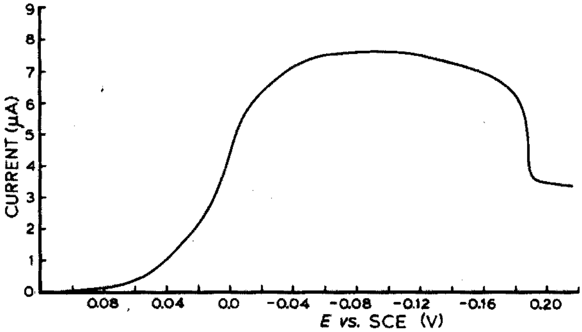

Fig. 5. Polarogram of $1.25 \cdot 10^{-3}$ *M* copper(II) in 0.9 *M* lithium nitrate, pH 1; three-electrode circuit, $m^{2/3}t^{1/6} = 0.95$ mg$^{2/3}$sec$^{1/6}$. Note the inflection point at *ca.* 0.005 V *vs.* SCE.

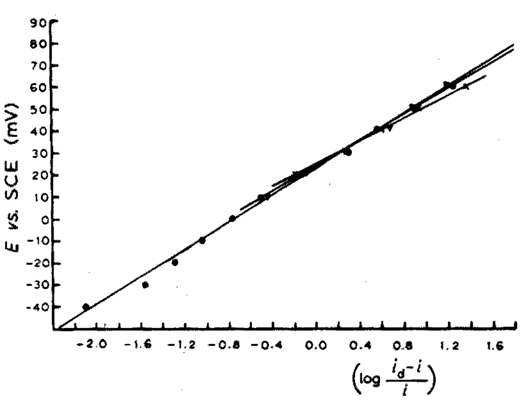

Fig. 6. Log-plots for system shown in Fig. 5 except: (●) $0.50 \cdot 10^{-3}$ *M* Cu(II); (▲) $1.25 \cdot 10^{-3}$ *M* Cu(II); (×) $1.75 \cdot 10^{-3}$ *M* Cu(II). For potentials anodic to *ca.* 0.00 V, the value of *n* is 2.06 ± 0.05.

at more negative potentials beyond the maximum. The curve shows a well-defined inflection point (*ca.* +0.005 V, Fig. 5) when the maximum begins on the rising portion of the polarogram.

The fact that the current is diffusion-controlled at potentials anodic to the inflection point is demonstrated by the fact that this portion of the curve follows the Heyrovsky-Ilkovič equation; logarithmic plots are shown in Fig. 6. Moreover, the current-*vs.*-time curves follow the Ilkovič equation here, but not at potentials cathodic to the inflection point. (The slope of a plot of log *i* *vs.* log *t* was found to be 0.20 ± 0.01 for the system described in Fig. 5 at potentials anodic to the inflection point indicating diffusion-control.)

The dependence of the potential of the inflection point on the concentration of depolarizer and on other experimental variables is the subject of further investigation.

This work was supported by the U.S. Army through the Themis contract DAABO7-69-C-0366. The work had been initiated with the help of a grant from the National Science Foundation. We are grateful to Dr. D. Britz for the construction of the potentiostat.

SUMMARY

Characteristics of polarographic maxima, studied by means of three-electrode circuitry, are described. There are major differences as compared with results obtained with two-electrode circuits; the literature on this subject has hitherto been restricted to studies in the latter category.

RÉSUMÉ

Une étude est effectuée sur les caractéristiques des maxima polarographiques, à l'aide d'un circuit à 3 électrodes. On remarque des différences importantes avec les résultats obtenus au moyen d'un circuit à deux électrodes. C'est à cette dernière catégorie que se limite la littérature sur ce sujet.

ZUSAMMENFASSUNG

Die Merkmale polarographischer Maxima, die mit einer Drei-Elektroden-Schaltung untersucht worden sind, werden beschrieben. Es sind grössere Unterschiede im Vergleich mit Ergebnissen vorhanden, die mit Zwei-Elektroden-Schaltungen erhalten worden sind; die Literatur auf diesem Gebiet beschränkte sich bisher auf Untersuchungen der letzteren Kategorie.

REFERENCES

1 J. J. LINGANE, *J. Amer. Chem. Soc.*, 62 (1940) 1665.
2 P. STURROCK, personal communication.
3 R. N. O'BRIEN, personal communication.
4 E. R. BROWN, D. E. SMITH AND G. L. BOOMAN, *Anal. Chem.*, 40 (1968) 1411.
5 J. HEYROVSKY AND J. KŮTA, *Principles of Polarography*, Academic Press, New York, 1966, pp. 429–63.
6 J. HEYROVSKY, *Actualités Scientifiques et Industrielles*, No. 90, Paris, 1934 (quoted in I. M. KOLTHOFF AND J. J. LINGANE, *Polarography*, 2nd Edn., Interscience, New York, 1952, pp. 156–188).

Analytica Chimica Acta
Elsevier Publishing Company, Amsterdam
Printed in The Netherlands

ELECTROCHEMICAL DETERMINATION OF DIFFUSION COEFFICIENTS OF SELECTED METALS IN DIMETHYLSULFOXIDE

JERRY L. JONES* AND HERBERT A. FRITSCHE, JR.**
Department of Chemistry, Texas A&M University, College Station, Texas 77840 (U.S.A.)

(Received 1st July 1971)

Numerous electrochemical investigations have been made in non-aqueous solvents. In such studies the diffusion coefficient can be of value in determining the nature of the diffusing species and the extent of the depolarizer–solvent interaction. However, only limited ionic or molecular diffusion coefficient data in non-aqueous systems are available.

In an earlier publication[1], a method was presented for the determination of ionic diffusion coefficients in aqueous solution. Excellent agreement between calculated diffusion coefficients and tracer diffusion coefficients was obtained. This investigation extends the method to a non-aqueous system and diffusion coefficients of lead, zinc, thallium and gadolinium in dimethylsulfoxide (DMSO) are reported. Gadolinium was selected for study to demonstrate the feasibility of performing electrochemical studies of the lanthanide elements in DMSO.

THEORY

Diffusion coefficients

The calculation of ionic diffusion coefficients from the complete Koutecky equation and instantaneous current data was demonstrated earlier[1]. It was pointed out that agreement between experimental instantaneous currents and theoretical currents predicted by the Koutecky equation could be expected only if the experimental parameters were carefully adjusted to satisfy the assumptions made in the derivation of the current equation. Non-aqueous systems require the same considerations. Diffusion control is accomplished as it is in aqueous systems. Current measurements at the end of the drop life insure the absence of capillary shielding effects, and measurement only on the first drop formed after application of the electrolysis voltage eliminates concentration polarization effects. For each capillary and each depolarizer solution, the influence of the flow rate on the diffusion coefficient must be determined. If the value of the diffusion coefficient varies with the mercury flow rate, then the capillary parameters must be adjusted to minimize the effect of back-pressure, so that it becomes negligible or is within the normal error of the polarographic measurement[2].

---

* Current address and address for reprint requests: Department of Chemistry, Central Washington State College, Ellensburg, Wash. 98926, U.S.A.

** Current address: Department of Clinical Pathology, M. D. Anderson Hospital and Tumor Institute, University of Texas at Houston, Houston, Texas 77025, U.S.A.

Gadolinium

Electrochemical investigations of the lanthanides in aqueous solution are complicated by the acidic nature of these elements. Interfering hydrolytic reactions produce undefined aquo-complexed or hydroxylated species and hydrogen gas production masks further electrochemical reduction of the lanthanides[3]. A number of non-aqueous systems have been investigated to find solvents which will yield solvated lanthanide species of reproducible composition without producing electrochemically active byproducts[4-7].

Gutmann *et al.*[8] have reported the polarography of gadolinium and other anhydrous lanthanide chlorides in DMSO and dimethylformamide. Europium, samarium and ytterbium gave two waves while all others gave one wave. Only the second waves of europium, samarium and ytterbium were reversible while all other reductions were irreversible. All reductions were diffusion-controlled. Maxima were not encountered in either solvent. The number of electrons involved in each electrochemical reduction was determined and metal amalgamation in all cases was verified. The effect of traces of water was reported to be negligible.

EXPERIMENTAL

Reagents

Triply distilled mercury and prepurified nitrogen were used without further purification. Reagent-grade DMSO was dried with molecular sieve (Linde 5A). Reagent-grade potassium perchlorate was used without further purification. Tetrabutylammonium perchlorate was prepared by reaction of the organic iodide with sodium perchlorate. The product was washed several times and dried at 60°[9].

Lead and thallium nitrates were dried for 6 h at 130°. Zinc nitrate was dried over phosphorus pentoxide for several days. Titrimetric determinations of the weighed salts in aqueous solution verified the absence of significant absorbed water. Standard solutions of these salts in DMSO were prepared directly by weighing.

Gadolinium chloride was obtained from Alfa Inorganics, Inc. The anhydrous salt was prepared by a modification of the method of Young and Hastings[10], and dissolved in DMSO and the metal content was determined by back-titration of excess EDTA with a standard zinc solution[11].

Apparatus

Instrumentation used for the recording of conventional polarograms and instantaneous current measurements was described earlier[1]. A Sargent capillary (2–5 sec drop time) was used. The radius of the capillary was $3.26 \cdot 10^{-3}$ cm as determined from drop weight data. Chronoamperometric investigations were made with a Model FS Polarograph and IR Compensator (E. H. Sargent Co.). A hanging mercury drop electrode (H.M.D.E.) was used as the working electrode and has been described earlier[12]. The usual drop area was 0.0540 cm^2.

Diffusion coefficient measurements

Conventional polarograms of the inorganic ion in DMSO were obtained first. Then a point on the plateau of the wave was selected for the determination of maximum currents on single drops[1]. The mercury flow rate was adjusted so that back-pressure influence was negligible. Maxima of the second kind, caused by excessive flow rates, were generally not present. The instantaneous maximum current was measured at the end of the drop life and the experimental data substituted into the complete Koutecky equation. The equation was solved for the diffusion coefficient by means of an iterative computer technique.

Gadolinium

The polarographic behavior of gadolinium in DMSO was further investigated using the technique of chronoamperometry with potentiostatic control of the working electrode. The electrochemical measurements were made under nearly anhydrous conditions and included the determination of the diffusion coefficient, the polarographic half-wave potential, the chronoamperometric peak potential and tests for diffusion-controlled electrochemical reactions and for electrochemical reversibility.

RESULTS AND DISCUSSION

Diffusion coefficients

The polarographic diffusion coefficients of lead(II), zinc(II) and thallium(I) were determined in DMSO with 0.100 *M* potassium perchlorate as supporting electrolyte. No attempt was made to do these determinations under completely anhydrous conditions since 8 drops of aqueous 0.1% gelatin solution were added to remove maxima of the first kind on the wave front. The water content was not greater than 1% after the addition of gelatin, as determined by Karl Fischer titrations. Maxima on the wave front could not be suppressed in the case of zinc but the limiting current plateau was well formed. The results of this study are given in Table I. The diffusion coefficients of these ions were much smaller in DMSO than in water. This is probably due to the higher viscosity of the dimethylsulfoxide and the fact that a larger, solvated cation exists in DMSO solutions[13].

TABLE I

POLAROGRAPHIC DIFFUSION COEFFICIENTS IN DIMETHYLSULFOXIDE[a]

Ion	*Concentration (mM)*	t_d *(sec)*	$\bar{m}$ *(mg sec^{-1})*	i_d *(μA)*	*Diff. coef.*[b] *(· 10^6)*
Pb(II)	1.047	7.50	0.952	3.32	2.36
Tl(I)	1.152	7.46	0.958	2.65	4.59
Zn(II)	1.047	6.35	0.957	3.18	2.26

[a] In the presence of gelatin and 0.100 *M* potassium perchlorate supporting electrolyte. Average of 6 measurements on first drops.
[b] ±2% of the reported value.

Butler[13] and Hamm *et al.*[14] have calculated approximate diffusion coefficients of these ions in DMSO from conventional polarographic diffusion current data and the Ilkovic equation. The diffusion coefficients determined in this study are compared to those given by Butler and Hamm in Table II and they were smaller than those given by Hamm but larger than those reported by Butler. In the earlier studies the

TABLE II

COMPARISON OF DIFFUSION COEFFICIENT DATA IN DIMETHYLSULFOXIDE[a]

Ion	*Diffusion coefficient* $\cdot 10^{-6}$	*Reference*[b]
Pb(II)	2.3	13
	2.36	
Zn(II)	5.4	13
	1.56	14
	2.26	
Tl(I)	3.56	14
	4.59	

[a] Supporting electrolyte was 0.100 *M* potassium perchlorate.
[b] Values without references were those determined in this study.

corrections for spherical diffusion, the back-pressure effect and the depletion effect were not considered. The lack of agreement between the data of Butler and those of Hamm may be due to several factors. First, maxima may not have been completely removed in all cases. It was noted in this study, for example, that maxima of the first kind in the case of zinc(II) could not be completely suppressed. Since some maxima are not always reproducible it is possible that a range of experimental diffusion currents would be obtainable.

Second, the diffusion coefficient may be a function of gelatin concentration or water concentration. The size of the diffusing species and hence the value of the diffusion coefficient would be seriously affected if the depolarizer associated with gelatin or water instead of dimethylsulfoxide molecules.

Gadolinium

Polarograms of gadolinium in DMSO were obtained with 0.100 *M* tetrabutylammonium perchlorate as the supporting electrolyte. The waves were well-defined and diffusion-controlled, as shown by the linear dependence of the limiting current on the square root of the height of the mercury column. The half-wave potential was determined to be -2.09 V *vs.* the aqueous saturated calomel electrode (S.C.E.). Gutmann *et al.*[8] reported the half-wave potential to be -2.16 V *vs.* the aqueous S.C.E.; however, a high resistance frit was used to separate the aqueous and non-aqueous cell compartments. This causes unknown liquid junction potentials to be present and makes less practicable comparison of half-wave potentials. Gutmann made only calculated corrections for the IR drop in the solution. It is believed that the potentiostatic control of the working electrode used in this study gives more nearly correct values. Gutmann reported this wave to be an irreversible, 3-electron reduction, which was diffusion-controlled and showed no maxima. Metal amalgamation of gadolinium with a mercury electrode was verified by analysis of gadolinium content in a mercury pool electrode[8].

Electrochemical reversibility tests were performed by plotting the potential of the polarized electrode against the natural logarithm of the current function, $i/(i_d - i)$. The slope of the linear plot was 54 mV. For a reversible, 3-electron reduction the slope should be 20 mV. The chronoamperometric peak potential of gadolinium(III) in DMSO was −2.16 V *vs.* the aqueous S.C.E. The half-wave potential calculated from this value was −2.15 V. The experimentally determined value by the conventional d.c. polarographic method was −2.09 V *vs.* the aqueous S.C.E. The lack of complete agreement between the calculated and the experimental half-wave potentials may be an indication of the presence of a rather slow step in the overall electrochemical reduction. Peak currents were measured as a function of the voltage scan rate. A linear dependence was obtained indicating that the limiting current in the electrochemical reduction of gadolinium in DMSO is diffusion-controlled.

The diffusion coefficient of gadolinium(III) in DMSO was determined and the experimental conditions and results of the determination are given in Table III. Despite the fact that the gadolinium wave was generally well formed, a slight maximum of the second kind was present. Neither an aqueous gelatin solution nor one prepared in DMSO had any effect on this maximum. It could only be removed by decreasing either the radius of the capillary or the height of the mercury column so as to reduce the flow rate of mercury. The value of the diffusion coefficient determined under these conditions was $4.05 \cdot 10^{-5}$ cm^2 sec^{-1}. The value of the diffusion coefficient at infinite dilution in water, determined[15] from conductance data, is $6.0 \cdot 10^{-6}$ cm^2 sec^{-1}. The value determined in this study may be slightly high since the effect of back-pressure could hardly be expected to be negligible under these conditions of low flow rates of mercury. In order to reduce the maximum, the flow rate of mercury had to be reduced to 0.254 mg sec^{-1} but this led to conditions wherein the back-pressure influence may not be negligible. When the diffusion coefficient is calculated from the Koutecky equation for a flow rate which is too low to meet fully the conditions of its derivation, the calculated diffusion coefficient is naturally adjusted upward in magnitude to satisfy the measured current, that is, it must increase slightly to allow for the small and slightly erroneous value of the flow rate.

TABLE III

DIFFUSION COEFFICIENT OF GADOLINIUM(III) IN DMSO[a]

Flow rate:	0.254 mg sec^{-1}
Drop rate:	7.08 sec
Diffusion current:	4.50 μA
Concentration:	0.382 m*M*
Applied potential:	2.10 V *vs.* aqueous S.C.E.
Diffusion coefficient:	$4.05 \cdot 10^{-5}$ cm^2 sec^{-1}

[a] The diffusion coefficient is the average of 6 diffusion current measurements on first drops and the reported value has an average deviation of ±2%.

The small maximum encountered at all except the lowest flow rates of mercury may not be the only source of difficulty since the use of an agar plug in the Luggin capillary to separate the aqueous and non-aqueous solutions may have also contributed to the high value of the diffusion coefficient. The plug was prepared from water, potassium chloride and agar. It was observed in this study that the plug in the presence of DMSO became useless after about an hour. This observation was based on increased demands placed on the potentiostat in order to compensate for the increased resistance in the plug. This effect could be brought about by the DMSO leaching out the water or potassium chloride or both. Because the plug was not more than 1 mm from the working electrode, the local concentration of water or potassium ions in the vicinity of the electrode could be appreciable. The presence of water may affect the nature of the diffusing gadolinium species by hydrolysis or water may itself be reacting electrochemically, increasing the diffusion current and hence the value of the diffusion coefficient. The presence of small amounts of potassium ion leads to the same results, that is, current enhancement due to the reduction of potassium ions to potassium metal. The presence of these impurities would not affect the determination of the diffusion coefficient of lead(II), zinc(II) or thallium(I) because the half-wave potentials of these ions are much more positive. In these cases, water and potassium ions were not significantly reduced at the potentials chosen for current measurements.

The effect of added water on the polarographic behavior of the gadolinium reduction in DMSO was briefly investigated. Addition of water up to the level of 1% by volume increased the diffusion current slightly. This effect may be due to the electrochemical reduction of water. Addition of water over the 1% level caused an increase in maximum formation and drop irregularity. This was observed by Gutmann *et al.*[8]. It should be noted that Karl Fischer determinations give the bulk water concentration. The local concentration of water at the electrode surface may possibly be higher, owing to leaching of water from the agar plug by the dimethylsulfoxide, or to dielectric saturation at the drop surface because of the very high electric field strength present there.

SUMMARY

Diffusion coefficients of lead, zinc, thallium and gadolinium in dimethylsulfoxide have been measured electrochemically by means of the complete Koutecky equation. Instantaneous currents were measured on first drops from a D.M.E. and calculations were made by an iterative computer technique. Half-wave potentials, polarographic wave reversibility, and diffusion control data are reported.

RÉSUMÉ

Des coefficients de diffusion du plomb, du zinc, du thallium et du gadolinium, dans le diméthylsulfoxide sont déterminés électrochimiquement, à l'aide de l'équation de Koutecky. Les courants instantanés sont mesurés sur les premières gouttes, en effectuant les calculs avec computer. On indique potentiels de demi-vague, réversibilité polarographique et valeurs de diffusion.

ZUSAMMENFASSUNG

Die Diffusionskoeffizienten von Blei, Zink, Thallium und Gadolinium in Dimethylsulfoxid wurden elektrochemisch unter Anwendung der vollständigen Koutecky-Gleichung ermittelt. Die Momentanströme wurden bei den ersten Tropfen aus einer tropfenden Quecksilberelektrode gemessen und die Berechnungen nach einem iterativen Computer-Verfahren ausgeführt. Halbwellenpotentiale, Reversibilität der polarographischen Wellen und Diffusionskontrolldaten werden vorgelegt.

REFERENCES

1 J. L. JONES AND H. A. FRITSCHE, *Anal. Chim. Acta*, 56 (1971) 97.
2 J. HEYROVSKY AND J. KUTA, *Principles of Polarography*, Academic Press, New York, 1966, p. 96.
3 T. MOELLER, *Chemistry of the Lanthanides*, Reinhold, New York, 1963, p. 39.
4 E. COKAL AND E. WISE, *J. Electroanal. Chem.*, 11 (1966) 406.
5 J. COETZEE AND W. SIAO, *Inorg. Chem.*, 2 (1963) 14.
6 J. GAUR AND K. ZUTSHI, *J. Electroanal. Chem.*, 11 (1966) 390.
7 L. HALL AND D. FLANIGAN, *Anal. Chem.*, 35 (1963) 2108.
8 G. GRITZNER, V. GUTMANN AND G. SCHOBER, *Monatsh. Chem.*, 96 (1965) 1056.
9 I. M. KOLTHOFF AND J. COETZEE, *J. Amer. Chem. Soc.*, 79 (1957) 870.
10 R. YOUNG AND J. HASTINGS, *J. Amer. Chem. Soc.*, 59 (1937) 765.
11 H. FLASCHKA, *Mikrochim. Acta*, (1955) 55.
12 J. JONES AND H. FRITSCHE, *J. Electroanal. Chem.*, 12 (1966) 334.
13 J. BUTLER, *J. Electroanal. Chem.*, 14 (1967) 89.
14 E. JOHNSON, K. POOL AND R. HAMM, *Anal. Chem.*, 39 (1967) 888.
15 A. PURUSHOTTAM AND B. RAO, *Anal. Chim. Acta*, 12 (1955) 589.

Analytica Chimica Acta
Elsevier Publishing Company, Amsterdam
Printed in The Netherlands

SHORT COMMUNICATIONS

Rapid determination of selenium by atomic absorption spectrophotometry

There is an ever-increasing need for rapid methods for determining selenium in geological and biological samples in connection with mineral exploration programs. To some extent existing methods are not entirely suitable for this purpose since they seldom combine the main requirements of speed, reliability and adequate sensitivity. A suitable method should allow the determination of at least 0.1 p.p.m. selenium and have an output of at least fifty samples per day.

Watkinson[1] has summarized the analytical chemistry of selenium. The most suitable methods for determining selenium in the p.p.m. range are X-ray fluorescence (Loftus-Hills *et al.*[2]—limit of detection, 15 p.p.m.), atomic absorption (Allan[3]—limit of detection, 0.5 p.p.m. with conventional burner and 0.015 with the flame-in-tube method), atomic fluorescence (Dagnall *et al.*[4]—limit of detection, 0.1 p.p.m.) and colorimetry (Stanton and McDonald[5]—limit of detection 0.1 p.p.m.). The atomic absorption and atomic fluorescence methods suffer from the disadvantage that the limits of detection are for aqueous solutions prepared from an original solid specimen so that when concentrations are referred to the dry weight of sample, limits of detection become at least an order of magnitude poorer. Atomic absorption and atomic fluorescence methods also suffer from scattering problems particularly at low wavelengths, so that the direct determination of selenium is seldom possible without a prior separation technique.

This paper reports a method developed for determining selenium at low levels in geological and biological samples. It involves dissolution of the sample, coprecipitation of selenium with arsenic, redissolution of the precipitation in a small volume of nitric acid and the subsequent determination of selenium by conventional atomic absorption.

This method incorporates the classical separation of selenium described by Luke[6] and has been employed as a preliminary stage of other methods developed by Cousins[7], Allaway and Cary[8], and Stanton and McDonald[5].

Experimental

Apparatus. The atomic absorption measurements were carried out with a Techtron AA5 atomic absorption spectrophotometer under the conditions listed below.

Source: ASL hollow-cathode lamp
Lamp current: 6 mA
Wavelength: 196.0 nm
Slit width: 0.30 mm
Burner: standard 10-cm laminar burner
Gas mixture: nitrogen, flow rate 7.5 scale units (15 lb. in^{-2} pressure); hydrogen, flow rate 3.5 scale units (3.5 lb. in^{-2} pressure)
Scale expansion, $\frac{3}{4}$ of full scale.

Reagents. Arsenic solution. Dissolve 250 mg of arsenic trioxide and 2 g of sodium hydroxide in water and dilute to 200 ml.

Standard selenium solution. Dissolve 50 mg of selenium in 10 ml of concentrated nitric acid (s.g. 1.42), boil gently to remove fumes of nitrogen dioxide, cool and dilute to 500 ml with water (100 p.p.m. Se).

Method

Digestion of the sample. Digest 1-g samples of vegetation, soil, rock, gossan or sulphide ore in 50-ml squat beakers with 20 ml of a (4+1) mixture of nitric acid (s.g. 1.42; A.R.) and perchloric acid (60%; A.R.). Digest very slowly for about 8 h until white fumes of perchloric acid become visible. If no organic matter is present, an alternative digestion involves adding 15 ml of (1+1) nitric–hydrofluoric acids to the sample contained in a polypropylene beaker and taking to dryness over a waterbath for 3–4 h.

Separation of selenium. Leach the residue with 20 ml of hot 6 *M* hydrochloric acid for 15 min and then transfer the mixtures to 50-ml centrifuge tubes. Centrifuge the samples for 3 min and decant each supernatant layer into another 50-ml centrifuge tube. Discard the residues. Add 2 ml of arsenic solution to each tube, mix, and add 5 ml of aqueous 50% (w/v) hypophosphorous acid solution. Place the tubes for 15 min in a hot waterbath (80°), then cool and allow to stand for at least 8 h to allow complete flocculation of the arsenic precipitate.

Remove the supernatant liquid completely by means of suction applied via an extruded thin glass tube. Wash the precipitate with 10 ml of 6 *M* hydrochloric acid, centrifuge the mixture and remove the supernatant phase as before. Redissolve the residue in 2 ml of 2 *M* nitric acid. For large quantities of selenium (>100 μg), add more nitric acid until dissolution is complete.

Atomic absorption determination of selenium. For routine samples, standards comprised 1, 5 and 10 p.p.m. selenium in 2 *M* nitric acid. For higher concentration of selenium, standards containing 10, 20, 50 and 100 p.p.m. were used. Beer's law was obeyed up to 10 p.p.m. Under the optimal instrumental conditions, a solution containing 50 p.p.m. selenium gave a meter deflection of 60% for the absorbance mode when no scale expansion was used.

Results and discussion

Recovery of selenium. Experiments were carried out to determine the relationships between the amount of arsenic added and the recovery of added selenium. Recovery of 1–2000 μg of selenium was complete when 2 ml of arsenic solution (*ca.* 1800 μg As) was used for the separation procedure. However, recoveries were only of the order of 75% when settling times shorter than 8 h were used. Recovery tests were carried out on a number of soil samples of known composition and with non-detectable amounts of selenium. Full recovery of selenium was achieved even when iron was present in high concentrations.

Method of digestion. No detectable difference in selenium levels was noted for 100 samples digested by either perchloric–nitric or hydrofluoric–nitric methods of attack. The latter procedure is preferable when no organic matter is present, because of hazards attendant on mixing perchloric acid with hypophosphorous acid.

Reproducibility and accuracy of the method. Table I summarizes analytical data

TABLE I

ANALYTICAL DATA FOR REPLICATE DETERMINATIONS OF SELENIUM IN SIX ROCK SAMPLES

Sample[a]	*No. of determinations*	*Mean concn. Se (p.p.m.)*	*Range*	*Coeff. of variation (%)*
1	12	4700	4000–4900	± 6.1
2	7	156	140–168	± 6.3
3	16	62	56–65	± 4.5
CAAS sulfide ore[9]	12	20.6	18.0–22.0	± 6.3
5	8	10.5	10.2–11.0	± 2.3
6	6	1.1	1.0–1.2	±10.0

[a] Samples 1–3, 5 and 6 are rock chip and ore samples from the seleniferous Yellow Cat Area, Utah. Samples by courtesy of H. L. Cannon and the U.S. Geological Survey.

for selenium in the standard sulphide ore (Webber[9]) and for replicates of five other selected samples chosen for their variable range of selenium concentrations. Coefficients of variation reported for each sample show that the reproducibility is more than adequate for geochemical prospecting.

Limit of detection. If the limit of detection is defined as a signal equal to twice the noise level, the method appears to have a detection limit of about 0.1 p.p.m. selenium when a conventional burner is used. This should be improved considerably by using the flame-in-tube method (Allan[2]).

Conclusions

It is concluded that the method has the required rapidity, reproducibility, and sensitivity for geochemical prospecting. For vegetation samples containing background selenium levels (*i.e.* 0.05 p.p.m. dry weight), the flame-in-tube method would have to be used for the atomic absorption part of this procedure.

Department of Chemistry and Biochemistry,
Massey University,
Palmerston North (New Zealand)

B. C. Severne
R. R. Brooks

1 J. H. Watkinson, *Selenium in Biomedicine*, Avie Publishers, Westport, Conn., 1967.
2 G. D. Loftus-Hills, D. I. Groves and M. Solomon, *Proc. Australasian Inst. Mining Met.*, 232 (1969) 55.
3 J. E. Allan, *Proc. Fourth Australian Spectrosc. Conf., Canberra, 1963.*
4 R. M. Dagnall, K. C. Thompson and T. S. West, *Talanta*, 14 (1967) 557.
5 R. E. Stanton and A. J. McDonald, *Analyst*, 90 (1965) 497.
6 C. L. Luke, *Anal. Chem.*, 31 (1959) 572.
7 F. B. Cousins, *Australian J. Exptl. Biol. Med. Sci.*, 38 (1960) 11.
8 W. K. Allaway and E. E. Cary, *Anal. Chem.*, 36 (1964) 1359.
9 G. R. Webber, *Geochim. Cosmochim. Acta*, 29 (1965) 229.

(Received 22nd July 1971)

Analytica Chimica Acta
Elsevier Publishing Company, Amsterdam
Printed in The Netherlands

Spectrophotometric determination of trace amounts of selenium in iron and steel with 4-methyl-*o*-phenylenediamine*

Because of the interest in the determination of selenium in metals and the importance of selenium in biological materials, various methods have been reported for selenium determinations. The determination of trace amounts of selenium is generally based either on the reduction of selenium(IV) to elementary selenium or the measurement of piazselenols formed by the reaction of selenous acid with aromatic *o*-diamines[1]. Reduction procedures are however laborious, time-consuming and relatively insensitive. 3,3′-Diaminobenzidine, introduced first by Hoste[2] and Hoste and Gillis[3], has been widely used because of its sensitivity and selectivity for selenium. In establishing a still more sensitive reagent, Parker and Harvey[4] have proposed 2,3-diaminonaphthalene as an excellent fluorimetric reagent for selenium. Toei *et al.*[5] and some others[6-9] have also proposed *o*-phenylenediamine and some 4-substituted *o*-phenylenediamines. Tanaka and Kawashima[10] have presented a critical study of 4-methyl-, 4-chloro- and 4-nitro-*o*-phenylenediamine as spectrophotometric reagents for selenium, 5-substituted piazselenols being formed.

For the determination of selenium in iron and stainless steel, several authors have reported various methods[11-16]. Cheng[12] and Clarke[16] have reported methods with 3,3′-diaminobenzidine involving masking of iron with EDTA, and with 2,3-diaminonaphthalene involving reduction of iron(III) to iron(II) with hydroxylammonium chloride, respectively; but for selenium contents of 0.01% or less, it is preferable to separate iron[15]. For this purpose, Kammori and Ono[13] have presented a method involving extraction of iron with methyl isobutyl ketone, but this method is unsatisfactory because of partial extraction of selenium with the iron. Tanaka *et al.*[17] have reported the extraction of iron(III) caprate with organic solvents and suggested the use of capric acid in the separation of iron from selenium[18].

In the present communication, a method of determination of selenium in iron and stainless steel is described which utilizes 4-methyl-*o*-phenylenediamine after extraction of iron(III) caprate with chloroform.

Apparatus

Hitachi Perkin-Elmer Model 139 u.v.–vis. spectrophotometer; Horiba Model F-5 pH meter.

Reagents

Stock selenium solution (1 *mg Se ml*$^{-1}$). Dissolve 2.2 g of anhydrous sodium selenite in 1 l of 0.1 *M* hydrochloric acid. Standardize the solution iodimetrically. Prepare a working solution (1.0 μg Se ml^{-1}) by suitable dilution of the stock solution with 0.1 *M* hydrochloric acid.

*4-Methyl-*o*-phenylenediamine hydrochloride solution.* The commercial product (Tokyo Chemical Industry Co., Ltd., Japan) is purified by recrystallization as described previously[10]. Prepare an aqueous 1% (w/v) solution freshly before use.

---

* Presented at the 19th Annual Meeting of the Japan Society for Analytical Chemistry, Nagoya, on 14th October, 1970.

1 M Capric acid–chloroform solution. Dissolve *ca.* 43 g of *n*-capric acid (Wako Pure Chemical Co., Ltd., Osaka, Japan) in 250 ml of chloroform.

2% Oxine solution. Dissolve 2 g of oxine in 5 ml of glacial acetic acid and dilute to 100 ml with water.

Extra-pure toluene was once distilled. Extra-pure chloroform was used without further purification. All other reagents used were of analytical grade.

Recommended procedure

Dissolve 0.1–0.3 g of sample (for 0.02–0.005 %Se) in a 200-ml conical beaker, in 20 ml of nitric acid (1 + 1) for iron, or in 3–4 ml of nitric and hydrochloric acid and water mixture (1 + 2 + 3) for steel, adding a further 20 ml of nitric acid (1 + 1) to the latter sample. When dissolution of the sample is complete, add 2–3 ml of 60% perchloric acid and heat gently on a hot plate. Evaporate to fumes and allow to fume gently for 10–20 min. Cool and add a few drops of 3% hydrogen peroxide to the cooled solution in order to reduce chromium(VI) to chromium(III). Transfer the solution to a 100-ml beaker. (For samples with selenium contents above 0.02%, dilute the prepared sample solution to 100 ml with 0.1 *M* hydrochloric acid in a volumetric flask, and take a suitable aliquot for the subsequent procedure.)

Add 3 ml of 1 *M* acetic acid and adjust the pH to 4.7–5 with 25% sodium acetate (pH meter). Transfer the solution to a 150-ml separatory funnel. Extract iron(III) twice with about 10 ml of capric acid in chloroform. Add 3 ml of 2% oxine solution to the aqueous solution and extract metal oxinates (molybdenum(VI), tungsten(VI), vanadium(V), etc.) with chloroform. Wash all the organic phases once with 5 ml of acetate buffer solution (pH 4.7–5). Combine the aqueous solutions and then wash the solution successively with choroform and toluene. Adjust the pH of the aqueous solution to 1.5–2.0 with 6 *M* hydrochloric acid (pH meter). Add 2–3 drops of 3% hydrogen peroxide, 1 ml of 0.25 *M* EDTA and 1 ml of 1% 4-methyl-*o*-phenylenediamine. After standing for 2 h at room temperature, extract the 5-methylpiazselenol formed with exactly 10 ml of toluene, the funnel being shaken for 10 min on a shaker. After the separation of the two phases, wash the toluene phase once with 0.1 *M* hydrochloric acid. Measure the absorbance of the toluene extract at 337 nm with toluene as reference.

Results and discussion

All the piazselenols previously studied[10] can be easily extracted with toluene. The absorption maxima and distribution ratios in toluene have been given previously[10]. 4-Methyl-*o*-phenylenediamine was selected as the reagent for this study because of its stability and smaller susceptibility to interferences. It was confirmed that the time required for full color development was about 2 h at 25° whereas 5 min of heating at 70° sufficed, and that constant absorbance was achieved when extraction was done in the pH range 1–2.5.

When the recommended procedure including the extraction of iron(III) with capric acid was followed, rectilinear calibration curves were found over the range 1–40 μg of selenium(IV) per 10 ml of toluene. There was no significant difference in the calibration curves obtained when 200 mg of iron(III) was added to all solutions.

Effect of diverse ions. The effect of higher concentrations of diverse ions than in the previous study[10] was examined. For this investigation, the diverse ion was added

TABLE I

EFFECT OF DIVERSE IONS
(19.7 μg of selenium at pH 1.7)

Diverse ion	*Added (mg)*	*Absorbance*	*Diverse ion*	*Added (mg)*	*Absorbance*
—	—	0.425	Fe(III)	10	0.070
—	—	0.424		50	0.062
				50[b2]	0.427
Cr(III)	50	0.423		50[c]	0.410
	100	0.416		200[c]	0.410
	200	0.399		300[c]	0.421
	300	0.366		400[c]	0.398
			Mo(VI)	500[c]	0.409
Cr(VI)	10	1.046		10	0.237
	10[a]	0.420		10[b1]	0.427
	40[a]	0.424	Te(IV)	5	0.430
			V(V)	2	0.434
Cu(II)	10	0.430		5	0.469
	20	0.471		5[b1]	0.440
	20[b1]	0.430	W(VI)	10	0.237
	50	0.457		10[b3]	0.424
	50[b2]	0.435		10[d]	0.427

[a] 2 ml of hydrogen peroxide (3%) was added. [b] Masked with 0.25 *M* EDTA. Volumes of EDTA added are: [b1] 2 ml, [b2] 5 ml and [b3] 10 ml. [c] Separated as a caprate. [d] Separated as an oxinate.

to 25 ml of solution containing 19.7 μg of selenium at pH 1.7, and the caprate extraction method was not included. The amounts (in mg) of the various ions which could be tolerated were as follows: Al(III) (200), As(V) (5), Ba(II) (500), Ca(II) (400), Cd(II) 200, Co(II) (200), Mg(II) (400), Mn(II) (400), Ni(II) (200). Other results are given in Table I. Oxidizing ions such as iron(III) and chromium(VI) interfere by forming colored products. Interference of iron(III) can be removed by extraction with caprate or by EDTA addition. Chromium(VI) can be reduced with hydrogen peroxide, to chromium(III) which does not interfere in amounts up to about 100 mg. Copper(II) (10 mg) and vanadium(V) (2 mg) do not interfere if the toluene phase is washed once with 0.1 *M* hydrochloric acid; the interference of larger amounts is mostly suppressed by EDTA. The interferences of molybdenum and tungsten can be removed by masking with EDTA or by extraction of the oxinates.

For the extraction of iron(III) with capric acid in chloroform[17], complete extraction of up to 100 mg of iron was found in the pH range 3–6; with larger amounts of iron, extraction is incomplete below pH 4, and the range 4.7–5 is recommended. These results were obtained by measuring the absorbance of the iron(III) caprate in the organic phase at 462 nm. Selenium(IV) does not react with capric acid in the pH range 0–5, and remains wholly in the aqueous phase.

Determination of selenium in iron and steel. Care is needed in the dissolution of the samples to avoid losses of selenium[11,19,20]. A mixture of nitric and perchloric acids is usually recommended[13,15,16,21], and it was confirmed that this mixture was satisfactory, provided that prolonged heating was avoided.

TABLE II

DETERMINATION OF SELENIUM IN IRON AND STEEL

Sample taken (g)	Se added (µg)	Se found (µg)	Se found (%)	
			Observed	Corrected for addition
Electric iron				
0.2	0	0	0	0
0.2	19.7	19.7	0.010	0
0.2	197	200	0.100	0
0.3	19.7	20.2	0.007	0
0.4	19.7	20.4	0.005	0
0.5	19.7	20.2	0.004	0
				Mean 0
Iron[a,b]				
0.3965	0	192, 193	0.049	0.049
0.4049	0	197, 200, 197	0.049	0.049
0.3981	98.7	296, 296	0.074	0.050
				Mean 0.049
17Cr–6 ~ 8Ni steel[a,c]				
0.1540	0	190, 190	0.123	0.123
0.1538	0	175, 179	0.115	0.115
0.1529	0	185, 185	0.121	0.121
0.1528	98.7	273, 274	0.179	0.115
				Mean 0.119

[a] The prepared sample solution was diluted to 100 ml with 0.1 *M* hydrochloric acid and a 10-ml aliquot was treated by the recommended procedure. [b,c] Standard sample cross-checked by members of the Japan Steel Maker's Association. Recommended values for selenium are: [b] 0.050 and [c] 0.13%.

The results obtained for iron and steel samples are shown in Table II. Recovery of added selenium was found to be quantitative, and the reproducibility was satisfactory.

The method proposed can be applied to many other samples with selenium contents below 0.01 % with slight modification.

The authors wish to thank Professors M. Kamada, Kagoshima University, and M. Tanaka, Nagoya University, for their stimulating and helpful discussions; and Dr. K. Tanaka, Industrial Research Institute of Kanagawa Prefecture, for the gift of iron and steel samples.

Chemical Institute, College of Liberal Arts,
Kagoshima University, Kamoike-cho, Kagoshima (Japan)
Takuji Kawashima
Akira Ueno

1 T. E. Green and M. E. Turley, in I. M. Kolthoff and P. J. Elving, *Treatise on Analytical Chemistry*, Part II, Vol. 7, Interscience, New York, 1961.
2 J. Hoste, *Anal. Chim. Acta*, 2 (1948) 402.
3 J. Hoste and J. Gillis, *Anal. Chim. Acta*, 12 (1955) 158.
4 C. A. Parker and L. G. Harvey, *Analyst*, 87 (1962) 558.

5 H. Ariyoshi, M. Kiniwa and K. Toei, *Talanta*, 5 (1960) 112.
6 M. Goto and K. Toei, *Talanta*, 12 (1965) 124.
7 L. S. Efros and Z. V. Todres-Selektor, *J. Gen. Chem. USSR*, 27 (1957) 1064.
8 P. Cukor, J. Walzcyk and P. F. Lott, *Anal. Chim. Acta*, 30 (1964) 473.
9 D. Demeyere and J. Hoste, *Anal. Chim. Acta*, 27 (1962) 288.
10 M. Tanaka and T. Kawashima, *Talanta*, 12 (1965) 211.
11 N. S. Mott, *Foundry*, 78 (1950) 121.
12 K. L. Cheng, *Chemist-Analyst*, 45 (1956) 67.
13 O. Kammori and A. Ono, *Jap. Anal.*, 15 (1966) 290.
14 F. J. Conrad and B. T. Kenna, *Anal. Chem.*, 39 (1967) 1001.
15 K. Tanaka, N. Takagi and H. Tsuzimura, *Jap. Anal.*, 18 (1969) 319.
16 W. E. Clarke, *Analyst*, 95 (1970) 65.
17 M. Tanaka, N. Nakasuka and S. Goto, in D. Dyrssen, J.-O. Liljenzine and J. Rydberg, *Solvent Extraction Chemistry*, North-Holland, Amsterdam, 1967, p. 154.
18 M. Tanaka, private communication.
19 E. B. Sandell, *Colorimetric Metal Analysis*, 3rd Edn., Interscience, New York, 1959, p. 73.
20 T. T. Gorsuch, *Analyst*, 84 (1959) 135.
21 C. L. Luke, *Anal. Chem.*, 31 (1959) 572.

(Received 3rd May 1971)

The determination of zirconium in steels

Zirconium is often present in welding electrodes and in the resulting weld metals and in this connection it was necessary to be able to determine the zirconium content of steels in the range 0.1–0.005%. The present standard method[1] was not sufficiently sensitive and an alternative method was sought.

A procedure described by Young and White[2] appeared to be particularly suitable; zirconium is extracted from acidic solution by tri-*n*-octylphosphine oxide in cyclohexane and then reacted in the organic phase with pyrocatechol violet. This procedure, or a modification of it, has been used to determine zirconium in niobium[3,4], and to determine trace amounts of zirconium in steels after a cupferron separation[5]. Wood and Jones[3] stated that their procedure could be modified for stainless steels. The basic method appeared to be sufficiently sensitive; it is also reasonably selective for zirconium. White[6] reported that Cr^{6+}, U^{4+}, Th^{4+}, Hf^{4+} and Zr^{4+} were extracted and formed coloured complexes. Hibbits *et al.*[5] claimed that manganese(VII) was extracted and reacted with pyrocatechol violet and that fluoride and phosphate ions interfered. Wood and Jones[3] reported that titanium and tantalum interfered but did not report interference from chromium.

The basic procedure with slight variations, *e.g.* a cupferron separation step, is to extract zirconium from acidic solution, usually 7 M in hydrochloric or nitric acid, with tri-*n*-octylphosphine oxide in either cyclohexane or cyclohexanone. The ratio of aqueous to organic phase can be between 1:1 and 15:1. Wood and Jones[3] reported that by increasing the concentration of the tri-*n*-octylphosphine oxide from 0.02 M[6] to 0.1 M, much greater quantities of sulphate ion can be tolerated in the aqueous solution. The organic extract is then washed with an acidic solution, which removes traces of titanium and molybdenum, and an aliquot is dissolved in ethanol and catechol violet and pyridine are added. The absorbance of the solution is measured at 655 nm. The present communication shows that this procedure can be modified to give a selective method for low levels of zirconium in mild and alloy steels without the need for a cupferron separation.

Reagents

Tri-n-octylphosphine oxide, 0.1 *M*. Dissolve 1.93 g of reagent in 50 ml of cyclohexane. This solution must be freshly prepared before use.

Standard zirconium solution, *250 µg Zr ml*$^{-1}$. Dissolve 0.25 g of high-purity zirconium metal in dilute hydrofluoric acid in a platinum dish. Add 2–3 drops of nitric acid (s.g. 1.42), heat to expel oxides of nitrogen and cool. Add 5 ml of sulphuric acid (s.g. 1.84) and evaporate to fumes of sulphuric acid; repeat this step, finally fuming for about 10 min to expel all the hydrofluoric acid. Cool, add 10 ml of water and transfer the solution to a 1-l flask, add 10 ml of sulphuric acid (s.g. 1.84) and dilute to 1 l with de-ionized water. Store the solution in a polyethylene bottle.

Apparatus

A Unicam SP 600 spectrophotometer was used.

Procedure

Weigh 1.0 g of steel into a 250-ml borosilicate beaker, add 15 ml of aqua regia, cover the beaker with a watch glass and heat gently until the sample is dissolved. Add 5 ml of perchloric acid (s.g. 1.70) and heat until dense white fumes are evolved. Cool, dilute with water and filter through a 7.5-cm Whatman No. 40 filter paper into a 100-ml graduated flask. Wash the residue, adding the washings to the filtrate, and dilute the filtrate to 100 ml with water. Transfer the residue and filter paper to a clean platinum basin and ash at 800°. Cool the residue, add 2 ml of sulphuric acid (s.g. 1.84) and 5 ml of 40% hydrofluoric acid, and heat to dryness on a hot plate. Fuse the residue with 2 g of sodium pyrosulphate, dissolve the product in (7+3) nitric acid and transfer to a 100-ml graduated flask.Dilute the solution to 100 ml with (7+3) nitric acid.

Transfer 10.0 ml of the filtrate and 10.0 ml of the residue solutions (equivalent to a 100-mg steel sample) to a clean, dry separating funnel, add 1 ml of aqueous 40% (w/v) sodium nitrite solution and 4 ml of nitric acid (s.g. 1.42) to give a total volume of 25 ml which is 7 *M* with respect to nitric acid. Add 5.0 ml of 0.1 *M* tri-*n*-octylphosphine oxide in cyclohexane, stopper the funnel and mechanically shake the solution for 15 min. Allow the two phases to separate and remove the aqueous layer. Add 25 ml of 7 *M* nitric acid and again shake for 15 min. Allow the two phases to separate and transfer 1.00 ml of the organic phase to a clean, dry 25-ml graduated flask. Then to this aliquot add 10 ml of isopropanol, 5 ml of catechol violet solution (0.015% w/v pyrocatecholsulphonphthalein in isopropanol) and 5 ml of pyridine in that order, mixing the solution after each addition. Dilute the solution to 25 ml with isopropanol. Prepare a blank solution by carrying out the entire procedure on 1 g of zirconium-free iron. Measure the absorbance of the solutions after 15 min in 1-cm or 4-cm cells at 655 nm, using the blank solution as the reference.

At the same time, prepare a calibration curve in a similar manner using 1 g of high-purity iron in 100 ml of solution and adding aliquots containing 0, 25, 50, 75, 100 and 125 μg of zirconium respectively to 10-ml aliquots (≡100 mg of iron) of the iron solution.

A graph of the calibration results gave a straight line passing through the origin from 0 to 25 μg of zirconium in the final 25-ml test solution.

Results

The proposed method was intended to determine zirconium in steels at a level at and below that determined by the conventional standard method[1]; hence it was not possible to compare results given by both methods on identical samples. Three analysed reference steels, National Bureau of Standards S.R.M. 462, 464 and 467, plus a series of zirconium-free steels "spiked" with known amounts of zirconium were analysed in replicate to determine the accuracy and precision of the proposed method; the results are given in Table I.

Discussion

In the reported method the variable factors that affect the efficient extraction of zirconium were fixed as follows. A 0.1 *M* solution of tri-*n*-octylphosphine oxide in cyclohexane was chosen as the extractant and the extraction time was kept at 15 min. Under these conditions, zirconium was completely extracted when the nitric acid concentration was in the range 6–10 *M*. Perchloric acid, which was present in the steel solutions in amounts up to 0.5 *M*, did not affect the extraction. Similarly, the ratio of the aqueous to organic phase could be varied between 1 : 1 and 15 : 1 with-

TABLE I

COMPARISON OF RESULTS OBTAINED BY PROPOSED METHOD ON N.B.S. STANDARD OR B.C.S. "SPIKED" SAMPLES

Sample	*B.C.S.* 149/2 *with* 0.125% *Zr added*	*B.C.S.* 149/2 *with* 0.025% *Zr added*	*B.C.S.* 149/2 *with* 0.005% *Zr added*	*B.C.S.* 149/2 *with* 0.025% *Zr added*	*N.B.S.* 462	*N.B.S.* 464	*N.B.S.* 467
Zirconium content of steel sample	0.125% Zr	0.025% Zr	0.005% Zr	0.025% Zr	Certified value 0.063% Zr	Certified value 0.010% Zr	Certified value 0.094% Zr
Operator	A	A	B	A	B	B	B
Cuvette size	1 cm	1 cm	4 cm	4 cm	1 cm	4 cm	1 cm
Mean result[a]	0.125	0.025	0.0051	0.025	0.063	0.0095	0.095
Maximum	0.129	0.029	0.0056	0.026	0.065	0.0116	0.097
Minimum	0.120	0.021	0.0046	0.024	0.059	0.0076	0.092
Range	0.009	0.008	0.0010	0.002	0.006	0.0040	0.005
Standard deviation	0.0027	0.0025	0.00032	0.00063	0.0018	0.0012	0.0016
Relative standard deviation	2.16	10.0	6.27	2.52	2.86	12.6	1.68

[a] Twelve separate determinations were done in each case.

out significantly affecting the extraction efficiency. The concentration of tri-*n*-octylphosphine oxide in cyclohexane could be reduced from 0.1 *M* to 0.01 *M*, when sulphuric acid was absent but if it was present, the extraction efficiency was lowered. In the presence of aqueous solutions containing 7 *M* nitric and 1 *M* sulphuric acids, over 99% of the zirconium was extracted with 0.1 *M* tri-*n*-octylphosphine oxide solution but with 0.01 *M* solutions less than 40% of zirconium was extracted.

The absorbance spectrum of the zirconium–catechol violet complex in a cyclohexane–isopropanol–pyridine medium shows a maximum at 655 nm; at this wavelength the absorbance of the reagents alone is low, less than 0.02 absorbance units. The molar absorptivity of the complex is about 37,500. If absolute ethanol is used, as suggested by Young and White[2], the molar absorptivity of the complex is increased to about 40,000. The proposed technique is therefore slightly less sensitive but it does have the advantage that dry ethanol is not required.

The colour formation is complete after 15 min. The absorbance is then stable for at least 1 h, after which it slowly decreases as the complex precipitates from solution.

The amount of pyridine in the final 25 ml of test solution can be varied between 3 and 7 ml; the reagents however must be added in the order given in the procedure to avoid the formation of immiscible phases.

Interferences

The effect of many cations on the determination was investigated. Sample solutions containing 10 mg of each element to be investigated plus 100 mg of iron and 100 μg of zirconium were prepared. The final sample solution volume was 25 ml and was made 7 *M* with respect to nitric acid. The extraction procedure was applied to these solutions and the zirconium content of the extract determined.

The following elements caused no significant interference, *i.e.* a relative error less than 5%: Al, Sb, As, Ba, Be, Bi, B, Cd, Ca, Ce, Cr, Co, Cu, In, K, La, Li, Pb, Mg, Mn, Mo, Na, Ni, Nb, Se, Ag, Si, Sr, Ta, Sn, Ti, V, W, Zn. White[6] reported that the rare earths are not extracted by tri-*n*-octylphosphine oxide, hence these also should not interfere with the proposed method.

Gold, thorium, uranium and hafnium were found to interfere, as shown in Table II. Chromium(VI) and manganese(VII) interfered but this interference could be overcome by reduction with sodium nitrite solution, even when the chromium content of the sample solution was increased to 20 mg. Wood and Jones[3] reported

TABLE II

EFFECT OF INTERFERING IONS ON THE DETERMINATION OF ZIRCONIUM IN STEEL

(In all cases, the aliquot taken contained 100 mg of iron and 100 μg of zirconium)

Interfering element (mg)	*Zirconium found (μg)*	*Interfering element (mg)*	*Zirconium found (μg)*	*Interfering element (mg)*	*Zirconium found (μg)*
Au 10	126	Th 1.0	246	U 10	240
Hf 0.15	166	Th 0.5	168	U 1.0	116
Hf 0.10	143	Th 0.1	114	U 0.5	109
Hf 0.05	122			U 0.1	101.6

that back-washing the organic phase removed traces of extracted titanium. This step was included in the method and no interference from titanium was found.

The effect of phosphate and fluoride was also studied. Up to 1.25 mg of phosphate and fluoride per 100 mg of iron caused no significant interference. Sulphate concentrations up to 1 *M* in the aqueous phase can be tolerated.

Conclusions

A method is described for the determination of zirconium in steels. It has been successfully applied to the analysis of welding electrodes, and weld metals. The only elements out of 40 tested found to interfere in the given procedure are gold, thorium, uranium and hafnium. Hafnium reacts in an identical manner to zirconium and is equally sensitive on a molar basis, *i.e.* the apparent zirconium content of a steel will be increased by 0.51% by every 1% of hafnium present. However, the hafnium–zirconium ratio in most compounds and alloys (other than specially purified zirconium alloys) is about 1:99 and will therefore not significantly affect the result. The other metals are extremely unlikely to be present in weld metals in large amounts and the method can be considered to be virtually specific for zirconium in these circumstances. The procedure has the additional advantage that a cupferron separation, as suggested by Hibbits *et al.*[5], is not required.

The precision of the method is such that eleven consecutive analyses of total zirconium in steel gave a mean value of 0.095% Zr (N.B.S. SRM No. 467, certified value 0.094% Zr) with a standard deviation about the mean of 0.0016%. Twelve steels can be analysed for acid-soluble zirconium in 3 h or for total zirconium content in 6 h.

The authors wish to thank the Director, Central Electricity Generating Board, Marchwood Engineering Laboratories for permission to publish this paper.

Central Electricity Generating Board,
Marchwood Engineering Laboratories,
Marchwood, Southampton (England)

D. B. Ratcliffe
C. S. Byford

1 British Standards Institution, *BS 1121, Part 46*, 1966.
2 J. P. Young and J. C. White, *Talanta*, 1 (1958) 263.
3 D. F. Wood and J. T. Jones, *Analyst*, 90 (1965) 125.
4 W. T. Elwell and D. F. Wood, *Analysis of the New Metals*, Pergamon Press, London, 1966, p. 243.
5 J. O. Hibbits, A. F. Rosenburg, R. T. Williams and S. Kallman, *Talanta*, 11 (1964) 1509.
6 J. C. White, *Oak Ridge Natl. Lab. Rep. ORNL-CF-56-9-18*, Sept. 1956.

(Received 27th August 1971)

Analytica Chimica Acta
Elsevier Publishing Company, Amsterdam
Printed in The Netherlands

Extraction-photometric determination of nitrite in fresh and sea water

Nitrite can be sensitively and accurately determined by spectrophotometry with sulfanilamide and N-1-naphthylethylenediamine[1,2] which form a red azo dye in the pH range 1–2. Nowadays, however, a more sensitive method is required for nitrite in natural waters.

Zeller[3] proposed extraction of the azo dye with *n*-butanol, and Wada and Hattori[4] studied concentration of the dye on cation-exchange resins; Macchi and Cescon[5] recently reported extraction of the yellow azo dye produced in the pH range 8.5–10.5, with chloroform. The positively charged azo dye can also be quantitatively extracted into carbon tetrachloride by coupling with the negatively charged *n*-dodecylbenzenesulfonate ion, and this extraction method has been successfully applied to the determination of trace amounts of nitrite in fresh water[6]. When this method was directly applied to sea water samples, however, some difficulties arose from turbidity in the carbon tetrachloride layer and from alteration of the wavelength of maximum absorption with changes in salt concentration. After several attempts, it was found that these difficulties could be eliminated by back-extraction.

Procedures

For fresh water. Since details have already been reported[6], the procedure is only outlined here.

To a 50-ml sample solution, add 1 ml of 1% sulfanilamide in 1.2 *M* hydrochloric acid solution and 1 ml of aqueous 0.1 % N-1-naphthylethylenediamine dihydrochloride solution. After 10 min, add 5 ml of carbon tetrachloride and 1 ml of aqueous 0.03% dodecylbenzenesulfonate solution. Extract the azo dye by shaking for 3 min, and measure the absorbance at 525 nm in a 1-cm cell.

For sea water. Transfer a 500-ml sea water sample to a 1-l separatory funnel and add 10 ml of 1% sulfanilamide in 2 *M* hydrochloric acid, followed by 5 ml of aqueous 0.1 % N-1-naphthylethylenediamine dihydrochloride solution during 2–8 min. After 10 min, add 5 ml of aqueous 0.5 % dodecylbenzenesulfonate solution and 50 ml of carbon tetrachloride. Extract the azo dye by shaking for 2 min, and transfer the organic layer to another 200-ml separatory funnel. Add 75 ml of acetone and 10 ml of 0.1 *M* hydrochloric acid, and then back-extract the azo dye into the hydrochloric acid layer by shaking for 5 sec. Measure the absorbance of the hydrochloric acid layer at 543 nm in a 2-cm cell, and deduct the blank value described below.

Notes to the procedure

The conditions of the procedure are not critical, *e.g.*, the addition of 5–13 ml of sulfanilamide solution and 3–7 ml of N-1-naphthylethylenediamine solution gives the same result. Variation in temperature from 5 to 30° has no effect on the result.

The azo dye produced is stable for 2 h in hydrochloric acid solution as well as in carbon tetrachloride, under diffuse light. It was, however, noticed that when the procedure was carried out under direct sunlight, a blue compound with maximum absorbance at 660 nm was formed in addition to the red azo dye, and the former was also extracted into carbon tetrachloride and back-extracted into the aqueous phase.

The blue substance seems to be an oxidized compound of N-1-naphthylethylenediamine. Since the substance causes a positive error, the procedure must be done under diffuse sunlight or artificial light.

Acetone is added to withdraw the azo dye into the aqueous layer. The volume of the aqueous layer changes with the amount of acetone added, because of mutual solubility in the carbon tetrachloride–acetone–hydrochloric acid system. As shown in Fig. 1, when 75 ml of acetone are added, the changes of the volume and of the absorbance of the aqueous phase are minimal.

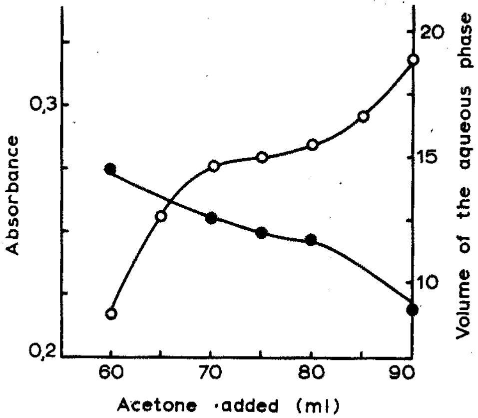

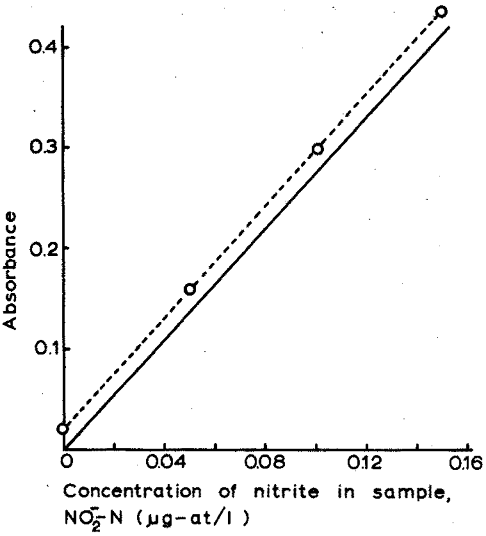

Fig. 1. Effect of the amount of acetone. (○) Absorbance; (●) volume of the aqueous phase.

Fig. 2. Working curve for nitrite.

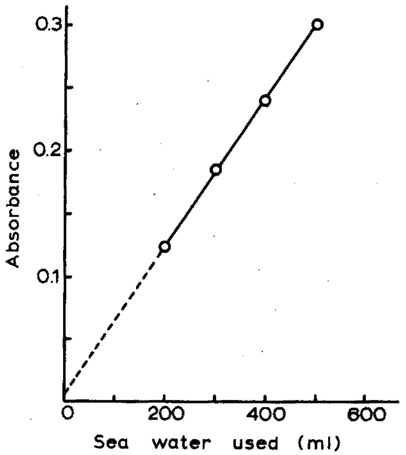

Fig. 3. Determination of blank value.

Working curve

To a sample of sea water, a known amount of nitrite is added and the solution is treated by the same procedure as for sea water. The absorbance is plotted against the added concentration of nitrite. As shown in Fig. 2, a straight line up to 0.16 μg-at. NO_2^--N l^{-1} is obtained. The working curve is then the solid line which is parallel to the broken line and starts from the zero absorbance.

Determination of the blank

The blank value under the same conditions as for samples is determined by the following procedure. A nitrite-enriched sea water solution whose concentration is about 0.1 μg-at. NO_2^--N l^{-1} is prepared. Portions (0.5, 0.4, 0.3 or 0.2 l) of the solution are placed in separatory funnels, and the absorbance is measured as described in the *Procedure*. As shown in Fig. 3, a straight line is obtained and its extrapolation to zero volume of the solution gives the blank value. In this case, the blank value was 0.006 in absorbance.

TABLE I

RECOVERY AND PRECISION FOR SEA WATER SAMPLE
(All results are given as μg-at. NO_2^--N l^{-1})

Original sea water	*Added*	*Found*[a]	*Standard deviation*
0.0065	0.0200	0.0269	0.0006
0.0065	0.1000	0.1071	0.0013

[a] Mean of 5 determinations.

Precision and sensitivity

The reproducibility of the method was determined by addition of nitrite to sea water samples (Table I). The relative standard deviation for 5 replicate determinations is about 2% at the 0.03 μg-at. level and 1% at the 0.1 μg-at. level.

The sensitivity for 0.001 absorbance in 1-cm cells is 0.0007 μg-at. NO_2^--N l^{-1} of sea water for this extraction method, while it is 0.02 μg-at. NO_2^--N l^{-1} for the ordinary method.

Department of Chemistry,
Faculty of Fisheries,
Hokkaido University,
Hakodate 040 (Japan)

K. Matsunaga
T. Oyama
M. Nishimura

1 M. B. Shinn, *Ind. Eng. Chem., Anal. Ed.*, 13 (1941) 33.
2 K. Bendschneider and R. J. Robinson, *J. Marine Res.*, 11 (1952) 87.
3 H. D. Zeller, *Analyst*, 80 (1955) 632.
4 E. Wada and A. Hattori, *22nd Annual Meeting, Chem. Soc. Japan*, Abstract, II (1969) 1189.
5 G. R. Macchi and B. S. Cescon, *Anal. Chem.*, 42 (1970) 1809.
6 M. Nishimura, K. Matsunaga and K. Matsuda, *Japan Analyst*, 19 (1970) 1096.

(Received 13th July 1971)

Analytica Chimica Acta
Elsevier Publishing Company, Amsterdam
Printed in The Netherlands

Determination of mercury in seawater by radioactivation

Methods reported for the determination of mercury in seawater[1,2] have followed classical schemes and require sample volumes of 5–10 l. It was desired to reduce this volume requirement by an order of magnitude. Accordingly, a method was developed which was based upon the inherently sensitive radioactivation technique. This report describes the method of isolating mercury from seawater before irradiation, the radiochemical purification process in the determination of radio-induced ^{197}Hg, and the results of the analysis of seawater.

Experimental

Chemicals. Copper carrier solution was prepared from 99.999% copper powder. The powder was dissolved in concentrated nitric acid and diluted with double distilled water to a concentration of 10 mg ml^{-1}. The final acid concentration was about 1 *M*.

Mercury carrier solution was prepared from mercury(II) nitrate hydrate at a concentration of 10 mg Hg ml^{-1} in 1.6 *M* nitric acid.

Comparator solution consisted of a standardized mercury solution diluted to a concentration of 2.00 μg Hg ml^{-1} in 1.6 *M* nitric acid.

Tin(II) chloride solution was prepared by adding about 30 ml of concentrated hydrochloric acid to 10 g of mossy tin. The mixture was allowed to stand for about 20 min before use.

Isolation of mercury from seawater. It was considered desirable to isolate mercury from seawater before neutron irradiation to reduce exposure to the levels of induced radioactivities which would otherwise develop from sea salts. The method of isolation depended upon coprecipitation of mercury with copper sulfide from acid solution.

Eleven 1-l polyethylene bottles were filled to within about 25 ml of their capacity with surface seawater. To each were added 10 ml of concentrated hydrochloric acid, 100 μl of copper carrier solution and a ^{197}Hg spike. Immediately, or 24 h after these additions, hydrogen sulfide was bubbled through the solution for 30 sec. The resultant precipitate was collected on a Millipore filter membrane (0.45 μm). The precipitate was transferred to a counting vial and then dissolved in about 10 ml of concentrated nitric acid. The walls of the original bottle were washed with about 10 ml of concentrated nitric acid and this solution was transferred to another counting vial. The gross γ-count rate of these solutions was determined with a NaI(Tl) detector. To determine the counting efficiency of the spike in each solution, each tube was then spiked with another aliquot of ^{197}Hg. From these data the recovery of mercury from seawater was computed. The results indicated that 100.1 ± 2.0% of the mercury activity is recovered from seawater by the coprecipitation process, independently of whether the copper sulfide was precipitated immediately or 1 day following addition of reagents. The quantity of mercury which was washed from the walls of the original vessel with concentrated nitric acid was generally about 2%.

Treatment of seawater sample. Seawater (8 l) was collected at a depth of 20 ft. off the end of the pier at the Scripps Institution of Oceanography, La Jolla, Calif. The sample was acidified on collection with concentrated hydrochloric acid (10 ml l^{-1} of seawater) and filtered through a Millipore filter membrane (0.45 μm). Aliquots of 0.5 l (exact volumes were gravimetrically determined) were transferred to each of twelve 1-l polyethylene containers which had been previously leached with concentrated nitric acid and subsequently rinsed with distilled water and about 100 ml of seawater sample. Groups of four samples received either none, 50 or 100 ng of mercury. To each sample were added 100 μl of copper carrier. Within 5 h of these additions, the copper was precipitated from solution and collected on a Millipore filter membrane as described above. The membrane was placed in a 15-ml polyethylene irradiation vial. The walls of the sample container were washed successively with 5-, 3- and 2-ml volumes of concentrated nitric acid and the washings were added to the irradiation vial.

Blanks and comparator. The copper carrier blank consisted of 100 μl of carrier solution together with 10 ml of concentrated nitric acid.

The hydrochloric acid blank was prepared in the following way: 5 ml of concentrated hydrochloric acid were added to 100 ml of double distilled water that contained 100 μl of copper carrier. Copper sulfide was precipitated and prepared for irradiation as in the procedure described for seawater samples. (Mercury tracer coprecipitated quantitatively with copper sulfide under these conditions.)

The Millipore membrane filter blank consisted of 3 Millipore filters dissolved in 10 ml of concentrated nitric acid.

The concentrated nitric acid and double distilled water used in the preparation of these blanks were obtained from sources previously shown to be free of detectable mercury[3].

Comparator solution (10 ml) served as the elemental standard.

Irradiation. Samples, comparators and blanks were irradiated for 1 h in a flux of $2 \cdot 10^{12}$ n cm^{-2} sec^{-1} in a rotating sample container (1 r.p.m.) at Gulf Energy and Environment Services, San Diego, Calif.

Radiochemical separations and measurements. After irradiation the sample or blank was quantitatively transferred to a vessel that contained 1 ml of mercury carrier. The solution was brought to pH 1–2 with ammonia liquor and 5 ml of tin(II) chloride were added. The precipitate which formed was isolated by centrifugation. The supernate was discarded and the precipitate was dissolved in 5–10 ml of aqua regia. Copper carrier (1 ml) was added to the solution, the pH was adjusted as above and precipitation with tin(II) was repeated. This precipitate was collected by filtration, and dissolved in aqua regia, and the solution was adjusted to pH 7 with ammonia liquor. Hydrogen sulfide gas was bubbled through the solution for 30 sec. The sulfide precipitate was collected on a Millipore filter and counted.

Comparators, after addition of 1 ml of mercury carrier, were precipitated directly as the sulfide and counted.

The 77-keV γ-ray of ^{197}Hg was measured one week after the irradiation with a NaI(Tl) detector coupled to a pulse-height analyzer.

After the radioactivity measurement the mercury sulfide was dissolved in 2 ml of aqua regia and diluted to 25 ml with water. The atomic absorptivity of this solution was compared to that of a mercury standard to obtain the carrier yield.

Results

The results of the assay of mercury in seawater appear in Fig. 1. The abscissa refers to the quantity of mercury added to the sample and the ordinate to the quantity determined through measurement of induced ^{197}Hg. The straight line represents a least-squares fit of the data. The standard deviation of experimental points from the computed line is 11.2%. The mercury content of the seawater sample derived from these data is 83.2±9.3 ng kg^{-1}.

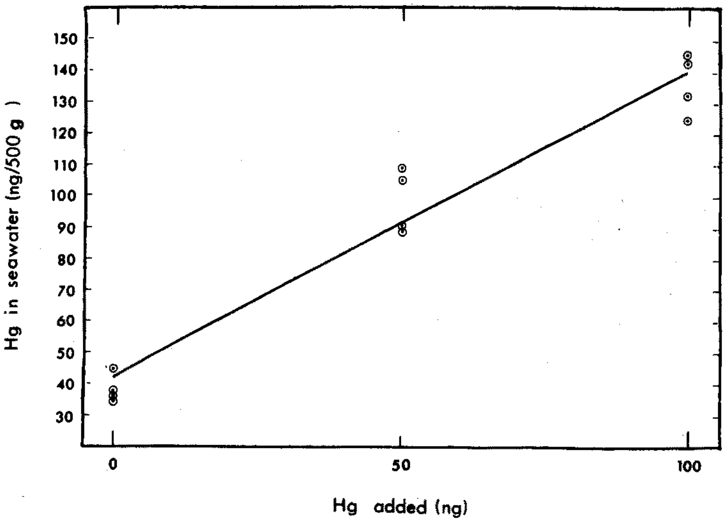

Fig. 1. The recovery of mercury from seawater.

The hydrochloric acid used in the pre-concentration step contained 1.6 ng Hg ml^{-1} and the data were corrected for this factor. The results of the other blank determinations indicated that the copper carrier and Millipore filter membranes were free of mercury.

Varying quantities of induced ^{24}Na were associated with the mercury(II) sulfide after the radiochemical separation. Most samples could be counted without interference from this radionuclide by the fourth day after irradiation. By the seventh day this source of interference was absent in all samples.

The mercury carrier yield was 81.1±9.8% for the twelve determinations. An analyst performs 4 radiochemical separations in 1 h. The sensitivity of the procedure, which is defined by a count rate in excess of 3 standard deviations from the background 7 days after the irradiation, is 4 ng.

Naval Undersea Research and Development Center, Herbert V. Weiss
San Diego, Calif. 92132 (U.S.A.)

Department of Chemistry, San Diego State College, Thomas E. Crozier
San Diego, Calif. 92115 (U.S.A.)

1 H. Hamaguchi, R. Kuroda and K. Hosohara, *Nippon Kagaku Zasshi*, 82 (1961) 347; *Chem. Abstr.*, 55 (1961) 15222c.
2 V. A. Stock and F. Cucuel, *Naturwiss.*, 22 (1934) 390.
3 H. V. Weiss, M. Koide and E. D. Goldberg, *Science*, Nov. (1971) in press.

(Received 9th July 1971)

Analytica Chimica Acta
Elsevier Publishing Company, Amsterdam
Printed in The Netherlands

The determination of uranium in exploration samples by X-ray emission spectrometry

The use of scattered tube radiation to correct for matrix effects in X-ray emission spectrometric analysis was first proposed by Andermann and Kemp[1] and has since been applied and discussed by others[2-4]. This communication describes the use of such a correction in the rapid and accurate determination of uranium in exploration samples.

Apparatus

Mixing of calibration standards was carried out in a Spex mixer/mill, 8000-11, with a steel vial (8001) and four 0.25-in. diam. steel balls.

A Philips PW 1540 spectrometer was used for all X-ray measurements. The following conditions were applied:

Air path; W-target tube at 50 kV and 20 mA; LiF (200) crystal: ULα line measured at $2\theta = 26.14°$, scattered tube radiation measured at $2\theta = 12.00°$ ($\lambda = 0.42$ Å); fine collimator; scintillation counter; pulse-height analyser set at: lower level 50 units, threshold, attenuation 2^1; 100-sec counts; sample spinner on.

Calibration

Calibration standards (26) were prepared by making additions of 97% U_3O_8 to an exploration sample (ground to 200 mesh) previously shown to be barren in uranium, to cover a range in % U_3O_8 from 0.003 to 1.923 (0.06–38.4 lb/short ton). Standards were mixed for 5 min. Standards were presented for X-ray measurements as a loose powder poured on to 6 μm Mylar film. Each standard was counted twice, being repoured on to the Mylar film before the second set of counts. Table I gives the results obtained.

The relationship between R, the ratio of the intensity of the ULα line to the intensity of the scattered tube radiation, and % U_3O_8 in the sample was found to be linear up to 1.4% U_3O_8, and is given by the least-squares method as

$$\%U_3O_8 = 0.337\,R - 0.111 \qquad (1)$$

A more detailed study of 13 standards containing up to 0.10% U_3O_8 indicated that the practical lower limit of detection is 0.010% U_3O_8.

Table I shows that, as expected, the relative reproducibility of the standards with only trace U_3O_8 was poor. However, for those standards containing greater than 0.020% U_3O_8, the relative error did not exceed ±4%, which was considered to be entirely satisfactory. Full calibration takes 2 man-shifts, comprising 1.5 man-shifts for weighing and mixing, and 0.5 man-shift for X-ray measurements.

Application

This calibration was applied to the determination of uranium in a suite of 507 samples from an exploration prospect. All samples were ground to 200 mesh and then presented for analysis as a loose powder poured on to 6 μm Mylar film. A calibration graph covering the range 0.01–0.1% U_3O_8 was used for $R < 0.65$, and a graph covering

TABLE I RESULTS FOR CALIBRATION STANDARDS

Standard	*% U_3O_8*	*A (c.p.s. at $2\theta=12.00°$)*	*B (c.p.s. at $2\theta=26.14°$)*	*$R=B/A$*	*Mean R*	*Reproducibility*	
						Absolute (% U_3O_8)	*Relative (%)*
0	0.000	3439	1178	0.343	0.340	±0.001	—
		3471	1174	0.338			
1	0.003	3756	1323	0.352	0.356	0.001	±33.3
		3638	1305	0.359			
2	0.008	3669	1265	0.345	0.347	0.001	12.5
		3548	1245	0.351			
3	0.014	3646	1309	0.359	0.358	0.001	7.1
		3672	1308	0.356			
4	0.020	3728	1417	0.380	0.382	0.001	5.0
		3649	1401	0.384			
5	0.029	3699	1495	0.404	0.406	0.001	3.4
		3633	1482	0.408			
6	0.041	3717	1633	0.439	0.442	0.001	2.4
		3653	1625	0.445			
7	0.049	3616	1699	0.470	0.466	0.002	4.1
		3717	1715	0.461			
8	0.060	3635	1807	0.497	0.494	0.001	1.7
		3687	1810	0.491			
9	0.072	3657	1949	0.533	0.531	0.001	1.4
		3673	1938	0.528			
10	0.078	3674	2001	0.545	0.548	0.001	1.3
		3688	2037	0.552			
11	0.089	3513	2091	0.595	0.596	0.001	1.1
		3599	2088	0.597			
12	0.100	3506	2194	0.626	0.636	0.003	3.0
		3402	2199	0.646			
13	0.203	3383	3147	0.930	0.931	0.001	0.5
		3391	3159	0.932			
14	0.298	3357	4103	1.222	1.218	0.001	0.3
		3433	4167	1.214			
15	0.402	3286	5095	1.551	1.563	0.004	1.0
		3316	5223	1.575			
16	0.494	3433	5912	1.722	1.766	0.015	3.0
		3270	5921	1.811			
17	0.593	3307	7199	2.179	2.154	0.009	1.5
		3238	6891	2.128			
18	0.694	3227	7740	2.399	2.419	0.007	1.0
		3220	7849	2.438			
19	0.800	3337	8578	2.571	2.606	0.012	1.5
		3209	8477	2.642			
20	0.885	3148	9467	3.007	2.968	0.013	1.5
		3204	9389	2.930			
21	0.980	3296	10161	3.083	3.165	0.021	2.1
		3186	10283	3.228			
22	1.163	3122	11616	3.721	3.726	0.002	0.2
		3111	11609	3.732			
23	1.344	3061	13547	4.426	4.410	0.005	0.4
		3006	13212	4.395			
24	1.509	2945	13946	4.735	4.800	0.022	1.5
		2931	14259	4.865			
25	1.732	2823	16127	5.713	5.787	0.025	1.4
		2865	16793	5.861			
26	1.923	2825	17597	6.229	6.345	0.039	2.0
		2772	17906	6.460			

the range 0.1–2.0% U_3O_8 was used for $R > 4.5$; eqn. (1) was used for all other values of R. Results were quoted as % U_3O_8, to the third decimal place as found.

Analysis time for a single determination was 4–5 min per sample.

Accuracy

Of the 507 U_3O_8 determinations made, 115 were checked in this laboratory by a colorimetric method in which the uranium is complexed with dibenzoylmethane[5]. Of these, 90 determinations which were within the practical lower detection limit of the X-ray method (0.010% U_3O_8) and the upper detection limit of the colorimetric method (0.90% U_3O_8), gave a mean difference between the methods of ±0.019% U_3O_8, and a mean bias (colorimetric–X-ray) of +0.009% U_3O_8. A further 30 determinations were checked by an outside laboratory, in an umpire capacity, by an unknown method. A mean difference between the methods of ±0.012% U_3O_8 was obtained, with a mean bias (outside laboratory–X-ray) of +0.002% U_3O_8. Thus the accuracy of the X-ray method is satisfactory.

Matrix effects

The matrix changes observed in this suite of samples were normal for such a suite. Particular variables were iron and silica. One sample was high in antimony; although count rates on this sample were reduced to approximately two-thirds of those on the standards, the X-ray determination of 0.208% U_3O_8 maintained agreement with the colorimetric determination of 0.212% U_3O_8. Thus the use of the intensity of the scattered tube radiation as a matrix correction is satisfactory.

Particle size effects

The effect of the 5-min mixing period on the standard samples was studied. Contrary to expectation, mixing produced a decrease in count rates, and a small increase in R. The omission of a similar mixing period for unknown samples may lower the determination of % U_3O_8 by up to 10% relative (although the colorimetric checks described above have not shown this in practice). Such an error is not significant in the evaluation of an exploration prospect, but can be eliminated by mixing all unknown samples in the Spex mixer/mill. Analysis time for a single determination is then increased to 6–7 min per sample. Count rates also varied according to packing density, but R remained unchanged.

Conclusion

The use of the ratio technique as described offers other analysts a rapid and accurate method for the evaluation of a uranium exploration prospect. Determination of U_3O_8 between 0.010% and 1.923% (0.2–38.4 lb/short ton) can be effected with an expected relative reproducibility of ±4%. Samples are presented as loose powder (200 mesh). Full calibration takes 2 man-shifts, and each sample has an analysis time of not greater than 7 min.

The authors thank Mount Isa Mines Limited for permission to publish this work.

Technical Services Department,
Mount Isa Mines Limited, Mount Isa
Queensland 4825 (Australia)

N. H. Clark
J. G. Pyke

1 G. Andermann and J. W. Kemp, *Anal. Chem.*, 30 (1958) 1306.
2 K. P. Champion, J. C. Taylor and R. N. Whittem, *Anal. Chem.*, 38 (1966) 109.
3 Z. H. Kalman and L. Heller, *Anal. Chem.*, 34 (1962) 946.
4 D. L. Taylor and G. Andermann, *Anal. Chem.*, 43 (1971) 712.
5 N. T. McHugh and R. J. Preston, private communication.

(Received 2nd September 1971)

Separation of cyclotron-produced cadmium-109 from the silver matrix, copper and zinc

For the preparation of carrier-free cadmium-109, cyclotron-produced by the ^{109}Ag(d, 2n)^{109}Cd reaction, a separation of submicrogram quantities of cadmium from several grams of silver is required. Several methods for this separation have already been described. Grachev *et al.*[1] precipitate silver and copper as the iodides, but losses of cadmium-109 by inclusion and adsorption on the precipitate are unavoidable. According to the distribution coefficients of cations on Dowex 1-X8 (200–400 mesh) anion-exchanger in hydrochloric acid[2], silver and cadmium may be separated in concentrated hydrochloric acid medium. This method has in the past been applied in this laboratory, but was replaced by a procedure based on anion exchange in hydrobromic acid[3]. This procedure was adopted because the hydrobromic acid medium allows a smaller starting solution and the distribution coefficients for cadmium and silver are sufficiently far apart. However, the method implies the elution of *ca.* 2 l of 6.8 *M* hydrobromic acid, 500 ml of 0.3 *M* nitric acid and 300 ml of 2 *M* nitric acid and is time-consuming: about 2 working days are spent on each separation. Furthermore, the ^{65}Zn decontamination is poor. Even if the elution with 0.3 *M* nitric acid is prolonged, the ^{65}Zn-contamination is not completely removed and amounts to 0.5% of the ^{109}Cd-activity in the cadmium fraction.

Hence, a completely new procedure was devised, based on deposition of the silver and anion exchange of the remaining solution. The procedure only takes half a working day and the decontamination of ^{109}Cd from silver and ^{65}Zn is very satisfactory.

Deposition of silver

Silver can be readily deposited by addition of copper to a solution, and this simple electrochemical reaction allows complete replacement of silver by copper. The tedious problems of separating cadmium from silver, copper and zinc can then be simplified to the separation of cadmium from copper and zinc. For the deposition process, the pH of the solution should not be too low, otherwise copper may be dissolved by the nitric acid used for dissolving the silver; the optimal pH was found to be between 2 and 7, complete deposition being accomplished in 15 min.

The deposition of silver on iron was also studied, but the medium must be made too acidic and iron must be present on the paper used for filtration to avoid redissolution of the silver. The amount of iron in solution becomes much higher than the equivalent necessary to precipitate the silver. Furthermore, the separation of copper(II) from zinc(II) and cadmium(II) is simpler than the separation of iron(III) from the latter metal ions.

The displacement of 5 g of silver brings about 1.5 g of copper(II) into solution. At pH 5 more than 99.85% of the silver is deposited in 15 min. Silver-110m was used to monitor the silver decontamination. After filtration the solution contains copper(II), ^{109}Cd and ^{65}Zn. ^{109}Cd can be separated from copper(II) and ^{65}Zn by anion exchange in dilute hydrochloric acid. Zinc is not absorbed on Dowex 1-X8[4] in 0.02 *M* hydrochloric acid, while cadmium is strongly retained; furthermore, copper(II) is not absorbed at all, so that relatively small columns can be used. The elution of copper was monitored by means of the blue colour of the amminocopper(II) complex. After percolation of the starting volume an additional 20 ml of 0.02 *M* hydrochloric acid eluted the copper(II) completely; a further 110 ml of the acid was needed to remove all the ^{65}Zn, while the ^{109}Cd was completely retained on the resin. Elution with 3 *M* nitric acid removed the ^{109}Cd from the resin. The results for the different separation steps are collected in Table I.

TABLE I

BEHAVIOUR OF SILVER, CADMIUM, COPPER AND ZINC IN THE DIFFERENT SEPARATION STEPS

Step	*Fraction*	*Volume*	*% of the elements in each fraction*			
			Ag	*Cd*	*Cu*	*Zn*
Precipitation	Ag precipitate		>99.85	<0.5		<0.3
	Filtrate	20 ml	<0.15	>99.5		>99.5
Ion exchange	HCl 0.02 *M*	110 ml		<0.03	>99.99	>99.995
	HNO_3 3 *M*	50 ml		>99.9	<0.01	<0.005

Recommended method

Dissolve the silver target in 10 ml of concentrated nitric acid, evaporate to dryness and add 20 ml of water. Adjust the solution to pH 5 and add 3 g of copper turnings. Stir for 15 min and filter. Wash the silver precipitate with distilled water. Evaporate the combined filtrate and washings almost to dryness, add 10 ml of concentrated hydrochloric acid, evaporate to dryness and redissolve the residue in 20 ml of 0.02 *M* hydrochloric acid. Percolate the solution through a Dowex 1-X8 column (200–400 mesh; 15-cm high bed with a volume of 25 ml). Elute with an additional 110 ml of 0.02 *M* hydrochloric acid and discard these fractions. Elute with 50 ml of 3 *M* nitric acid to collect the ^{109}Cd. Evaporate this solution and make up with the desired solute.

Discussion

It can be seen from Table I that more than 99.4% of the cadmium-109 is collected in the nitric acid fraction. ^{65}Zn contamination is less than 0.005% of the original content and is undetectable. Silver and copper are also separated quantitatively. The silver chloride precipitation test and the amminocopper(II) test are both negative in the cadmium fraction.

The method requires only a filtration, evaporation to dryness, redissolution and elution of relatively convenient volumes. It is much quicker and more efficient than the formerly used anion-exchange method in hydrobromic acid medium[3].

National Physical Research Laboratory,
South African Council for Scientific and
Industrial Research,
Pretoria (South Africa)
R. D. Neirinckx

1 S. A. Grachev, V. N. Melkinov, Tu. A. Ryukhin and M. A. Toropova, *Radiokhim.*, 3 (1961) 116.
2 K. A. Kraus and F. Nelson, *Proc. Int. Conf. Peaceful Uses At. Energy, Geneva, 1955*, 7 (1956) 113.
3 F. W. E. Strelow, W. J. Louw and C. H.-S. W. Weinhert, *Anal. Chem.*, 40 (1968) 2021.
4 S. Kallmann, H. Oberthin and R. Liu, *Anal. Chem.*, 32 (1960) 58.

(Received 17th August 1971)

Spectropolarimetric determination of copper(II) with L(−)proline

Several papers concerning polarimetric titrations have been published[1-9]; the determination of metal ions with optically active titrants such as the disodium salts of D(−)PDTA and of D(−)DCTA[3-9] is particularly noteworthy.

In the compleximetric titrations of metal ions the main requirements are as follows:

1. the conditional formation constant of the complex must be higher than about 10^6;
2. the specific rotation of the ligand and of the complex must be different enough to permit a good appreciation of the end-point.

In the selection of the proper wavelength it is advisable to avoid regions of high absorbance because this could decrease the sensitivity of the instrument. Preliminary experiments proved that in the case of the polarimetric titration of copper(II) with L(−)proline these requirements could be satisfied.

Experimental

Apparatus. A Perkin-Elmer 141 M spectropolarimeter equipped with a 5-ml flow-through cell which had an optical depth of 1 dm was used. The cell was connected with a titration vessel of the type described by Palma and Pearson[4]. The measurements were carried out at room temperature and at 1.00 *M* ionic strength (KNO_3).

Reagents. L(−)Proline (BDH) was chromatographically homogeneous; its purity was checked by measuring its specific rotation ($[\alpha]_D^{25} = -85.1°$ in aqueous solution[10]). The solutions were prepared by weighing and the concentrations were checked polarimetrically; they were stable for about 48 h.

Copper nitrate and potassium nitrate (Carlo Erba, reagent-grade) were used without further purification; the solution of copper(II) was standardized against EDTA.

Buffers. A mixture which was 1.00 *M* in ammonium nitrate and 5.56 *M* in ammonia was used as buffer pH 10.00; a 1.00 *M* triethanolamine–0.63 *M* nitric acid solution was used as buffer pH 8.00.

All solutions were prepared with twice-distilled water.

Procedure. In the solution to be titrated the concentration of copper(II) ranged from $1.00 \cdot 10^{-3}$ to $5.00 \cdot 10^{-3}$ *M*; various buffer concentrations (1–3 ml for each 100 ml of solution) were used, with enough potassium nitrate to bring the ionic strength to 1.00. After introduction of the solution into the reaction vessel, proline ($7.61 \cdot 10^{-2}$ or $1.00 \cdot 10^{-1}$ *M*) solution was added by means of a microsyringe. The time required for complete mixture of the reagents was about 30 sec. The polarimeter readout was zeroed in respect to air.

Results and discussion

The absorption spectra of 1:1 solutions of copper(II) and L(−)proline up to $5.00 \cdot 10^{-3}$ *M* at pH 10.00 show that their absorbance is low enough from 350 to 450 nm. In this range, with the apparatus used, it was possible to select wavelengths of 365.015, 404.660 and 435.834 nm. The molar rotations of the titrant and of the 1:1 complex (the latter calculated from titration plots at the equivalent point) at the above wavelengths are given in Table I. They are different enough to permit a graphical evaluation of the end-point in the above-mentioned experimental conditions.

TABLE I

VALUES OF THE MOLAR ROTATION (ϕ) OF PROLINE AND OF ITS 1:1 COMPLEX WITH COPPER(II) AT OPERATING WAVELENGTHS

Wavelength (nm)	ϕ *proline*	ϕ *complex*
365.015	−310	−710
404.660	−240	−550
435.834	−200	−500

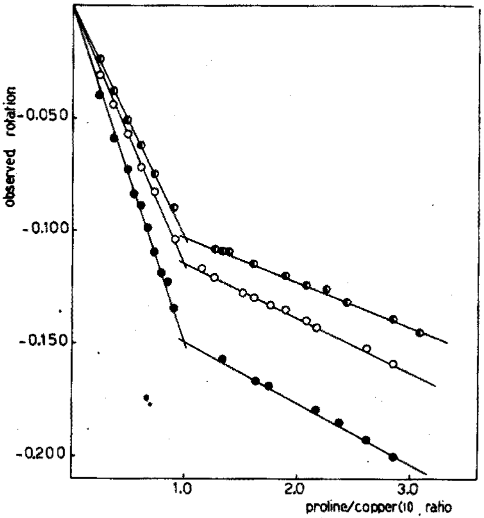

Fig. 1. Spectropolarimetric titration of copper(II) nitrate ($2.00 \cdot 10^{-3}$ *M*) with L(−)proline ($7.61 \cdot 10^{-2}$ *M*) at pH 10.00 and unit ionic strength. (●)$\lambda = 365.015$ nm; (○)$\lambda = 404.660$ nm; (◐)$\lambda = 435.834$ nm.

Figure 1 shows the titration data for copper(II) ($2.00 \cdot 10^{-3}$ M) at pH 10.00 and at the above wavelengths. The experimental points lie on straight lines whose intersection corresponds to a 1:1 metal–titrant ratio. The plot does not indicate the formation of a 1:2 complex as reported in the literature in the absence of ammonia[11,12]. This could suggest the formation of a mixed complex copper(II)–proline–ammonia in the present experimental conditions, as found in the case of copper(II)–glycine complexes[13].

The titration curves shown in Fig. 2 were obtained by using the same concentration of copper(II) at two different concentrations of the ammonia buffer; clearly, the amount of buffer affects the slope of the line after the equivalence point, and it seems advisable to use a small concentration of buffer in order to improve the accuracy of end-point detection. The average deviation of the end-point from the true equivalence point as calculated from about twenty titrations at different concentrations of cop-

TABLE II

RESULTS OF SPECTROPOLARIMETRIC TITRATIONS

Wavelength (nm)	*Copper (mg)*		*Deviation*	
	Taken	*Found*	*mg*	*%*
365.015	6.040	6.003	−0.037	−0.61
365.015	57.98	57.45	−0.43	−0.91
365.015	24.16	24.27	+0.11	+0.46
404.660	24.16	24.27	+0.11	+0.46
435.834	24.16	23.99	−0.17	−0.70
365.015	132.88	132.75	−0.13	−0.10

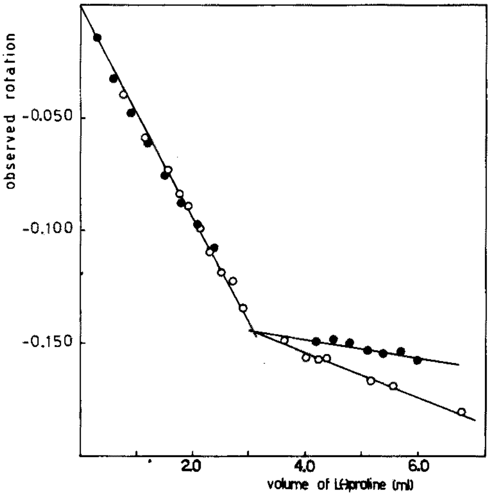

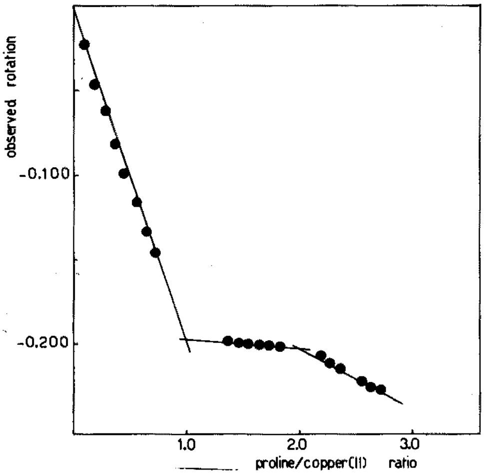

Fig. 2. Spectropolarimetric titration of copper(II) nitrate ($2.00 \cdot 10^{-3}$ M) with L(−)proline ($7.61 \cdot 10^{-2}$ M) at 365.015 nm, pH 10.00 and unit ionic strength. Total volume = 120 ml. (●) 2.0 ml of buffer; (○) 2.4 ml of buffer.

Fig. 3. Spectropolarimetric titration of copper nitrate ($4.90 \cdot 10^{-3}$ M) with L(−)proline ($1.00 \cdot 10^{-1}$ M) at 435.834 nm and pH 8.00.

per(II) (1.00–5.00 · 10^{-3} M) was found to be about −0.5%. Table II shows typical data of titrations.

Other titrations were made at pH 8.00 with the triethanolamine–nitric acid buffer. A titration plot is given in Fig. 3. It shows two break points, corresponding to copper(II)–proline ratios of 1:1 and 1:2. This could be attributed to the formation of both complexes of copper(II) with proline. The break point at the 1:1 ratio can be easily detected with an average deviation of −0.8%.

The present investigation was supported by Italian Council of Research (C.N.R.).

Istituto di Chimica Analitica,
Università di Torino,
10125 Torino (Italy)

Ennio Campi
Piero Mirti

1 S. Kirschner and D. C. Bhatnagar, *Anal. Chem.*, 35 (1963) 1069.
2 K. H. Pearson and S. Kirschner, *Anal. Chim. Acta*, 48 (1969) 339.
3 R. J. Palma, P. E. Reinbold and K. H. Pearson, *Anal. Letters*, 2 (10) (1969) 553.
4 R. J. Palma and K. H. Pearson, *Anal. Chim. Acta*, 49 (1970) 497.
5 D. L. Caldwell, P. E. Reinbold and K. H. Pearson, *Anal. Chim. Acta*, 49 (1970) 505.
6 R. J. Palma, P. E. Reinbold and K. H. Pearson, *Anal. Chem.*, 42 (1970) 47.
7 D. L. Caldwell, P. E. Reinbold and K. H. Pearson, *Anal. Chem.*, 42 (1970) 416.
8 J. R. Baker and K. H. Pearson, *Anal. Chim. Acta*, 50 (1970) 255.
9 P. E. Reinbold and K. H. Pearson, *Talanta*, 17 (1970) 391.
10 M. C. Otey, J. P. Greenstein, M. Winitz and S. M. Birnbaum, *J. Amer. Chem. Soc.*, 77 (1955) 3112.
11 A. Albert, *Biochem. J.*, 47 (1950) 531.
12 N. C. Li and E. Doody, *J. Amer. Chem. Soc.*, 76 (1954) 221.
13 M. Bonnet, R. P. Martin and R. A. Paris, *Bull. Soc. Chim. France*, (1965) 176.

(Received 16th July 1971)

Analytica Chimica Acta
Elsevier Publishing Company, Amsterdam
Printed in The Netherlands

The determination of nitrilotriacetic acid in granular detergent formulations with a Technicon AutoAnalyzer

Titrimetric[1], polarographic[2,3], electrophoretic[4] or thermometric[5,6] procedures have been used successfully in the past for the determination of nitrilotriacetic acid (H_3NTA) or its sodium salt in detergents. However, none of these are suitable for assaying large numbers of samples. It is clear that the only solution in this situation is automation of the NTA analysis.

The method described in this communication is based on the colorimetric measurement of the blue-green color of the nickel–NTA chelate. The method is automated by the use of a Technicon AutoAnalyzer and operates at a rate of 15 samples per hour.

Experimental

Reagents. All chemicals used were of reagent-grade quality. The nickel sulfate solution is 0.1 *M* buffered at pH 5.0 with an acetate buffer: weigh 26.3 g of nickel sulfate hexahydrate and 68.0 g of sodium acetate trihydrate and dissolve in 900 ml of distilled water; adjust to pH 5.0 with anhydrous acetic acid and add 1 ml of BRIJ 35; bring to volume in a 1-l volumetric flask and filter before use. The solution contains BRIJ 35 (Technicon) to lubricate the transmission tubes.

Apparatus. A Technicon AutoAnalyzer comprising the following modules was used: Sampler II, cam 20/1/1; proportioning pump, single or two speed; manifold (Fig. 1); double dialyzer with cuprophan membranes (Technicon C 105–1058 membranes) placed in a water bath at 50°; 15-mm flow cell colorimeter with 600-nm filters; recorder with absorbance chart paper and 4× range expander.

Procedure. For the calibration curve, use four standard solutions containing exactly 0.25, 0.50, 0.75 and 1.00% Na_3NTA in distilled water.

For sample solutions, dissolve 15.0±0.1 g of sample in a 1-l volumetric flask. If the sample contains perborate, destroy the perborate with about 0.1 g of catalase

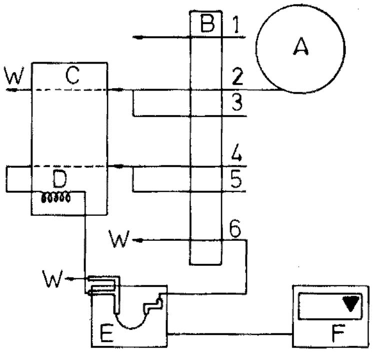

Fig. 1. (A) Sampler II; (B) proportioning pump; (C) double dialyzer 50°; (D) 3 single mixing coils at 50°; (E) 15-mm flow cell colorimeter with 600-nm filters; (F) recorder and 4× range expander.
(B_1) 2.00 ml min^{-1} distilled water to sampler; (B_2) sample 1.60 ml min^{-1}; (B_3) air 0.42 ml min^{-1}; (B_4) nickel sulfate 1.60 ml min^{-1}; (B_5) air 0.42 ml min^{-1}; (B_6) from colorimeter 0.60 ml min^{-1}; (W) waste.

(see below). When the foam has settled, use the following standard and sample solution sequence on the Technicon sampler: standard 0.25%, 0.50%, 0.75%, 1.00%; sample 1 to 10; standard 0.25%, 0.50%, 0.75%, 1.00%; distilled water. Repeat this cycle until all samples have been analyzed.

Calculation. Use the mean of the absorbance of the paired standards to plot a calibration curve of absorbance *vs.*% Na_3NTA. The results are expressed as percent trisodium nitrilotriacetate.

Accuracy and precision

The accuracy of the method was tested by adding known amounts of Na_3NTA to detergents containing 20% perborate. The average recovery was 99.5% (see Table I). The precision was estimated from results obtained on one detergent analyzed 10 times; the standard deviation was 0.17% and the relative standard deviation 0.61% on an average result of 28.61% Na_3NTA.

TABLE I

STANDARD ADDITION OF Na_3NTA TO DETERGENTS CONTAINING 20% PERBORATE

Detergent	*% Na_3NTA added*	*% Na_3NTA found*	*% Recovery*
1	29.18	29.00; 28.83	99.09
2	30.23	29.83; 30.00	98.96
3	31.47	31.17; 31.33	99.30
4	32.33	32.17; 32.33	99.75
5	33.35	33.33; 33.50	100.19

Interferences

Detergent matrix. On 10 detergent base powders, no matrix effect was noted: all calibration curves coincided with the Na_3NTA calibration curve in distilled water. However, it is advisable to test matrix effects of new detergents by comparing a calibration curve of Na_3NTA in distilled water to one in distilled water with NTA-free detergent.

Perborate. There is no influence from perborate on freshly prepared solutions. However, results become lower as the solution ages; after 24 h a 25% loss is observed. This is probably due to the formation of NTA-oxide with different complexing abilities from NTA itself. In order to be able to prepare sample solutions long before assay, the perborate is destroyed with catalase. After destruction of perborate the solutions remain stable for at least 8 h.

Iron(III) and copper(II). Iron(III) and copper(II) should interfere because the formation constants of their complexes with NTA are larger ($K = 15.8$ and 12.6, respectively) than the formation constant of nickel(II) with NTA, and the molar absorptivities of the complexes at 600 nm are larger than that of the nickel(II)–NTA complex. However, since the level of iron(III) and copper(II) in detergents is so low (5–20 p.p.m.), the interference of these ions cannot be observed. Hence, iron(III) and copper(II) cause no error in the described method.

EDTA. The nickel–EDTA complex absorbs at 600 nm and would therefore interfere with the method. However, EDTA is not usually present in detergents already containing NTA.

Mr. R. Campens' assistance during the experimental part of the work is gratefully acknowledged.

Procter and Gamble Company,
European Technical Centre,
1820 Strombeek-Bever (Belgium)

N. Vanwelssenaers
G. G. Clinckemaillie

1 G. G. Clinckemaillie, *Anal. Chim. Acta*, 43 (1968) 520.
2 R. L. Daniel and R. B. H. Blanc, *Anal. Chem.*, 31 (1959) 1221; R. B. H. Blanc, *Anal. Chem.*, 31 (1959) 1840.
3 R. N. P. Farrow and A. G. Hill, *Analyst*, 90 (1965) 241.
4 M. A. Doran, *Anal. Chem.*, 33 (1961) 1752.
5 M. Theis, *Z. Anal. Chem.*, 144 (1955) 275.
6 F. E. Freeberg, *Anal. Chem.*, 41 (1969) 54.

(Received 23rd August 1971)

Preparation of 2,4-dinitrophenyl derivatives of amino acids in dipolar aprotic solvents*

Sanger first used the reagent 2,4-dinitrofluorobenzene to derivatize amino acids[1,2]. Since his classic work on insulin, 2,4-dinitrofluorobenzene has been used routinely for the determination of the N-terminal amino acid of peptides and proteins.

The dinitrophenylation procedures commonly in use have two distinct disadvantages: long reaction time and low yields. The Sanger procedure as modified by Rao and Sober[3] required stirring for 2–5 h with sodium bicarbonate and excess of 2,4-dinitrofluorobenzene in 50% ethanol–water at room temperature. Ethanol is removed by evaporation, the excess of 2,4-dinitrofluorobenzene is extracted with ether and the aqueous phase is acidified, precipitating the crude derivative. The yields of the pure derivatives are low, varying between 10 and 70%. In an attempt to improve the yields Schroeder and LeGette[4] developed a procedure which produced yields of 76–100%. However, this method involved 11 extractions and 3 washings, thus requiring a lengthy work-up period.

In an effort to improve the yield and reaction time, a search was made for a solvent system that was different from the ethanol–water medium commonly used. Since the reaction is a nucleophilic substitution, it seemed that dipolar aprotic solvents might be suitable. Such reactions have their rates greatly increased upon changing from protic solvents, such as alcohols and water, to dipolar aprotic solvents[5]. Yields of nucleophilic reactions in dipolar aprotic solvents are often increased because of the lack of side reactions which occur in the nucleophilic protic solvents. In the case of water as a solvent, 2,4-dinitrofluorobenzene can react with the nucleophilic water to produce 2,4-dinitrophenol. Bunnett and Hermann[6] have found that the reaction of sodium glycinate with 2,4-dinitrofluorobenzene is 200 times faster in 90% dimethylsulfoxide–10% water than in pure water. The present study describes the use of some

---

* A preliminary account of this work was presented at the Pittsburgh Conference of Analytical Chemistry and Applied Spectroscopy, Cleveland, Ohio, March 1971.

dipolar aprotic solvents in the preparation of 2,4-dinitrophenyl derivatives of representative amino acids.

Preparation of 2,4-dinitrophenyl derivatives of amino acids

Dissolve 1 g of sodium bicarbonate in 10 ml of water. To this solution add 0.5 g of amino acid and stir the mixture until the amino acid dissolves. Add 20 ml of dipolar aprotic solvent, followed by an excess of 2,4-dinitrofluorobenzene (1 ml), and stir the mixture at room temperature for 15 min or less. Transfer the reaction mixture to a separatory funnel with 100 ml of water. Extract the excess of 2,4-dinitrofluorobenzene twice with two 20-ml portions of ether. Then acidify the aqueous layer with 6 *M* hydrochloric acid to the Congo red end-point. Usually, the 2,4-dinitrophenyl amino acid precipitates on acidification, but for some amino acids it is necessary to refrigerate overnight. Isolate the solid derivative by suction filtration, wash with water, and air-dry. In all but a very few cases, the melting point of the crude derivative is not improved by recrystallization.

Solvent effects

The effect of the nature of the solvent was investigated by comparing the rates of formation and yields of 2,4-dinitrophenyl derivatives of amino acids in ethanol and the dipolar aprotic solvents, dimethylsulfoxide (DMSO), dimethylformamide (DMF), and dimethylacetamide (DMAC). The results are shown in Table I. It can be seen that the rates in dipolar aprotic solvents are much faster than those in ethanol and that the yields in dipolar aprotic solvents are also greater than the yields in ethanol. The yield in DMAC is slightly lower than the yield in DMSO and DMF. DMF and DMSO were found to give similar results with respect to rates and yields, however, DMF is a cheaper solvent and will probably have greater usage.

The yields of various 2,4-dinitrophenyl derivatives in DMF and DMSO are shown in Table II.

The procedure described in this paper is rapid and simple, producing a nearly quantitative yield of 2,4-dinitrophenyl derivatives. Work is continuing on the application of this method for the derivatization and determination of the N-terminal residue of peptides and proteins.

TABLE I

SOLVENT EFFECT ON RATES AND YIELDS

Amino acid	*Reaction time*	*% Yields*[a]			
		Ethanol	*DMF*[b]	*DMSO*[c]	*DMAC*[c]
Glycine	60 sec	47	95	91	82
Glycine	15 min	1	—	80	—
Phenylalanine	60 sec	29	—	59	—
Phenylalanine	15 min	68	100	100	91

[a] Crude yield of dinitrophenyl derivative after reaction of 2,4-dinitrofluorobenzene with the amino acid in 20 ml of solvent and 10 ml of water.

[b] Aldrich reagent-grade DMF was used, although comparable results were obtained with technical grade DMF, *e.g.* phenylalanine 93%.

[c] Technical grade solvents were used.

TABLE II

PERCENTAGE YIELDS OF 2,4-DINITROPHENYL DERIVATIVES OF AMINO ACIDS IN DMF AND DMSO

Amino acid	*% Yield*[a]	
	DMF	*DMSO*
Glycine	97	91
DL-Alanine	98	—
DL-Valine	92	—
DL-Phenylalanine	100	100
L-Tyrosine	100	99
L-Histidine (bis-derivative)	99	100
L-Arginine	99	—
DL-Threonine	—	99
DL-Methionine	—	99
DL-Aspartic acid	96	95
DL-Asparagine	95	93
L-Cystine	90	—
L-Cysteine (bis-derivative)	100	—

[a] Yield after 15 min at room temperature.

The authors would like to thank Crown Zellerbach Corporation for a generous sample of dimethylsulfoxide and E. I. du Pont de Nemours for samples of dimethylformamide and dimethylacetamide.

Chemistry Department,
Washington and Jefferson College,
Washington, Pa. 15301 (U.S.A.)

J. A. Vinson
L. D. Pepper

1 F. SANGER, *Biochem. J.*, 39 (1945) 507; 40 (1946) 261.
2 R. R. PORTER AND F. SANGER, *Biochem. J.*, 42 (1948) 287.
3 K. R. RAO AND H. A. SOBER, *J. Amer. Chem. Soc.*, 76 (1954) 1328.
4 W. A. SCHROEDER AND J. LEGETTE, *J. Amer. Chem. Soc.*, 75 (1953) 4612.
5 A. J. PARKER, *Quart. Rev. (London)*, 16 (1962) 163.
6 J. F. BUNNETT AND D. H. HERMANN, *Biochemistry*, 9 (1970) 816.

(Received 3rd August 1971)

Analytica Chimica Acta
Elsevier Publishing Company, Amsterdam
Printed in The Netherlands

The monitoring of reactions in solid-phase peptide synthesis with picric acid

The determination of reaction rates could be an important expedient in improving the purity and yield of peptides synthesized by the solid-phase method[1]. Currently used methods are based on amino acid analysis[1], nitrogen analysis, determination of reaction products which are radioactive[2] or have suitable spectroscopic properties[3-5], mass spectrometry[6,7], Schiff base formation[8], and chloride titration[9]. Since some of these methods require sophisticated equipment and are laborious or not generally applicable, there are few reports on the kinetic aspects of reactions involving amino acid and peptide derivatives bound to a solid support. This communication deals with a convenient and fast procedure for the measurement of amine in an insoluble polymer. It can therefore be used for the determination of rates of solid-phase reactions involving the appearance or disappearance of amino groups.

The amine-containing resin is treated with a solution of picric acid to form a salt with the polymer-bound amino groups. After thorough washing to remove excess of picric acid, the resin is treated with an excess of a strong base which quantitatively releases the picrate from the polymer into solution. The concentration of picrate in this solution is determined spectrophotometrically and reflects the amine content of the resin.

General procedure

Allow the resin to swell in dichloromethane for 5 min, neutralize with 5% (v/v) diisopropylethylamine in dichloromethane (2 × 3 min), wash with dichloromethane (3 × 2 min), treat with 0.1 *M* picric acid in dichloromethane (2 × 3 min) and wash with dichloromethane (5 × 2 min). Elute the picrate with the above diisopropylethylamine solution or with 0.1 *M* pyridine hydrochloride in dichloromethane (2 × 3 min) and then with dichloromethane (3 × 2 min). After dilution with 95% ethanol, measure spectrophotometrically. The molar absorptivity of diisopropylethylamine picrate ($\epsilon_{358} = 14{,}500$) is constant in the concentration range $1\text{–}20 \cdot 10^{-5}$ *M* if the ethanolic measuring solution contains less than 20% dichloromethane. A practical ratio of resin to solvent is 1:20 (w/v).

Results and discussion

In order to check the reproducibility of the determinations, 50 mg of tert-butyloxycarbonyl-L-prolyl resin (obtained by coupling of tert-butyloxycarbonyl-L-proline to hydroxymethyl resin with carbonyldiimidazole) was deprotected with 50% trifluoroacetic acid in dichloromethane (2 × 10 min). Four consecutive picrate determinations according to the standard procedure gave 590, 594, 602 and 599 μeq g^{-1}, indicating a reproducibility of ±2%.

The correlation of picrate determinations to amino acid analyses is shown in Table I. Tert-butyloxycarbonyl-L-proline (36 mmole) which had been activated by one equivalent of N,N′-carbonyldiimidazole was allowed to react at room temperature with hydroxymethyl resin (54 meq) in 250 ml of dichloromethane (experiment A). Samples of the resin were withdrawn periodically and both picrate and amino acid were determined. Tert-butyloxycarbonyl-glycyl resin was prepared and analyzed

TABLE I

CORRELATION OF PICRATE AND AMINO ACID DETERMINATION

Experiment	*Reaction time (h)*	*Found (μequiv. g⁻¹)*[a]		
		Proline	*Glycine*	*Picrate*
A	2	31		38
	6	116		114
	18	307		288
	42	453		449
	66	568		527
B	3		708	685
	9		726	715
	27		761	750
	73		793	787

[a] Amino acid analyses were performed on a Beckman Spinco amino acid analyzer 120 B after hydrolysis of the resins with propionic acid–conc. HCl (1+1, v/v) in sealed tubes at 130–140° for 4–6 h[10].

in an analogous manner (experiment B). For substitutions most frequently used in solid-phase peptide synthesis ($>100\ \mu eq^{-1}$ g) the results of the two methods correlate within a range of 1–8%.

An application of the described procedure, namely, the determination of rates of formation of diketopiperazines from dipeptide resins will be published elsewhere[11].

The author wishes to thank Professor R. B. Merrifield for helpful discussions and Mr. Arun Dhundale for expert technical assistance.

Department of Biochemistry,
The Rockefeller University,
New York, N.Y. 10021 (U.S.A.)

B. F. Gisin

1 R. B. Merrifield, *J. Amer. Chem. Soc.*, 85 (1963) 2149.
2 C. L. Krumdieck and C. M. Baugh, *Biochemistry*, 8 (1969) 1568.
3 M. Bodanszky and J. T. Sheehan, *Chem. Ind. (London)*, (1966) 1597.
4 V. Gut and J. Rudinger, in E. Bricas, *Peptides 1968*, North-Holland, Amsterdam, p. 185.
5 Su-Sun Wang and R. B. Merrifield, *Intern. J. Protein Res.*, 1 (1969) 235.
6 F. Weygand and R. Obermeier, *Z. Naturforsch.*, 23b (1968) 1390.
7 E. Beyer and W. A. Koenig, *J. Chromatogr. Sci.*, 7 (1969) 95.
8 K. Esko, S. Karlsson and J. Porath, *Acta Chem. Scand.*, 22 (1968) 3342.
9 L. C. Dorman, *Tetrahedron Letters*, 28 (1969) 2319.
10 J. Scotchler, R. Lozier and A. B. Robinson, *J. Org. Chem.*, 35 (1970) 3151.
11 B. F. Gisin and R. B. Merrifield, in preparation.

(Received 18th August 1971)

Analytica Chimica Acta
Elsevier Publishing Company, Amsterdam
Printed in The Netherlands

BOOK REVIEWS

Progress in Analytical Chemistry. Vol. 3. *X-Ray and Electron Probe Analysis in Biochemical Research,* Edited by K. M. Earle and A. J. Tousimis, Plenum Press, New York–London, 1969, ix + 105 pp., price $ 12.50.

This slender, rather expensive volume contains six edited papers from an Eastern Analytical Symposium, held in 1967. It is hoped that the publication will stimulate an increased application in biomedical research of techniques now commonplace in such fields as metallurgy. The publishers suggest that the book is of particular interest to scientists in the fields of analytical chemistry, applied spectroscopy, biochemistry, biophysics, molecular biology and medical research. Perhaps it would be more accurate to say that it will be of general interest to many in all of these fields, but of especial interest to few.

Three papers are given on X-ray analysis: in Forensic Medicine, metal poison determination; in dispersive and non-dispersive analysis of biological material; in the elemental analysis of Parkinsonian and normal brain tissue. The paper by Louis Zeitz of the Sloan–Kettering Institute is weightiest, including a description of non-dispersive (*i.e.*, energy dispersion), dispersive (diffraction) and mixed instrumental techniques.

Similarly, there are three contributions on electron probe microanalysis: in the examination of asbestos bodies and anthracotic pigment in human lung tissue; in the study of amino-acid transport in the small intestine; and a general paper on the electron probe microanalysis of biological structures. The accurate location of specific elements in biological structures is emphasised in all these papers. However, the use of electron rather than the less spectacular X-ray images to illustrate the texts is disappointing. Quantitative data are sparse.

On the whole instrumentalists will not gain a great deal from this book. Descriptions of instruments and instrumental technique are restricted; succint and more up-to-date information is to be obtained in manufacturers' advertising matter. On the other hand, sections on specimen handling are interesting and there are interdisciplinary references. There is a brief index.

J. P. G. Farr (Birmingham)

Organic Reaction Mechanisms 1969, Edited by B. Capon and C. W. Rees, Interscience Publishers–J. Wiley and Sons, Inc., New York, 1970, xii + 709 pp., price £ 11.00.

This annual survey of the literature of 1969 has arrived several months late owing to circumstances beyond the control of authors and publisher. This is a pity, but it says much for the value of this series that the volume is still most welcome.

Once again, there is an increase in the number of references dealt with (over 4,000). The subject matter is discussed under the same headings as before; many of the most interesting studies are described in some detail whereas the rest are listed. One feels now that the size of the book has reached a limit of usefulness.

The book has been produced in conformity with the high standards of its predecessors. This year the increase in price matches the increase in size, but the price has now gone beyond the stage where a soft-backed edition would be more widely sold. However, this book is still a must for libraries.

D. W. Turner, C. Baker, A. D. Baker and C. R. Brundle, *Molecular Photoelectron Spectroscopy. A Handbook of He 584 Å Spectra*, Wiley–Interscience, London, 1970, 386+x pp., price £ 7.00.

This book is a useful contribution to the literature of a new and rapidly expanding branch of spectroscopy. The field is largely the creation of the research group headed by the senior author, and specialists will probably all possess their own copies of this book by now. However, the book is not a review of the whole field, nor a first introduction for the non-specialist. The first two chapters do give an introduction to the basis of the method, and some details of the spectrometers which have been used, but those who require only an overall view of the subject would probably find one of the several recent review articles to be an easier introduction.

The subtitle of the book, *A handbook of He 584 Å Spectra*, is unduly modest. In addition to illustrations of a large number of spectra, many not published elsewhere, there are detailed analyses of the spectra of some diatomic and triatomic molecules, and of a number of molecules of fundamental importance in organic chemistry. The literature pertinent to these analyses is covered fully to the beginning of 1969. A trivial but possibly confusing point is that, in the diagram of the orbitals of SO_2, the x and y axes are interchanged; apart from this and some less important details, the volume is comparatively free of errors. A careful reading of the text is strongly recommended to anyone considering entry to the field.

D. R. Lloyd (Birmingham)

Analytica Chimica Acta
Elsevier Publishing Company, Amsterdam
Printed in The Netherlands

PUBLICATIONS RECEIVED

Absorption Spectra in the Ultraviolet and Visible Region, Vol. XIV, Edited by L. Lang, Akademiai Kiado, Budapest, 1970, 400 pp., price £ 7.00

Organic Mass Spectrometry, Vol. 4, Supplementary Volume with Cumulative Chemical Compound Index, Heyden and Sons, Ltd., London, 1970, £ 15.75.

R. Reuber, H. Wellens and K. Gruss, *Chemikon (Chemie in Übersichten), Vols. III, IV, VII and VIII*, Umschlau Verlag, Frankfurt-am-Main, 1971.

These small paperbacks contain a miscellany of information on many chemical topics, and should be useful to undergraduate and graduate students for revision work.

NATIONAL BUREAU OF STANDARDS PUBLICATIONS

The following items have recently become available. They can be obtained from the Clearinghouse for Federal Scientific and Technical Information, Springfield, Va. 22151, U.S.A. The relevant number should be quoted and foreign remittances must include an additional 1/4 of the purchase price to cover mailing costs.

Status of Thermal Analysis, Edited by O. Menis, Proceedings of a Symposium on the Current Status of Thermal Analysis, Maryland, April, 1970, N.B.S. Special Publication 338, October 1970, 189 pp., $ 1.00.

Selected Tables of Atomic Spectra, Atomic Energy Levels and Multiplet Tables (CI–CVI), Edited by C. E. Moore, NBS-NSRDS-NBS 3, Section 3, November 1970, $ 1.00.

Ionization Potentials and Ionization Limits Derived from the Analysis of Optical Spectra, Edited by C. E. Moore, NBS-NSRDS-NBS 34, September 1970, 22 pp., 75 cents.

R. C. Paule and J. Mandel, *Standard Reference Materials: Analysis of Interlaboratory Measurements on the Vapor Pressures of Cadmium and Silver*, N.B.S. Special Publication 260–21, January 1971, 30 pp., 30 cents.

A. Napolitano and E. G. Hawkins, *Standard Reference Materials: Viscosity of a Standard Borosilicate Glass*, N.B.S. Special Publication 260–23, December 1970, 10 pp., 25 cents.

Space Simulation, Edited by J. C. Richmond, Proceedings of a Conference held at Gaithersburg, Md., September, 1970, N.B.S. Special Publication 336, October 1970, 984 pp., $ 5.25.

Activities of the N.B.S. Spectrochemical Analysis Section, 1969–1970, Edited by B. F. Scribner, N.B.S. Technical Note 542, November 1970, 114 pp., $1.25.

Damage in Laser Materials, Edited by A. J. Glass and A. H. Guenther, Proceedings of an A.S.T.M.–N.B.S. Symposium held at Boulder, Colo., June 1970, N.B.S. Special Publication 341, December 1970, 126 pp., $ 1.25.

VOL. 58 NO. 1 ANALYTICA CHIMICA ACTA JANUARY 1972

CONTENTS

An integrator for low absorbance samples in atomic absorption spectroscopy
H. Nishita, R. Farmer and S. Peterson (Los Angeles, Calif., U.S.A.) (Rec'd 8th July 1971) 1

Evaluation of atomic absorption with a heated graphite atomizer for the direct determination of trace transition metals in sea water
D. A. Segar and J. G. Gonzalez (Miami, Fla., U.S.A.) (Rec'd 2nd August 1971) . 7

Analysis of metals for trace impurities by sealed cell atomic absorption
J. P. Pemsler and E. J. Rapperport (Lexington, Mass., U.S.A.) (Rec'd 18th June 1971) 15

The determination of noble and base metals in osmiridium, native platinum and sperrylite by atomic absorption spectrophotometry
J. G. Sen Gupta (Ottawa, Ont., Canada) (Rec'd 23rd July 1971). 23

Atomic absorption and fluorescence spectroscopy with a carbon filament atom reservoir. Part VIII. The determination of manganese by atomic absorption spectroscopy
L. Ebdon, G. F. Kirkbright and T. S. West (London, England) (Rec'd 20th June 1971) 39

The determination of lead in blood by atomic absorption with the high-temperature graphite tube
E. Norval and L. R. P. Butler (Pretoria, South Africa) (Rec'd 14th August 1971) . 47

The use of a glow-discharge lamp as a light source in the spectrometric analysis of gold
H. Jäger (Pretoria, South Africa) (Rec'd 5th July 1971) 57

Zur Berechnung von Interelementeffekten bei der Röntgenfluoreszenzspektralanalyse
K. H. Grothe und H. Rackur (Hannover, Deutschland) (Eing. den 2. August 1971) . 65

A semi-solid surface fluorescence method for the determination of lactate dehydrogenase
R. L. Zimmerman, Jr. and G. G. Guilbault (New Orleans, La., U.S.A.) (Rec'd 30th June 1971) 75

Determination of total iodine and iodate in sea water and in various evaporites
M. M. Schnepfe (Washington, D.C., U.S.A.) (Rec'd 2nd August 1971) 83

Excited state prototropism and solvent dependence of the fluorescence of 3-aminoquinoline
S. G. Schulman and A. C. Capomacchia (Gainesville, Fla., U.S.A.) (Rec'd 29th June 1971) 91

Ligand structure and fluorescence of metal chelates; N-heterocyclic hydrazones with zinc
D. E. Ryan, F. Snape and M. Winpe (Halifax, N.S., Canada) (Rec'd 26th July 1971) 101

A new sensitive method for the extractive – spectrophotometric determination of nickel
R. S. Barratt, R. Belcher, W. I. Stephen and P. C. Uden (Birmingham, England) (Rec'd 20th July 1971) 107

Spectrophotometric determination of small amounts of reagents used in solvent extraction processes. Part I. α-Hydroxyoximes
A. W. Ashbrook (Ottawa, Ont., Canada) (Rec'd 12th July 1971) 115

Spectrophotometric determination of small amounts of reagents used in solvent extraction processes. Part II. Bis(2-ethylhexyl)phosphoric acid
A. W. Ashbrook (Ottawa, Ont., Canada) (Rec'd 12th July 1971) 123

Studies of substituted dihydroxy-*p*-benzoquinones as precipitate-exchange reagents
J. E. Barney II and D. D. Rosebrook (Kansas City, Mo., U.S.A.) (Rec'd 21st May 1971) 131

Specific method for the determination of ozone in the atmosphere
S. L. Sachdev, J. P. Lodge, Jr. and P. W. West (Baton Rouge, La., U.S.A.) (Rec'd 23rd August 1971) 141

The distribution of salts of large cations between water and organic solvents. Part I. Studies on the extraction of quaternary phosphonium and arsonium salts over a range of cation and anion concentrations
N. A. Gibson and D. C. Weatherburn (Sydney, N.S.W., Australia)(Rec'd 13th August 1971) 149

(continued on page 4 of cover)

Continued from inside page of cover

The distribution of salts of large cations between water and organic solvents. Part II. Factors affecting the magnitude of the distribution ratio
N. A. Gibson and D. C. Weatherburn (Sydney, N.S.W., Australia) (Rec'd 13th August 1971) 159

The direct gas-chromatographic separation and determination of impurities in terephthalic acid
J. E. Hicks and R. S. Jessee (Kingsport, Tenn., U.S.A.) (Rec'd 5th August 1971) . . 167

Thermal properties of some compounds of lutidinic acid with divalent metals
G. D'Ascenzo, U. Biader Ceipidor and G. de Angelis (Rome, Italy) (Rec'd 16th July 1971) 175

A direct electrochemical method for the determination of allopurinol and uric acid mixtures. Adsorption of uric acid at the pyrolytic graphite electrode
G. Dryhurst and P. K. De (Norman, Okla., U.S.A.) (Rec'd 1st September 1971) . . 183

Electrochemical studies of the uranium(VI) – diethylenetriaminepentaacetic acid complexes
E. Jacobsen, G. O. Kalland and O. Lykkjen (Oslo, Norway) (Rec'd 31st August 1971) 193

Polarographic maxima of the first kind: characteristics in absence of resistance-controlled currents
F. M. Hawkridge, T. W. Holt and H. H. Bauer (Lexington, Ky., U.S.A.) (Rec'd 22nd July 1971) 203

Electrochemical determination of diffusion coefficients of selected metals in dimethylsulfoxide
J. L. Jones and H. A. Fritsche Jr. (College Station, Tex., U.S.A.) (Rec'd 1st July 1971) 209

Short Communications

Rapid determination of selenium by atomic absorption spectrophotometry
B. C. Severne and R. R. Brooks (Palmerston North, New Zealand) (Rec'd 22nd July 1971) 216

Spectrophotometric determination of trace amounts of selenium in iron and steel with 4-methyl-*o*-phenylenediamine
T. Kawashima and A. Ueno (Kagoshima, Japan) (Rec'd 3rd May 1971) 219

The determination of zirconium in steels
D. B. Ratcliffe and C. S. Byford (Southampton, England) (Rec'd 27th August 1971) 223

Extraction–photometric determination of nitrite in fresh and sea water
K. Matsunaga, T. Oyama and M. Nishimura (Hakodate, Japan) (Rec'd 13th July 1971) 228

Determination of mercury in seawater by radioactivation
H. V. Weiss and T. E. Crozier (San Diego, Calif., U.S.A.) (Rec'd 9th July 1971) . . . 231

The determination of uranium in exploration samples by X-ray emission spectrometry
N. H. Clark and J. G. Pyke (Mount Isa, Qld., Australia) (Rec'd 2nd September 1971) 234

Separation of cyclotron-produced cadmium -109 from the silver matrix, copper and zinc
R. D. Neirinckx (Pretoria, South Africa) (Rec'd 17th August 1971) 237

Spectropolarimetric determination of copper(II) with L(—)proline
E. Campi and P. Mirti (Torino, Italy) (Rec'd 16th July 1971) 239

The determination of nitrilotriacetic acid in granular detergent formulations with a Technicon AutoAnalyzer
N. Vanwelssenaers and G. G. Clinckemaillie (Strombeek-Bever, Belgium) (Rec'd 23rd August 1971) 243

Preparation of 2,4-dinitrophenyl derivatives of amino acids in dipolar aprotic solvents
J. A. Vinson and L. D. Pepper (Washington, Pa., U.S.A.) (Rec'd 3rd August 1971) . 245

The monitoring of reactions in solid-phase peptide synthesis with picric acid
B. F. Gisin (New York, N.Y., U.S.A.) (Rec'd 18th August 1971) 248

Book Reviews 250